Behavior of Piled Raft Foundations Subjected to Static Horizonal Loading and Seismic Loading

KAKEN
2002
10

BEHAVIOR OF PILED RAFT FOUNDATIONS SUBJECTED TO STATIC HORIZONTAL LOADING AND SEISMIC LOADING

(Project No.: 12450188)

Research report of a Grants-in-Aid for Scientific Research (Exploratory Research (B)(2)) supported by the Ministry of Education, Culture, Sports, Science and Technology (MEXT) and the Japan Society for the Promotion of Science (JSPS)

March 2003

Head investigator: Tatsunori Matsumoto
(Department of Civil Engineering, Faculty of Engineering, Kanazawa University)

パイルド・ラフト基礎の水平抵抗および耐震性能に関する研究

（課題番号：12450188）

平成 12 年度～平成 14 年度科学研究費補助金（基盤研究(B)(2)）研究成果報告書

平成 15 年 3 月

研究代表者

松本樹典（金沢大学工学部土木建設工学科）

PREFACE

This report summarizes the results of the research on "Behavior of piled raft foundations subjected to static horizontal loading and seismic loading" supported by the Ministry of Education, Culture, Sports, Science and Technology (MEXT) and the Japan Society for the Promotion of Science (JSPS) from April 2000 to March 2003. The intended goal of this research is to establish the design method of piled raft foundations subjected to seismic loading, because Japan is one of the highly seismic areas. In order to achieve this goal, it is required to clarify the behavior of piled rafts under static vertical loading and horizontal loading as well as under seismic loading.

In this research, static load tests on model piled rafts and model pile groups, and shaking table tests on them were conducted at 1-g were conducted at 1-g gravitational field and centrifugal field using a centrifuge device. Although the centrifuge tests took an important role in this research, the experiments at 1-g field complemented the centrifuge tests because the number of the centrifuge tests was limited due to its cost and time required.

As for analytical method, a simplified analytical method was developed to analyze the three dimensional deformation of piled rafts and pile groups. The propose method makes use of a hybrid model in which the flexible raft is modeled as thin plates and the piles as elastic beams and the soil is treated as springs. Both the vertical and lateral resistances of the piles as well as the raft base are incorporated into the model. Pile-soil-pile, pile-soil-raft and raft-soil-raft interactions are taken into account based on Mindlin's solutions for both vertical and lateral forces. The validity of the proposed method was verified through comparisons with several existing methods for single piles, pile groups and piled rafts, and three-dimensional FEM analyses.

The research constitution was mainly consisted of the Geotechnical Research Group of the Department of Civil Engineering, Kanazawa University, and the Technical Center of Taisei Corporation. The centrifuge tests were conducted using the centrifuge device at the Technical Center of Taisei Corporation. Much support from Mr. Y. Matsuotka (Manager of the Technical Center), Mr. Y. Shiba (Manager of Soil Mechanics Section) and other members of the Technical Center of Taisei Corporation is greatly appreciated.

The model tests at 1-g gravitational field were carried out at Kanazawa University. The disaster prevention research group is appreciated for their permission to use their shaking table test facilities for this research. Many students graduated from the Geotechnical Research Group of the Department of Civil Engineering, Kanazawa University, Mr. Hiroshi Yamada, Mr. Hiroshi Ito, Mr. Masaya Kitaguchi, Mr. Atsuo Yamada, Mr. Naotsugu Ebuchi, Miss. Ai Ohno and Miss. Nao Kanefusa, took part in this research through their graduation projects. Mr. Takayuki Yamakami, Technician of the Geotechnical Research Group is greatly acknowledged for his help in conducting the 1-g model tests.

RESEARCH CONSTITUTION

Research representative: Tatsunori Matsumoto (Dept. of Civil Eng., Kanazawa University)

Research partaker: Kenichi Horikoshi (Technology Center, Taisei Corporation)

Kinya Miura (Dept. of Civil Eng., Toyohashi Technical College)

Masaru Kitaura (Dept. of Civil Eng., Kanazawa University)

Fawu Wang (Dept. of Civil Eng., Kanazawa University)

Toshiyuki Takahara (Dept. of Civil Eng., Kanazawa University)

Research supporter: Toru Watanabe (Technology Center, Taisei Corporation)

Hideki Fukuyama (former graduate student of Graduate School, Kanazawa University)

Yoshinori Hashizume (former graduate student of Graduate School, Kanazawa University)

Kitiyodom Pastsakorn (Doctoral student of Graduate School, Kanazawa University)

Kazuyuki Fukumura (Graduate student of Graduate School, Kanazawa University)

RESEARCH BUDGET

(unit: 1,000 yen)

Term	Direct	Indirect	Total
April 2000 to March 2001	6,400	0	6,400
April 2001 to March 2002	2,900	0	2,900
April 2002 to March 2003	1,700	0	1,700
Ground sum	11,000	0	11,000

はしがき

本報告書は，パイルド・ラフト基礎の合理的な地震時設計法を確立することを念頭に置き，パイルド・ラフトおよび従来の群杭基礎の静的水平載荷実験と振動実験，組合せ荷重を受けるこれらの基礎に対する三次元簡易変形解析法の開発，開発した解析手法を用いた実験の解析を３カ年にわたって実施した結果をとまとめたものである。

実験については，本研究では，1g 場での小型模型の静的載荷実験，1g 場での小型模型の振動実験，遠心装置を利用した静的載荷実験と振動実験と，多岐に渡ってパイルド・ラフトの挙動を調べた。解析手法に関しては，弾性論に基づいて杭－地盤－杭，杭－地盤－ラフト，ラフト－地盤－ラフトの相互作用を考慮した，三次元簡易解析手法を開発した。

本研究の特徴は，大学と民間企業（大成建設㈱）が両者の特色と得意分野を有効に利用して，実務に役立つ成果を得たことである。遠心実験については，大成建設㈱技術センターの遠心実験装置を利用した。遠心実験装置の利用に際し，多大な便宜を図って頂いた松岡康訓所長，土質研究室志波由紀夫室長をはじめ，同技術センターの皆様に深謝の意を表する。また，研究の実施にあたっては，下記の研究組織に加えて，金沢大学土木建設工学科地盤研究室の多くの卒業生の協力があったことを記し，謝意を表する。

平成 15 年 4 月　研究代表者　松本樹典

研究組織

研究代表者：松本樹典（金沢大学工学部土木建設工学科）
研究分担者：堀越研一（大成建設株式会社、技術センター）
三浦均也（豊橋技術大学建設工学系）
北浦　勝（金沢大学工学部土木建設工学科）
汪　発武（金沢大学工学部土木建設工学科）
高原利幸（金沢大学工学部土木建設工学科）
研究協力者：渡邊　徹（大成建設株式会社、技術センター）
福山英樹（元金沢大学大学院博士前期課程院生）
橋爪芳徳（元金沢大学大学院博士前期課程院生）
Kitiyodom Pastsakorn（金沢大学大学院博士後期過程院生）
福村和之（金沢大学大学院博士前期課程院生）

交付決定額（配分額）

（金額単位：千円）

	直接経費	間接経費	合　計
平成１２年度	6,400	0	6,400
平成１３年度	2,900	0	2,900
平成１４年度	1,700	0	1,700
総　計	11,000	0	11,000

LIST OF PUBLICATION

Journals & Proceedings

No	Authors	Title	Publication	Vol., No., page, year
1	Pastsakorn, K. Matsumoto, T. Takahara, T. Todo, H.	A simplified analytical method for deformation analysis of piled raft foundations with batter piles	Proc. 5th Int. Conf. on Deep Foundation Practice incorporating Piletalk Int. 2001, Singapore	319 - 326 2001.4..
2	Watanabe, T. Fukuyama, H. Horikoshi, K. Matsumoto, T.	Centrifuge modelling of piled raft foundations subjected to horizontal loads	Proc. 5th Int. Conf. on Deep Foundation Practice incorporating Piletalk Int. 2001, Singapore	371 - 378 2001.4.
3	堀越 研一 松本 樹典 福山 英樹 渡邊 徹	パイルド・ラフト基礎の地震時挙動に関する基本実験	杭基礎の耐震設計法に関するシンポジウム論文集，東京	43 - 48 2001.9.
3	Horikoshi, K. Matsumoto, T. Fukuyama, H. Watanabe, T.	Fundamental experiments on behavior of piled raft foundations under seismic loads (in Japanese)	Proc. of Symp. on Sesimic Design of Pile Foundations, JGS, Tokyo	43 - 48 2001.9.
4	堀越 研一 松本 樹典 福山 英樹 渡邊 徹	水平荷重を受けるパイルド・ラフト基礎の挙動	第46回地盤工学シンポジウムー地盤・構造物の変形とその評価ー，東京	241 - 246 2001.11.
4	Horikoshi, K. Matsumoto, T. Fukuyama, H. Watanabe, T.	Behavior of piled raft foundations subjected to horizontal loading (in Japanese)	Proc. of 46th Geotechnical Symp., JGS, Tokyo	241 - 246 2001.11.
5	Pastsakorn, K. 松本 樹典	斜杭パイルド・ラフトおよび群杭基礎の簡易三次元変形解析プログラムの開発	第46回地盤工学シンポジウムー地盤・構造物の変形とその評価ー，東京	247 - 252 2001.11
5	Pastsakorn, K. Matsumoto, T.	Development of a computer program for simplified deformation analysis of piled rafts and pile groups with batter piles (in Japanese)	Proc. of 46th Geotechnical Symp., JGS, Tokyo	247 - 252 2001.11.
6	Horikoshi, K Matsumoto, T. Fukuyama, H. Watanabe, T.	Performance of piled raft foundations subjected to seismic loads	Proc. Int. Workshop on Design codes and Soil Investigation in view of International Harmonization and Performance Based Design, Tokyo	381 - 389 2002.4.

No	Authors	Title	Publication	Vol., No., page, year
7	Pastsakorn, K. Hashizume, Y. Matsumoto, T.	Lateral load tests on model pile groups and piled raft foundations in sand	Proc. Int. Conf. on Physical Modelling in Geotechnics, St. John's, Canada	709 - 714 2002.7.
8	Horikoshi, K Watanabe, T. Fukuyama, H. Matsumoto, T.	Behavior of piled raft foundations subjected to horizontal loads	Proc. Int. Conf. on Physical Modelling in Geotechnics, St. John's, Canada	715 - 721 2002.7.
9	Matsumoto, T. Hashizume, Y. Fukumura, K. Pastsakorn, K. Horikoshi, K.	Preliminary study on behavior of model pile foundations in sand using shaking table	Jour. of Engineering Geology	Vol.10, 502 - 508, 2002.10
10	Pastsakorn, K. Matsumoto, T.	Recent development in simplified deformation analysis program PRAB for piled raft foundations	Jour. of Engineering Geology	Vol.10, 509 - 515, 2002.10
11	Pastsakorn, K. Matsumoto, T.	A simplified analysis method for piled raft and pile group foundations with batter piles	Int. J. Numer. and Anal. Methods in Geomech.	Vol.26, 1349-1369, 2002.11
12	Pastsakorn, K. Matsumoto, T.	A simplified analysis method for piled raft foundations in non-homogeneous soils	Int. J. Numer. and Anal. Methods in Geomech.	Vol.27, 85-109, 2003.2
13	Kitiyodom, P. Matsumoto, T. Kanefusa, N.	Numerical analysis of the influence of reaction piles on static axial pile load test results	BGA Int. Conf. on Foundations 'Innovations, observations, design and practice', Dundee, Scotland	2003 (submitted)
14	Fukumura, K. Matsumoto, T. Ohno, A. Hashizume, Y.	Experimental study on behavior of model piled raft foundations in sand using shaking table at 1-g gravitational field	BGA Int. Conf. on Foundations 'Innovations, observations, design and practice', Dundee, Scotland	2003 (submitted)
15	Horikoshi, K. Matsumoto, T. Hashizume, Y. Watanabe, T. Fukuyama, H.	Performance of pile raft foundations subjected to static vertical loading and horizontal loading	Int. Journal of Physical Modelling in Geomechanics.	2003 (submitted)
16	Horikoshi, K. Hashizume, Y. Matsumoto, T. Watanabe, T.	Performance of pile raft foundations subjected to dynamic loading	Int. Journal of Physical Modelling in Geomechanics.	2003 (submitted)
17	Kitiyodom, P. Matsumoto, T. Kanefusa, N.	Influence of reaction piles on the behaviour of test pile in static load testing	Canadian Geotechnical Jour.	2003 (to be submitted)

No	Authors	Title	Publication	Vol., No., page, year
18	Ikemoto, T. Miyajima, M. Kitaura, M.	Inverse analysis of dynamic soil parameters using acceleration records	Proc. of 12th World Conf. on Earthquake Engineering (12WCEE), Auckland, New Zealand	CD-R paper 1794 2000.
19	Murata, A. Kitaura, M. Miyajima, M.	Prediction of damage to wooden houses by using fatigue response spectra considering the number of seismic response cycles	Proc. of 12th World Conf. on Earthquake Engineering (12WCEE), Auckland, New Zealand	CD-R paper 1870 2000.
20	Hashimomo, T. Miyajima, M. Yoshida, M. Yasuda, M. Murata, A. Kitaura, M.	Damage characteristics of buildings close to fault in the 1999 Ji-Ji Earthquake, Taiwan	Proc. of 6th Int. Conf. on Seismic Zonation (61CSZ), Palm Springs, California, USA	CD-R 2000.11

Oral presentations in Annual Meetings of Japanese Geotechnical Society
（地盤工学研究発表会での口頭発表）

No.	Authors 氏　名	Title 講　演　題　目	Serial No., place	page, year 頁・年
地1	山田　博志 松本　樹典	砂地盤におけるパイルドラフト基礎の模型載荷実験	第31回 （北見）	1677 - 1678 1996.7.17-20
地2	伊東　弘 山田　博志 松本　樹典	単杭パイルドラフト基礎の模型載荷実験における杭の支持力特性	第32回 （熊本）	1495 - 1496 1997.7.15-17
地3	山田　博志 伊東　弘 松本　樹典	複数杭パイルドラフト基礎の模型載荷実験における杭の支持力特性	第32回 （熊本）	1497 - 1498 1997.7,15-17
地4	北口　雅也 松本　樹典 山田　博志	パイルドラフト基礎の水平抵抗力の発生機構に関する基礎的実験	第33回 （山口）	1513 - 1514 1998.7.14-16
地5	山田　淳夫 松本　樹典 福山　英樹	砂地盤での模型パイルド・ラフト鉛直載荷実験における寸法効果	第34回 （東京）	1483 - 1484 1999.7.21-23
地6	福山　英樹 松本　樹典 山田　淳夫	砂地盤における模型パイルド・ラフトの水平載荷実験	第34回 （東京）	1485 - 1486 1999.7.21-23
地7	浦田　芳孝 松本　樹典 岡田　範彦	鉛直荷重を受けるパイルド・ラフトおよび群杭基礎の簡易三次元弾性変形解析例	第35回 （岐阜）	1855 - 1856 2000.6.13-15
地8	松本　樹典 岡田　範彦 浦田　芳孝	組合わせ荷重を受けるパイルド・ラフトおよび群杭基礎の簡易三次元弾性変形解析例	第35回 （岐阜）	1857 - 1858 2000.6.13-15
地9	江渕　直嗣 福山　英樹 松本　樹典	砂地盤における模型パイルド・ラフトの水平載荷実験（その３） －杭配置の違いによる水平抵抗力の比較－	第35回 （岐阜）	1859 - 1860 2000.6.13-15
地10	福山　英樹 江渕　直嗣 松本　樹典	砂地盤における模型パイルド・ラフトの水平載荷実験（その４） －群杭とパイルド・ラフトの水平抵抗力の比較－	第35回 （岐阜）	1861 - 1862 2000.6.13-15
地11	K. Pastsakorn 松本　樹典	Miudlinの第2解に基づく横方向地盤反力係数の評価と杭基礎への応用	第36回 （徳島）	1677 - 1678 2001.6.12-14
地12	橘爪　芳徳 松本　樹典 K. Pastsakorn 福山　英樹	砂地盤における模型パイルド・ラフトの水平載荷実験（その５）	第36回 （徳島）	1679 - 1680 2001.6.12-14
地13	福山　英樹 渡邊　徹 堀越　研一 松本　樹典	水平荷重を受けるパイルド・ラフト基礎の挙動に関する遠心実験	第36回 （徳島）	1681 - 1682 2001.6.12-14

No.	Authors 氏　名	Title 講　演　題　目	Serial No., place	page, year 頁・年
地14	藤堂　治彦 松本　樹典 高原　利幸 K. Pastsakorn	水平荷重を受けるパイルド・ラフトの三次元FEM解析結果と簡易解析結果との比較	第36回 （徳島）	1683 - 1684 2001.6.12-14
地15	松本　樹典 K. Pastsakorn	組合せ荷重を受ける斜杭パイルド・ラフトおよび群杭基礎の簡易三次元変形解析	第36回 （徳島）	1685 - 1686 2001.6.12-14
地16	茂原 裕志 K. Pastsakorn 松本 樹典	パイルド･ラフトの三次元FEM弾性変形解析結果に及ぼすメッシュ寸法の影響	第37回 （大阪）	CD-R, 2pp. 2002.7.16-18 番号743
地17	橋爪 芳徳 福村 和之 松本 樹典 堀越 研一	1g 場における模型パイルド･ラフトの振動実験 (その1)　- 模型砂地盤の振動特性 -	第37回 （大阪）	CD-R, 2pp. 2002.7.16-18 番号744
地18	橋爪　芳徳 福村　和之 松本　樹典 茂原 裕志	1g 場における模型パイルド・ラフトの振動実験 (その２)　- １本杭パイルド・ラフトの振動実験 -	第37回 （大阪）	CD-R, 2pp. 2002.7.16-18 番号745
地19	福村 和之 橋爪 芳徳 松本 樹典 K. Pastsakorn	1g 場における模型パイルド・ラフトの振動実験 （その３）－先端固定杭基礎の振動実験－	第37回 （大阪）	CD-R, 2pp. 2002.7.16-18 番号746
地20	K. Pastsakorn 茂原　裕志 松本 樹典	パイルド・ラフト基礎の簡易変形解析における相互作用を有する鉛直・水平地盤ばね導入の重要性	第37回 （大阪）	CD-R, 2pp. 2002.7.16-18 番号747
地21	金房　奈緒 K. Pastsakorn 松本　樹典	杭の静的鉛直載荷実験結果に及ぼす反力杭の影響	第38回 （秋田）	CD-R, 2pp. 2003.7.2-4 （投稿済）
地22	橋爪　芳徳 K. Pastsakorn 金房　奈緒 松本　樹典	杭の静的水平載荷実験結果に及ぼす反力杭の影響	第38回 （秋田）	CD-R, 2pp. 2003.7.2-4 （投稿済）
地23	K. Pastsakorn 金房　奈緒 松本　樹典	地盤の非線形性を考慮した簡易変形解析による杭静的載荷遠心模型実験の逆解析	第38回 （秋田）	CD-R, 2pp. 2003.7.2-4 （投稿済）
地24	福村　和之 大野　愛 松本　樹典 橋爪　芳徳	1g 場における模型パイルド・ラフトの振動実験 (その 4) －4本杭パイルド・ラフトの振動実験－	第38回 （秋田）	CD-R, 2pp. 2003.7.2-4 （投稿済）
地25	大野　愛 福村　和之 松本　樹典	1g場における模型パイルド・ラフトの振動実験 （その5）－4本杭パイルド・ラフトの振動実験と静的水平載荷実験との比較－	第38回 （秋田）	CD-R, 2pp. 2003.7.2-4 （投稿済）

Oral presentations in Annual Meetings of Japanese Society for Civil Engineers
（土木学会年次学術講演会での口頭発表）

No.	Authors 氏　名	Title 講　演　題　目	Serial No., place	Page, year 頁・年
土1	山田　博志 松本　樹典	鉛直荷重を受けるパイルドラフト基礎の模型実験	第51回 （名古屋）	第３部(B), 34 - 35, 1996.9.
土2	松本　樹典 山田　博志	薄板要素－杭ばね－地盤ばねモデルによるパイルド・ラフトの鉛直変形解析プログラムの開発	第53回 （神戸）	第３部(B), 40 - 41, 1998.10.
土3	山田　博志 松本　樹典	水平載荷を受けるパイルドラフト基礎のFEM解析	第53回 （神戸）	第３部(B), 42 - 43, 1998.10.
土4	福山　英樹 松本　樹典	砂地盤における模型パイルド・ラフトの水平載荷実験（その２）	第54回 （広島）	第３部(A), 832 - 833, 1999.9.
土5	岡田　範彦 松本　樹典	三次元変形簡易解析プログラムにパイルドラフト基礎の解析例	第54回 （広島）	第３部(A), 834 - 835, 1999.9.
土6	福山　英樹 堀越　研一 渡邊　徹 松本　樹典	遠心載荷実験による単杭およびラフトの沈下特性の検討	第55回 （仙台）	第３部(A), 2000
土7	橋爪　芳徳 松本　樹典 P. Kitiyodom 藤堂　治彦	砂地盤における斜杭パイルド・ラフトの水平載荷実験	第56回 （熊本）	CD-R版 2001.10. III-A362
土8	福山　英樹 松本　樹典 堀越　研一 渡邊　徹	水平荷重を受けた際のパイルド・ラフト基礎の挙動（静的載荷実験）	第56回 （熊本）	CD-R版 2001.10. III-A363
土9	堀越　研一 渡邊　徹 福山　英樹 松本　樹典	水平荷重を受けた際のパイルド・ラフト基礎の挙動（模型振動実験）	第56回 （熊本）	CD-R版 2001.10. III-A364
土10	P. Kitiyodom 松本　樹典	有限深さ地盤におけるパイルド・ラフトの簡易変形解析（その１：PRABの拡張）	第57回 （札幌）	CD-R版 2002.9. III-A652
土11	P. Kitiyodom 松本　樹典 茂原　裕志	有限深さ地盤におけるパイルド・ラフトの簡易変形解析（その２：PRABとFEMの比較解析）	第57回 （札幌）	CD-R版 2002.9. III-A653

No.	Authors 氏　名	Title 講　演　題　目	Serial No., place	Page, year 頁・年
土12	橋爪　芳徳 松本　樹典 福村　和之	砂地盤における模型パイルド・ラフトの水平載荷実験（その６）	第57回 （札幌）	CD-R版 2002.9. III-A655
土13	福村　和之 橋爪　芳徳 松本　樹典	一本杭パイルド・ラフト模型および模型ラフトの水平載荷実験	第57回 （札幌）	CD-R版 2002.9. III-A656
土14	渡邊　徹 堀越　研一 松本　樹典 橋爪　芳徳	杭頭剛結度が静的水平載荷時のパイルド・ラフト基礎の挙動に与える影響	第57回 （徳島）	CD-R版 2003.9. （投稿済）
土15	松本　樹典 橋爪　芳徳 堀越　研一 渡邊　徹	杭頭剛結度が振動載荷時のパイルド・ラフト基礎の変位特性に与える影響	第57回 （徳島）	CD-R版 2003.9. （投稿済）
土16	橋爪　芳徳 松本　樹典 堀越　研一 渡邊　徹	杭頭剛結度が振動載荷時のパイルド・ラフト基礎の荷重分担性状に与える影響	第57回 （徳島）	CD-R版 2003.9. （投稿済）
土17	Kitiyodom, P. 松本　樹典 橋爪　芳徳 堀越　研一	簡易解析プログラムPRABを用いた水平載荷時のパイルド・ラフトの挙動解析	第57回 （徳島）	CD-R版 2003.9. （投稿済）

CONTENS

CHAPTER 1

INTRODUCTION

1.1. BACKGROUND OF THE RESEARCH

Piled raft foundations have been widely recognized as one of the most economical foundation systems since Burland et al (1977) presented the concept of settlement reducers . Some design concepts and their applications have been reported (Kakurai et al., 1987; Randolph, 1994; Horikoshi and Randolph, 1998; Katzenbach et al., 1998; Horikoshi and Randolph, 1999; Shinozaki et al., 1999). Furthermore, design codes and guidelines for piled raft foundations have been published (Architectural Institute of Japan, 2001; Katzenbach and Moormann, 2001; Placzek et al, 2001).

In piled raft foundations, piles are extensively used to reduce the settlement of foundations to an acceptable level, rather than to support the weight of upper structures. Although a number of works on the settlement of piled raft foundations have been reported, the work that deals with the behavior of piled raft foundations subjected to horizontal loading seems to be very limited. The establishment of a seismic design concept for piled raft foundations is necessary especially in highly seismic areas such as Japan.

Although piled raft foundations have already been used for the actual foundations in Japan, most of them seemed to be treated as rafts alone in the seismic design by ignoring any horizontal contributions from the piles. Considering current trends toward the performance based design in the field of geotechnical engineering, the behavior of the piled raft foundation needs to be rationally explained.

1.2. REVIEW OF PREVIOUS RESEARCH WORKS

1.2.1. Experimental research

Centrifuge modeling has great advantages to observe the interactions between the piles and the raft through the soil. A number of works such as Sommer et al. (1991), Thaher and Jessberger (1991), Horikoshi and Randolph (1996) used centrifuge modeling to examine the settlement behavior of piled rafts.

As for pile rafts subjected to horizontal loads, Watanabe et al (2000) reported the results of horizontal loading tests on a square raft model on an actual ground, where 4 slender piles were installed beneath the square raft of 2 m width. However, the detailed behavior of the piled raft foundations subjected to horizontal loads still has not been well clarified.

1.2.2. Analytical methods

Much research on the analysis of piled raft foundations has been done, for instance, the works of Hain and Lee (1978), Poulos and Davis (1980), Kuwabara (1989), Clancy and Randolph (1993), Poulos (1994), Randolph (1994), Yamashita et al (1994), Ta and small (1996), Horikoshi and Randolph (1998) and Horikoshi and Randolph (1999). However, most of the previous research is related to piled rafts subjected to vertical loading.

A complete three-dimensional analysis of a pile raft foundation system can be carried out by a finite element analysis (e.g. Smith and Wang (1998)). The use of the finite element approach removes the need for the approximate assumptions inherent in the above-mentioned simplified approaches. However, a finite element analysis is more suited to obtaining benchmark solutions against which to compare simpler analysis methods, or to obtaining solutions of a detailed analysis for the final design of a foundation, rather than as a preliminary routine design tool. In the present study, a computer program PRAB (Piled Raft Analysis with Batter piles) has been developed based on a hybrid model, which sufficiently minimizes the size of the stiffness matrix and the amount of computation. This model was first proposed by O Neill et al (1977). The response of each pile is modelled using the load-transfer method, and the interaction between the piles through the soil, is calculated based on Mindlin s solution. In Chow (1987), this hybrid model was used for the analysis of general three-dimensional pile groups. Clancy and Randolph (1993) extended the hybrid model by including thin plate bending finite elements to model the raft. The results of the analysis of piled rafts were present in Clancy and Randolph (1993), however, only vertical loading was considered in their work In PRAB, the lateral resistance of the piles as well as the raft base is incorporated into the hybrid model so as to be able to analyze the deformation of piled rafts subjected to lateral and moment loads as well as vertical loads.

1.3. OBJECTIVES AND CONSTITUTION OF THE RESEARCH

Principle objectives in this research are as follows:

1. provide comprehensive experimental data of behaviors of piled rafts and freestanding pile groups, and their components such as single piles and rafts alone subjected to static vertical and horizontal loading,

2. provide comprehensive experimental data of behaviors of piled rafts and freestanding pile groups subjected to dynamic (seismic) loading,

3. provide comprehensive experimental data for calibration of piled rafts subjected to static horizontal loading and dynamic loading,

4. develop a simple method for deformation analysis of piled rafts and freestanding pile groups subjected to vertical, horizontal and moment loads,

5. examine the validity of the developed analysis method through comparisons with existing analytical methods and simulation of the experiments, and

6. give a design concept of piled rafts subjected to static horizontal loads and dynamic loads.

In order to achieve the above objectives, this research consists of the following contents:

In Chapter 2, a series of static horizontal load tests of model piled rafts and free standing pile groups in model sand ground are conducted first to investigate the influence of the sharing of the vertical load by the raft and the piles on the raft base resistance and the resistance of the piles beneath the raft, varying the number of piles, the pile spacing and the raft size. It is shown that the horizontal resistance of a piled raft is greater than that of a freestanding pile group with the same number of piles as the piled raft, and that the resistance of the pile beneath the raft also is larger than that of a single pile, and that the increase in the number of piles in a piled raft does not necessarily lead to the increase in the horizontal resistance of the piled raft.

In Chapter 3, a series of static vertical and horizontal load tests of model single piles, model rafts alone and model piled rafts in model sand ground are conducted in a centrifugal field of 50g, in order to explore the test results obtained in Chapter 1 in more detail and to provide comprehensive experimental data used for the design of pile raft foundations in sand.

Regarding the details of the piled raft designs, there is a discussion as to whether the pile head connection should be rigid or hinged. Since the main objective of the piles in piled rafts is to reduce the settlement of structures, a hinged or even detached pile head connection with the raft base may satisfy the required performance to reduce the settlement. In the present study, the influences of the rigidity of the pile head connection on the horizontal behavior are investigated by designing rigidly fixed and hinged pile head connection models. Much emphasis was placed on the stiffness and the proportion of the load carried by each component of the two different pile head connections.

In Chapter 4, dynamic (seismic) loading tests of 4-pile piled raft models with the rigid and the hinged pile head connections and a 4-pile freestanding pile group model with the hinged pile head connection are conducted in the centrifuge. Chapter 4 provides the behaviors of such foundation models and compares them with the results from the static horizontal loading tests

It is well known that centrifuge tests have many advantages in geotechnical modeling

because the stress state in a prototype model can be realized in a corresponding model test and the similitude rules for the centrifuge testing has been established. However, the number of centrifuge tests is usually limited because of cost and time, and centrifuge apparatuses are available in limited numbers of institutions or organizations. Therefore, model tests at 1-g gravitational field still play important roles in pile foundation engineering area. Hence, in Chapter 5, shaking table tests of model piled rafts and model freestanding pile group models are conducted at 1-g gravitational field. In the dynamic loading tests conducted in Chapter 4, the frequency of the input motion is sufficiently lower than the natural frequencies of the foundation models. In contrast, frequencies of input motions ranges from very low to very high compared to the natural frequencies of the model foundations in the shaking table tests at 1-g gravitational field. The behaviors of the piled raft model and the freestanding pile group models near their natural frequencies are presented in Chapter 5.

The design of pile foundations is changing from the conventional allowable stress design to a performance based design. A precise estimation of deformation of a pile foundation and of stresses of their structural members is a vital issue in the framework of the performance based design. In the preliminary design stage, a number of alternative calculations are required, varying the number of piles, the pile length, the pile spacing, the locations of the piles, and so on. Hence, a feasible but reliable deformation analysis method of piled raft foundations is sought for. In Chapter 6, a simplified method of numerical analysis is developed to estimate the deformation and load distribution of piled raft foundations subjected to vertical, lateral, and moment loads, using a hybrid model in which the flexible raft is modeled as thin plates and the piles as elastic beams and the soil is treated as springs. Both the vertical and lateral resistances of the piles as well as the raft base are incorporated into the model. Pile-soil-pile, pile-soil-raft and raft-soil-raft interactions are taken into account based on Mindlin s solutions for both vertical and lateral forces. The propose analysis method was incorporated into a computer program PRAB (Piled Raft Analysis with Batter Piles) (Kitiyodom & Matsumoto, 2002).

In Chapter 7, the computer program PRAB was extended for the analysis of axially and laterally loaded piled raft foundations embedded in nonhomogeneous soils that are encountered often in practice (Kitiyodom & Matsumoto, 2003).

In Chapter 8, the program PRAB was employed to analyse the static horizontal load tests of the piled raft models conducted in Chapter 4.

In Chapter 9, the conclusions from this research is summarized

REFERENCES

1) Architectural Institute of Japan 2001. Recommendations for Design of Building Foundation.
2) Burland, J. B., Broms, B. B. and De Mello, V. F. B. (1977): Behaviour of foundations and structures , *Proc. 9th ICSMFE*, Tokyo, **2**: 496-546.
3) Chow, Y. K. (1986): Analysis of vertically loaded pile groups , *Journal of Geotechnical Engineering* ASCE, **113**(6): 637-651.
4) Clancy, P. and Randolph, M. F. (1993): An approximate analysis procedure of piled raft foundations , *International Journal for Numerical and Analytical Methods in Geomechanics*, **17**: 849-869.
5) Hain, S. J. and Lee, I. K. (1978): The analysis of flexible raft-pile systems , *Géotechnique*, **28**(1): 65-83.
6) Horikoshi, K. and Randolph, M. F. (1996): Centrifuge modeling of piled raft foundations on clay , *Géotechnique*, **46**(4): 741-752.
7) Horikoshi, K. and Randolph, M. F. (1998): A contribution of optimum design of piled rafts , *Géotechnique*, **48**(3): 301-317.
8) Horikoshi, K. and Randolph, M. F. (1999): Estimation of overall settlement of piled rafts , *Soils and Foundations*, **39**(2): 59-68.
9) Kakurai, M., Yamashita, K. & Tomono, M. (1987): Settlement behavior of piled raft foundation on soft ground , *Proc. 8th ARCSMFE*, 373-376.
10) Katzenbach, R. and Moormann, C. (2001): Recommendations for the design and construction of piled rafts , *Proc. 15th ICSMGE*, Istanbul, Vol. 2: 927-930.
11) Katzenbach, R. Arslan, U. and Reul, O. (1998): Soil-structure-interaction of a piled raft foundation of a 121 m high office building on loose sand in Berlin , *Proc. Deep Foundation on Bored and Auger Piles*, 215-221.
12) Kitiyodom, P. and Matsumoto, T. (2002): A simplified analysis method for piled raft and pile group foundations with batter piles *International Journal for Numerical and Analytical Methods in Geomechanics*, **26**:1349-1369.
13) Kitiyodom, P. and Matsumoto, T. (2003): A simplified analysis method for piled raft foundations in non-homogeneous soils . *International Journal for Numerical and Analytical Methods in Geomechanics*, **27**: 85-109.
14) Kuwabara, F. (1989): An elastic analysis for piled raft foundations in a homogeneous soil , *Soils and Foundations*, **29**(1): 82-92.
15) O Neill, M. W., Ghazzaly, O. I. and Ha, H. B. (1977): Analysis of three-dimensional pile groups with nonlinear soil response and pile-soil-pile interaction , *Proc. 9th Offshore Technology Conference*, Vol. 2: 245-256.
16) Poulos, H. G. (1994): An approximate numerical analysis of pile-raft interaction ,

International Journal for Numerical and Analytical Methods in Geomechanics, **18**: 73-92.

17) Poulos, H. G. and Davis, E. H. (1980): Pile Foundation Analysis and Design, Wiley, New York.

18) Placzek, D., Jentzsch, E. and Schulte, K. (2001): A contribution to the analysis and the design concept of piled raft foundations , *Proc. 15th ICSMGE*, Istanbul, Vol. 2: 985-989.

19) Randolph, M. F. (1994). Design methods for pile groups and piled rafts , *Proc. 13th ICSMGE*, New Delhi, Vol. 5: 61-82.

20) Shinozaki, Y. Nishio, H., Kobayashi, Nagao, T., Kuwabara, F. (1999): Study on the settlement behavior of piled raft foundations (Part 3) , Summaries of Technical papers of Annual Meeting Architectural Institute of Japan: 731-732 (in Japanese).

21) Smith, I. M. and Wang, A. (1998): Analysis of piled rafts , *International Journal for Numerical and Analytical Methods in Geomechanics*, **22**: 777-790.

22) Sommer, H., Tamaro, G. and DeBenedittis, C. (1991): Messe Turm, foundations for the tallest building in Europe , *Proc. 4th Int. Conf. on Piling and Deep Foundations*, 139-145.

23) Ta, L. D. and Small, J. C. (1996): Analysis of piled raft systems in layered soils , *International Journal for Numerical and Analytical Methods in Geomechanics*, **20**: 57-72.

24) Thaher, M. and Jessberger, H. L. (1991): The behavior of Piled-raft Foundations, Investigated in Centrifuge Model Tests , *Proc. Centrifuge 91*, Colorado, Balkema, 225-234.

25) Watanabe, T., Kobayashi, H., Nagao, T., Nagataki, Y., Majima, M. and Kuwabara, F. (2000): Horizontal loading tests of piled raft foundation , Vol. 33, Report of Taisei Research Institute, 125-128 (in Japanese).

26) Yamashita, K., Kakurai, M. and Yamada, T. (1994): Investigation of a piled raft foundation on stiff clay , *Proc. 13th ICSMGE*, New Delhi, Vol. 2: 543-546.

CHAPTER 2

HORIZONTAL LOAD TESTS ON MODEL PILED RAFT AND PILE GROUP FOUNDATIONS AT 1-G GRAVITATIONAL FIELD

(*N.B.* This chapter was published in Proc. Int. Conf. on Physical Modelling in Geotechnics, St. John's, Canada, pp.709-714, entitled "Lateral load tests on model pile groups and piled raft foundations in sand" by Pastsakorn, Hashizume & Matsumoto)

ABSTRACT

This paper presents the results obtained from lateral load tests on model pile groups and model piled raft foundations in Toyoura sand in a 1g field. In the test series, raft size, number of piles, pile spacing and pile rake angle were varied. It was found that for model foundations with the same configuration, the piled raft foundation exhibited about 2 times higher lateral resistance than that of the pile group foundation. In pile groups, lateral resistance of the foundation increased almost linearly with the increasing number of piles. In piled rafts, the lateral resistance did not necessarily decrease with a decreasing number of piles, since the lateral resistance of the raft base compensated for the reduction of the number of piles. Use of the batter piles greatly improved the performance of both piled raft and pile group foundations under lateral loading.

2.1 INTRODUCTION

In foundation design, piled raft foundations have been widely recognized as an economical foundation type, since the bearing capacity of the raft base is included in the design, and piles are used in order to reduce the settlement of the foundation to an acceptable level. Much research on the settlement of piled raft foundations has been done (for instance, Cooke et al. 1981, Horikoshi & Randolph 1996, 1998, 1999, Katzenbanch 1998, Kakurai et al. 1987, Randolph 1994, Yamashita et al. 1994). However, research on the behavior of piled raft foundations subjected to lateral loads seems to be very limited.

In highly seismic areas such as Japan, estimation of the behavior of the piled raft during earthquakes becomes an important factor in the foundation design process. In a traditional method of seismic design in Japan, dynamic loads acting on the foundation are modeled by an equivalent static lateral load. And, as the behavior of piled rafts under lateral loading has not been completely understood, piled raft foundations are generally treated as raft foundations or pile foundations. In recent years, there has been some research aiming to

clarify the behavior of piled rafts subjected to lateral loading. The results of a series of centrifuge model tests of piled raft foundations subjected to lateral loads are described in Watanabe et al. (2001).

In this study, a series of lateral load tests on model piled rafts and model pile groups have been conducted in a 1g field. This paper presents and discusses a part of the test results.

2.2 TEST APPARATUS

Figure 2.1 shows a schematic illustration of the test equipment. The details of each component are described below.

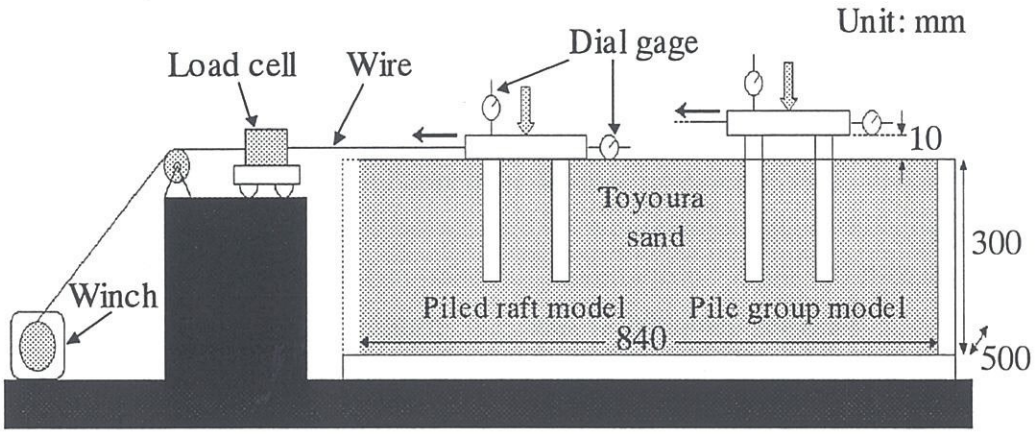

Figure 2.1. Schematic illustration of test equipment.

2.2.1. Model ground

Dry Toyoura sand was used for the model ground throughout the present study. The physical properties of Toyoura sand are summarized in **Table 2.1**. Toyoura sand was prepared in an acrylic box having dimensions of 500 mm in width, 840 mm in length, and 300 mm in depth. The soil was compacted to nearly its maximum relative density by vibration and tapping, in order to maintain the uniformity and consistency in the soil strength throughout the test series.

The uniformity of the soil strength was examined through the tests by using a miniature cone penetrometer with a diameter of 16.2 mm and an apex angle of 60 degrees. The cone penetration tests (CPTs) were conducted at a total of 4 locations as shown in **Figure 2.2**. The rate of penetration was set at 0.1 mm/s. The measured strengths are summarized in **Figure 2.3**. The figure shows that the strength increases with depth, and that the uniformity of the strength between the tests at different locations was excellent especially until a depth of 200 mm which is equal to the pile length. The increase in the soil strength at deep levels at locations C and D was thought to be due to effects of the sidewall of the acrylic box.

Table 2.1. Physical properties of Toyoura sand.

Property	Value
ρ_t (t/m^3)	1.616-1.660
D_{50} (mm)	0.162
ρ_s (t/m^3)	2.661
ρ_{dmax} (t/m^3)	1.654
ρ_{dmin} (t/m^3)	1.349

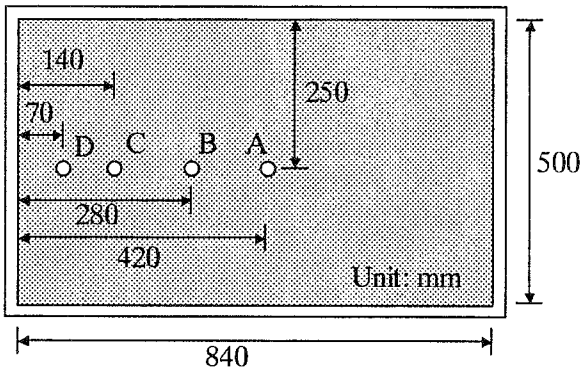

Figure 2.2. Positions of CPTs (Top view).

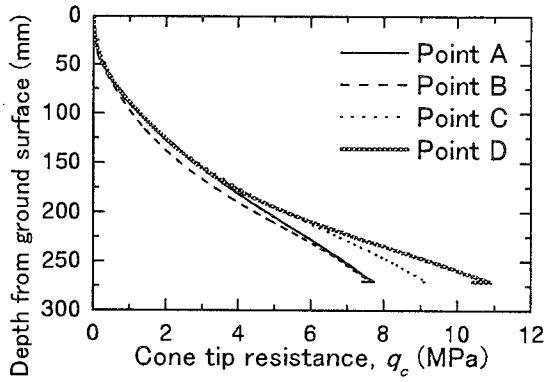

Figure 2.3. Distributions of cone tip resistance.

2.2.2. Model foundations

Aluminum pipes were used for the model piles, the properties of which are listed in **Table 2.2**. The model piles had an outer diameter of 20 mm, an inner diameter of 18 mm, and a length of 200 mm below the soil surface. The pile toes were capped with a thin aluminum plate. Young s modulus, E_p, and Poisson s ratio, ν_p, have been estimated from bending tests of the model piles. Each pile was instrumented with foil strain gages along the pile shaft as shown in **Figure 2.4** in order to measure the distribution of the axial forces, the shear forces, and the bending moments of the pile.

Table 2.2. Properties of the model pile.

Propertry	Value
Material	Aluminium
Diameter, D	Outer 20 mm, Inner 18 mm
Length, L	200 mm (from ground surface)
Young s modulus, E_p	70632 MN/m^2
Poisson s ratio, ν_p	0.345

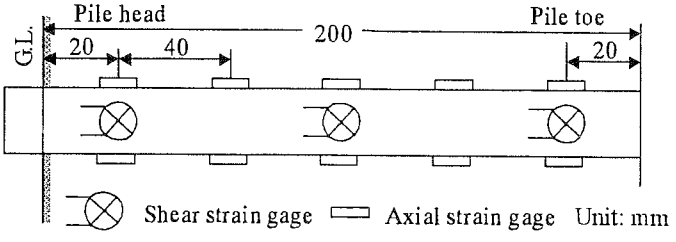

Figure 2.4. Model pile instrumented with strain gages.

Rectangular model rafts were made of duralumin plates with a thickness, t_r, of 22 mm, Young s modulus, E_r, of 68670 MN/m^2 and Poisson s ratio, ν_r, of 0.335. Various models of piled rafts and pile groups were prepared with combinations of different sizes of rafts and the model piles.

2.2.3 Test procedure

First the model foundation was set near the center point of the model ground in order to minimize the effects of the sidewalls. Then dry Toyoura sand was slowly poured into the acrylic box and the sand was compacted by vibration and tapping to make a layer of about 30 mm in thickness. This procedure was iterated until the model ground of 300 mm in depth was obtained. For pile group models, a gap of 10 mm was maintained in order to keep the raft base away from the soil surface. After the soil preparation was finished, all the instrumentation such as dial gages, a load cell and a pulling wire were arranged.

In the first step of loading stage, weights were placed on the raft surface. Then the lateral loading was initiated by pulling the raft by means of a winch and a wire at a slow displacement rate less than 1 mm/min. The raft displacement and the loads transferred to the whole foundation, the raft and the piles were monitored throughout the test.

2.3 TEST SERIES

In the present study, a series of lateral load tests on model pile foundations were performed as summarized in **Figure 2.5** and **Table 2.3**. The model foundations were separated into two types, pile groups (denoted as PG) and piled rafts (PR), so that the comparison of the performance of the two types could be made. For each foundation type, the number of piles was varied from 1 (denoted as 1p) to 9 (9p) in order to investigate the effect of group efficiency and the effect of pile spacing.

Additionally, the foundations were also divided into two categories. The first category (denoted as u) is various combinations of unit capped-piles, where the unit capped-pile is made from a 75 × 75 mm unit-raft and one pile. Hence, pile spacing of the foundations in the first category was 75 mm. The second category is foundations with rafts of the size 225 × 225 mm. The number of piles in the second category was varied as 9, 6 and 4. In the second category, some unit-rafts were not directly supported by a pile, allowing pile spacing to be varied.

In the case of foundations containing 6 piles, two different loading directions were employed so that number of front piles in the direction perpendicular to the loading direction became 2 (denoted as 2f) or 3 (3f).

Furthermore, in order to investigate the effects of pile rake angle, the piles were raked in the loading direction at angles of 0, 10, 20 and 30 degrees (denoted as 10d, 20d, 30d), while the number of piles was four and the raft size was 225 × 225 mm.

Weights were placed on the raft of each foundation prior to lateral loading to obtain a corresponding vertical pressure of 52.3 kN/m^2. The coefficient of friction between the raft base and Toyoura sand was obtained as 0.301 from a direct shear test.

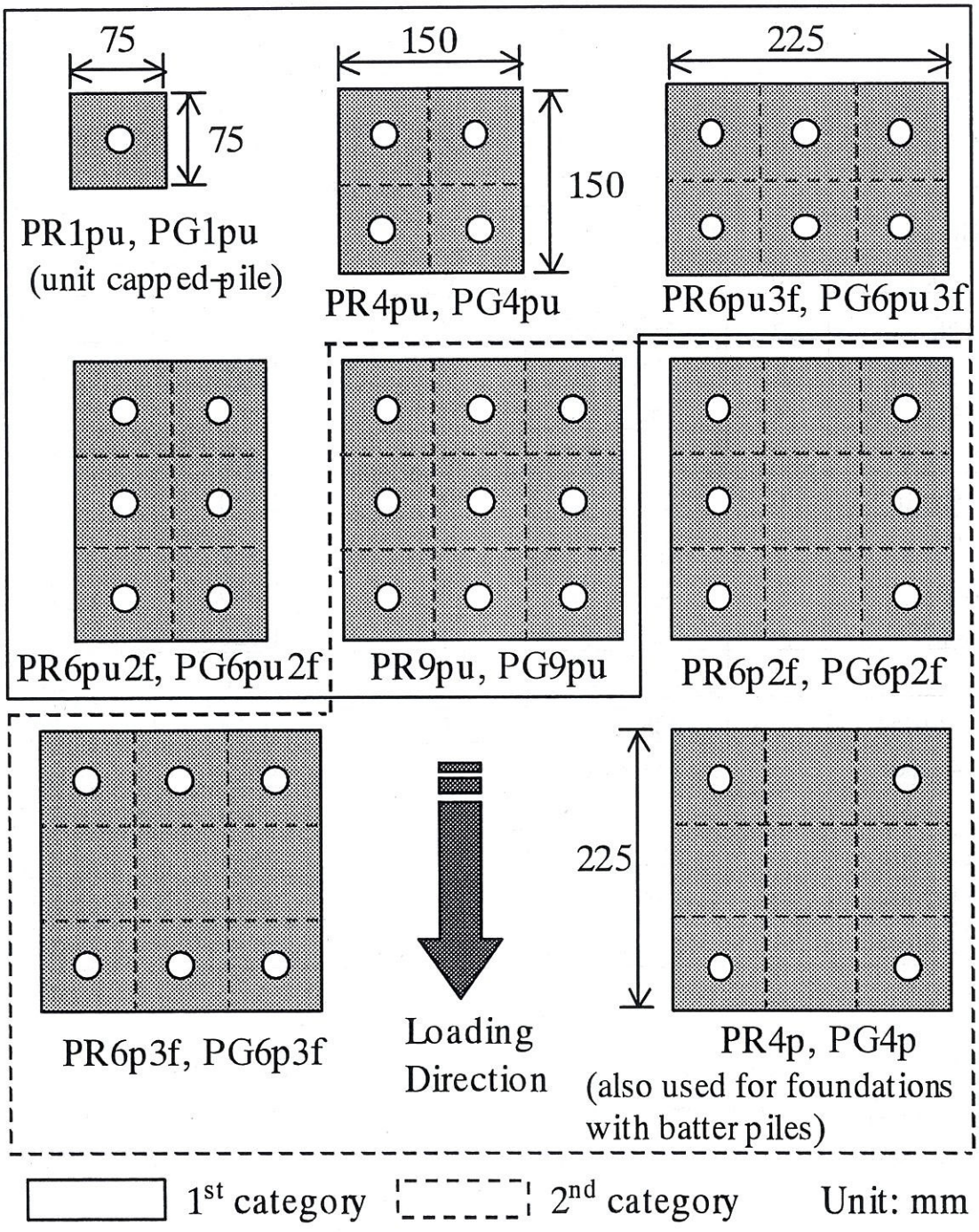

Figure 2.5. Raft and pile arrangements (Top view).

Table 2.3. Experimental cases and their conditions.

Case	No. of piles	Raft size (mm × mm)	Pile rake angle (deg.)	Soil density (t/m^3)	Vertical load (kN)
PG1pu	1	75 × 75	0	1.616	0.29
PG4pu	4	150 × 150	0	1.660	1.18
PG6pu2f	6	150 × 225	0	1.630	1.77
PG6pu3f	6	225 × 150	0	1.630	1.77
PG9pu	(Not available)				
PG6p2f	6	225 × 225	0	1.632	2.65
PG6p3f	6	225 × 225	0	1.621	2.65
PG4p	4	225 × 225	0	1.660	2.65
PR1pu	1	75 × 75	0	1.628	0.29
PR4pu	4	150 × 150	0	1.660	1.18
PR6pu2f	6	150 × 225	0	1.660	1.77
PR6pu3f	6	225 × 150	0	1.660	1.77
PR9pu	9	225 × 225	0	1.660	2.65
PR6p2f	6	225 × 225	0	1.660	2.65
PR6p3f	6	225 × 225	0	1.620	2.65
PR4p	4	225 × 225	0	1.660	2.65
PG4p10d4		225 × 225	10	1.618	2.65
PG4p20d4		225 × 225	20	1.621	2.65
PG4p30d4		25 × 225	30	1.619	2.65
PR4p10d4		225 × 225	10	1.635	2.65
PR4p20d4		225 × 225	20	1.619	2.65
PR4p30d4		225 × 225	30	1.622	2.65

2.4 TEST RESULTS OF FOUNDATIONS WITH VERTICAL PILES

The lateral load at the normalized displacement (lateral displacement, u, divided by the outer pile diameter, D) equal to 1, 5 and 10 % are summarized in **Table 2.4** for all cases of pile foundations with vertical piles. In the case of piled raft foundations, the proportion of vertical load carried by the raft before lateral loading is also shown in **Table 2.4.**

2.4.1 Pile groups

It can be seen from **Table 2.4** that the lateral resistance of the pile groups tended to increase almost linearly with the number of piles. However, the effects of pile spacing on the lateral

resistance can be seen from detailed comparison of the test results. For instance, let us compare PG4pu and PG4p. The number of piles in these cases was the same, four, but the pile spacing was different in these two cases, 75 mm in PG4pu and 150 mm in PG4p. It was found that the lateral resistance was slightly higher in PG4p that had higher pile spacing. The same tendency was found in the cases of pile groups with 6 piles. The lateral resistance of PG6p3f was higher than that of PG6pu3f, where the pile spacing in the former case in the loading direction was greater than that of the latter case. This trend can also be seen in the comparison of PG6p2f and PG6pu2f where the pile spacing in the direction perpendicular to the loading direction was greater in PG6p2f.

The effect of the number of piles in a row is also seen from the comparison of PG6p3f and PG6p2f, even though the total number of piles is the same, six, in both cases. The lateral resistance of PG6p3f, which had 3 front piles and 3 back piles, was slightly greater than PG6p2f that had 2 piles in each of the front, middle and back rows. This tendency is also found in the comparison between PG6pu3f and PG6pu2f.

Table 2.4. Summary of the lateral load test results.

Case	Lateral load at normalized disp. (kN)			Load Ratio (%)
	at u/D = 1 %	at u/D = 5 %	at u/D = 10 %	
PG1pu	0.027	0.060	0.080	
PG4pu	0.170	0.350	0.450	
PG6pu2f	0.220	0.530	0.690	
PG6pu3f	0.260	0.560	0.720	
PG9pu	(Not available)			
PG6p2f	0.275	0.570	0.760	
PG6p3f	0.300	0.590	0.790	
PG4p	0.175	0.440	0.580	
PR1pu	0.065	0.150	0.200	8.7
PR4pu	0.310	0.550	0.710	32.3
PR6pu2f	0.423	0.740	1.050	28.4
PR6pu3f	0.410	0.870	1.210	28.8
PR9pu	0.470	0.950	1.310	29.3
PR6p2f	0.435	0.930	1.280	30.0
PR6p3f	0.710	1.230	1.500	33.3
PR4p	0.540	1.060	1.420	42.4

2.4.2 Piled rafts

Lateral resistance of the piled rafts was about two times higher than that of the corresponding pile groups. In the test series of the 1st category, the proportions of the vertical load carried by the raft prior to lateral loading were almost the same, 30 %, excluding PR1pu. The lateral resistance of the piled rafts in the 1st category increased with the increasing number of piles, which was similar to the results obtain for the pile groups.

On the other hand, in the case of the piled rafts in the 2nd category, where the raft size was the same, 225 × 225 mm, and the vertical load was the same, 2.65 kN, the lateral resistance did not necessarily increase with the increasing number of piles as shown in **Table 2.4** and **Figure 2.6**. The largest resistance was obtained in PR6p3f and the second largest resistance was obtained in PR4p, exceeding PR9pu in which the number of piles was the highest. Another interesting point is that the effect of the loading direction was pronounced in the cases of piled rafts as can be seen from the comparison between PR6p2f and PR6p3f. These aspects are discussed below.

Figures 2.7(a)-2.7(d) show the relationship between the lateral resistance and the normalized displacement of the piled rafts. Included in the figures are the lateral resistance carried by the raft base, all piles, and each pile row (front, middle and back piles in PR6p2f and PR9pu, and front and back piles in PR4p and PR6p3f). Note that the total lateral resistance was measured by the load cell, and the lateral pile resistance was obtained from the shear forces measured near the pile heads. The raft base resistance was calculated by subtracting the sum of the pile resistances from the total lateral resistance, which is indicated by the shaded area in the figures.

Let us first compare the result of PR4p with that of PR9pu. The lateral resistance of PR4p was slightly greater than the resistance of PR9pu even though the number of piles was smaller in PR4p. It is clearly seen that the raft base resistance in PR4p was much greater than that of PR9pu. The potential of the lateral resistance of the raft base is the product of the vertical reaction of the raft base and the interface friction coefficient between the raft base and the soil. It should be noted that the proportion of the vertical load carried by the raft prior to lateral loading was 42.4 % in PR4p, which was 1.44 times higher than the 29.3 % in PR9pu. Hence, the higher raft base resistance in PR4p is caused by the higher vertical reaction compared with PR9pu.

If the maximum raft base resistance in PR4p is estimated from the vertical raft base reaction of 1.12 kN prior to lateral loading and the interface friction coefficient of 0.301, an estimate of 0.34 kN is obtained. This is comparable to the measured value at u/D=10%. Similarly, the potential of the lateral raft base resistance in PR9pu was estimated as 0.23 kN.

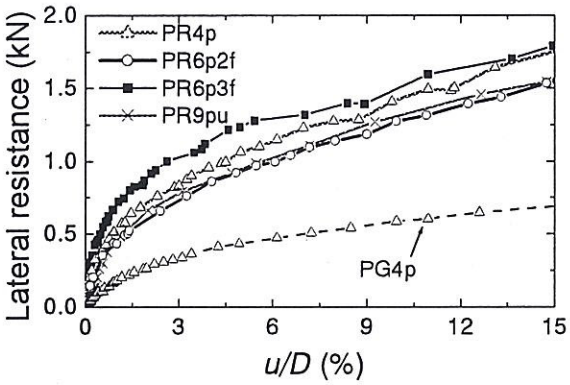

Figure 2.6. Load-displacement relationship.

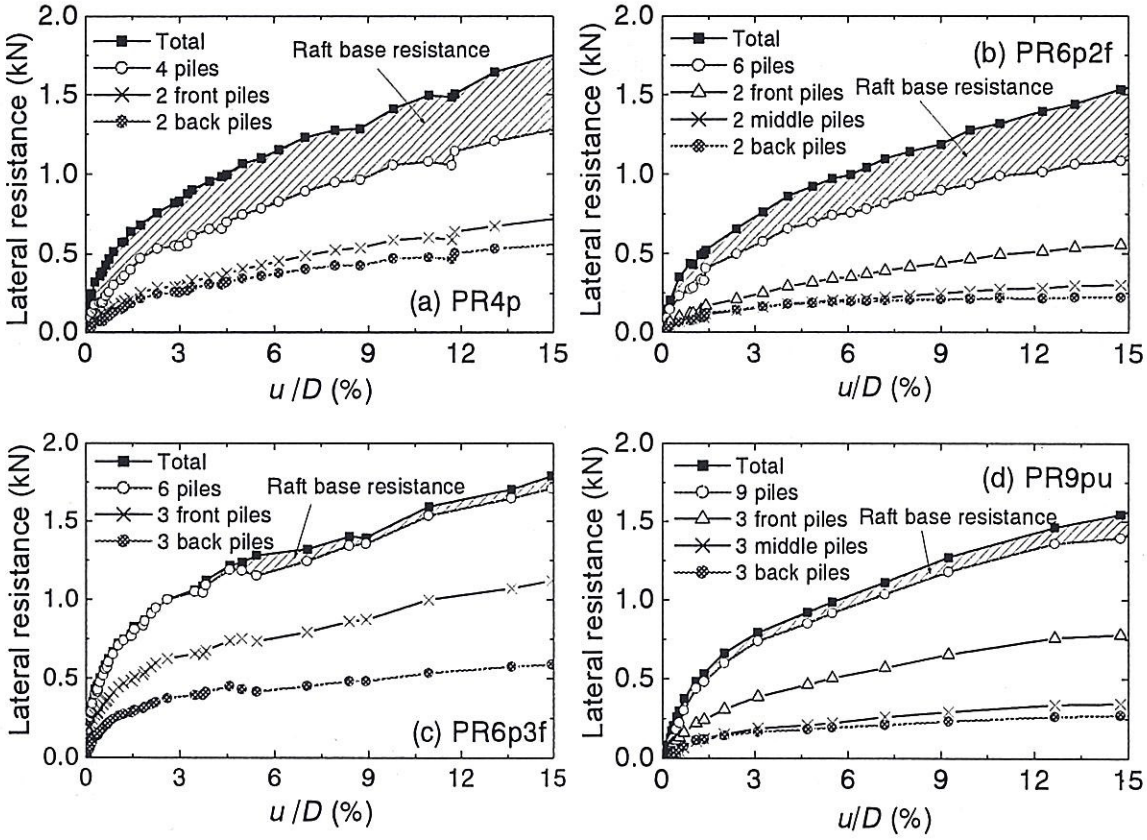

Figure 2.7. Load-displacement relationships of components.

However, the measured value for PR9pu was much less than this estimated value. This reduction in the raft base resistance in PR9pu is thought to be due to effect of the piles that were located closely together with a pile spacing of 75 mm. This pile spacing is a half of that in PR4p. The soil beneath the raft surrounded by the narrowly spaced piles in PR9pu was thought to move together with the raft, resulting in a mobilized raft base resistance smaller than the expected value.

The above effect in the lateral resistance of the piled raft can also be found from the comparison of PR6p2f and PR6p3f. Remember that PR6p3f had 3 front piles with a pile spacing of 75 mm and PR6p2f had 2 front piles with a pile spacing of 150 mm, although

the number of piles is the same, 6, in both cases. The lateral resistance of the piles was higher in PR6p3f than in PR6p2f, indicating that an arching effect in the soil occurred in the former case. The soil beneath the raft is again thought to move together with the raft due to this arching effect in PR6p3f, resulting in lower raft base resistance compared to PR6p2f.

From the test results, the case of PR4p seems to be the most efficient piled raft foundation tested. The results of this case will be discussed below.

Figure 2.8 shows the proportion of the lateral load carried by the piles and the raft. At the initial stage of lateral loading, the proportion of the lateral load carried by the raft was much higher than that of the piles. However, until u/D = 2 %, the proportion of the load carried by the piles significantly increased while that of the raft decreased accordingly, and the proportion of the lateral load carried by the raft became lower than that of the piles. For the normalized displacements exceeding 2 %, the load sharing ratio became almost constant.

The lateral load-displacement relationship for each pile in PR4p is shown in **Figure 2.9**. The results obtained from the case of a single pile (PG1pu) and a pile group with 4 piles (PG4p) are also indicated. The figure shows that the lateral pile resistance in the pile group (PG4p) was higher than that of the single pile alone. This is due to the difference between the deformation mechanisms of the foundations. In the case of the single pile, the pile deformed with a free pile head condition, whereas in the cases of the pile group and the piled raft, the pile acted with a fixed pile head condition. The lateral pile resistance and deformation stiffness became significantly higher in the case of the piled raft compared with the pile group. This increase in the stiffness and strength of the foundation is thought to be due to the increase in the stiffness and the strength of the soil surrounding the piles beneath the raft, which was caused by the load transfer through the raft base to the soil.

It can also be seen from **Figure 2.9** that the front piles carried more load than the back piles in the cases of both the pile group and the piled raft. The difference between lateral loads on the front and back piles was much smaller in the piled raft. This behavior is important when considering failure of the piles in pile foundation design.

Inclination of the raft during the loading tests of a pile group of 4 piles and a 4 pile piled raft is shown in **Figure 2.10**. In the case of the pile group, the inclination of the raft increased almost linearly with the increasing lateral displacement from the beginning of the lateral loading. On the other hand, no inclination was observed in the case of the piled raft even at the normalized displacement equal to 15 %. This fact has important implications for the limit state design of pile foundations.

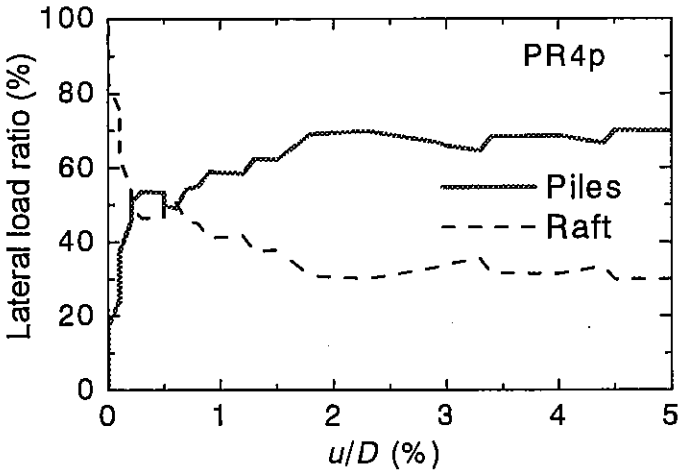

Figure 2.8. Proportions of lateral load carried by raft and piles.

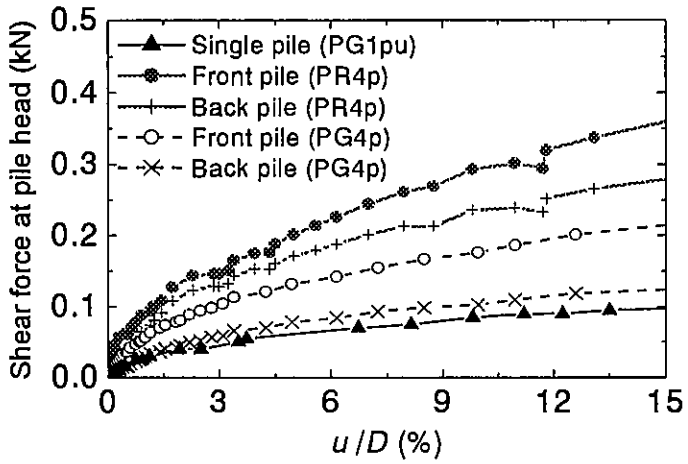

Figure 2.9. Behavior of a pile in the foundation.

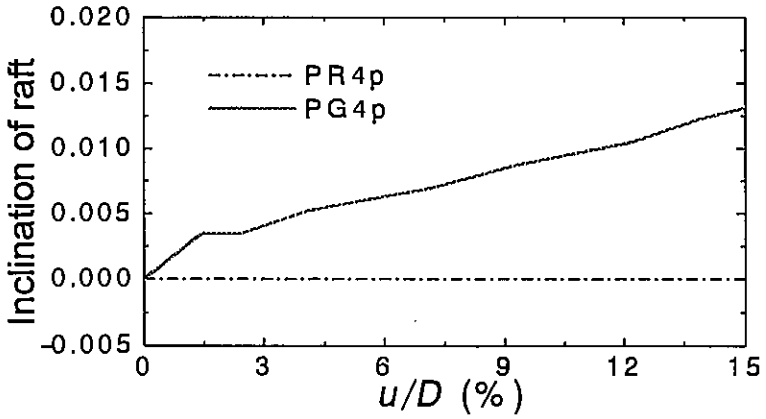

Figure 2.10. Inclination of the raft.

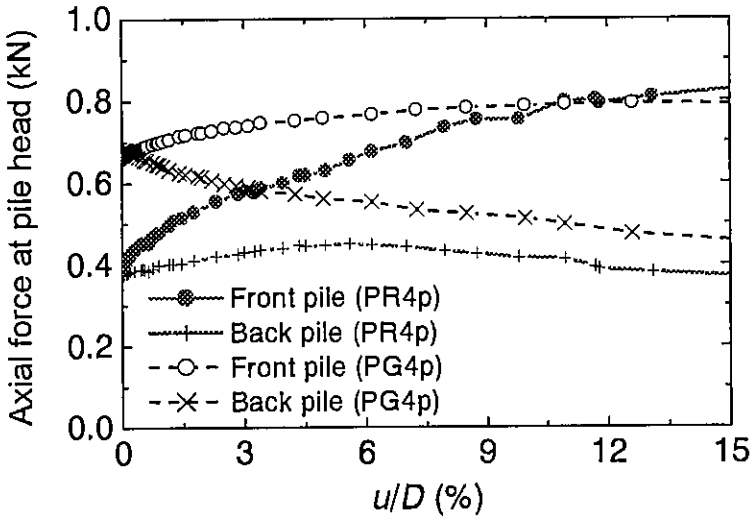

Figure 2.11. Axial force at pile head.

Figure 2.11 shows the relationships between the axial force at the pile head and the lateral displacement for PR4p and PG4p. Before the starting of lateral loading, both the back piles and the front piles carried almost the same vertical load in each case. In the case of the pile group, the axial force of the front piles increased while the axial force of the back piles decreased at almost the same rate. However, in the case of the piled raft, the axial force of the back piles did not decrease immediately at the early stages of lateral loading, but slightly increased. This behavior matches very well with results from the direct shear test of dense sands. It is thought that at the beginning of lateral loading, the soil beneath the raft tended to reduce its volume due to 'negative dilatancy' even for the dense sand. This led to the decrease in the vertical load carried by the raft as well as the increase in the vertical load carried by the piles, including even the back piles. As the normalized lateral displacement exceeded 5 %, the axial force of the back piles started to decrease with the increasing lateral displacement.

The behavior of a 4 pile piled raft foundation subjected to lateral loading has also been reported in Watanabe et al. (2001), in which a series of centrifuge model tests of piled raft foundations were conducted. Although there are some differences in the test procedures and the scale of the models, their work tends to support the conclusions of this study concerning foundations with vertical piles.

2.4.3. Foundations with batter piles

Figure 2.12 shows the relationships between the lateral load and the lateral displacement in 4 pile groups with 4 batter piles and 4 pile piled rafts with 4 batter piles. It can be clearly seen that use of the batter piles increased the lateral resistance of the foundations. This tendency is the same for both piled rafts and pile groups. Increase in the rake angle of the batter piles greatly improved the performance of the foundation.

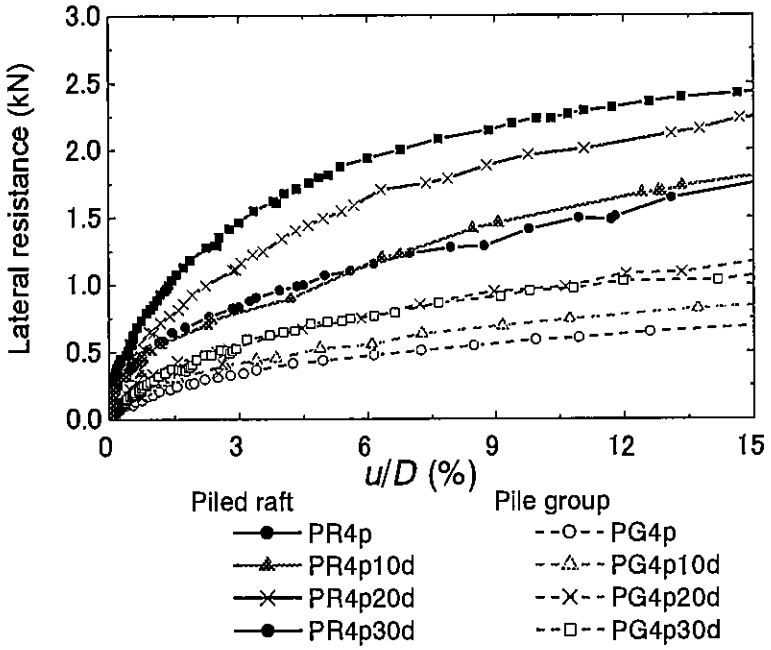

Figure 2.12. Load-displacement relationships of foundations with batter piles.

2.5 CONCLUSIONS

A series of model lateral load tests were conducted with the aim to investigate the behavior of piled raft foundations subjected to lateral loading. In this study, model loading tests on pile groups, and foundations with batter piles were also carried out. The main findings from the experiments in the 1g field are summarized qualitatively as follows:

1 Piled rafts had about 2 times higher lateral resistance than the pile groups, for model foundations with the same configuration.
2 The use of the batter piles greatly improved the performance of both model piled raft and pile group foundations under lateral loading.
3 In model pile groups, lateral resistance of the foundation increased almost linearly with the increasing number of piles.
4 In model piled rafts, the lateral resistance did not necessarily decrease with a decreasing number of piles, since the lateral resistance of the raft base compensated for the reduction of the number of piles.
5 In the initial stages of lateral loading of model piled rafts, most of the lateral load was carried by the raft base, however, as the lateral displacement increased, the proportion of the load carried by the raft base decreased.

REFERENCES

Cooke, R. W., Bryden-Smith, D. W., Gooch, M. N., Sillet, D. F. 1981. Some observations of the foundation loading and settlement of a multi-storey building on a piled raft foundation in London clay, *ICE*, 170(1).

Horikoshi, K. & Randolph, M. F. 1996. Centrifuge modeling of piled raft foundations on clay, *Géotechnique* 46(4): 741-752.

Horikoshi, K. & Randolph, M. F. 1998. A contribution of optimum design of piled rafts, *Géotechnique* 48(3): 301-317.

Horikoshi, K. & Randolph, M. F. 1999. Estimation of overall settlement of piled rafts, *Soils & Foundations*, 39(2): 59-68.

Katzenbanch, R., Arslan, U., Reul, O. 1998. Soil-structure-interaction of a piled raft foundation of a 121 m high office building on loose sand in Berlin, *Proc. Deep Foundation on Bored and Auger Piles*: 215-221.

Kakurai, M., Yamashita, K., Tomono, M. 1987. Settlement behavior of piled raft foundation on soft ground, *Proc. 8th ARCSMFE; Kyoto*:373-376.

Randolph, M. F. 1994. Design methods for pile groups and piled rafts, *Proc. 13th ICSMFE; New Delhi*, 5: 61-82.

Watanabe, T., Fukuyama, H., Horikoshi, K., Matsumoto, T. 2001. Centrifuge modeling of piled raft foundations subjected to horizontal loads, *Proc. 5th Int. Conf. on Deep Foundation Practice incorporating PILETALK International 2001; Singapore*: 371-378.

Yamashita, K. Kakurai, M. and Yamada, T. 1994. Investigation of a piled raft foundation on stiff clay, *Proc. 13th ICSMFE; New Delhi*, 2: 543-546.

CHAPTER 3

BEHAVIOR OF PILED RAFTS SUBJECTED TO STATIC VERTICAL AND HORIZONTAL LOADS IN CENTRIFUGE TESTS

(*N.B.* This chapter was submitted to Int. Jour. of Physical Modelling in Geomechanics entitled "Performance of pile raft foundations subjected to static horizontal loads," 2003)

ABSTRACT

A series of static loading tests was conducted vertically and horizontally on piled raft models on sand with the use of geotechnical centrifuge, as well as the loading tests of their components (single piles and rafts alone). Much focus was placed on the load-displacement relationship and the load sharing between the piles and the raft in the piled raft system. Effects of the rigidity at pile head connection on the piled raft behavior were also examined. This paper provides basic information on the performance of piled rafts subjected to horizontal loads through the responses of the components. Principal findings from the present study are:

1) The stiffness and the resistance of the single pile in piled raft foundations are highly different from those observed in the loading test of isolated single piles, due to the difference in the confining stress condition around the piles; 2) The piles play a important role in the horizontal ultimate resistance of piled raft foundations; 3) The initial horizontal stiffness of the piled raft is not always higher than that of the raft alone; 4) Higher horizontal load is transferred to the piles in the piled raft with rigid pile head connection, which leads to higher initial horizontal stiffness compared with that in the piled raft with hinged connection; 5) The proportion of the horizontal load carried by piles in the piled raft is more dependent on the horizontal displacement than the proportion of the vertical load carried by the piles during the horizontal loading.

Key words: centrifuge modeling, sand, raft, single pile, piled raft, loading test, load sharing, design

3.1. INTRODUCTION

Piled raft foundations have been widely recognized as one of the most economical foundation systems since Burland et al. (1977) presented the concept of settlement reducers . Some design concepts and their applications have been reported (Kakurai et al., 1987; Randolph, 1994; Horikoshi and Randolph, 1998; Katzenbach et al., 1998; Shinozaki et al., 1999; Kobayashi et al., 2000). Furthermore, design codes and guidelines for piled raft foundations have also been published (Architectural Institute of Japan, 2001; Katzenbach and Moormann, 2001; Placzek et al., 2001).

In piled raft foundations, piles are extensively used to reduce the settlement of foundations to an acceptable level, rather than to support the weight of super structures. Although a number of works on the settlement of piled raft foundations have been reported, the work that deals with the behavior of piled raft foundations subjected to horizontal loads seems to be very limited. Watanabe et al. (2000) reported the results of horizontal loading tests on a square raft model on an actual ground, where 4 slender piles were installed beneath the square raft with a width of 2 m. Pastsakorn et al. (2002) also carried out a series of horizontal loading tests on small piled raft models at 1 g. However, the detailed behavior of the piled raft foundations subjected to horizontal loads still has not been well clarified, and the establishment of a seismic design concept for piled raft foundations is necessary especially in highly seismic areas such as Japan. Although piled raft foundations have already been applied to actual structures in Japan, most seismic designs seem to treat piled rafts as rafts alone by ignoring the existence of piles. Considering the current trends toward the performance-based design in the field of geotechnical engineering, the behavior of the piled raft foundation subjected to horizontal loads needs to be more rationally explained.

In this paper, the centrifuge modeling technique was used to examine the behavior of piled raft foundations. Centrifuge modeling has great advantages to observe the interactions between the piles and the raft through the soil. A number of works such as Sommer et al. (1991), Thaher and Jessberger (1991), Horikoshi and Randolph (1996) used centrifuge modeling to examine the settlement behavior of piled rafts. Watanabe et al. (2001), Horikoshi et al. (2001, 2002) and Mano et al. (2002) employed the technique to investigate the piled raft behavior under horizontal loading.

Among a series of static and dynamic centrifuge model tests on piled raft foundations on sand performed in this project, this paper mainly provides the results from static horizontal loading tests on piled raft models in both vertical and horizontal directions, as well as the loading tests of the piled raft components, i.e. single piles and rafts alone.

Regarding the details of the piled raft designs, there is a discussion as to whether the pile head connection should be rigid or hinged. Since the main objective of the piles in piled rafts is to reduce the settlement of structures, a hinged or even detached pile head connection with the raft may satisfy the required performance to reduce the settlement. In

the present study, the influences of the rigidity of the pile head connection on the horizontal behavior are investigated by designing rigidly fixed and hinged pile head connection models. Much emphasis was placed on the stiffness and the proportion of the load carried by each component for the different pile head connection models.

Note that model scale is used in the following results and discussions in this paper.

3.2. MODEL DESIGNS

3.2.1. Centrifuge package

The geotechnical centrifuge used in the present study was described in detail by Nagura et al. (1994). The effective radius of the centrifuge is 2.65 m. A centrifugal acceleration of 50 g was applied to a 1/50 model (here g denotes gravity level).

In the present study, all the models, i.e. single piles, rafts alone and piled rafts, were loaded vertically or horizontally in separate tests. **Figure 3.1** shows a schematic illustration of the centrifuge package used for this study. A rigid box with a length of 700 mm, a width of 400 mm and a height of 700 mm was used. Teflon sheets were attached to the sidewalls of the box to reduce the friction between the soil and the sidewalls. Generally two models were placed on the model ground, and loaded one by one for experimental efficiency.

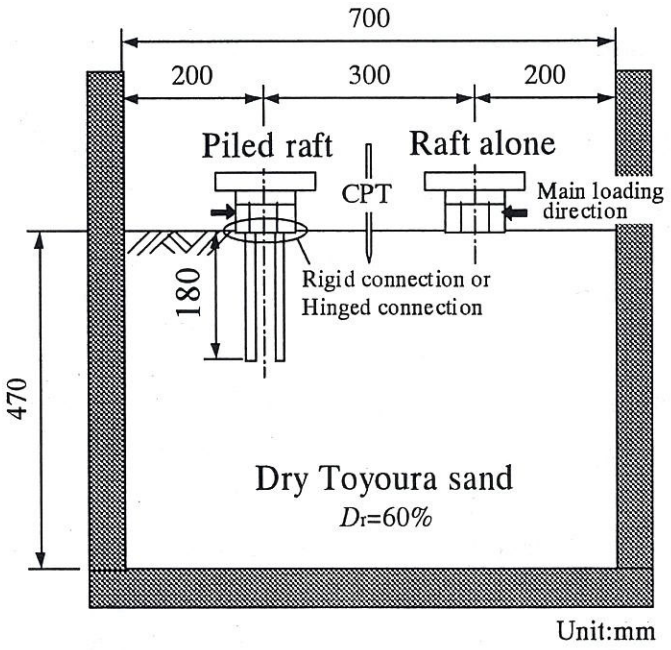

Fig. 3.1. Schematic figure of centrifuge package

3.2.2. Model raft and pile

Square aluminum rafts with widths of 80 mm (4 m at prototype scale) and 120 mm (6 m at prototype scale) were prepared for the vertical loading tests of the rafts alone. The thickness of the raft was set at 25 mm, which was thought to be very rigid. In the vertical

loading test, the raft was loaded by using an actuator at a constant displacement rate of 0.01mm/s. A raft model with the same width but with the different weight and thickness was prepared for the horizontal loading test. On the horizontal loading test, the vertical load was applied by using the raft mass with a weight of 2296 N at 50 g, as described later.

Figure 3.2 shows the model pile used for (isolated) single pile loading tests both in the vertical and horizontal directions. An aluminum pipe with an outer diameter of 10 mm and an inner diameter of 8 mm was used, which is set at the same conditions as the piles used for the piled raft models. The pile tip was closed by using an aluminum plate. Although the total length was 250 mm, the embedment length was varied in each vertical loading test. The pile was instrumented with foil strain gages as shown in the figure to measure axial forces and bending moments along the pile shaft.

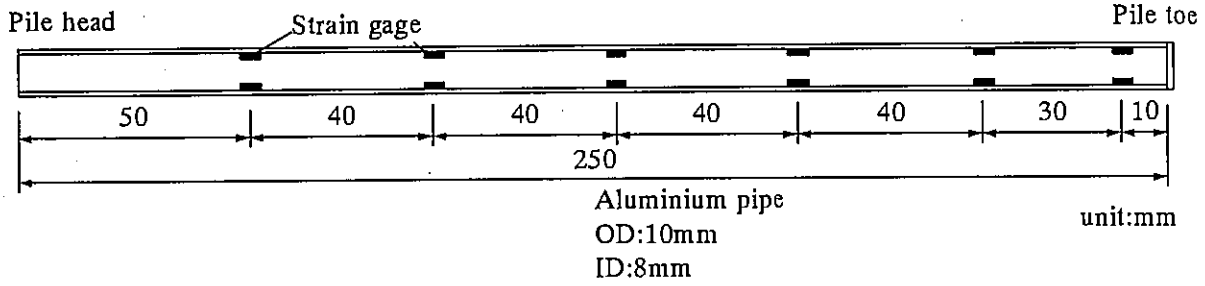

Fig. 3.2. Details of model pile used for loading tests of (isolated) single pile

Table 3.1. Properties of the model pile and the corresponding prototype pile

Properties	Centrifuge model	Prototype
Material	Aluminum	Concrete
Diameter	10 mm	500 mm
Wall thickness	1 mm	Solid
Pile length, L_p	180 mm	9.0 m
Young s modulus, E_p	71 GN/m^2	41.7GN/m^2
Cross-sectional rigidity, E_pA_p	2.0×10^{-3} GN	5.0 GN
Bending rigidity, E_pI_p	2.0×10^{-8}GNm^2	0.13 GNm^2

The properties of the model pile are summarized in **Table 3.1**. Considering the similarity rules for centrifuge modeling, both axial rigidity and bending rigidity of the pile should be considered appropriately since the piles are subjected to both vertical and horizontal directions in the piled raft models. The elastic modulus shown in the table corresponds to the modulus calculated based on the bending rigidity. According to the table, the model pile is approximately equivalent to a solid concrete pile with a diameter of 500 mm at prototype scale. Note that, in the present study, the strength of the prototype concrete pile was not simulated, since different materials were used between the model and the prototype. It was confirmed that the pile stress was below the yield stress in the majority of the present

loading tests. According to separate tensile loading tests of the pile material, yield stress was 149 MN/m^2, and failure stress was 243 MN/m^2.

3.2.3. Piled raft model with rigid pile head connection

Figure 3.3 shows the plan view of the piled raft model with rigid pile head connection. The authors initially used another design of the piled raft model, where the pile head connection was neither perfectly rigid nor perfectly hinged (Watanabe et al., 2001; Horikoshi et al. 2002). In this paper, the piled head connections were set at in the two extreme conditions: rigid and hinged. The degree of the pile head rigidity for the model shown in **Figure 3.3** was examined by a separate loading test, and it was confirmed that the pile head connection was substantially rigid.

The geometries of the piled raft model were determined with reference to the vertical loading tests of the piled raft components, i.e. single piles and rafts alone of the same size, with the consideration of the possible soil box size.

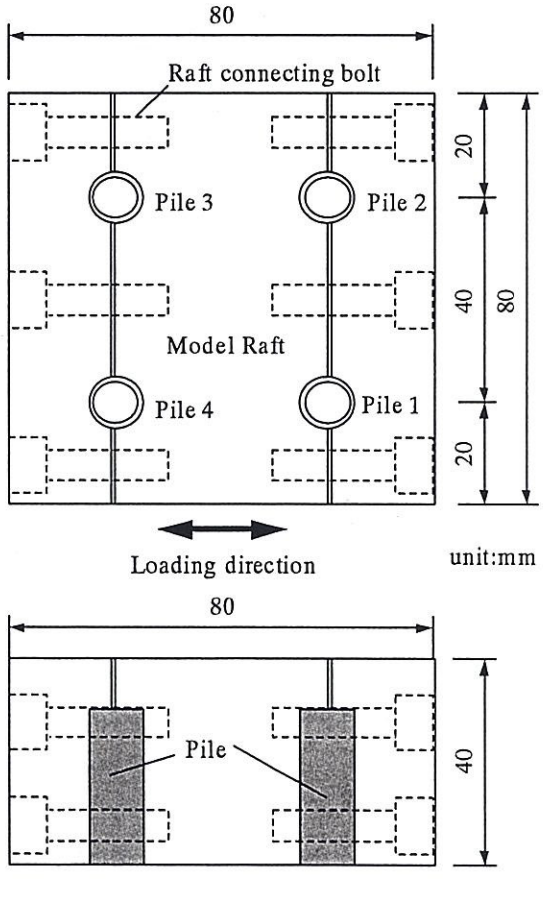

Fig. 3.3. Details of model raft with for piled rigid pile head connection

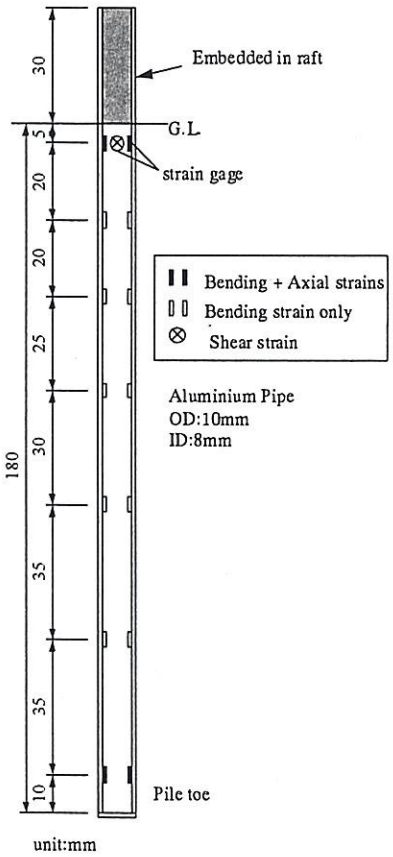

Fig. 3.4. Details of model pile used raft with rigid pile head connection

A square model raft with a width of 80 mm (4.0 m at prototype scale) consists of three separable solid aluminum plates as shown in **Figure 3.3**, which enabled the raft to be connected to the piles after the first flight allowing for the self-weight settlement of the models. The raft base was roughened to increase the frictional resistance. Four piles having a embedment length of 180 mm were installed beneath the raft at a center-to-center spacing of 40 mm. Out of 4 piles installed beneath the raft, two piles were fully instrumented with strain gages along the pile shaft as shown in **Figure 3.4** to measure the distributions of the axial loads and the bending moments. For the other two piles, only the pile head load was measured. Shear strain gages were attached near the pile head (5 mm below the raft base) for all the piles to measure the horizontal loads transferred from the raft. Most of the strain gages were attached inside the pipe to create a smooth shaft surface and to keep the pile diameter uniform along the pile length.

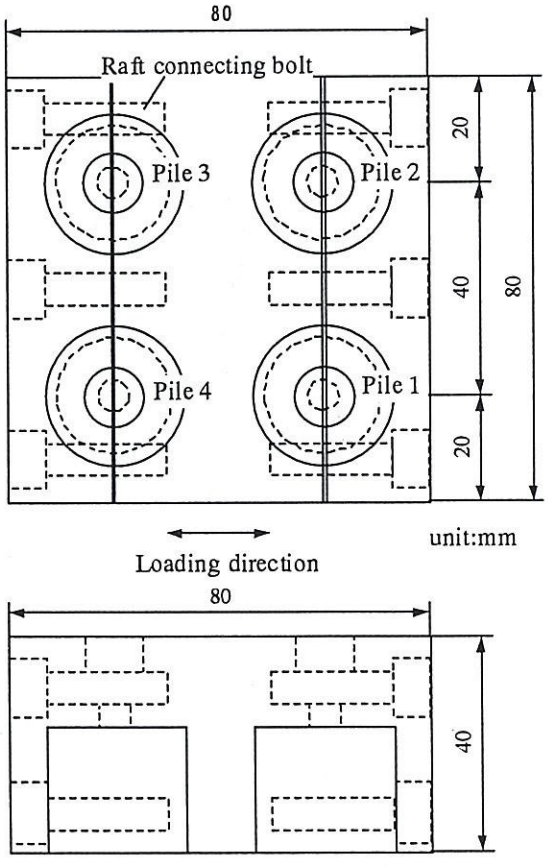

Fig. 3.5. Details of model raft with hinged pile hinged head connection

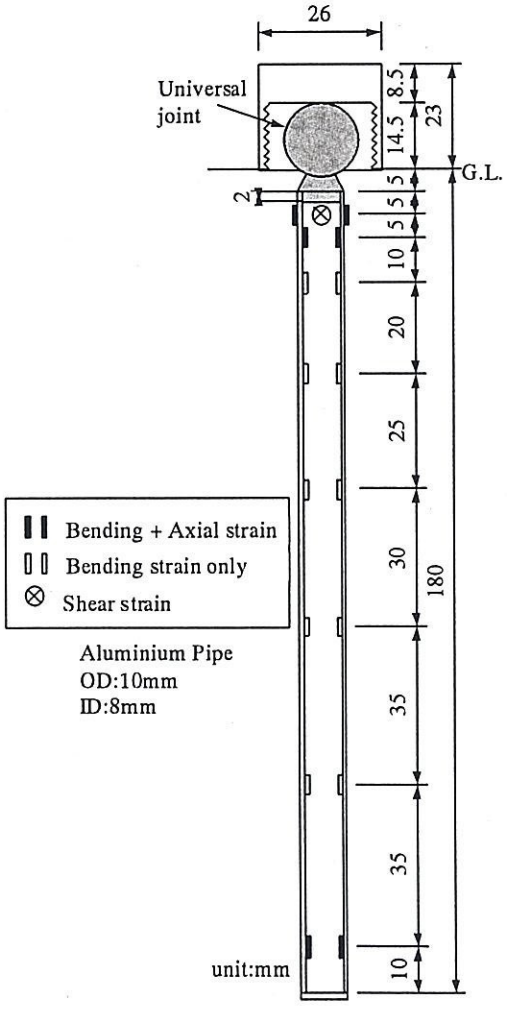

Fig. 3.6. Details of model pile with pile connection

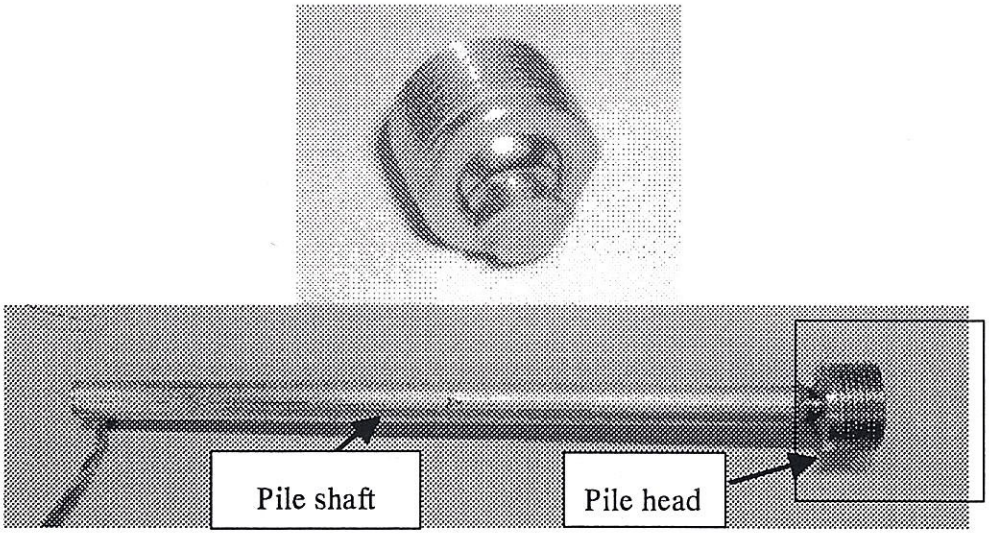

Photo 3.1. Universal joint used for hinged pile head connection

3.2.4. Piled raft model with hinged pile head connection

As shown in **Figures 3.5 and 3.6,** a piled raft with hinged pile head connections was designed to examine the influences of the pile head conditions on the behavior during horizontal loading. Commercially available universal joint (THK Corp. type TBS8, see **Photo 3.1**) was attached at each pile head. The joint can rotate at any direction with essentially negligible resistance.

3.2.5. Horizontal loading device

Figure 3.7 illustrates a cross-section of the piled raft model and the horizontal loading device. The piled raft was loaded cyclically at a height of 25 mm above the soil surface through stainless rollers to minimize the friction between the rods and the piled raft model (see **Photo 3.2**). Added mass was set on the raft to give the intended vertical load to the piled raft. The horizontal and vertical displacements of the model were measured at several points by using laser displacement transducers.

3.2.6. Model ground

Air-pluviated dry Toyoura sand was used throughout the present project. The physical properties of the Toyoura sand are summarized in **Table 3.2**. The relative density of the Toyoura sand was about 60 % after applying the centrifugal acceleration of 50 g, i.e. before the loading test.

The distribution of the soil strength and its repeatability were examined by using an in-flight miniature cone penetrometer with a diameter of 10 mm and an apex angle of 60 degrees. The penetration rate was set at 1.0 mm/s. The measured tip resistances, q_c are summarized in **Figure 3.8** from all the tests conducted for the present study. The figure shows that the strength increases linearly with depth, and the repeatability of the strength between the different tests was excellent.

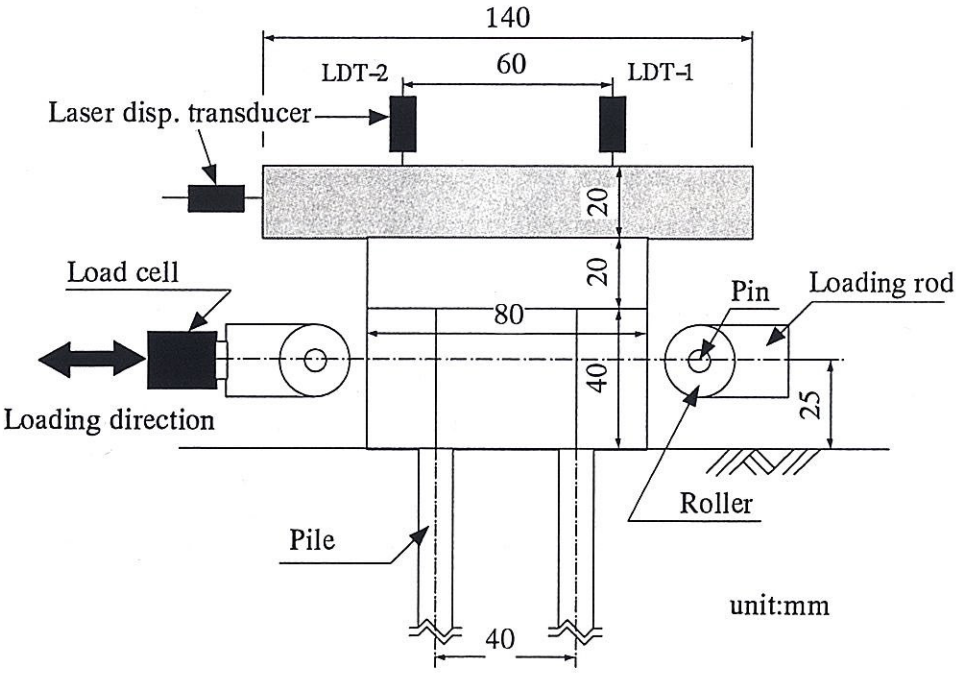

Fig. 3.7. Illustration of horizontal loading system

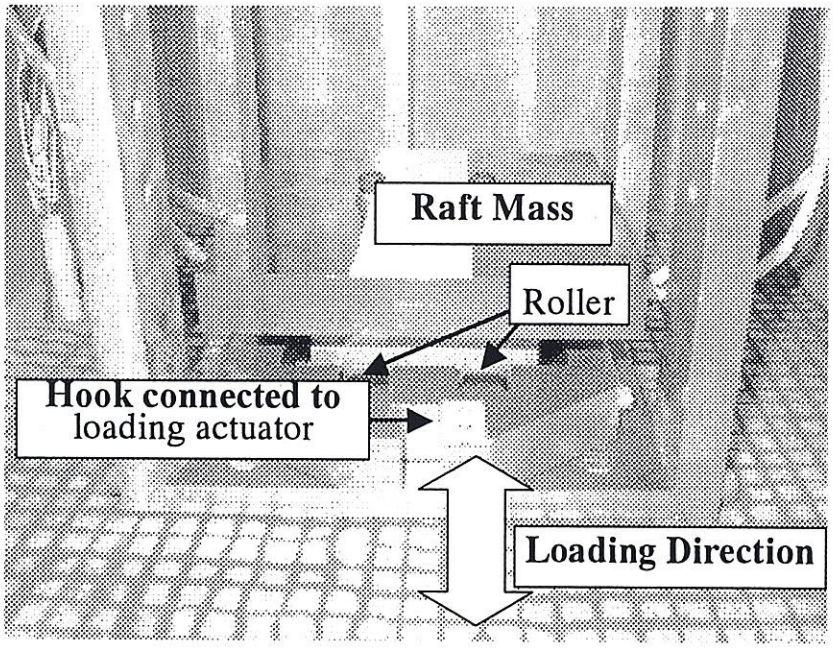

Photo 3.2. Horizontal loading device

Table 3.2. Properties of Toyoura sand

Properties	Value
Density of soil particle, ρ_s (t/m^3)	2.661
Mean grain size, D_{50} (mm)	0.162
Maximum dry density, ρ_{dmax} (t/m^3)	1.654
Minimum dry density, ρ_{dmin} (t/m^3)	1.349

Table 3.3. Experimental cases and their conditions

Model Type	Loading direction	
	Vertical loading	Horizontal loading
Single Pile	L_p = 120, 170, 200 mm h = 505 mm	L_p = 170 mm h = 440 mm
Raft (alone)	B = 80, 120 mm M_r = 0.36 kg h = 470 mm	B = 80 mm M_r = 4.69 kg h = 460 mm
Piled Raft	L_p = 170 mm B = 80 mm, 120 mm M_r = 0.90 kg h = 470 mm	L_p = 180 mm B = 80 mm M_r = 4.69 kg h = 460 mm Rigid or hinged pile head conditions

L_p: Pile length, B: Square raft width, M_r: Mass of raft, h: Soil thickness

3.2.7. Test procedures

The test procedures for the static loading tests are as follows:

1) Set four piles at the corresponding positions by using an adjusting apparatus,
2) Pour dry sand into the rigid box,
3) Apply centrifugal acceleration up to 50 g to allow for self-weight settlement of the soil and the piles,
4) Check soil strength distribution through cone penetration tests,
5) Place model raft on sand after halting the first flight,
6) Connect the model raft and the piles, and place added mass on the raft,
7) Set all instrumentations, and apply centrifugal acceleration up to 50 g again, and
8) Apply horizontal load to the piled raft.

3.3. TEST CASES

Experimental cases and their conditions considered in this paper are summarized in **Table 3.3**. Both vertical loading tests and horizontal loading tests were conducted for the single piles, the rafts alone, and the piled rafts with different sizes. The pile length and the raft width were varied in the vertical loading tests of the single pile and the raft alone, respectively, in order to evaluate the basic performance of the piled raft components.

During the tests, the same soil container was used. However, as shown in the table, the soil thickness varied slightly. This was due to the limitation of the space above the soil surface which was given for the loading apparatus. It was thought that the effects of the difference in the soil thickness on the behavior of the models subjected to horizontal loads were very small, since the pile was relatively short compared with the soil thickness. The load was applied to the model vertically or horizontally at a constant displacement rate of about 0.01 mm/s. Note that the same piled raft models as used in the (static) horizontal

loading tests were used in the dynamic loading tests to compare the model behavior, the results of which are described in another paper by Horikoshi et al. (2003).

3.4. VERTICAL LOADING TESTS OF PILED RAFT FOUNDATIONS AND COMPONENTS

3.4.1. Single pile and raft alone

The load-settlement relationships obtained from the vertical loading tests on the single piles are summarized in **Figure 3.9** for different initial embedment lengths of 120, 170 and 200 mm. The initial secant stiffness, i.e. load divided by settlement, of each pile is summarized in **Table 3.4.** In the calculation of the stiffness, the load at the settlement of 1 mm was taken since the profiles showed significant nonlinear responses from the beginning. The figure and the table show the increase in the secant stiffness and the axial capacity as the pile embedment length increases.

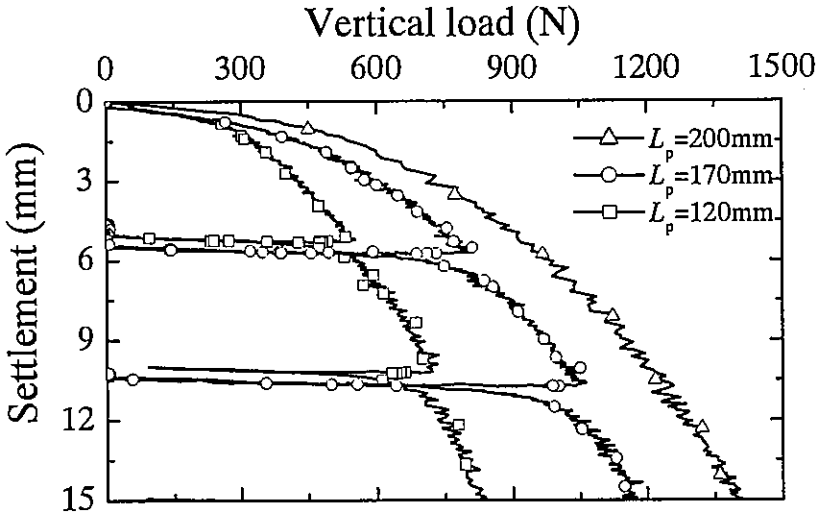

Fig. 3.9. Load-settlement behavior obtained from single pile loading tests

Table 3.4. Effects of pile length on vertical stiffness

Pile length (mm)	120	170	200
Stiffness (N/mm)	306	376	458

Figure 3.10 shows the distribution of the axial forces along the pile shaft. The figure shows that at least 50 % of the pile head load is transferred to the pile toe. This was thought to be due to the effects of the increase in the soil stiffness with depth as demonstrated in the cone resistance (**Figure 3.8**).

Figure 3.11 shows the results of the vertical loading tests for the rafts alone. The stiffness of the raft was calculated as 3.03 kN/mm and 5.24 kN/mm for the raft widths of 80 mm and 120 mm, respectively. The stiffness was much greater than that of the single pile.

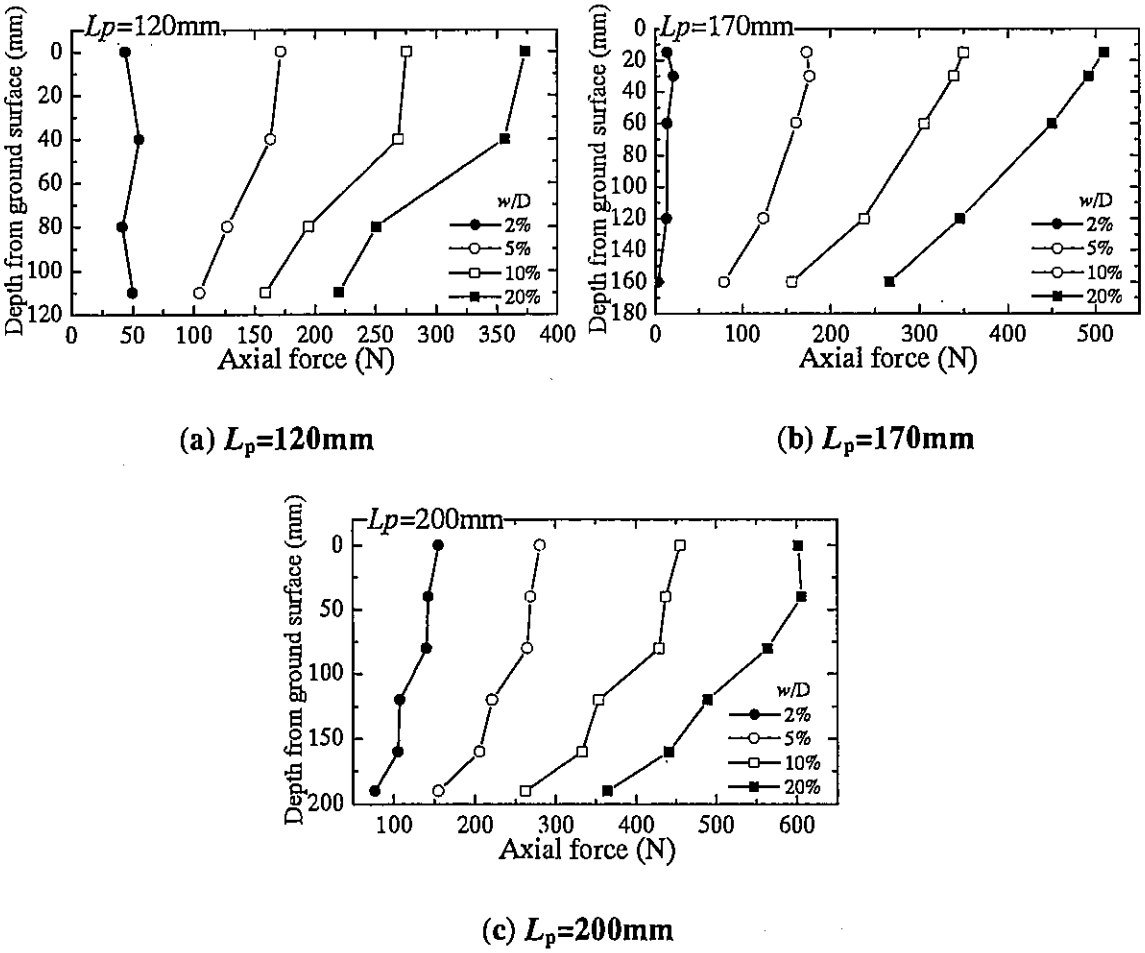

(a) L_p=120mm

(b) L_p=170mm

(c) L_p=200mm

Fig. 3.10. Axial force distributions measured during vertical loading tests

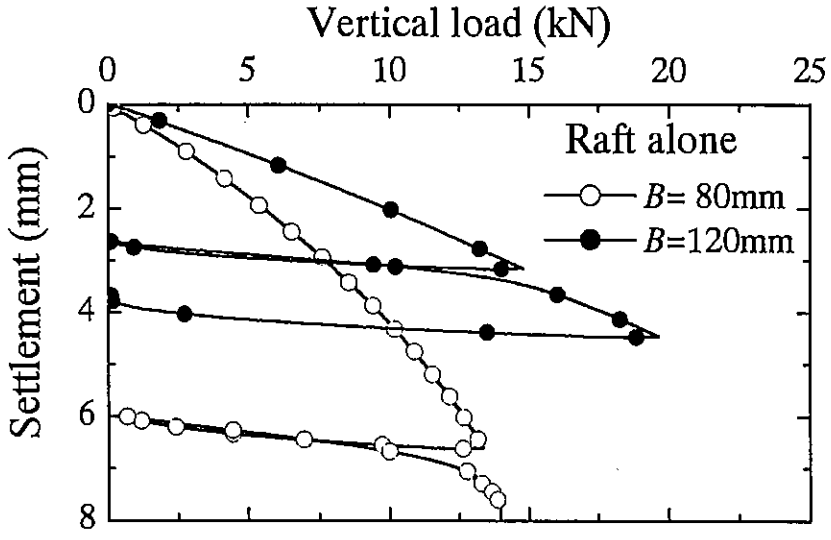

Fig. 3.11. Load-settlement relationships obtained from vertical loading tests of rafts alone

3.4.2. Piled raft foundations

Figure 3.12 shows the load settlement relationship of the piled raft model described by Watanabe et al. (2000). The width of the raft and the pile length was set at 80 mm and 170 mm respectively. The vertical load carried by each component is also shown in the figure, where the raft load was calculated by extracting the pile loads from the total applied load. The initial load applied to the piled raft, i.e. self-weight of the raft, was 441 N at 50 g, and the model was loaded vertically at the constant displacement rate of 0.01 mm/s. The measured initial vertical stiffness of the piled raft was 2.91 kN/mm.

The proportion of the vertical load carried by the raft and the 4 piles is shown in **Figure 3.13.** During the initial loading stage, the piles carried the majority of the applied load, and then the proportion decreased gradually, as was also reported by Horikoshi and Randolph (1996) for the piled raft models on soft clay.

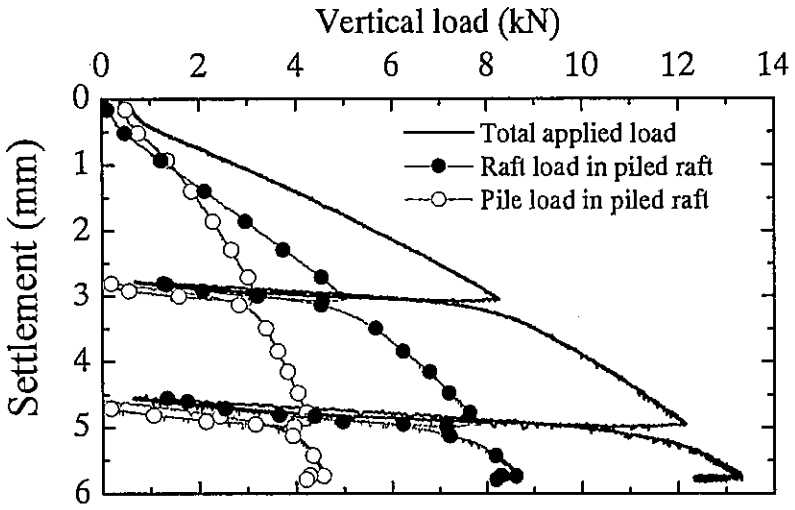

Fig. 3.12. Load-settlement relationship obtained from vertical loading test of piled raft

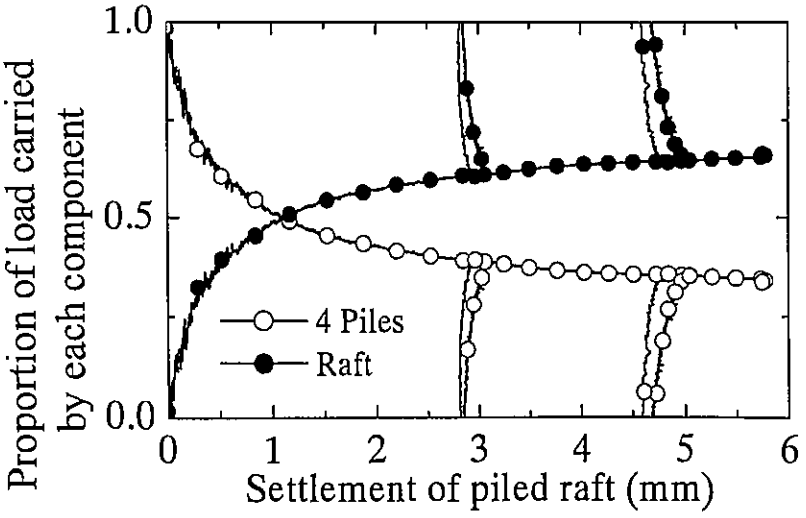

Fig. 3.13. Proportion of vertical load carried by each component

Figure 3.14 shows the load-settlement behavior of a pile as a component of the piled raft, in comparison with that obtained from the isolated single pile loading test with the same geometries. In the former pile response, the vertical displacement was taken from the piled raft settlement. According to the figure, a meaningful increase in the pile capacity was observed in the pile as a component of the piled raft, which is thought to be due to the increase in the soil stiffness and the strength beneath the raft related to increase in the confining stress around the piles. The results suggest that the load-displacement behavior of a pile in a piled raft can be highly different from that observed in the isolated single pile loading test. Such behavior may affect the estimate of the load sharing between the raft and the piles. In other words, modifications from the single pile loading tests are necessary with consideration of increase in the confining stress for the accurate estimation of piled raft behavior.

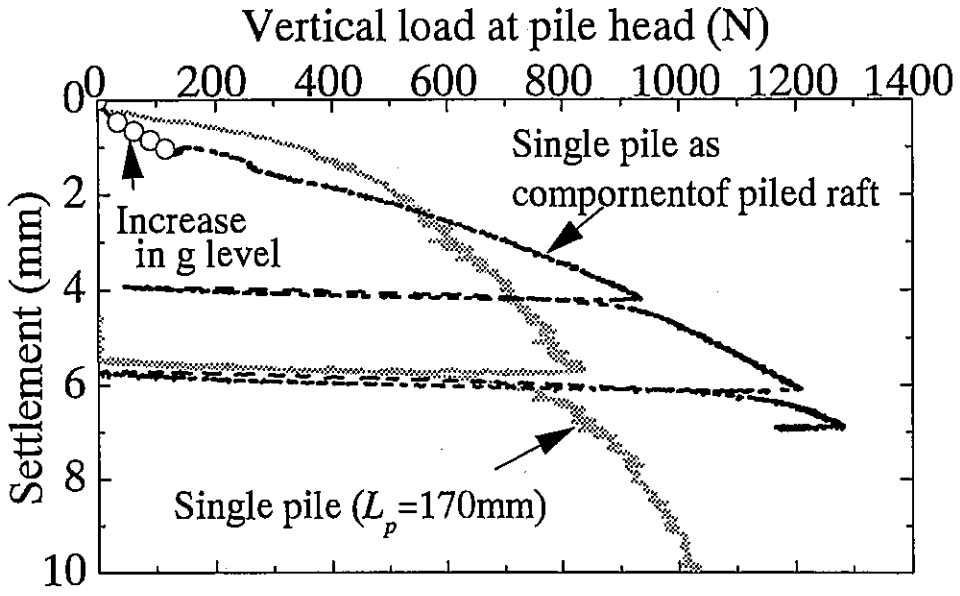

Fig. 3.14. Behavior of single pile as component of piled raft compared with result from single pile loading test

3.5. HORIZONTAL LOADING TESTS OF PILED RAFT FOUNDATIONS AND COMPONENTS

3.5.1. Single pile and raft alone

The result of the horizontal loading test of the single pile is shown in **Figure 3.15** for the pile with the length of 170 mm. In the test, a constant displacement rate of 0.01 mm/s was applied to the pile at 25 mm above the soil surface. The initial horizontal stiffness of the single pile was calculated as 40 N/mm. **Figure 3.16** shows the distributions of the bending moments along pile shaft at the initial stage. The maximum bending moment was observed at a depth of about 65 mm below the soil surface.

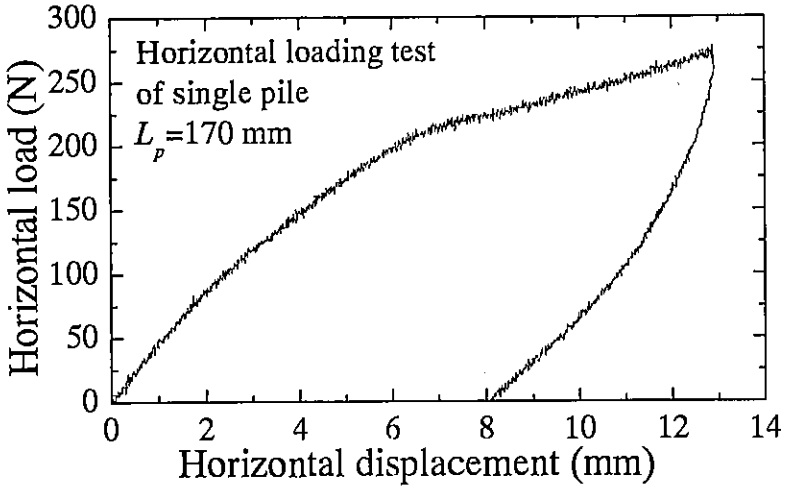

Fig. 3.15. Horizontal load-displacement relationship of single pile (L_p= 170 mm)

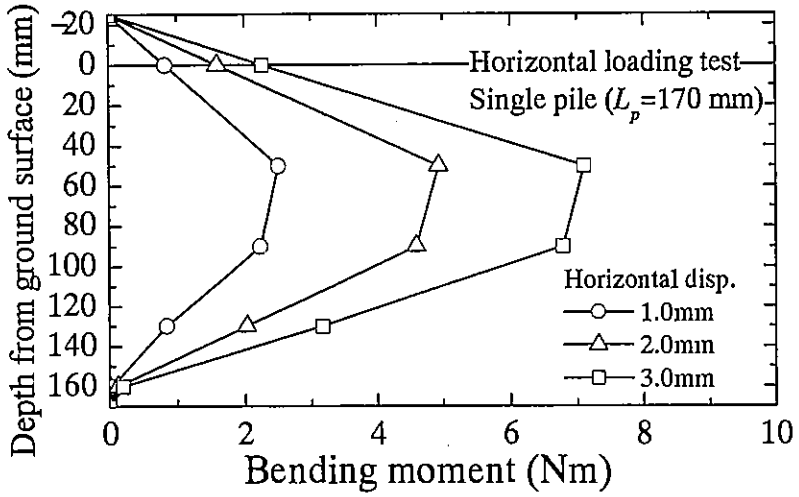

Fig. 3.16. Distributions of bending moments along pile shaft

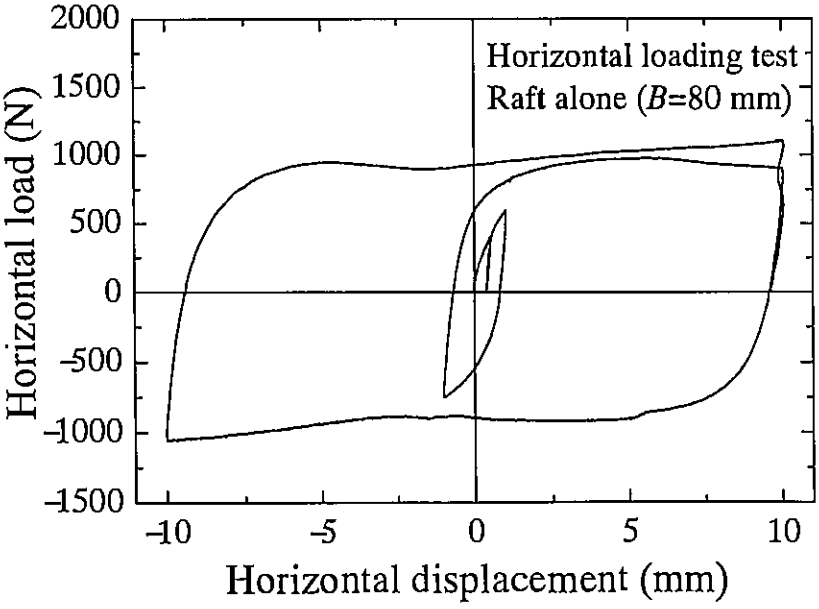

Fig. 3.17. Horizontal load-displacement relationship of raft alone

The horizontal load-displacement relationship of the raft alone with a width of 80 mm is shown in **Figure 3.17**. The raft weight was same as that used for the horizontal loading test of the piled raft model (2298 N at 50 g). The figure shows that the raft resistance reached the ultimate value of 973 N at a displacement of about 5 mm, which corresponded to the coefficient of friction of 0.423 (interface angle of 22.9 degrees).

Figures 3.18 and **3.19** show the settlement and the inclination of the raft alone during the horizontal loading. It can be seen that the raft settled and inclined as the cyclic horizontal displacements progressed. The increase in the inclination was almost in proportion with the horizontal displacement. Note that clock-wise inclination of the raft was taken as positive in the figure.

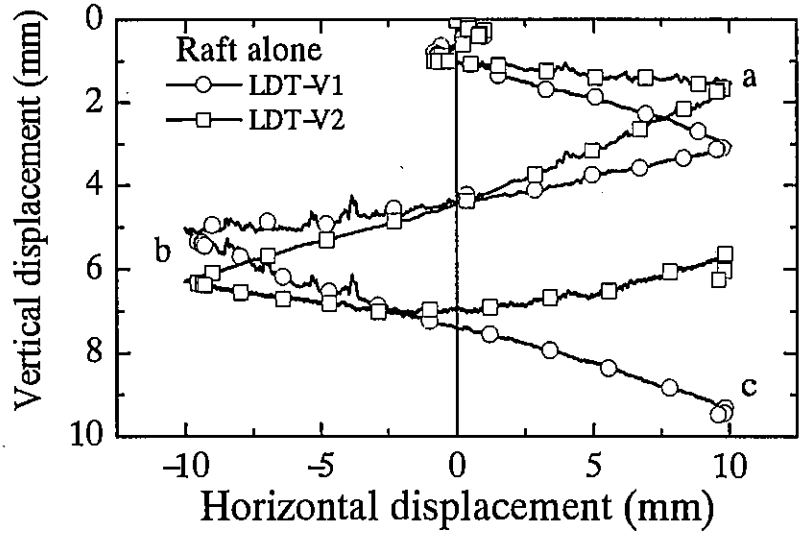

Fig. 3.18. Vertical displacements of model raft during horizontal loading

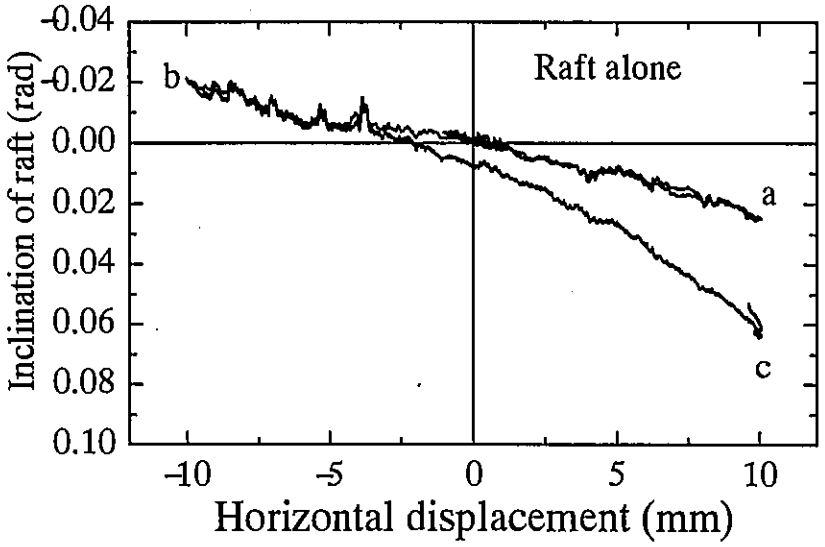

Fig. 3.19. Inclination of model raft during horizontal loading

3.5.2. Piled raft foundations

Considering the actual behavior of piled rafts, horizontal loads should be applied after applying vertical loads in-flight. However, in the present study, the vertical load was applied by increasing the initial raft mass to 2298 N at 50 g as described earlier, so as to simplify the experimental apparatus and procedures. It was thought that achieving the consistent load-sharing between the raft and the piles was the most important consideration, rather than applying the vertical load in a strict manner.

In the following results, the behavior of the piled raft models with the different pile head connections, i.e. rigid pile head connection and hinged pile head condition, is examined and compared. Note that the pile length was 180 mm for horizontal loading tests of the piled rafts, whereas the length was 170 mm for the vertical loading test. This is because the piled raft model for horizontal loading was initially designed for shaking table tests of a free-standing pile group with an embedment length of 170 mm allowing for a gap of 10 mm between the raft base and the soil surface (see Horikoshi et al, 2003).

Figure 3.20 shows the vertical loads carried by each component of the piled rafts during the stage of increasing in g level to 50 g. The figures show that about 40 % of the loads were carried by the 4 piles before the horizontal loading test consistently in both models. The proportion of the load was almost consistent with the behavior observed in the vertical loading test (see **Figures 3.12 and 3.13**).

Figure 3.21 shows the horizontal load-displacement relationships of the piled rafts. Cyclic horizontal loads were applied to the models. The result from the raft alone model with the same properties (**Figure 3.17**) is also added to the figures. In the figure, the raft load in the piled raft is estimated by extracting all the pile head shear forces from the total applied horizontal load. The horizontal stiffness was calculated as about 1790 N/mm and 1260 N/mm for the rigid connection model and the hinged connection model, respectively.

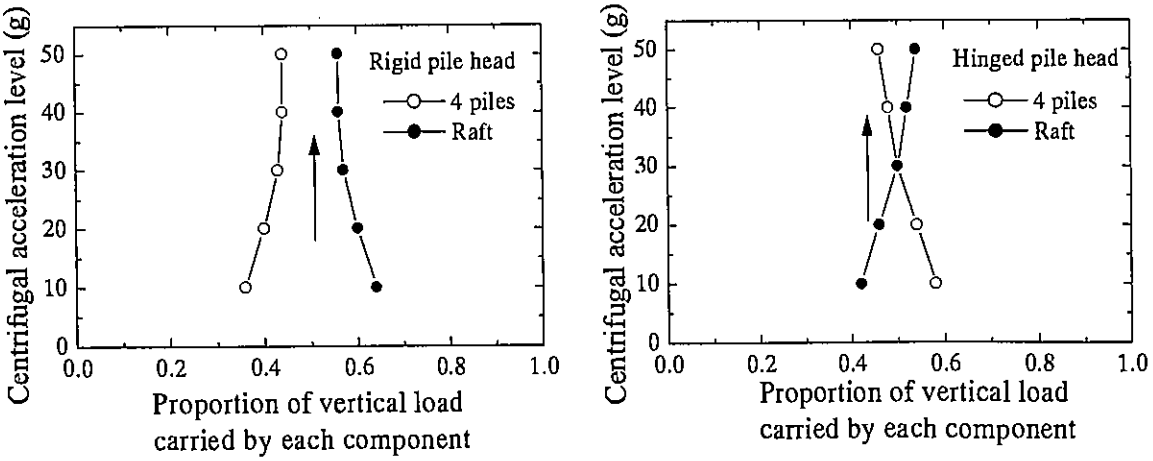

(a) Rigid connection model **(b) Hinged connection model**

Fig. 3.20. Proportion of vertical load carried by each component during the stage of increasing in g level to 50 g

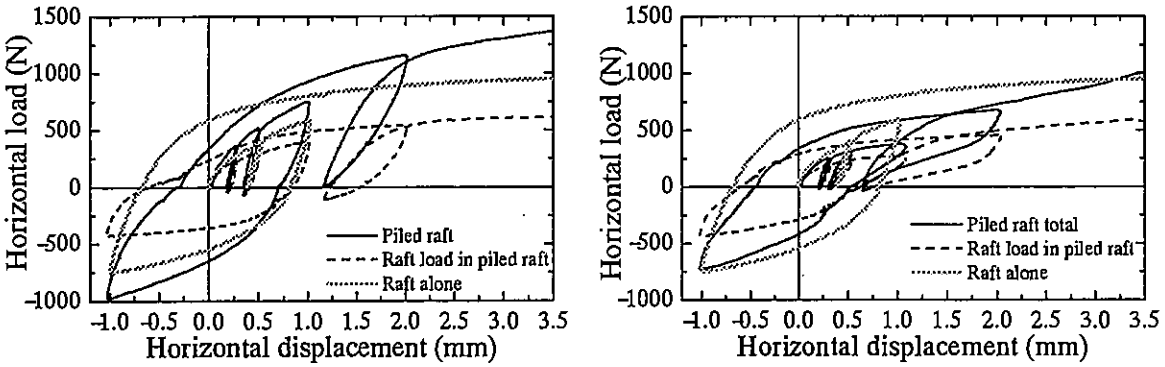

(a) Rigid connection model **(b) Hinged connection model**

Fig. 3.21. Horizontal load-displacement relationship of piled rafts

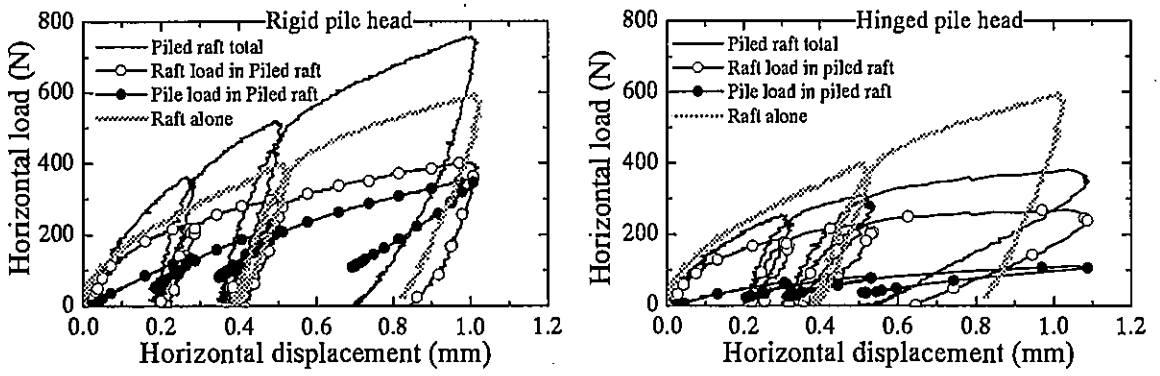

(a) Rigid connection model **(b) Hinged connection model**

Fig. 3.22. Horizontal load-displacement relationship of piled rafts (initial parts enlarged)

Figure 3.22 shows the initial parts of the load-displacement relationships and the contribution of each component (i.e. 4 piles and raft). According to the figures, the total horizontal resistance of the rigid connection piled raft is higher than that of the raft alone, whereas the total resistance is interestingly lower in the hinged connection model. The horizontal loads carried by the raft were almost the same between the different pile head connection models. That is, the higher total horizontal resistance of the rigid connection piled raft is attributed to the higher horizontal resistance of the piles.

It should also be noted that the horizontal stiffness of the raft in the piled raft was slightly smaller than that of the raft alone according to **Figure 3.22.** In the raft (alone) model, the total vertical load was directly transferred to the soil through the raft base, whereas only 60% of the vertical load was transferred to the soil through the raft base in the piled rafts (see **Figure 3.20**). Thus, the soil confining stress beneath the raft was smaller in the piled raft models, resulting in the smaller horizontal stiffness and the strength of the soil just beneath the piled raft model.

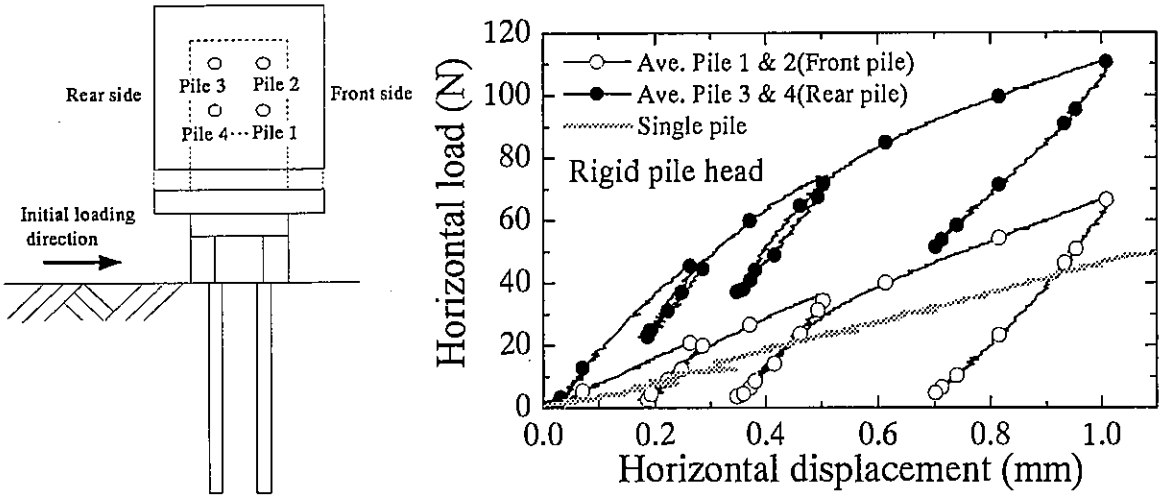

Fig. 3.23. Horizontal load-displacement relationships of piles in rigid pile head model, together with that of single pile

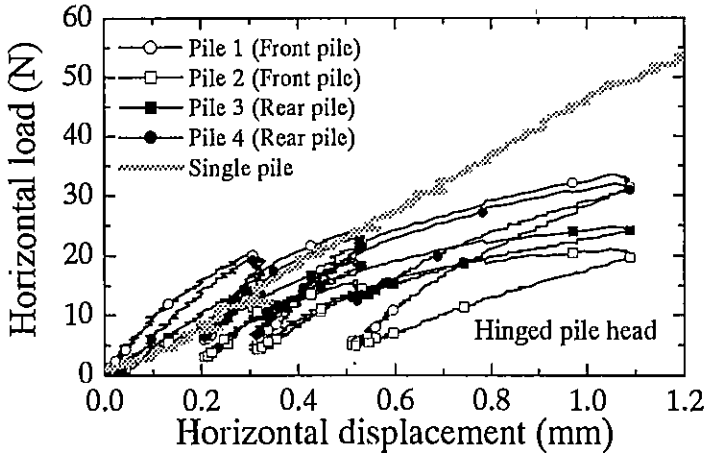

(a) Each pile response

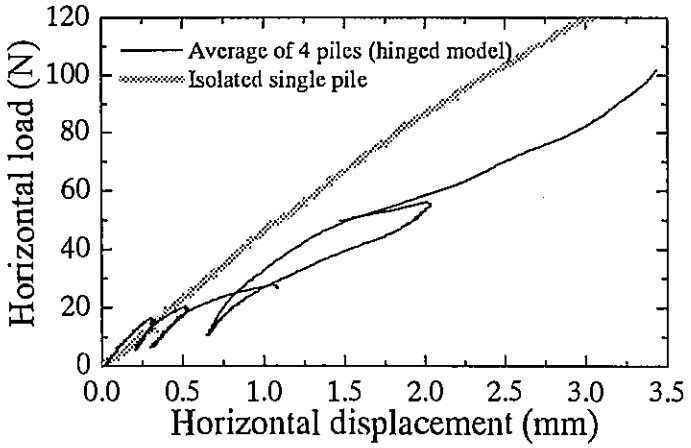

(b) Averaged response of 4 piles

Fig. 3.24. Horizontal load-displacement relationships of piles in hinged pile head model, together with that of single pile

Figure 3.23 compares the single pile responses in the rigid pile head model with the response observed in the isolated single pile (**Figure 3.15**). The horizontal displacement of the pile in the piled raft was taken from the measured piled raft displacement, and the horizontal load was taken from the shear force measured near the pile head. The figure clearly shows higher stiffness and resistance of the single pile as a component of the piled raft compared with those of the isolated single pile. The reason for the behavior was considered to be the difference in pile head flexibility and the confining stress around the piles as also explained in the vertical pile response (**Figure 3.14**).

Figure 3.24(a) shows the same relationships for the hinged connection piled raft, together with that of the isolated single pile. According to the figure, horizontal load transferred to each pile is relatively uniform depending on the line in the loading direction. For example, the loads transferred to the piles 1 and 4, which were in line in the loading direction, are almost the same. The average load of the 4 piles is plotted against horizontal displacement in **Figure 3.24(b)** together with the isolated single pile response. The figure shows that the averaged horizontal stiffness of the piles in the hinged piled raft model was smaller than that of the isolated single pile, indicating that the interaction between the piles and the raft base probably reduce the stiffness per pile in the piled raft model. In the rigid pile head mode, the higher pile head rigidity and the confining stress prevailed over the interaction effects between the piles and the raft base.

Figure 3.25 shows the distributions of the bending moments of the piles along the shafts in the piled raft models. The maximum bending moments in the hinged connection model was much smaller than those observed in the rigid connection model for the same horizontal displacements. Considering the bending moment distributions at the pile head, the shear force of the pile in the rigid connection model is much higher than that of the hinged connection model, which means that the piles in the rigid model carry more horizontal loads as shown in **Figures 3.22** and **3.23**.

The proportion of the horizontal load transferred to each component is shown in **Figure 3.26.** In the figure, the profiles in the unloading stage are not shown to provide simpler profiles. In both piled rafts, the raft carries much of the load in the early stages of the horizontal loading as was also observed in the previous piled raft model by the authors (Watanabe et al, 2000; Horikoshi et al, 2002). The proportion of the raft load rapidly decreased as the piled raft displacement increased, which shows the proportion is highly dependent on the horizontal displacement. The reduction in the proportion of the raft load was more significant in the rigid connection model (**Figure 3.26(a)**) related to a higher horizontal stiffness of the piles. The figures also indicate the importance of the consideration of the non-linear response for the accurate estimation of the piled raft behavior subjected to horizontal loads.

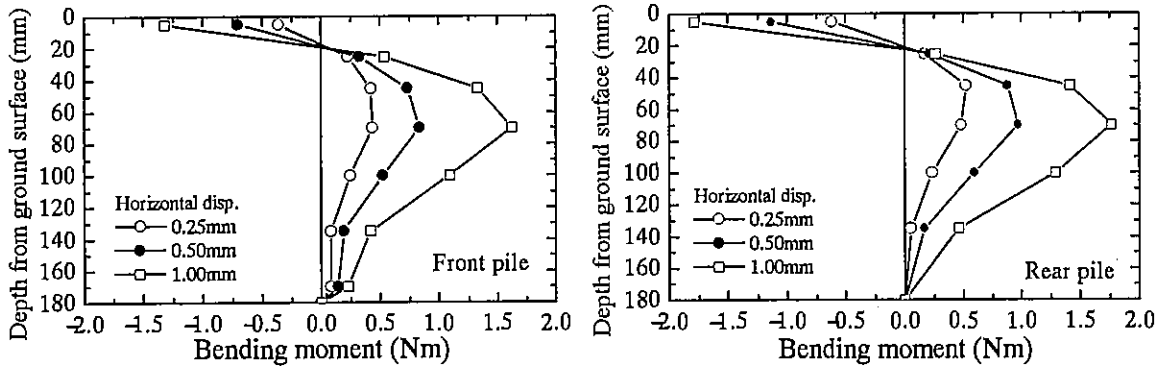

(a) Rigid connection model

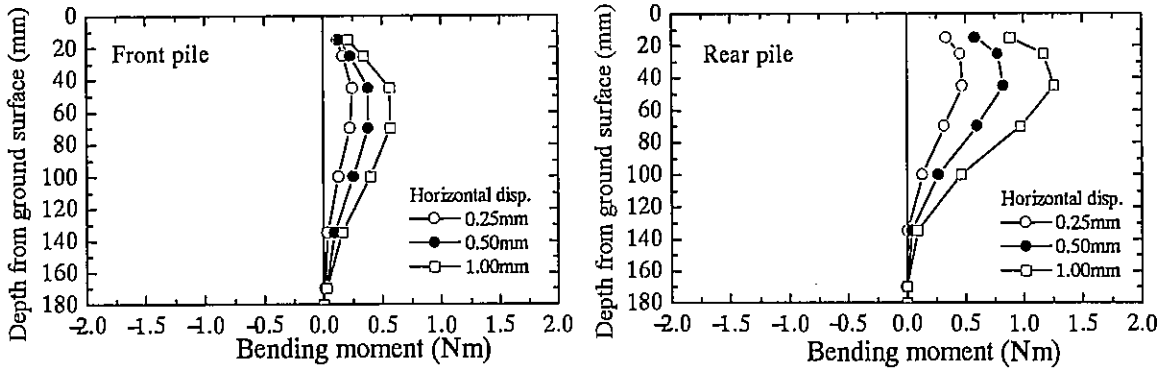

(b) Hinged connection model

Fig. 3.25. Distributions of bending moments along pile shaft

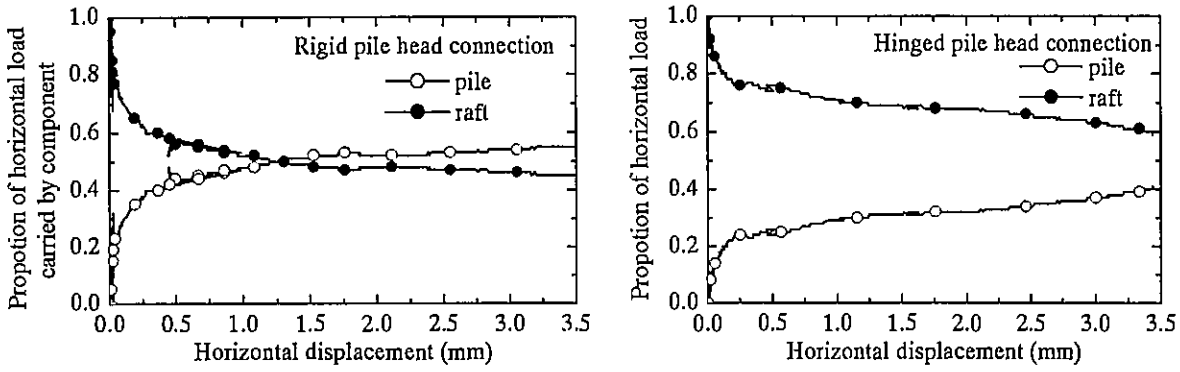

(a) Rigid connection model **(b) Hinged connection model**

Fig. 3.26. Proportion of horizontal load carried by each component

The proportion of the vertical load carried by each component during the horizontal loading is shown in **Figure 3.27**. The raft initially carried about 60% of the total load. The change in the proportion was smaller than that of the horizontal load (**Figure 3.26**), and this tendency was clearer in the hinged connection model. The proportion of the vertical load carried by the piles decreased with the increase in the horizontal displacement. This behavior corresponded to the changes in the axial forces at the pile heads shown in **Figure**

3.28. The force at the rear pile decreased with the increase in the horizontal displacement while that at the front pile remained almost constant. Thus, the decrease in the axial force of the rear pile is compensated by the increase in the vertical load carried by the raft base.

As for the raft resistance in each model, the resistance corresponding at the horizontal displacement of **3** mm was 586 N in the rigid connection model (see **Figure 3.21**). At this stage, the proportion of the vertical load carried by the raft was 73%. Since the interface friction coefficient was 0.423 and the weight of the raft mass was 2298 N, the raft resistance was estimated as 710 N. The measured value (586 N) was 83 % of the estimated (see **Table 3.5**). It was thought that the soil beneath the raft was constrained by the existence of the piles which reduced the shear deformation of the soil just beneath the raft base, and thus the mobilized shear stress at the interface between the raft and the soil was less than the estimated resistance. On the other hand, in the case of the hinged connection model, the shear deformation of the soil beneath the raft may not be highly constrained compared to the case of the rigid connected model. In fact, the estimated horizontal raft resistance of 584 N was closer to the measured value of 552 N.

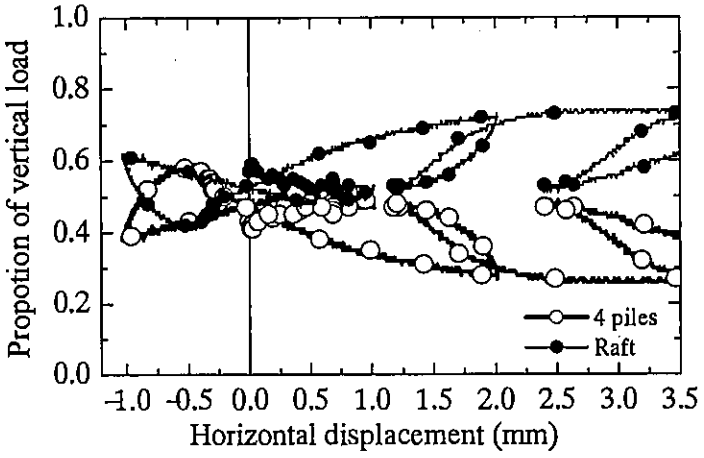

(a) Rigid connection model

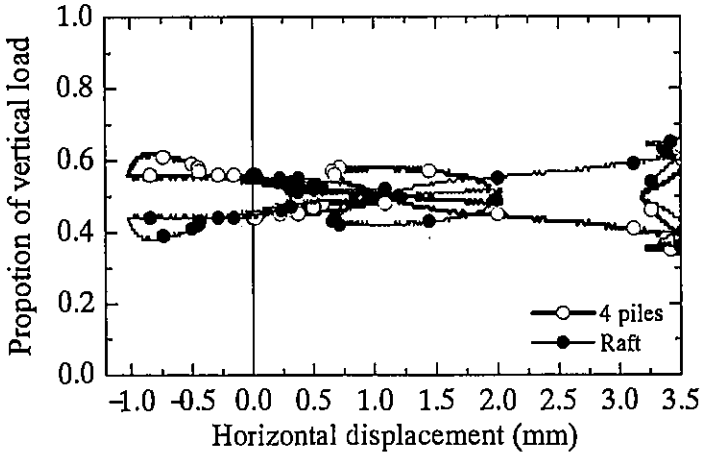

(b) Hinged connection model

Fig. 3.27. Proportion of vertical load carried by each component

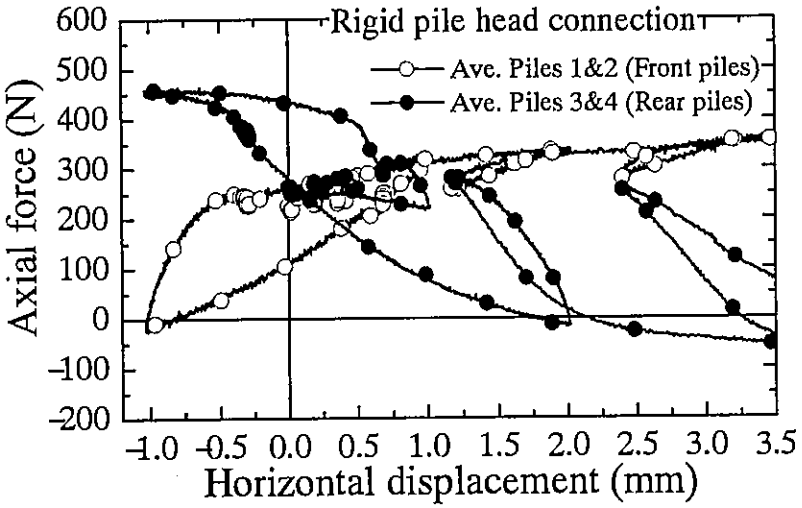

(a) Rigid connection model

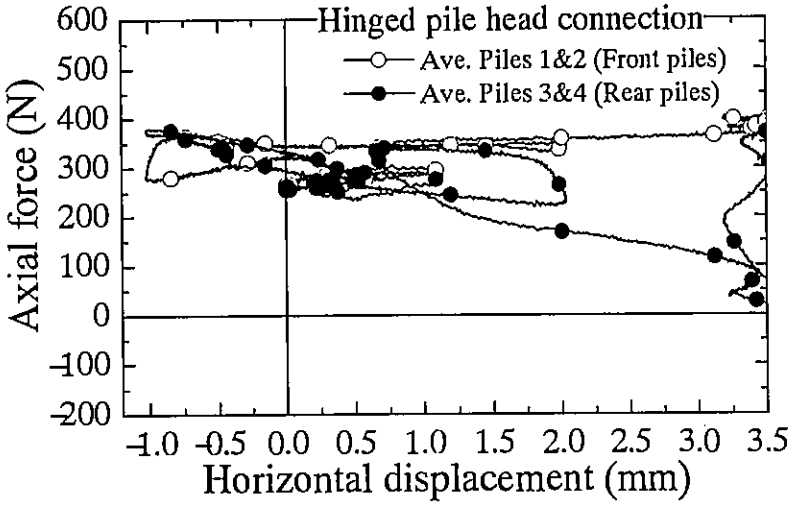

(b) Hinged connection model

Fig. 3.28. Pile head axial force during horizontal loading test

Table 3.5. Measured and estimated raft resistance in the piled rafts

	Raft resistance (N)	
	Measured value	Estimated value
Rigid piled raft	586 (0.83)	710
Hinged piled raft	552 (0.95)	584

The value in ( ) shows the ratio: Measured/Estimated

3.6. CONCLUSIONS

A series of vertical loading tests and horizontal loading tests were conducted on piled raft models and their components (single piles and rafts alone) on dry sand by using geotechnical centrifuge. The influences of the rigidity in the pile head connection on the horizontal piled raft behavior were also examined by designing two piled raft models with the rigid and hinged connections. Although the examined piled raft conditions are still limited, the following conclusions are drawn:

1. The stiffness and the ultimate resistance of the single pile in the piled raft are highly different from those observed in the loading test of the isolated single pile. The increase in the confining stress around the pile due to the load transferred through the raft base should be considered in the evaluation of the pile response in the piled raft design, as well as the interaction effects between the components.
2. As for the rigid pile head connection model, the ultimate horizontal resistance was much higher than that of the raft alone. The piles play important roles in the ultimate resistance of piled raft foundations. Ignoring the pile existence in piled raft designs against horizontal loads may lead to conservative horizontal resistance.
3. As far as the present centrifuge models are concerned, the initial horizontal stiffness of the piled raft was not always higher than that of the raft alone. Since the smaller load is transferred from the raft base to the underlying soil in the piled raft, the stiffness of the sand beneath the raft may also be smaller due to the smaller confining stress. This behavior suggests that care is required in the selection of the soil modulus in the design of the piled raft foundations.
4. The ultimate frictional resistance of the raft component in the piled raft was smaller (rigid pile head connection) or almost the same (hinged pile head connection) compared with the estimates from the raft vertical loads and the coefficient of the friction between the raft base and the soil. It was thought that the soil beneath the raft was constrained by the piles which may reduce the shear deformation of the soil just beneath the raft base, and thus the mobilized shear stress at the interface was smaller. This constrained effect may be higher in the rigid pile head connection model.
5. As for the proportion of the horizontal load carried by each component, the raft initially carried more load than the piles, with larger displacements the piles more than the raft in the piled raft with rigid pile head connection. In the piled raft with hinged pile head connection, the contribution of the piles was much smaller. Overall, however, the proportion is highly dependent on the piled raft displacement, and it is therefore important to consider such non-linear response in the designs of piled raft foundations.

6. The change in the proportion of the vertical load carried by the piles during the horizontal loading was smaller than that observed in the horizontal load. Hinged pile head connection gave the smaller change than the rigid pile head connection.
7. As far as the present centrifuge models are concerned, higher horizontal load was transferred to the piles with rigid pile head connection, which led to the higher initial horizontal stiffness compared with that of the hinged pile head connection. On the other hand, bending moments of the piles were much smaller in the piled raft with the hinged pile head connection for the same piled raft displacement.
8. In the piled raft with the hinged pile head connection, the horizontal resistance of the single pile in the piled raft was slightly smaller than that observed in the isolated single pile despite the higher confining stress around the piles beneath the raft. This was thought to be due to the possible interactions between the raft and the piles, i.e. the raft contribution was higher to the mobilization of the shear resistance.

ACKNOWLEDGEMENT

This study was supported by a Grant-in-Aid for Scientific Research (Grant No. 12450188) of Japanese Ministry of Education, Culture, Sports, Science and Technology.

The authors would also like to express their special appreciation to Mr. Yoshimasa Handa, Taisei Service Corporation for his special support in carrying centrifuge tests.

REFERENCES

1) Architectural Institute of Japan (2001): Recommendations for Design of Building Foundation (in Japanese).
2) Burland, J. B., Broms, B. B. and De Mello, V. F. B. (1977): Behaviour of foundations and structures, Proc. 9th ICSMFE, Tokyo, 2, pp. 496-546.
3) Horikoshi, K. & Randolph, M. F. (1996): Centrifuge modeling of piled raft foundations on clay, Géotechnique 46, No. 4, pp. 741-752.
4) Horikoshi, K. & Randolph, M. F. (1998): A contribution of optimum design of piled rafts, Géotechnique 48, No. 3, pp. 301-317.
5) Horikoshi, K. & Randolph, M. F. (1999): Estimation of overall settlement of piled rafts, Soils and Foundations, Vol. 39, No. 2, pp. 59-68.
6) Horikoshi, K., Matsumoto, T., Fukuyama, H. and Watanabe, T. (2001): Behavior of piled raft foundations subjected to horizontal loads, Proc. 46th JGS Geotechnical Symposium, pp. 241-246 (in Japanese).
7) Horikoshi, K., Watanabe, T., Fukuyama, H. and Matsumoto, T. (2002): Behavior of piled raft foundations subjected to horizontal loads, Proc. Int. Conf. on Physical Modelling in Geotechnics, St. John's, Canada, pp.715-721.

8) Horikoshi, K., Hashizume, Y., Matsumoto, T. and Watanabe, T. (2003): Performance of piled raft foundations subjected to dynamic loading, Int. Jour. of Physical Modelling in Geotechnics (to be submitted).
9) Kakurai, M., Yamashita, K. and Tomono, M. (1987): Settlement behavior of piled raft foundation on soft ground, Proc. 8th ARCSMFE, pp. 373-376.
10) Katzenbach, R. & Chr. Moormann (2001): Recommendations for the design and construction of piled rafts, Proc. 15th ICSMGE, Istanbul, Vol. 2, pp. 927-930.
11) Katzenbach, R. Arslan, U. and Reul, O. (1988): Soil-structure-interaction of a piled raft foundation of a 121 m high office building on loose sand in Berlin, Proc. Deep Foundation on Bored and Auger Piles, pp. 215-221.
12) Kobayashi, H., Nagao, T., Watanabe, T., Shinozaki, Y., Nishio, H. and Majima, M. (2000): Study on the behaviour of piled raft foundations, Part 2:Application to the low building and the observation of settlement, Report of Taisei Research Institute, Vol. 33, pp. 121-124 (in Japanese).
13) Mano, H., Nakai, S., Takanashi, K. and Ishida, R. (2002): Static dynamic tests of a piled raft foundation subjected to horizontal loading, Proc. 11th Japan Earthquake Engineering Symposium, pp.1143-1148 (in Japanese).
14) Nagura, K., Tanaka, M., Kawasaki, K. and Higuchi, Y. (1994): Development of an earthquake simulator for the Taisei centrifuge, Proc. Centrifuge 94, pp. 151-156.
15) Pastsakorn, K., Hashizume, Y. and Matsumoto, T. (2002): Lateral load tests on model pile groups and piled raft foundations in sand, Proc. Int. Conf. Physical Modelling in Geomechanics, St. John's, Canada, pp. 709-714.
16) Placzek, D., Jentzsch, E. and Schulte, K. (2001): A contribution to the analysis and the design concept of piled raft foundations, Proc. 15th ICSMGE, Vol. 2, Istanbul, pp. 985-989.
17) Randolph, M. F. (1983): Design of pile raft foundations, Proc. Int. Symp. on Recent Developments in Laboratory and Field Tests and Analysis of Geotechnical Problems, Bangkok, pp. 525-537.
18) Randolph, M. F. (1994): Design methods for pile groups and piled rafts, Proc. 13th ICSMGE, Vol. 5, New Delhi, pp. 61-82.
19) Shinozaki, Y. Nishio, H., Kobayashi, Nagao, T. and Kuwabara, F. (1999): Study on the settlement behavior of piled raft foundations (Part 3), Summaries of Technical papers of Annual Meeting Architectural Institute of Japan: 731-732 (in Japanese).
20) Sommer, H., Tamaro, G. and DeBenedittis, C. (1991): Messe Turm, foundations for the tallest building in Europe, Proc. 4th Int. Conf. on Piling and Deep Foundations, pp. 139-145.

21) Thaher, M. & Jessberger, H. L. (1991): The behavior of Piled-raft Foundations, Investigated in Centrifuge Model Tests, Proc. Centrifuge 91, Colorado, Balkema, pp. 225-234.

22) Watanabe, T., Kobayashi, H., Nagao, T., Nagataki, Y., Majima, M. and Kuwabara, F. (2000): Horizontal loading tests of piled raft foundation , Vol. 33, Report of Taisei Research Institute, pp. 125-128 (in Japanese).

23) Watanabe, T., Fukuyama, H., Horikoshi, K. and Matsumoto, T. (2001): Centrifuge modeling of piled raft foundations subjected to horizontal Loads, Proc. 5th Int. conference on deep foundation practice incorporating PILETALK international 2001, Singapore, pp. 371-378.

CHAPTER 4

BEHAVIOR OF PILED RAFTS SUBJECTED TO DYNAMIC LOADS IN CENTRIFUGE TESTS

(*N.B.* This chapter was submitted to Int. Jour. of Physical Modelling in Geomechanics entitled "Performance of pile raft foundations subjected to dynamic loading", 2003)

ABSTRACT

A series of shaking table tests were conducted on piled raft foundations on sand by using geotechnical centrifuge. The results were compared with those obtained from the static horizontal loading tests of the same models which have been reported by Horikoshi et al. (2003). Effects of the rigidity at pile head connection on the dynamic behavior were examined. Also shown are the results of the dynamic loading test of a free-standing pile group with the same number of piles to examine the contribution of the load transferred through the raft base.

Principal findings from a number of studies on the dynamic behavior of piled raft foundations are: 1) The horizontal load-displacement relationships and the bending moment distributions agree well between the dynamic models and static models, and the proportion of the horizontal load carried by each component is highly dependent on the horizontal displacement of the piled raft system; 2) The horizontal stiffness of the piled raft with the hinged pile head connection was smaller than that of the piled raft with the rigid pile head connection; 3) The proportion of the vertical load carried by the piles does not change significantly during dynamic loading; 5) The inclination of the piled raft during the shaking is much smaller than that of the pile group due to the contribution of the soil resistance just beneath the raft.

Key words: centrifuge modeling, shaking table test, piled raft, pile group, load sharing, displacement, sand

4.1. INTRODUCTION

Piled raft foundations have been widely recognized as one of the most economical foundation systems. Since piles are used as settlement reducers in piled rafts, a number of studies on the settlement of piled raft foundations have been reported (for example, Poulos et al, 2001). These works have proved that the number of piles can be significantly reduced in piled raft foundations compared to the conventional pile groups. The static centrifuge modeling by Horikoshi et al., 2003 and the field experiments with relatively large models by Watanabe et al. (2000) have shown that piles play an important role in the behavior of piled raft foundations subjected to horizontal loads, even when the piles are designed principally as settlement reducers. However, the research on the dynamic behavior of piled rafts is still very limited (Horikoshi et al., 2001 & 2002; Mano et al. 2002)

Estimation of the behavior of piled rafts during earthquakes has become an important task in the design process especially in highly seismic areas such as Japan. Since a much smaller number of piles is installed in piled raft foundations, the performance such as load-displacement behavior and the load sharing between the piles and the raft base needs to be understood well.

Although piled raft foundations have already been applied to actual structures in Japan, most seismic designs of piled rafts were substantially treated as rafts alone by ignoring the existence of the piles as described by Horikoshi et al. (2003). Some design concepts of piled raft foundations are introduced in the latest codes and guidelines (Architectural Institute of Japan, 2001; Katzenbach, R. and Moormann, 2001), however, no detailed methods of design have been described. Considering the current trend towards performance-based design, it is essential to establish rational seismic design concepts for piled raft foundations through detailed observation of the dynamic. To this end, a series of dynamic centrifuge tests was carried out to examine the detailed dynamic behavior and to give useful information on the seismic designs of piled raft foundations. In the centrifuge modeling, the same piled raft models were used as the static modeling by Horikoshi et al. (2003).

Regarding the details of the piled raft designs, there is a discussion as to whether the pile head connection should be rigid or hinged. Since the main objective of the piles in piled rafts is to reduce the settlement of structures, a hinged or even detached pile head connection with the raft base may satisfy the required performance to reduce the settlement. In the present study, the influences of the rigidity of the pile head connection on the dynamic behavior are therefore investigated by designing rigidly fixed and hinged pile head connection models as demonstrated in the static modeling by Horikoshi et al. (2003).

The results of the dynamic loading tests are compared with those obtained from the static horizontal loading tests of the same piled raft models conducted by Horikoshi et al. (2003). Furthermore, a dynamic loading test on a free-standing pile group is performed to

investigate the contribution of the raft contact with the soil surface.

Note that model scale is used in the following results and discussions in this paper.

4.2. MODEL DESIGNS

4.2.1. Centrifuge package

The geotechnical centrifuge used in the present study was described in detail by Nagura et al. (1994). The effective radius of the centrifuge is 2.65 m. A centrifugal acceleration of 50 g was applied to a 1/50 model (here g denotes gravity).

Figure 4.1 shows schematic illustrations of the centrifuge package used for the dynamic centrifuge modeling of the piled raft foundations. Shaking table tests were conducted for two piled raft models with different pile head connection conditions, and the free-standing pile group model. A laminar box with a length of 560 mm, width of 210 mm and height of 400 mm was used. The dynamic responses of the models were measured by means of a number of accelerometers and laser displacement transducers.

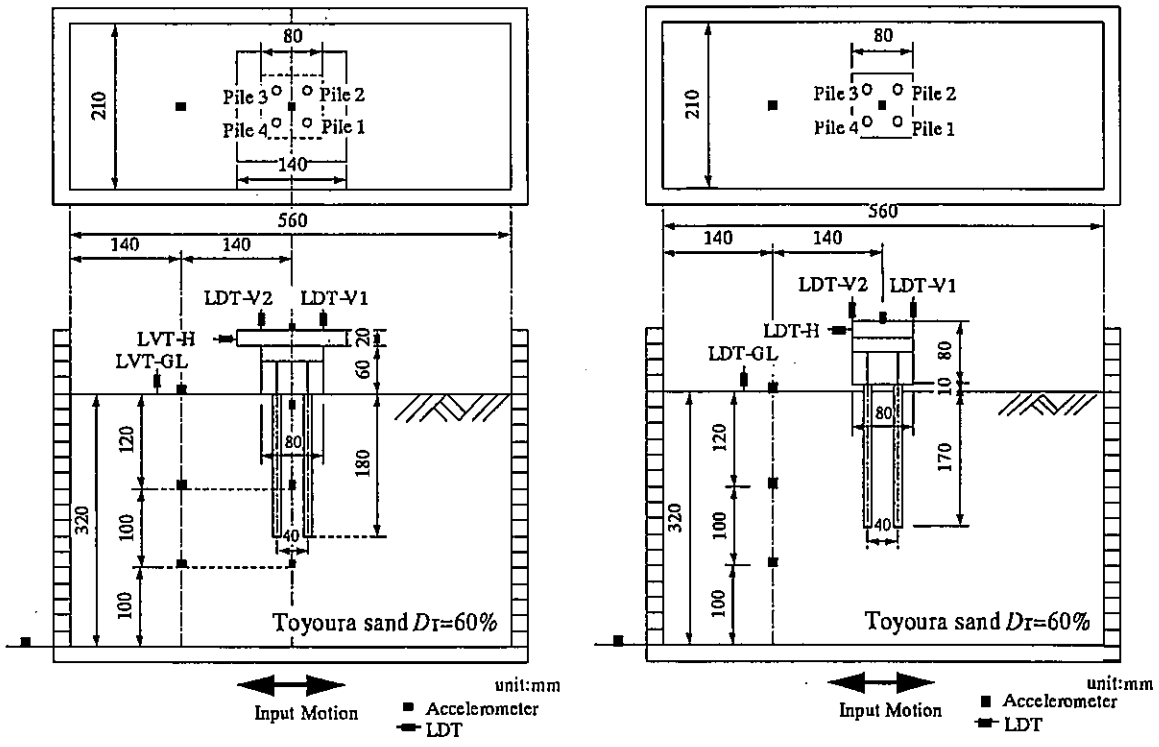

(a) Piled raft **(b) Free-standing pile group**

Fig. 4.1. Schematic figure of centrifuge package

4.2.2. Piled raft models

The same piled raft models as used for the static loading tests were used for the dynamic loading tests. Details of the static models were explained by Horikoshi et al. (2003).

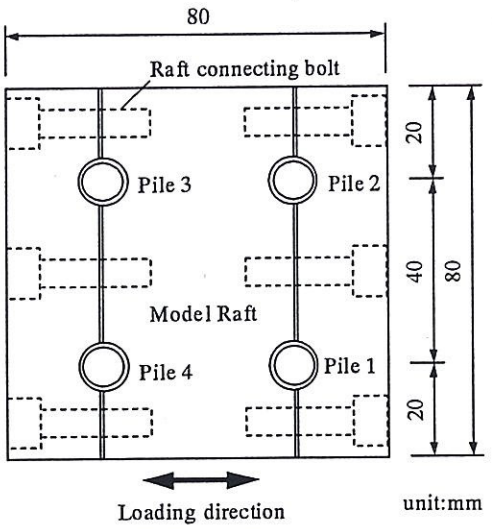

Fig. 4.2. Details of model raft with rigid pile head connection

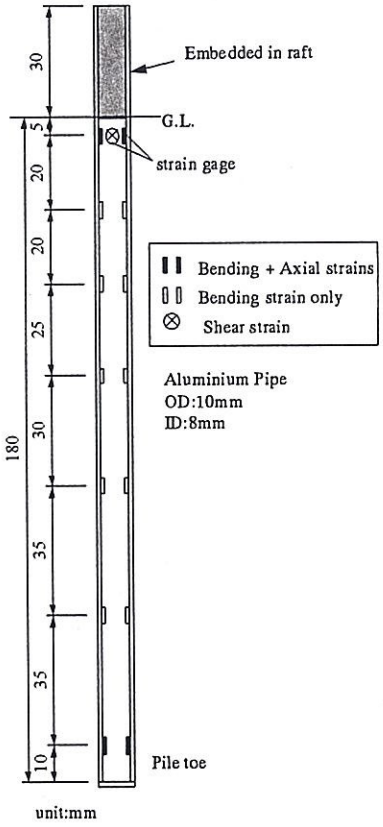

Fig. 4.3. Details of pile used for rigid pile head connection

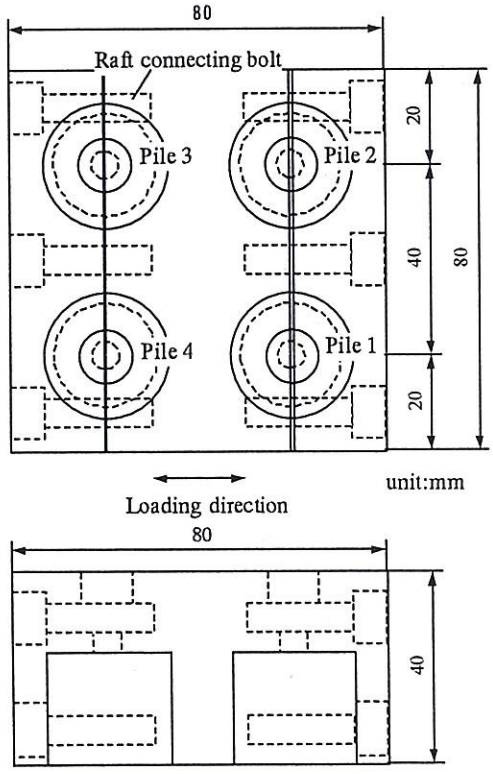

Fig. 4.4. Details of model raft with hinged pile head connection

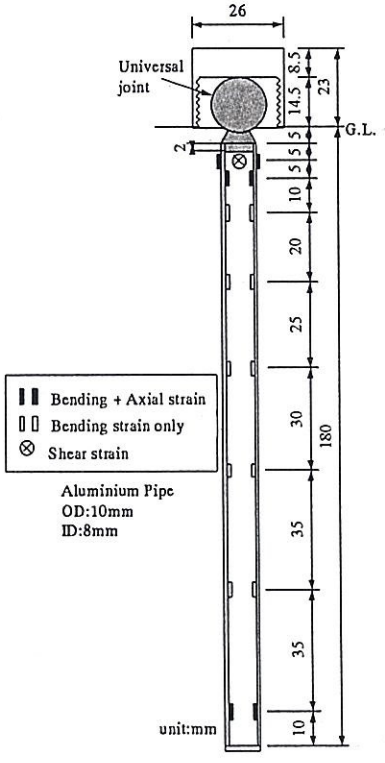

Fig. 4.5. Details of pile used for hinged pile head connection

Table 4.1. Properties of model pile and corresponding prototype pile

	Centrifuge model	Prototype
Material	Aluminum	Concrete
Diameter	10mm	500mm
Wall thickness	1mm	Solid
Pile length, L_p	180mm/170mm	9.0m/8.5m
Young s modulus, E_p	71 GN/m^2	41.7GN/m^2
Cross-sectional rigidity, E_pA_p	2.0×10^{-3} GN	5.0 GN
Bending rigidity, E_pI_p	2.0×10^{-8} GNm^2	0.13 GNm^2

Figures 4.2 and 4.3 show the plan view of the piled raft model with the rigid pile head connection, and the details of the model pile respectively. **Figures 4.4 and 4.5** show the models with the hinged pile head connection. Commercially available universal joints (THK Corp., type TBS8) were attached at each pile head for the hinged pile head connection model.

Square rafts with a width of 80 mm (4 m at prototype scale) were made of aluminum plates. The raft mass was set at 4.69 kg, and the raft base was roughened to increase the frictional resistance between the base and the sand. The coefficient of interface friction was observed as 0.423 from static loading tests of the raft alone (Horikoshi et al., 2003).

The properties of the model pile are summarized in **Table 4.1**, which are the same as those designed in the static loading. The model pile is approximately equivalent to a solid concrete pile with a diameter of 500 mm at prototype scale. Note that the strength of the prototype concrete pile was not modeled, since different materials were used between the model and the prototype. It was confirmed that the pile stress was below the yield point (149 MN/m^2) during the shaking table tests. The pile was instrumented with foil strain gages mainly inside the aluminum tube as shown in **Figures 4.3 and 4.5** to obtain axial forces and bending moments along the pile shaft, and the shear force at the pile head.

For the dynamic loading test of the free-standing pile group, the piled raft model with rigid connection was used by allowing a gap of 10 mm between the raft base and the soil surface. This led to a slightly shorter embedment pile length of 170 mm for the pile group model, which compares with 180 mm for the piled raft model.

4.2.3. Model ground

As for the model ground, air-pluviated dry Toyoura sand was prepared throughout the present study. The physical properties of the Toyoura sand are summarized in **Table 4.2**. The relative density of the sand was 60-63% after applying the centrifugal acceleration of 50 g before the shaking table test.

Table 4.2. Properties of Toyoura sand

Property	Value
Density of soil particle, ρ_s (t/m^3)	2.661
Mean grain size, D_{50} (mm)	0.162
Maximum dry density, ρ_{dmax} (t/m^3)	1.654
Minimum dry density, ρ_{dmin} (t/m^3)	1.349

Before the shaking table tests, the distribution of the soil strength and its repeatability were examined by an in-flight miniature cone penetrometer with a diameter of 10 mm and an apex angle of 60 degrees. The penetration rate was set at 1.0 mm/s. The measured tip resistances, q_c, are summarized in **Figure 4.6** from all the dynamic tests conducted for the present study. It can be seen that the variation in the q_c values was slightly higher in a deeper soil. Also noted is that the resistance measured at a deeper soil was smaller compared with that measured in the same properties of the soil in the rigid box which was used for static loading tests of the same piled raft models (Horikoshi et al, 2003). Since the space on the soil surface for the cone penetration tests was very limited with the existence of the piled raft model in the laminar box, there might be some effects of the sidewall boundary where rubber membrane was attached. However, the q_c values at shallower depths, which are more important in the horizontal resistance of the piles, were almost the same between the model grounds for the static model and for the dynamic model, and so it was considered that the difference in the model grounds between the static model and the dynamic model was small.

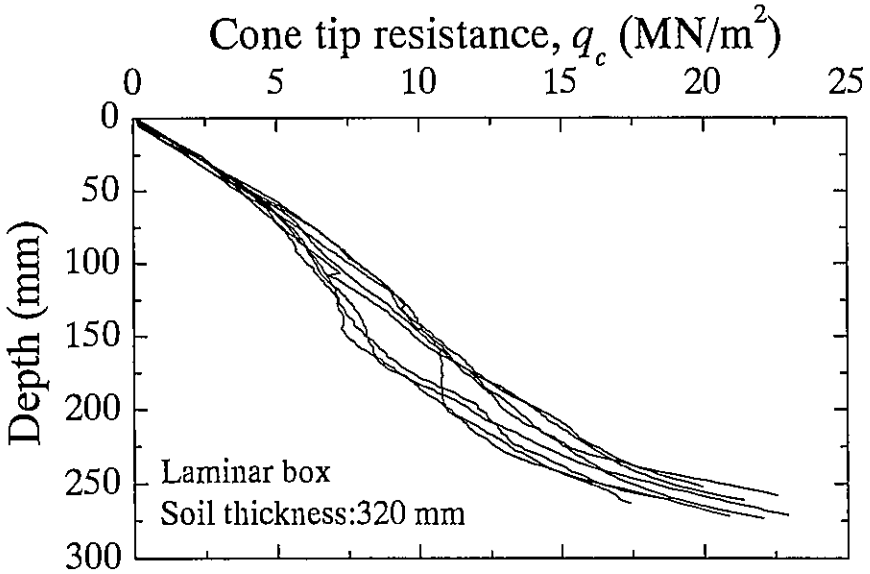

Fig. 4.6. Profiles of cone tip resistance

Table 4.3. Experimental cases and their conditions

Model Type	Loading direction		
	Vertical loading (see Horileshi et al. 2003)	Horizontal loading (see Horileshi et al. 2003)	Dynamic loading (present study)
Single Pile	L_p = 250mm L_d = 120, 170, 200 mm h = 505 mm	L_p = 250mm L_d = 170 mm h = 440 mm	
Raft (alone)	B = 80, 120 mm M_r = 0.36 kg h = 470 mm	B = 80 mm M_r = 4.69 kg h = 460 mm	
Piled Raft	L_p = 170 mm B = 80 mm, 120 mm M_r = 0.90 kg h = 470 mm	L_p = 180 mm B = 80 mm M_r = 4.69 kg h = 460 mm Rigid or hinged pile head conditions	L_p = 180 mm B = 80 mm M_r = 4.69 kg h = 320 mm Rigid or hinged pile head conditions
Free-standing Pile group			L_p = 180 mm L_d = 170 mm B = 80 mm M_r = 2.35 kg h = 320 mm Rigid pile head conditions

L_p: Pile length, L_d: Embedment length, B: Square raft width, M_r: Mass of raft, h: Soil thickness

4.2.4. Test procedure

The test procedures for the dynamic loading tests are as follows:

1) Set four model piles at the corresponding positions using an adjusting apparatus,
2) Pour dry sand into the laminar box,
3) Apply centrifugal acceleration up to 50 g to allow for self-weight settlement of the soil and the piles,
4) Check soil strength distribution through cone penetration tests,
5) Place model raft on sand after halting the first flight,
6) Connect the model raft and the piles, and place added mass on the raft,
7) Set all instrumentations, and apply centrifugal acceleration up to 50 g again, and
8) Apply horizontal load to the piled raft.

4.3. TEST CASES

In the present study, three dynamic loading tests, i.e. two tests on the piled rafts and one on the free-standing pile group, were carried out as summarized in **Table 4.3**, in addition to the static vertical and the static horizontal loading tests of the piled rafts and their components that have already been reported by Horikoshi et al. (2003). One of the main objectives of the dynamic loading tests is to compare and to confirm the behavior with that observed in the static loading tests. Note that the test conditions such as the model configurations and the intended soil conditions are the same between the static and the dynamic models except for the container size and the loading conditions. The soil thickness was set at 320 mm in the shaking table test as shown in **Figure 4.1**, which compares with 460 mm for the static models. It was considered that the influence of the soil thickness on the horizontal behavior of the piled raft was small since the loading direction was horizontal and the soil profiles within the pile embedment length were almost the same. Since the laminar box allows for shear deformation of model ground, the effects of the sidewalls on the horizontal behavior of the model were thought to be very small.

4.4. SHAKING TABLE TESTS OF PILED RAFT FOUNDATIONS

In this section, the results of the dynamic loading tests are presented both for the rigid connection model and the hinged connection model, in comparison with the behavior obtained from the static loading tests.

4.4.1. Vertical load sharing during period of increasing g level

In the present study, the vertical load was applied by using the raft mass as discussed by Horikoshi et al. (2003). **Figure 4.7** shows the profiles of the vertical load sharing with increasing centrifugal acceleration for both piled raft models. The piled raft models settled about 3 mm due to the self-weight. Since the raft mass was 4.69 kg, the vertical load applied to the raft base at 50 g was calculated to be about 2,298 N.

At 50 g, the piles carried 40% and 45% of the total load for the rigid connection model and the hinged connection model, respectively, which were almost the same as for the static model.

4.4.2. Input acceleration to model

Figure 4.8 shows the input acceleration measured at the base of the model. A sinusoidal wave with an amplitude of 50 m/s^2 (100 gal at the prototype scale) and a frequency of 50 Hz (1 Hz at the prototype scale) was applied to the model.

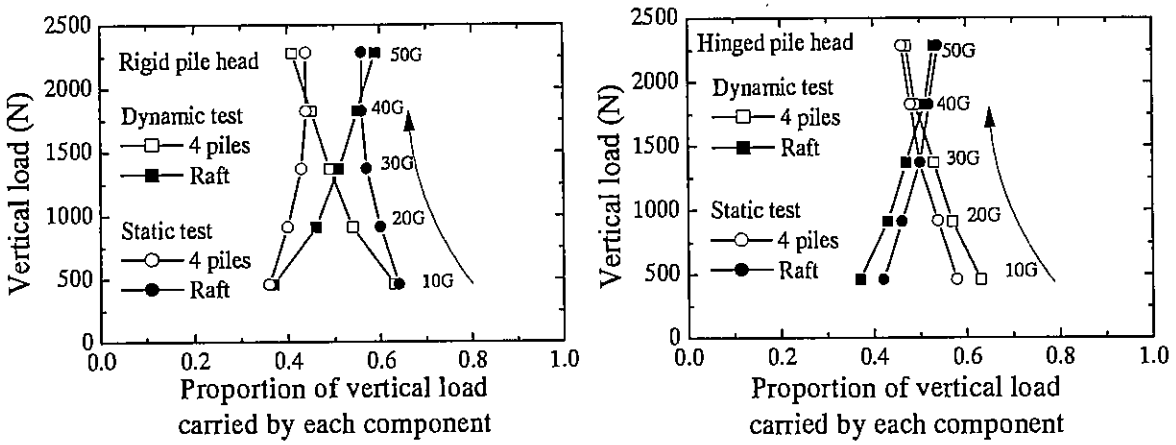

(a) Rigid connection model **(b) Hinged connection model**

Fig. 4.7. Proportion of vertical load carried by each component during the stage of increasing in g level to 50 g

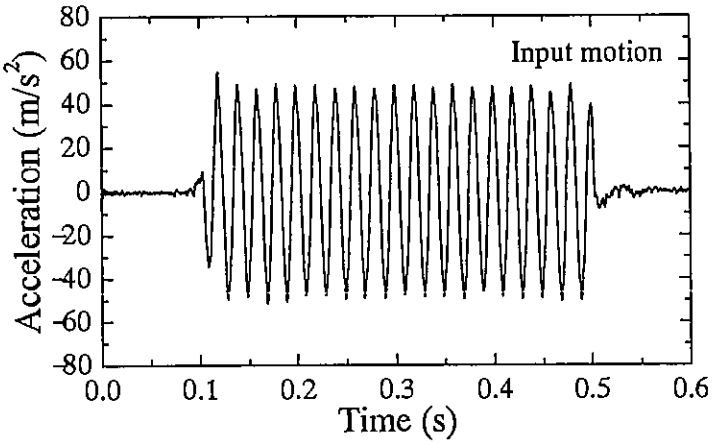

Fig. 4.8. Time history of input acceleration

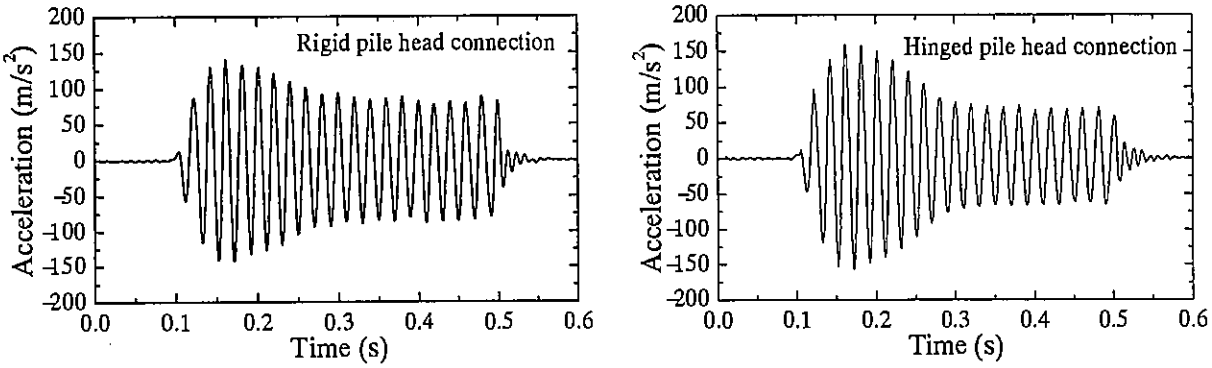

(a) Rigid connection model **(b) Hinged connection model**

Fig. 4.9. Acceleration responses measured on piled raft models

4.4.3. Dynamic responses of piled rafts

Figure 4.9 shows the time history of the horizontal acceleration observed on the piled raft model. The peak values were 135 m/s^2 and 160 m/s^2 for the rigid connection model and the hinged connection model, respectively. The reason for the higher amplitude by about 20% in the hinged connection model was thought to be related to the difference in the structural flexibility between the two models. It is of interest that, after reaching the peak value, the acceleration decreased with time and became an almost stable state in each model.

Figure 4.10 shows the time history of the horizontal displacement. The amplitude of the displacement also decayed with time as observed in the acceleration response. Residual displacements of about 0.4 mm were observed in both piled rafts, even though sinusoidal input waves were applied. This was thought to be due to the effects of non-linear load–displacement characteristics of the models and some uncertainty introduced during the model preparation. Considering that the conventional design of pile foundations allows only for a displacement of less than 1% of pile diameter and 15 mm (for example, see Japan Road Association (2002)), the centrifuge modeling gave sufficiently large displacement to the piled raft model.

The settlements of the piled raft and the ground surface during shaking are shown in **Figure 4.11**, together with the relative settlement between the model and the ground surface. The settlements of the ground surface in both tests were consistent. However, the final settlement of the hinged connection model was 20% larger than that of the rigid connection model.

Figure 4.12 compares the amplitude of the horizontal displacement in each cycle with the profiles of the relative settlement. The piled rafts settled rapidly during the first several cycles of the shaking. It can be seen that the relative settlements clearly correspond to the amplitude of the horizontal displacements. It can therefore be considered that the attenuation of the horizontal displacement was caused by the increase in the relative settlement, i.e. increase in the embedment of the raft into the ground.

The horizontal load-displacement behavior is compared with that observed in the static test in **Figure 4.13**. The horizontal load in the dynamic test was calculated as the product of the raft mass and the acceleration measured on the raft. The figure shows that the overall load-displacement behavior was consistent between the static and the dynamic tests, although the loading-unloading hysteresis curves shifted gradually in the dynamic tests due to the occurrence of the residual displacement. In the static tests, the horizontal stiffness was calculated as 1786 N/mm and 1264 N/mm for the rigid connection model and the hinged connection model, respectively.

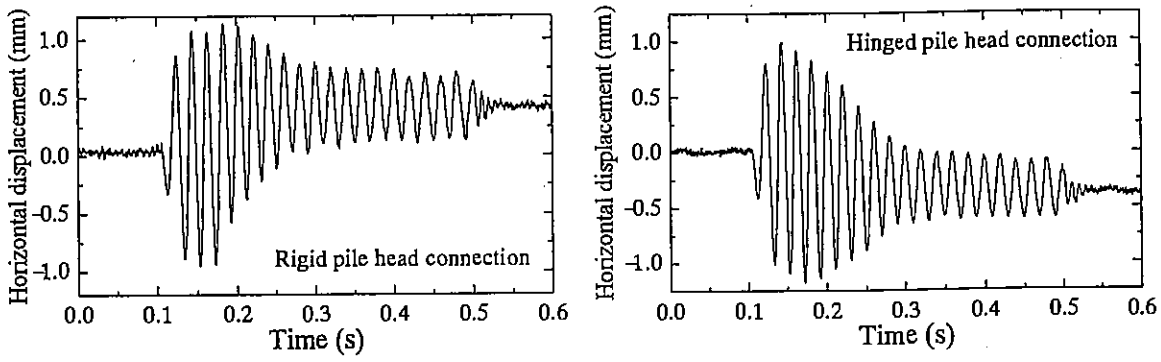

(a) Rigid connection model (b) Hinged connection model

Fig. 4.10. Horizontal displacement of piled rafts during shaking period

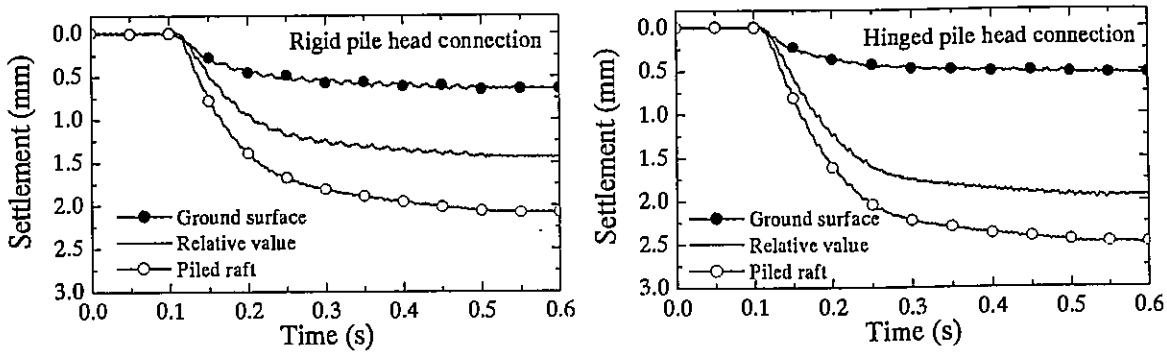

(a) Rigid connection model (b) Hinged connection model

Fig. 4.11. Settlement of piled rafts and ground surface during shaking period

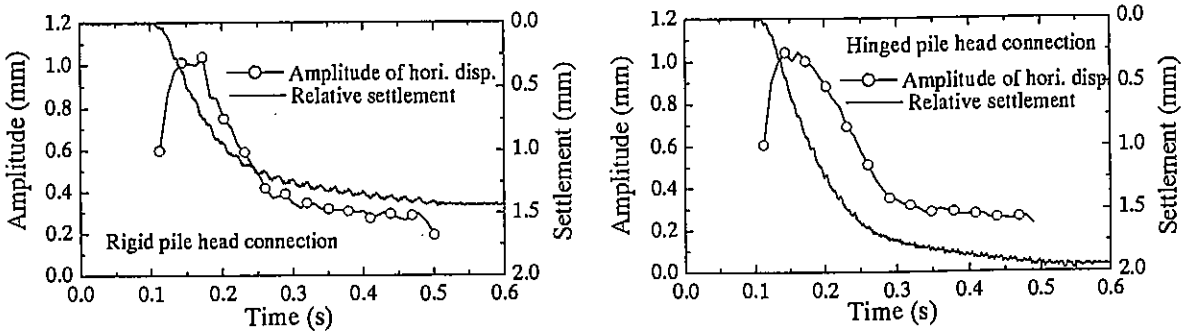

(a) Rigid connection model (b) Hinged connection model

Fig. 4.12. Amplitude of horizontal displacement in comparison with relative settlement of piled raft model

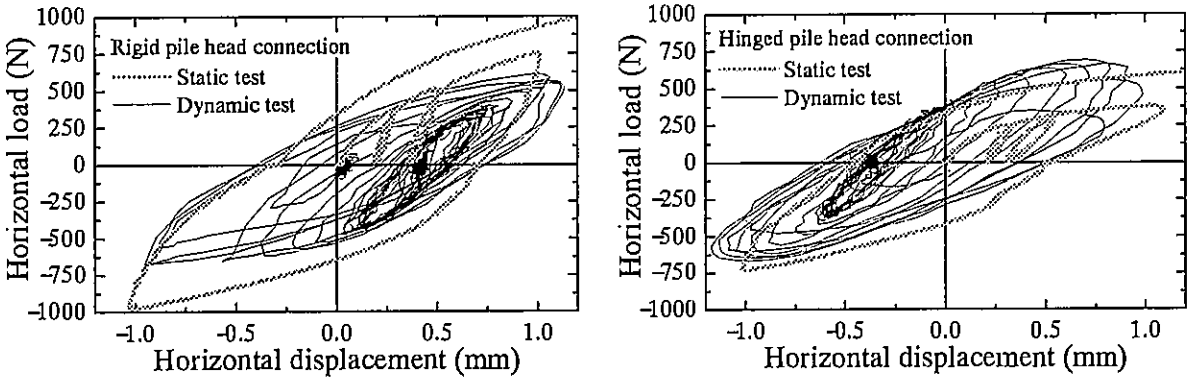

(a) Rigid connection model **(b) Hinged connection model**

Fig. 4.13. Horizontal load displacement relationships of piled rafts compared with results of static tests

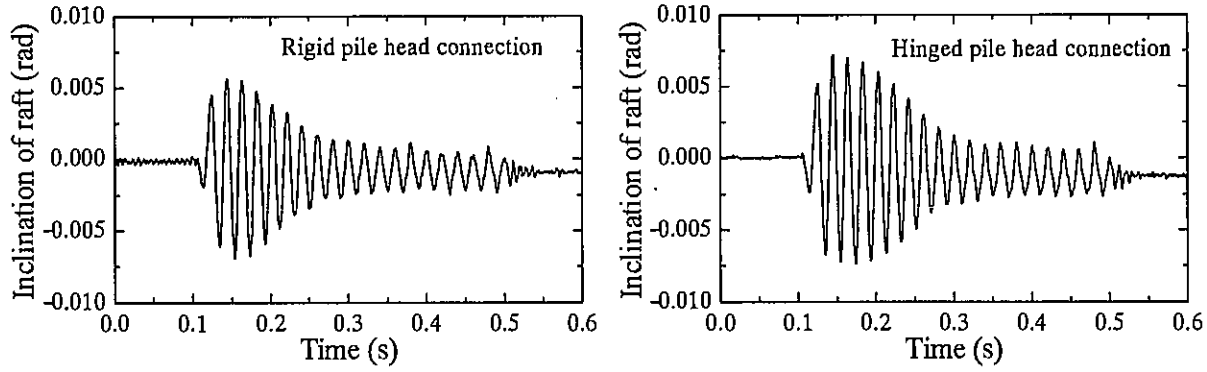

(a) Rigid connection model **(b) Hinged connection model**

Fig. 4.14. Inclination of piled rafts during shaking period

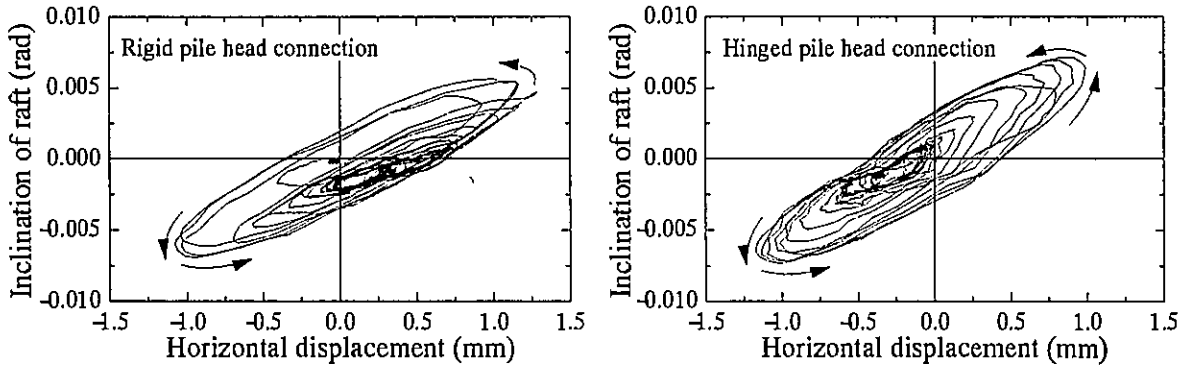

(a) Rigid connection model **(b) Hinged connection model**

Fig. 4.15. Relationship between inclination and horizontal displacement of piled raft

Figure 4.14 shows the inclination of the raft in the piled raft model by taking clock-wise inclination as positive. The inclination was calculated from the vertical displacements measured by the two laser displacement transducers (LDT-V1 and LDT-V2 in **Figure 4.1**). The figures show the rocking motions and the amplitude of the inclination in each cycle attenuated with time as was seen in the horizontal acceleration and the displacement responses. The relationship between the horizontal displacement and the inclination is shown in **Figure 4.15**. It seems that the point at a peak horizontal displacement coincides to the point at peak raft inclination in the rigid pile head connection model, whereas both did not coincide in the hinged connection model. The raft inclination becomes peak value after the peak of the horizontal displacement in the hinged pile head model.

Figure 4.16 shows the time history of the proportion of the horizontal load carried by the four piles. Overall, it seems that the proportion is higher in the rigid connection model as also shown in **Figure 17**. A rapid increase in the load carried by the piles during the initial stage of the shaking was observed in both piled rafts.

The profiles of the proportion of the load carried by piles obtained from the dynamic loading tests, are compared with the results obtained from the static loading tests in **Figure 4.17**. The results from the dynamic tests and the static loading tests were consistent in both piled rafts.

Figure 4.18 shows the profiles of the bending moment distributions along the pile shaft observed in the static and dynamic tests. The applied horizontal load of 600 N (26 % of the raft weight) was chosen for both the models for comparison. In the shaking table tests, unlike the static loading where only the upper structure is loaded, the ground itself has a dynamic displacement response which can influence the structural. However, since the mass of the raft model is relatively large, inertia effects seem to be much dominant compared with the kinematic effects, thus the dynamic responses were similar to the static responses.

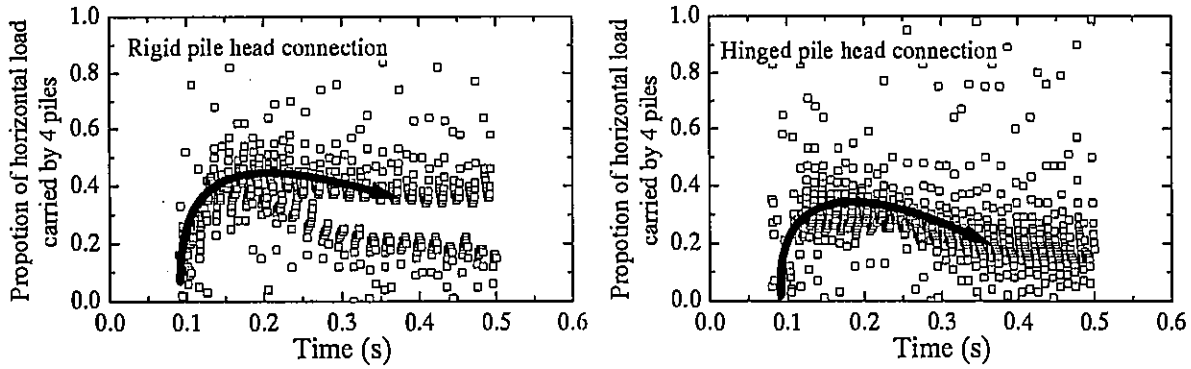

(a) Rigid connection model **(b) Hinged connection model**

Fig. 4.16. Proportion of horizontal load carried by 4 piles during shaking period

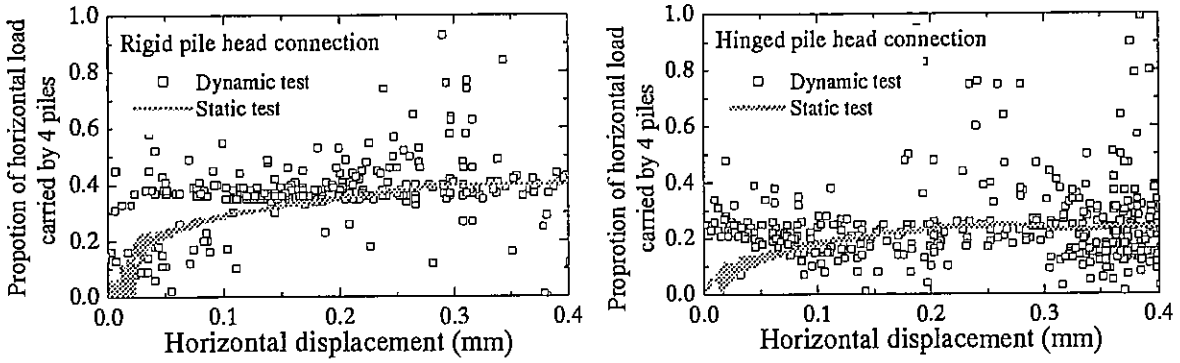

(a) Rigid connection model **(b) Hinged connection model**

Fig. 4.17. Proportion of horizontal load carried by 4 piles during shaking period in comparison with results of static tests

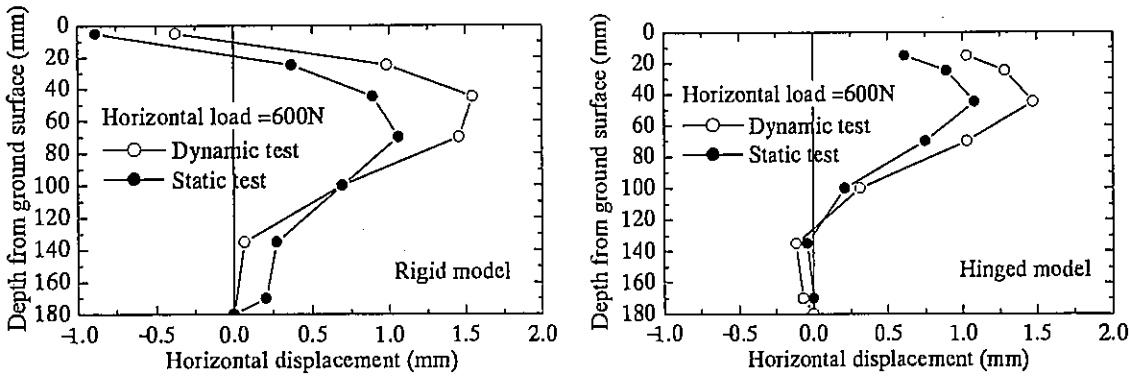

(a) Rigid connection model **(b) Hinged connection model**

Fig. 4.18. Distributions of bending moment along pile shaft

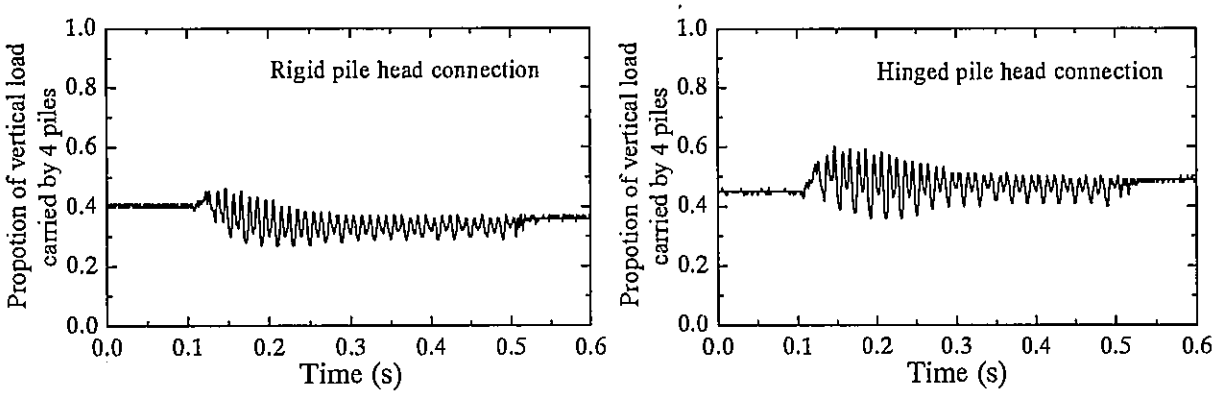

(a) Rigid connection model **(b) Hinged connection model**

Fig. 4.19. Proportion of vertical load carried by 4 piles during shaking period

Figure 4.19 shows the proportion of the vertical load carried by the piles during the shaking period. The load carried by the piles did not change significantly before and after the shaking.

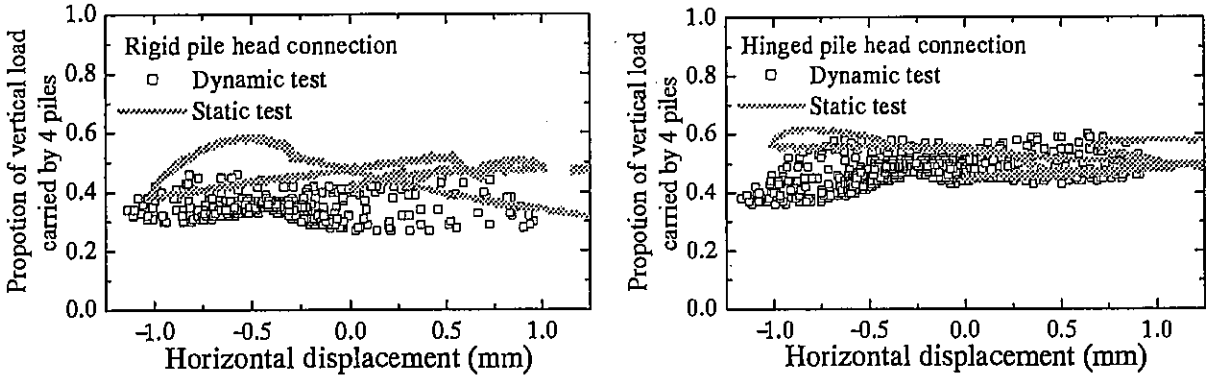

(a) Rigid connection model **(b) Hinged connection model**

Fig. 4.20. Proportion of vertical load carried by 4 piles in comparison with results of static tests

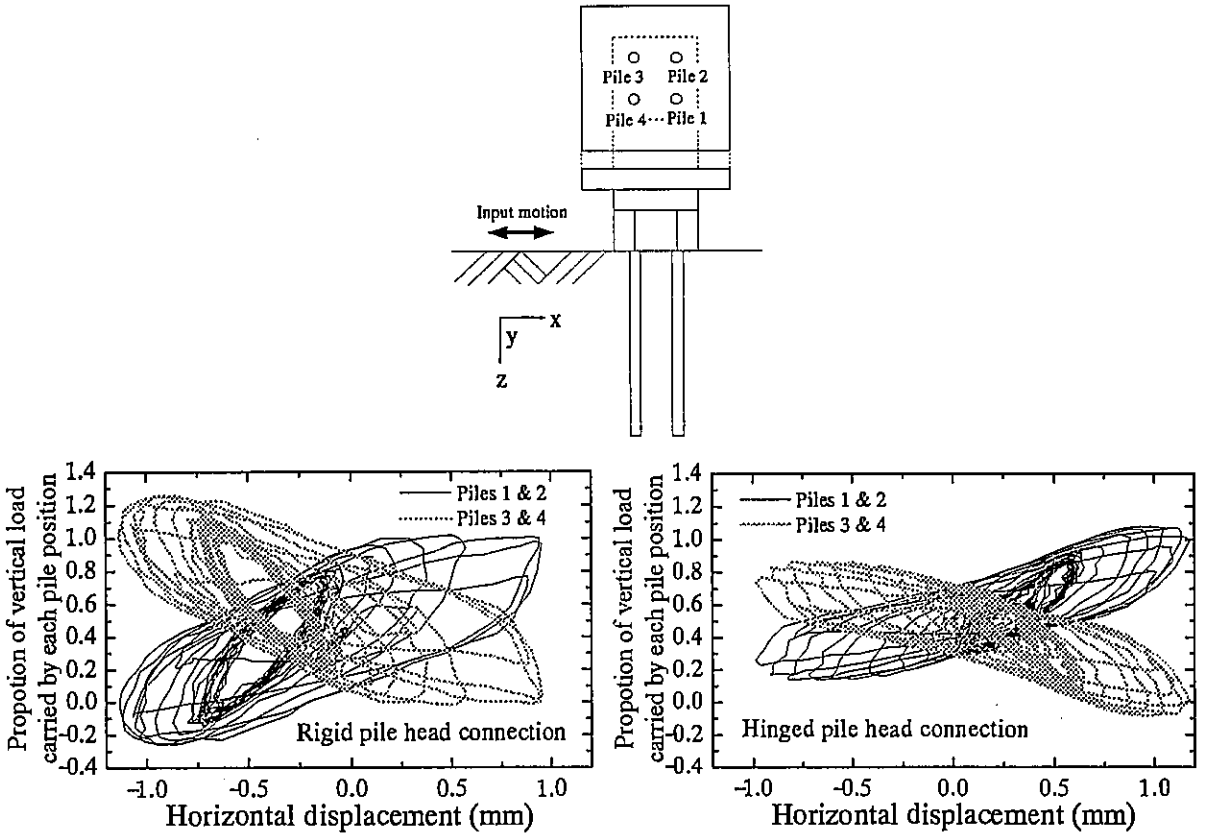

(a) Rigid connection model **(b) Hinged connection model**

Fig. 4.21. Proportion of vertical load carried by piles at different pile positions

The vertical load sharing is compared with that obtained from the static tests in **Figure 4.20.** The figure also shows the consistent trend between the dynamic and static loading tests.

Figure 4.21 shows the proportion of the vertical load carried by each pile position in the piled raft model. Since piles 1 & 2 and 3 & 4 are located in the same position, the results are summarized according to their positions.

It can be seen that piles 1 & 2 carried a larger load when the horizontal displacement was positive, while piles 3 & 4 carried a larger load when the horizontal displacement was negative. Interestingly, the degree of change in the axial load was more significant in the rigid connection model compared with that observed in the hinged connection model. This means that the piles in the hinged connection model tended to carry more uniform vertical load within the group. A similar trend was observed in the static horizontal loading tests of the piled rafts (Horikoshi et al., 2003).

4.4.4. Shaking Table Tests with higher input motion

It was considered that the proportion of the vertical load carried by piles after strong seismic motion might be another interest among engineers, since a change in the proportion could lead to further settlement of structures during the service life. An attempt was made to apply another shaking to the same model just after the first shaking described in the previous section. The magnitude of the input acceleration was increased to 150 m/s^2, which was three times higher than that applied in the first test.

The soil surface settled about 2.1 mm and 2.9 mm, and the relative settlements between the model and the soil surface was were 3.5 mm and 4.8 mm in the rigid connection model and the hinged connection model, respectively. The observed vertical load sharing is shown in **Figure 4.22.** The figures indicate that the change in the proportion of the vertical load carried by the piles before and after the shaking was still relatively small, although the amplitude of the proportion during the shaking period became larger compared with that shown in **Figure 4.19** for smaller input motion. The centrifuge result is consistent with the observation by Yamada et al. (2001) before and after the Hyogoken-Nambu Earthquake, in which the pile forces, earth pressures and pore pressures at the foundation slab of a 12-story building were measured in Osaka from 1991 to 1996.

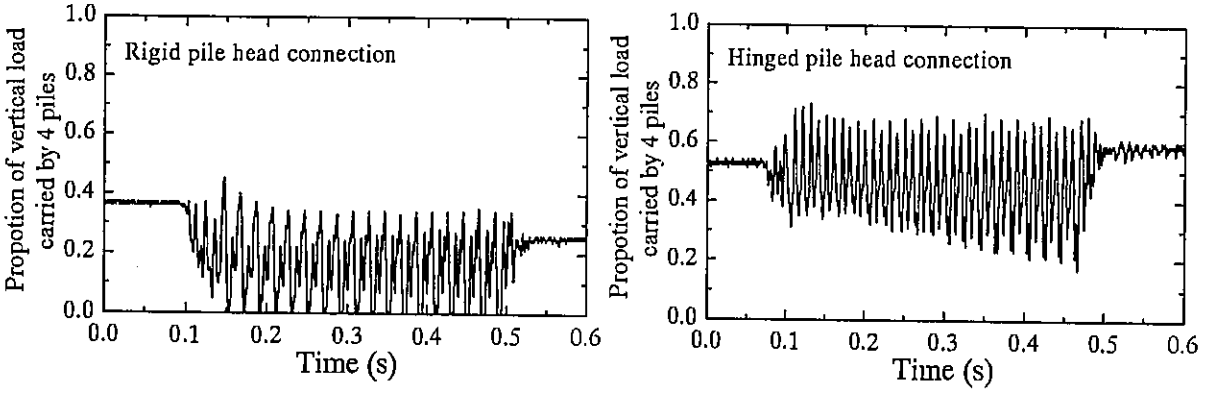

(a) Rigid connection model **(b) Hinged connection model**

Fig. 4.22. Proportion of vertical load carried by 4 piles for higher input motion

4.4.5. Shaking table test of free-standing pile group

During the series of tests, the contribution of the raft contact with soil to the dynamic response of the model was examined by conducting another shaking table test of a free-standing pile group. The piled raft model with the rigid head connection was used by allowing a gap of 10 mm between the raft base and the soil as shown in **Figure 4.1(b)**. Considering the fact that the vertical loading test of the same single pile indicated the vertical resistance of about 400 N taking the load at a settlement of 10 % of the pile diameter (see Horikoshi et al. 2003), as many as 15 piles are required to support the weight of the upper structure if a conventional safety factor of 3 is applied. It should therefore be noted that the aim of the shaking table test of the free-standing pile group was to compare the behavior with that observed in the piled raft system of the same geometries, rather than to examine the behavior of the conventional pile group. The initial vertical load applied to four piles was set at the same condition as the piled raft model. Since the proportion of the vertical load carried by the piles was 40-45% in the piled rafts (see **Figure 4.7**), the raft mass of 2.35 kg (about a half of the raft mass for the piled raft) was applied to the model. Note that the height of the gravity center was almost the same between the piled raft model, and the pile group model. During the stage of increasing the g level to 50 g, the gap between the raft base and the ground surface was reduced to 8.4 mm from 10 mm due to the model settlement. The same input motion as shown in **Figure 4.8** was then applied to the model.

Figure 4.23 shows the measured horizontal accelerations on the pile group. Unlike the behavior observed in the piled raft model (**Figure 4.9(a)**), no attenuation was observed in the response. Even though the mass of the upper structure was about half in the pile group model, the acceleration response was much higher. The difference in the acceleration response indicates the significant contribution of the raft contact with the soil surface. **Figures 4.24** and **4.25** show the settlement and the inclination of the free-standing pile group. These figures also show much larger settlement and the inclination in the free-standing pile group, indicating that the contribution of the raft base in the piled raft system was significant.

Figure 4.26 compares the distribution of the bending moments along the pile shafts with those measured in the piled raft model for the same horizontal load of 400 N. The maximum bending moment of the pile in the piled raft was significantly reduced to about one fourth of that in the free-standing pile group, indicating a large contribution of the raft also in reducing the bending moments in the pile.

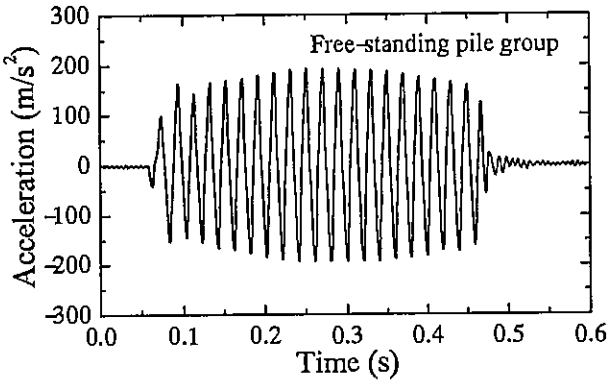

Fig. 4.23. Acceleration response measured on free-standing pile group model

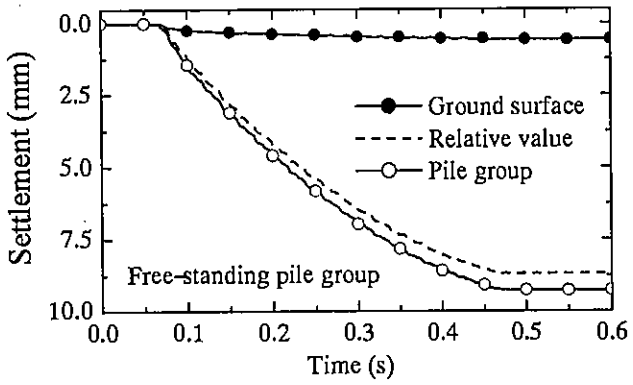

Fig. 4.24. Settlement of the free-standing pile group during shaking period

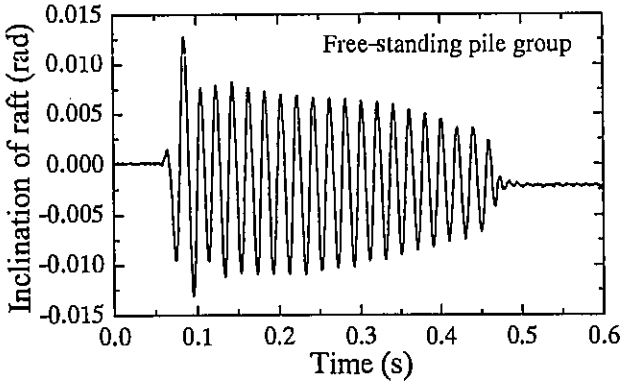

Fig. 4.25. Inclination of the free standing pile group during shaking period

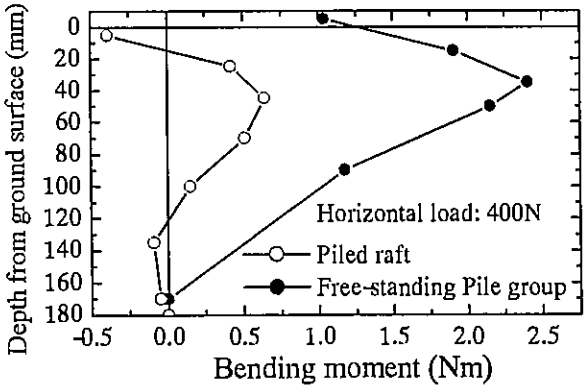

Fig. 4.26. Distributions of bending moments along pile shaft

4.5. CONCLUSIONS

A series of dynamic centrifuge tests was conducted for the piled raft and the free-standing pile group models. The influences of pile head connection with the raft base were also examined. The results provided various information on the dynamic piled raft behavior which has not been well examined. The following findings were obtained from the present study:

1) In the piled raft designs, evaluation of the displacement (settlement, horizontal displacement, and inclination) and the proportion of the load carried by the components are the most important factors. The dynamic behaviors of the above factors were intensively examined in this paper.
2) As was also shown in the static modeling by the authors, the dynamic tests also indicate that the proportion of the horizontal load carried by each component is highly dependent on the horizontal displacement of the piled raft system. The evaluation of horizontal displacement is therefore important in the seismic design of piled rafts.
3) The change in the vertical load sharing between the piles and the raft base was relatively small compared with the horizontal load, even when the piled rafts were subjected to relatively strong input motion.
4) As far as the model conditions in the present study are concerned, the rigid pile head connection gave higher horizontal stiffness than the hinged pile head connection. The acceleration response and the inclination of the model were also smaller in the rigid pile head connection model.
5) The proportion of the horizontal load carried by the piles was smaller in the hinged pile head connection model, indicating the role of piles in the horizontal resistance of the piled raft was smaller in the hinged pile head connection model.
6) According to the comparison of the behavior between the piled raft and the free-standing pile group, the contact of raft base with the soil surface played highly important roles in reducing the horizontal acceleration, the inclination, and the bending moments of the piles.

ACKNOWLEDGEMENTS

This study was supported by a Grant-in-Aid for Scientific Research (Grant No. 12450188) of the Japanese Ministry of Education, Culture, Sports, Science and Technology.

The author thanks Mr. Yoshimasa Handa, Taisei Service Corp., for his special support in carrying out the centrifuge tests.

REFERENCES

1) Architectural Institute of Japan (2001): Recommendations for Design of Building Foundation (in Japanese).
2) Horikoshi, K., Matsumoto, T., Hashizume, Y., Watanabe, T. and Fukuyama, H. (2003): Performance of pile raft foundations subjected to static horizontal loads, Int. Jour. of Physical Modelling in Geomechanics (submitted).
3) Horikoshi, K., Matsumoto, T., Fukuyama, H. and Watanabe, T. (2001): Behavior of piled raft foundations subjected to horizontal loads, Proc. 46th JGS Geotechnical Symposium, pp. 241-246 (in Japanese).
4) Horikoshi, K., Watanabe, T., Fukuyama, H. and Matsumoto, T. (2002): Behavior of piled raft foundations subjected to horizontal loads, Proc. Int. Conf. on Physical Modelling in Geotechnics, St. John's, Canada, pp.715-721.
5) Japan Road Association (2002): Specifications for Highway Bridges, Part IV Substructures .
6) Katzenbach, R. & Chr. Moormann (2001): Recommendations for the design and construction of piled rafts, Proc. 15th ICSMGE, Istanbul, Vol. 2, pp. 927-930.
7) Mano, H., Nakai, S., Takanashi, K. and Ishida, R. (2002): Static dynamic tests of a piled raft foundation subjected to horizontal loading, Proc. 11th Japan Earthquake Engineering Symposium, pp.1143-1148 (in Japanese).
8) Nagura, K., Tanaka, M., Kawasaki, K. and Higuchi, Y. (1994): Development of an earthquake simulator for the Taisei centrifuge, Proc. Centrifuge 94, pp. 151-156.
9) Pastsakorn, K., Hashizume, Y. and Matsumoto, T. (2002): Lateral load tests on model pile groups and piled raft foundations in sand, Proc. Int. Conf. Physical Modelling in Geomechanics, St. John's, Canada, pp. 709-714.
10) Poulos, H. G., Carter, J. P. and Small, J. C. (2001): Foundations and retaining structures-Research and practice, Proc. 15th International Conference on Soil Mechanics and Geotechnical Engineering, Istanbul, Vol. 4, pp. 2527-2606.
11) Watanabe, T., Kobayashi, H., Nagao, T., Nagataki, Y., Majima, M. and Kuwabara, F. (2000): Horizontal loading tests of piled raft foundation , Vol. 33, Report of Taisei Research Institute, pp. 125-128 (in Japanese).
12) Yamada, T., Yamashita, K., Kakurai, M., Tsukatani, H. (2001): Long-term behaviour of tall building on raft foundation constructed by top-down method, Proc. 5th Int. conference on deep foundation practice incorporating PILETALK international 2001, Singapore: 411-417.

CHAPTER 5

SHAKING TABLE TESTS ON MODEL PILED A RAFT AND A PILE GROUP AT 1-G GRAVITATIONAL FIELD

(*N.B.* This chapter was submitted to BGA Int. Conf. on Foundations, Dundee, Scotland, 2003, entitled "Experimental study on behavior of model piled raft foundations in sand using shaking table at 1-g gravitational filed" by Fukumura, Matsumoto, Ohno & Hashizume.)

5.1. INTRODUCTION

Piled raft foundations have been widely recognized as an economical and rational type of pile foundations when they are subjected to vertical loading, because the vertical load is supported by the raft as well as the piles, resulting in smaller settlements with a reduced number of piles compared to pile groups (for examples, Poulos & Davis 1980, Randolph 1994, Horikoshi & Randolph 1999, and Katzenbach & Moorman 2001).

In highly seismic areas such as Japan, estimation of the behavior of pile groups and piled rafts subjected to lateral loading or seismic loading becomes a vital issue in seismic design of pile foundations. Behavior of model piled rafts and model pile groups subjected to static horizontal loads have been intensively investigated in 1-g field model tests (Pastsakorn, Hashizume & Matsumoto, 2002) and in centrifuge tests (Horikoshi, Watanabe, Fukuyama & Matsumoto 2002). These test results show that piled rafts are also economical and rational foundations even for static horizontal loading. Horikoshi *et al.* (2002) also conducted dynamic loading tests of model piled rafts in centrifugal field. However, the number of the tests is limited, because the centrifuge test needs higher cost and time.

The authors conducted shaking table tests of model pile foundations at 1-g gravitational field in parallel with the above-mentioned tests. In this paper, the shaking table tests of a model piled raft and a model pile group at 1-g gravitational field were conducted to investigate the behavior of those models subjected to dynamic (seismic) loads. Static horizontal loads tests of the model piled raft and the model pile group were also carried out to compare the test results with the results of the shaking table tests.

5.2. SIMILITUDE FOR SHAKING TABLE TESTS IN I-G GRAVITATIONAL FIELD

It is important to take the similitude rule into account, to deduce the behavior of a prototype structure from the behavior of the corresponding model. Iai (1989) proposed the similitude rule for the shaking tests at 1-g field. His proposal is briefly reviewed below. Let λ be the geometrical scaling factor (prototype size / model size). Then, the scaling factor for stress, λ_σ, is given by the following relation in the case where the same soil as the prototype soil is used for the model ground, since the gravity accelerations in the prototype and the model are identical equal to 1-g:

Table 5.1. Similitude for model test (Iai, 1989).

Items	prototype / model	
	1-g filed	Centrifuge
Length (Size)	λ	λ
Density	1	1
Stress	λ	1
Strain	$\lambda^{1/2}$	1
Time	$\lambda^{3/4}$	λ
Frequency	$1/\lambda^{3/4}$	$1/\lambda$
Displacement	$\lambda^{3/2}$	λ
Velocity	$\lambda^{3/4}$	λ
Acceleration	1	λ
EI	$\lambda^{7/2}$	λ^4
EA	$\lambda^{3/2}$	λ^2

$$\sigma_p / \sigma_m = \lambda_\sigma = \lambda \tag{5.1}$$

where σ is the stress in the soil and subscripts 'm' and 'p' denote 'model' and 'prototype', respectively.

Many experimental results have shown that the stiffness of sands at small strain levels is approximately proportional to the square root of the confining pressure, $\sqrt{\sigma}$. Hence, the scaling factor for the strain, λ_ε, is given by

$$\varepsilon_p / \varepsilon_m = \lambda_\varepsilon = \sqrt{\lambda} \tag{5.2}$$

If the relation of Equation (5.2) is valid for the model soil, the similitude for model test at 1-g field can be summarized as shown in **Table 5.1**. The similitude for 1-g field model tests is rather complex compared to the centrifuge testing.

As described in detail later in this paper, dry Toyoura sand with a relative density, D_r, of

95 % was used for the model grounds throughout this study. One-dimensional compression tests of the Toyoura sand were conducted using an oedometer test device to confirm the one-dimensional modulus, E_c, of the sand is proportional to the square root of the vertical stress, σ_v', or not. A typical result of the compression tests is shown in **Figure 5.1**. The vertical stress, σ_v', was applied to a soil specimen of D_r = 95% in steps up to 2.43 MPa. The vertical strain, ε_a, of the specimen was plotted against σ_v' in **Figure 5.1(a)**. The value of E_c at each loading step was calculated as $E_c = \Delta\sigma_v'/\Delta\varepsilon_a$ and was plotted against σ_v' in **Figure 5.1(b)**. Fitting lines were calculated by means of the following equation:

$$E_c = E_{c0}\left(\sigma_v'/\sigma_{v0}'\right)^n \tag{5.3}$$

where E_{c0} is the values of E_c at a reference stress σ_{v0}' (= 100 kPa in this paper).
It can be seen from **Figure 5.1(b)** that the measured values of E_c are fitted by Equation (5.3) with E_{c0} = 35 MPa and n = 0.4 to 0.6. For σ_v' less than 0.3 MPa, the calculated line with E_{c0} = 28 MPa and n = 0.5 gave a best fit. Therefore, the similitude for 1-g gravitational field in **Table 5.1** may be applicable to the tests in this study.

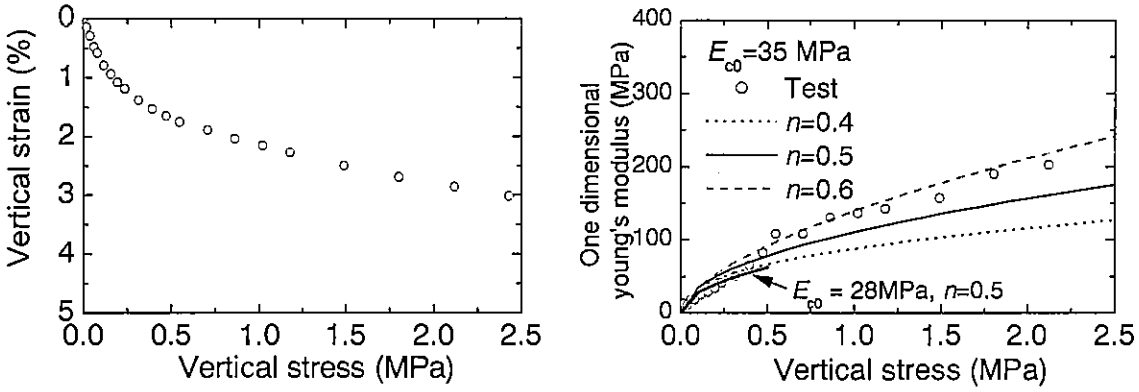

(a) Load - settlement relationship (b) One dimensional young's modulus

Figure 5.1. Result of consolidation test.

5.3 TEST DESCRIPTION

5.3.1 Model foundation

Figure 5.2 is the plan and top views of the model foundation used in the experiments. The square model raft, with a width of 80 mm, was made of an aluminum plate with a thickness of 25 mm. The mass of the model raft was 0.4 kg (3.92N in weight). In order to increase the friction at the raft base, the base was roughened. The interface frictional angle between the raft base and the model ground was 30.5 degrees, i.e., the coefficient of frictional angle was 0.59.

Four model piles were connected to the model raft with a pile spacing of 40 mm. The head of each pile was rigidly connected to the raft.

Aluminum pipes with an outer diameter of 10 mm, an inner diameter of 8 mm, and a length of 170 mm were used for the model piles. Each pile toe was capped with a thin aluminum plate. Young's modulus, E_p, and Poisson's ratio, ν_p, were determined from bending tests of the model piles. Each pile was instrumented with foil strain gages along the pile shaft as shown in **Figure 5.2** in order to obtain the distributions of the axial forces, the shear forces, and the bending moments of the pile.

The geometrical and mechanical properties of the model pile are listed in **Table 5.2**. **Table 5.2** also shows the properties of a corresponding prototype pile when the geometrical scaling factor, λ, is taken to be 50.

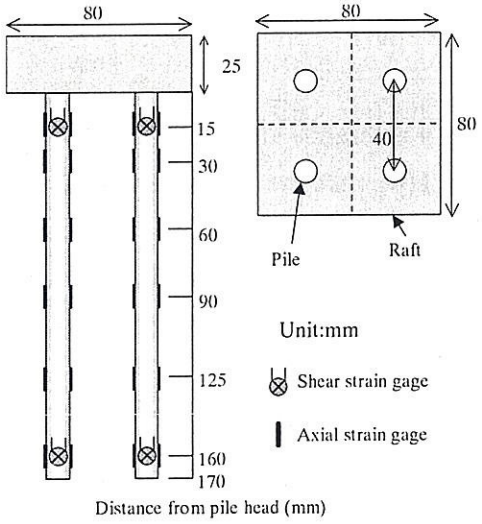

Figure 5.2. Plan and top views of the model foundation.

Table 5.2. Geometrical and mechanical properties of the model pile together with those of a prototype pile.

	Model	Prototype (λ=50)
Outer diameter (mm)	10	500
Wall thickness (mm)	1	50
Length (mm)	170	8500
Young's modulus, E_p (kPa)	6.71×10^7	6.71×10^7
Poisson's ratio, ν_p	0.345	0.345
Bending rigidity, E_pI(Nm^2)	19.4	17.2×10^6
Longitudinal rigidity, E_pA (N)	1.9×10^6	670.8×10^6

5.3.2. Static horizontal load test

Figure 5.3 shows an illustration of the equipment of the static horizontal load test. First, the model foundation was set near the center point of the model ground in order to minimize the effects of the sidewalls. Then dry Toyoura sand was slowly poured into the acrylic box with dimensions of 500 mm in width, 840 mm in length, and 300 mm in depth. The physical properties of the Toyoura sand are summarized in **Table 5.3**.

Table 5.3. Physical properties of Toyoura sand.

Property		Value
Density at test	ρ_t (t/m^3)	1.635
Density of soil particle	ρ_s(t/m^3)	2.661
Maximum density	ρ_{dmax} (t/m^3)	1.654
Minimum density	ρ_{dmin} (t/m^3)	1.349
Mean grain size	D_{50}(mm)	0.162
Relative density at test	D_r(%)	95
Internal friction angle	ϕ'(deg.)	44

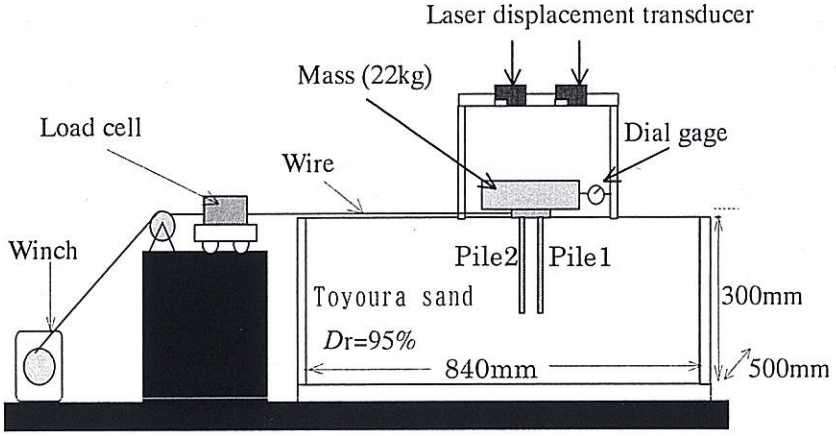

Figure 5.3. Illustration of the static horizontal load test equipment.

The sand was compacted to nearly its maximum relative density by vibration and tapping for each sand layer of about 30 mm in thickness. This procedure was repeated until the model ground had a depth of 300 mm. The relative density of the model ground was reached to 95 %. After the soil preparation was finished, all the instrumentation such as a dial gage, two laser displacement transducers, a load cell and a pulling wire were arranged.

In the first step of loading stage, a loading mass (22kg) was placed on the top of the raft. Then the horizontal load was applied by pulling the raft by means of a winch and a wire at a slow displacement rate less than 1 mm/min. The raft displacement and the loads transferred to the whole foundation, the raft and the piles were monitored throughout the test.

The static horizontal load tests of the piled raft and the pile group were carried out separately. In the tests of the pile group, a gap of 5 mm between the raft base and the ground surface was made. Therefore, the embedment length of the piles is the test of the pile group was reduced to 165 mm.

5.3.3 Shaking table test

Figure 5.4.shows an illustration of the final stage of the test set-up just before starting shaking test. The model foundation was set near the center location of a laminar box with a

special rig before making the model ground. The laminar box with dimensions of 210 mm in width, 560 mm in length, and 310 mm in depth was consisted of 16 layers of aluminum frames with a thickness of 20mm. Ball bearing were intercalated between the aluminum frame layers to minimize friction between them.

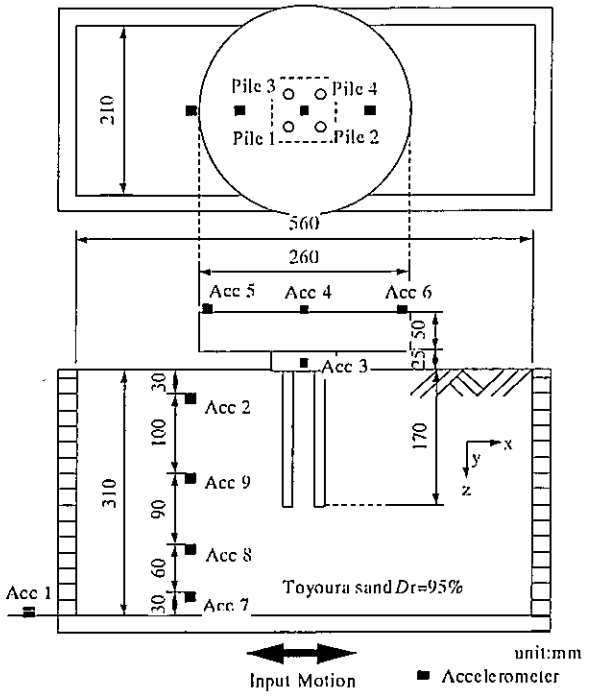

Figure 5.4. Illustration of the final stage of the test set-up in shaking table tests.

The dry Toyoura sand was used again for the model ground. The sand was poured in the laminar box and compacted by applying small vibrations using the shaking table. The relative density of the model ground was reached to 95% that is the same as in the static horizontal load test.

Accelerometers were embedded in the model ground (Acc. 2, 7, 8 and 9) and attached to the side and the top of the model foundation (Acc. 3 to 6). An accelerometer (Acc. 1) was placed on the shaking table to measure the input acceleration. After the completion of the preparation of the model ground, a loading mass of 22 kg (215.7 N in weight) was placed on the top of the raft and bolted to the raft. The total mass on the model piles was 22.4 kg, including the masses of the model raft (0.4 kg) and the loading mass (22 kg). The height of the center of gravity is 49.3 mm from the ground surface in the case of the piled raft, and 54.3 mm in the case of the pile group.

In each case, two series of shaking tests were carried out with a target amplitude of 100gal. In the 1st series, sinusoidal input waves of the frequencies of 18.8 Hz, 37.6 Hz, 56.4 Hz and 75.2 Hz (1 Hz, 2 Hz, 3 Hz and 4 Hz at the prototype scale of λ = 50) were applied. In the 2nd series of the tests, sinusoidal input waves of the frequencies from 5Hz to 95Hz at intervals of 5 Hz were applied.

5.4 TEST RESULTS

5.4.1 Shaking table tests

The shaking tests were conducted for the model ground alone, the piled raft and the pile group.

Figure 5.5 shows the transfer functions of the horizontal accelerations. In the figure, the vertical axis is the response factors that are the ratios of the response accelerations measured by Acc. 2 (the ground surface) and Acc. 4 (top of the loading mass) to the input acceleration monitored by Acc. 1 (the shaking table, see **Figure 5.4**). It can be seen that the natural frequencies of the model piled raft and the pile group were 15 Hz and that of the model ground alone was 60 Hz.

Hereafter, the test results of the model piled raft and the pile group at the input frequency of 18.8 Hz (1 Hz at the prototype scale λ =50) are focused.

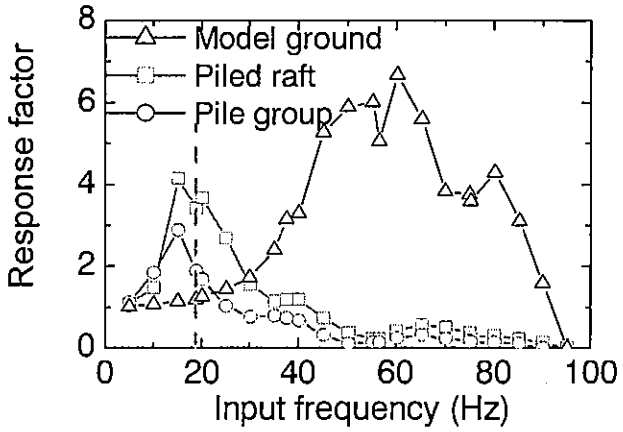

Figure 5.5. Transfer function of horizontal acceleration.

When the loading mass of a weight of 215.7 N was placed on the top of the raft of the piled raft prior to shaking test, the piles carried 62 % of the vertical load.

Figure 5.6 shows the input acceleration waves. The response horizontal accelerations on the top of the loading mass of the piled raft and the pile group are compared in **Figure 5.7**. At this input frequency, the amplitude of the horizontal acceleration of the piled raft was larger than that of the pile group. The response factor of the piled raft was 3.41 and that of pile group was 1.88, showing that the pile group was more stable against the input motion in respect of the horizontal movement.

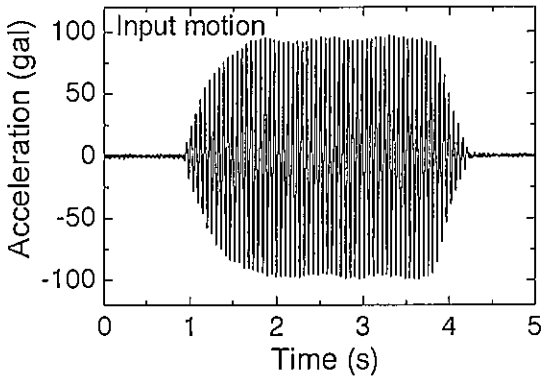

Figure 5.6. Input acceleration (18.8 Hz).

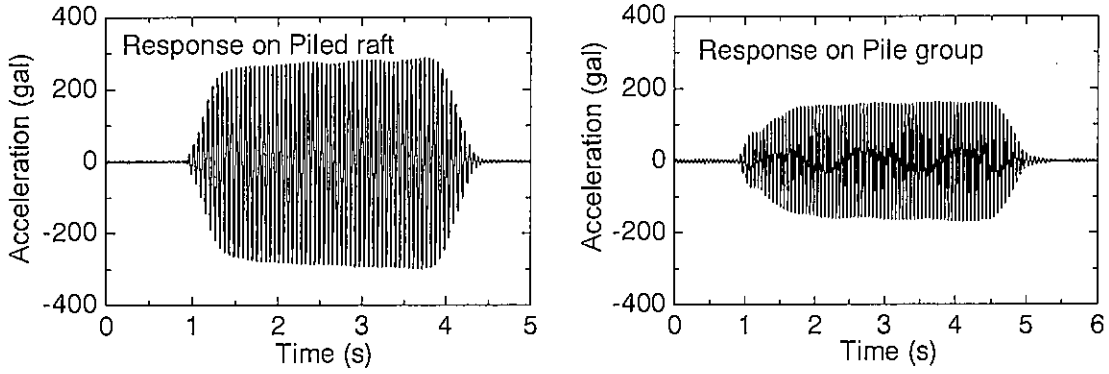

(a) Piled raft (b) Pile group

Figure 5.7. Response accelerations of the model foundations.

Figure 5.8 shows the time histories of the horizontal load, the horizontal pile resistance and the horizontal raft resistance in a loading cycle. The horizontal load was calculated as the product of the acceleration measured by Acc 4 and the total mass (22.4 kg) on the piles. The pile resistance was the total shear force at the pile heads of 4 piles, and the raft resistance was obtained by subtracting the pile resistance from the horizontal load, i.e. the negative value of the horizontal load was treated as the total resistance including the pile resistance the raft resistance.

In the case of the piled raft (**Figure 5.8(a)**), the mobilized pile resistance was higher than the mobilized raft resistance when the absolute value of the horizontal load was below 60 N. The pile resistance was about 30 N at peak and exhibited a softening behavior after the peak resistance. On the other hand, the raft resistance continued to increase after the peak of the pile resistance and the horizontal load proportion carried by the raft became higher than the piles.

In the case of the pile group (**Figure 5.8(b)**), the pile resistance was almost identical with the horizontal load until the horizontal when the absolute value of the horizontal load was below about 30 N. The pile resistance was about 30 N at peak and exhibited a softening behavior after the peak resistance, as was seen in the piles in the piled raft.

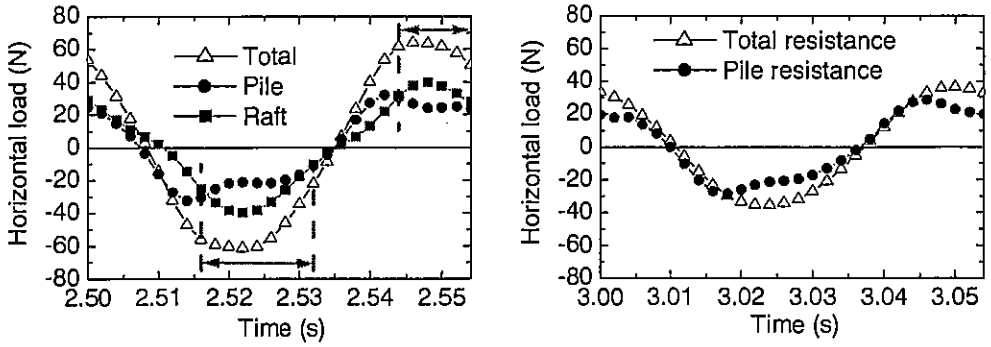

(a) Piled raft (b) Pile group

Figure 5.8. Time histories of the horizontal load and the horizontal resistance.

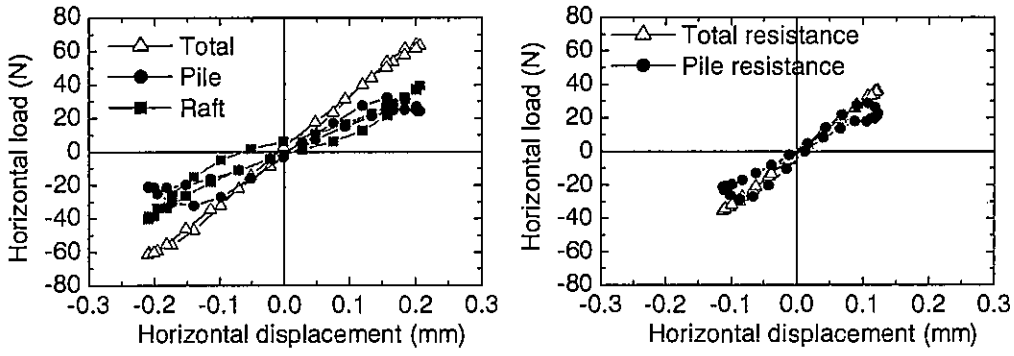

(a) Piled raft (b) Pile group

Figure 5.9. Horizontal load displacement relation.

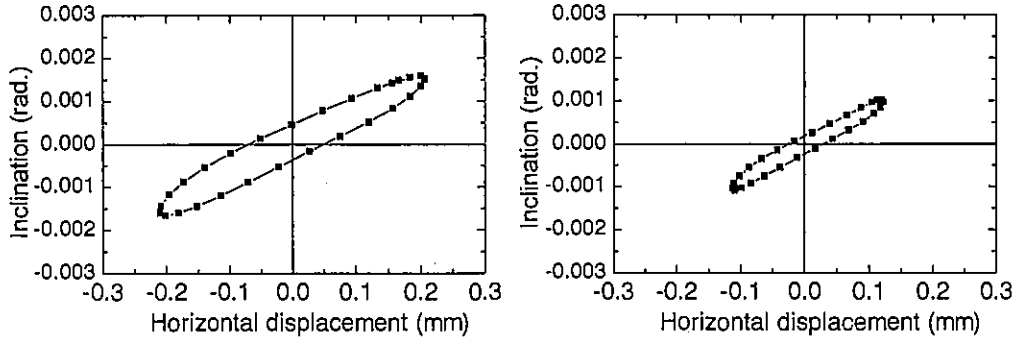

(a) Piled raft (b) Pile group

Figure 5.10. Horizontal displacement vs inclination of the raft.

Figure 5.9 shows the relationship between the horizontal resistance and the horizontal displacement of the raft. The horizontal displacement was obtained from twice integration of the acceleration measured with respect to time. The pile resistance in the piled raft reached its peak at a horizontal displacement of 0.15 mm while that of the pile group reached its peak at a smaller horizontal displacement of 0.1 mm. It can be clearly seen from **Figure 5.9**(a) that the raft resistance was effectively mobilized in the piled raft even during seismic loading.

Figure 5.10 shows the relationship between the inclination of the raft and the horizontal displacement. The inclination of the raft tended to increase with increasing the horizontal displacement in both foundations, although hysteresis loops were observed. Comparing both figures, the ratios of the inclination to the horizontal displacement were comparable in both foundations.

Figure 5.11 shows the time history of the horizontal load proportion carried by the piles in the piled raft. It can be seen that the plots of the horizontal load proportion carried by the piles concentered in a range from 30 % to 50 %. This range corresponds to the range of time indicated by the double-headed arrows in **Figure 5.8**. The horizontal load at out of this time range was small. Therefore, even when the proportion of the horizontal load carried by the piles become higher than 50 %, there may be no risk of pile failures.

Figure 5.12 shows the time history of the vertical load proportion carried by the piles in the piled raft. Although the vertical load proportion carried by the piles oscillated within a range from 50 % to 70 % during the shaking period, the vertical proportion carried by the piles did not change between before and after shaking. Similar result is reported by Horikoshi et al. (2002) where a shaking test of a piled raft was conducted in centrifuge of 50 g.

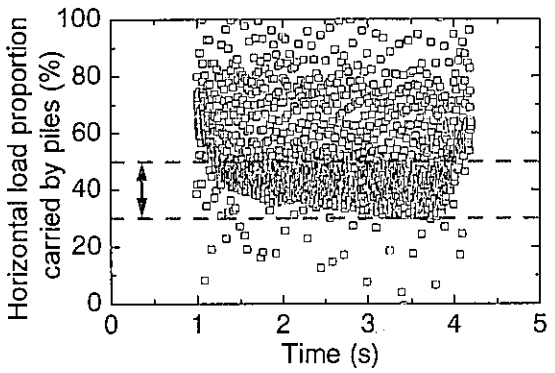

Figure 5.11. Proportion of the horizontal load carried by the piles in the piled raft.

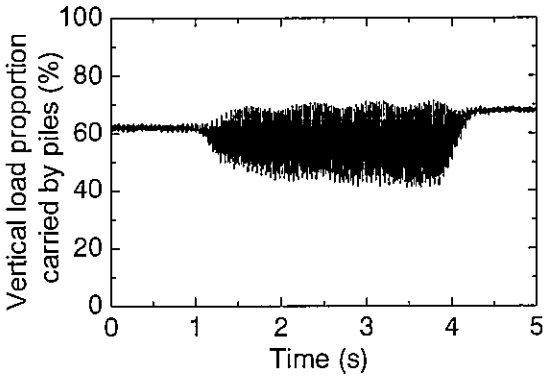

Figure 5.12. Proportion of the vertical load carried by the piles in the piled raft.

Figures 5.13 and 5.14 show the distributions of the bending moments and the shear forces along the pile shaft of each pile. For the positions of pile I and pile 2, refer to **Figure 5.4.** The horizontal displacement in the direction from the position of pile 1 to the position of pile 2 is taken as positive in this paper. The distributions at the horizontal load of 30 N are shown for the piled raft and the pile group for comparison. At this moment, the horizontal displacements of both foundations were 0.1 mm in the positive direction. It can be seen from both figures that the bending moments and the shear forces of the piles in the piled raft are smaller than those in the pile group. It is also seen that pile 2 (front pile at this

moment) carried higher bending moments and shear forces, compared to pile 1 (back pile at this moment). However, the difference of load carrying between pile 1 and pile 2 was smaller in the piled raft.

Figure 5.15 shows the axial forces on the piles vs the horizontal displacement in the piled raft. The axial forces on piles 1 and 3 and on piles 2 and 4 are indicated in the figure. It can be seen that the piles 2 and 4 carried much load when the horizontal displacement was positive, while piles 1 and 3 carried much load when the horizontal displacement was negative. **Figure 5.16** shows the shear forces at the pile heads vs the horizontal displacement in the piled raft. The horizontal resistance was mobilized in the piles 2 and 4 alone when the horizontal displacement was positive, while the horizontal resistance was mobilized in the piles 1 and 3 alone when the horizontal displacement was positive. Similar behaviors were observed also in the pile group.

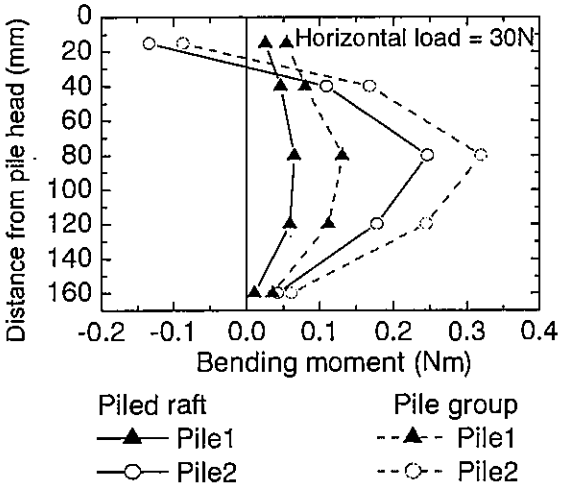

Figure 5.13. Distributions of the bending moments of the piles.

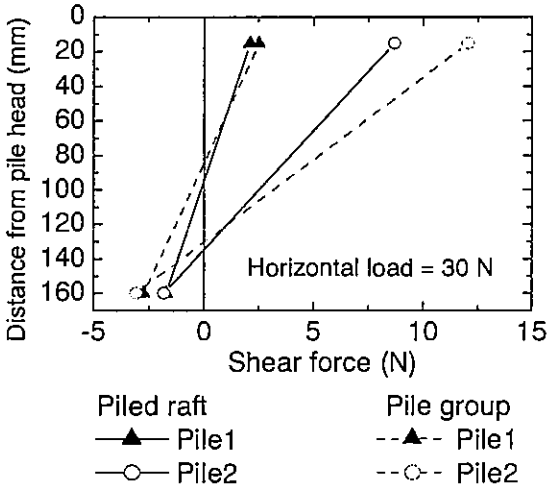

Figure 5.14. Distributions of the shear forces of the piles.

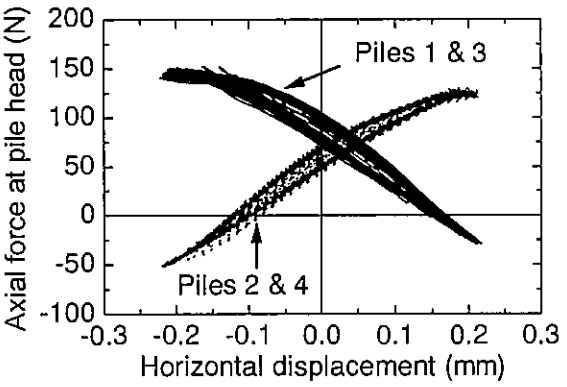

Figure 5.15. Axial force at the pile head vs the horizontal displacement in the piled raft.

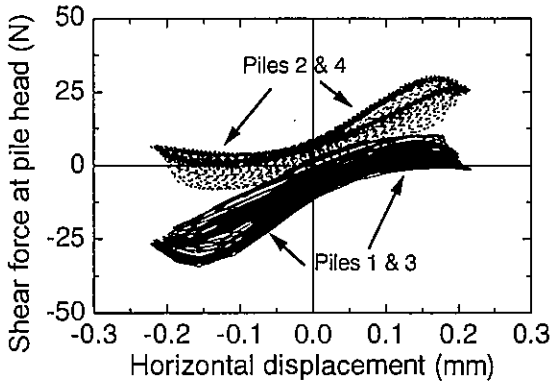

Figure 5.16. Shear force at the pile head vs the horizontal displacement in the piled raft.

It should keep the above results in mind in the design of piled rafts and pile groups under seismic loading, because the piles do not necessarily carry even load, even though even load carrying is prescribed in some pile design codes in Japan.

5.4.2 Static horizontal loads tests

When the loading mass of a weight of 215.7 N was placed on the top of the raft of the piled raft prior to horizontal loading, the piles carried 75 % of the vertical load, which was 13 % larger than the case of the shaking test. It was thought that this difference was caused by the different soil containers used in both tests.

Figure 5.17 shows the relationships between the horizontal load and the horizontal displacement of the piled raft and the pile group. The pile resistances are also indicated in the figure. The raft base resistance was obtained as the difference between the horizontal load and the pile resistance in the case of the piled raft and indicated by the shaded area. The horizontal resistance of the piled raft was more than twice of that of the pile group. The pile resistance in the piled raft was increased compared to that in the pile group. It is thought that this increase was caused by the increase in the stiffness and the strength of the soil beneath the raft due to a vertical load transfer from the raft base to the soil. It should be noted that, as shown in **Figures 5.8 and 5.9**, the pile resistances in the piled raft and in the pile group were almost the same in the shaking tests.

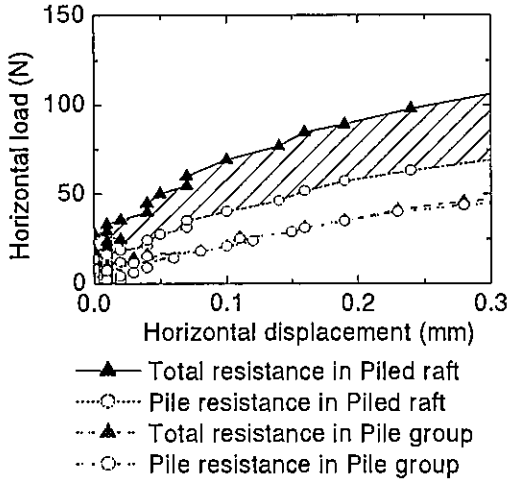

Figure 5.17. Load-displacement relationships of the piled raft and the pile group.

Figure 5.18 shows the proportion of the horizontal load carried by the piles and the raft obtained from the static horizontal load test on the piled raft. The raft carried much of the load in the early loading stages, which contributed to a reduction of the horizontal displacement. The load carried by the raft significantly decreased as the horizontal displacement increased, and the leveled off at a horizontal displacement of 0.2 mm. The results of **Figure 5.18** were completely different from the test results obtained from the

shaking test of the piled raft. As shown in **Figures 5.8(a) and Figure 5.9(a)**, the piles carried much of the horizontal load at small displacements. Note here that the trend of the change with time in the horizontal displacement is identical that of the horizontal load shown in **Figure 5.8(a)**. Hence, it is seen from **Figure 5.8(a)** that the piles carried much of the horizontal load at small displacements as mentioned, and that the raft resistance exceeded the pile resistance after the pile resistance attained to its peak values.

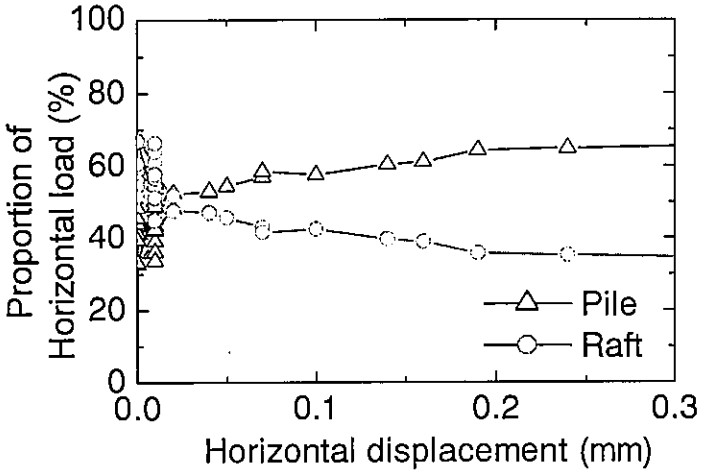

Figure 5.18. Proportion of the horizontal load obtained from the static load test of the piled raft.

Figure 5.19 shows the relationship between the inclination of the raft and the horizontal displacement. In both foundations, the inclination tended to increase in proportion with the increase in the displacement. However, the inclination of the piled raft was smaller than that of the pile group, indicating a contribution of the raft to suppress the inclination.

Let us compare the results of **Figure 5.19** with the results from the shaking tests (**Figure 5.10**). Although the slope of the inclination to the horizontal displacement of the piled raft during shaking was a little bit of smaller than that of the pile group (**Figure 5.10**), the effect of the raft to suppress the inclination is not expected as in the static horizontal load tests.

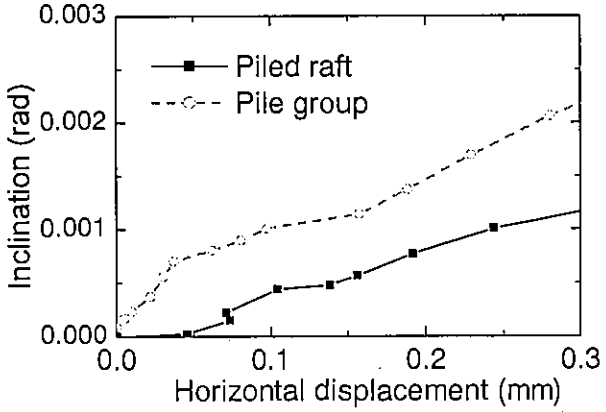

Figure 5.19. Inclination vs horizontal

Figures 5.20 and 5.21 show the distributions of the bending moments and the shear forces along the pile shaft of each pile in the piled raft. For the positions of pile 1 and pile 2, refer to **Figure 5.4**. The distributions at a static horizontal load of 60 N are shown in the figure. Also shown are the distributions of the bending moments and the shear forces obtained from the shaking test of the piled raft at a horizontal load of 60 N. The horizontal displacements of the pile head were 0.07 mm and 0.15 mm in the static horizontal test and the shaking test, respectively. In the static load test, the distributions of the bending moments and the shear forces were very similar between pile 1 (back pile) and pile 2 (front pile), which is comparable to a result from deformation analysis for the piled raft in an elastic state considering interactions. On the other hand, the behaviors of pile 1 and pile 2 were completely different in the shaking test, as described in **Figures 5.13 to 5.16.**

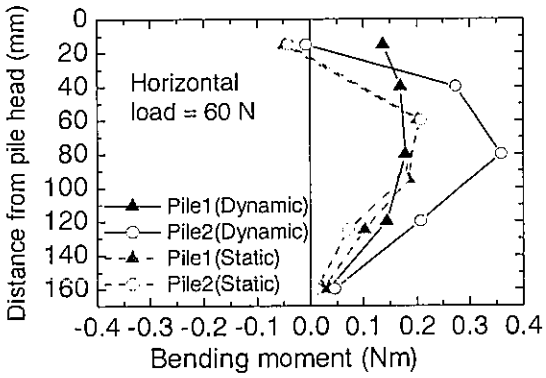

Figure 5.20. Distributions of the bending moments along the piles in the piled raft obtained from the static horizontal load test and the shaking test.

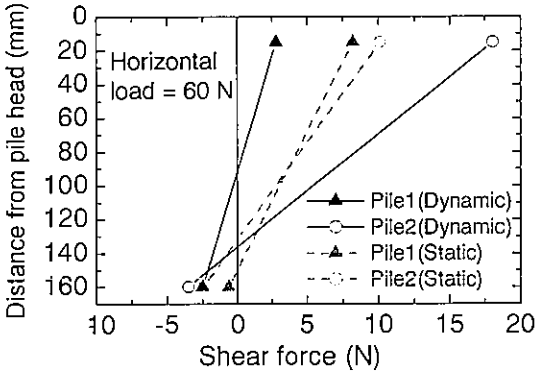

Figure 5.21. Distributions of the shear forces along the piles in the piled raft obtained from the static horizontal load test and the shaking test.

5.5. CONCLUSIONS

A series of static horizontal load tests and shaking table tests was conducted on a model piled raft and a model pile group at 1-g gravitational field. The behaviors of the model foundations under shaking at their natural frequencies were intensively investigated and compared with their behaviors under static horizontal loading.

Principle findings from the experiments in this study are summarized as follows:

The horizontal stiffness and the horizontal resistance of the piled raft in the static horizontal load test were larger than that of the pile group. Under seismic loading, the horizontal stiffness of the piled raft and the pile group were almost the same.

1. The pile resistance in the piled raft in the horizontal load test was larger than that in the pile group, due to the increase in the stiffness and the strength of the soil beneath the

raft caused by a vertical load transfer from the raft base to the soil. Under seismic loading, the pile resistance in the pile group was the same as that in the pile group.

2. The inclination of the piled raft in the horizontal load test was reduced compared to the pile group, indicating a contribution of the raft to suppress the inclination. Under seismic loading, the raft did not contribute effectively to reduce the inclination of the piled raft.
3. The distributions of the bending moments and the shear forces along the pile shaft were similar in each pile in the static horizontal load test. Under seismic loading, the bending moments and the shear forces of the piles fronted to the direction of displacement at that moment were increased very much compared to the back piles.
4. The magnitude of he horizontal acceleration of the raft of the piled raft was about 2 times that of the pile group under seismic loading at near the natural frequencies of the piled raft and the pile group. Nevertheless, the bending moments and the shear forces of the piles in the piled raft were smaller than those in the pile group. This means that risk of structural failure of the piled raft is reduced compared to the pile group.

Many of the above findings in this study are conflicting the results from Horikoshi et al.(2003). They concluded that the behavior of the piled raft during seismic loading is comparable with the behavior under static horizontal loading. In the centrifuge model tests by Horikoshi et al. (2003), the frequency of the input motion was about a half of the natural frequency of the model foundation.

Further experimental and analytical investigations on the behavior of pile foundations under seismic loading at their natural frequencies will be required to establish a seismic design of pile foundations.

REFERENCES

Iai, S. Similitude for shaking table tests on soil-structure-fluid model in 1g gravitational field, *Soils and Foundations* 1989; 29(1), 105-118.

Katzenbach, R and Moormann, C. Recommendations for the design and construction of piled rafts, *Proc. 15th ICSMGE* 2001, Istanbul; 2, 927-930.

Horikoshi, K and Randolph, MF. Estimation of overall settlement of piled rafts, *Soils and Foundations* 1999, 39(2), 59-68.

Horikoshi K, Watanabe, T, Fukuyama, H and Matsumoto, T. Behavior of piled raft foundations subjected to horizontal loads, *Proc. Int. Conf. on Physical Modelling in Geotechnics* 2002, St. John's, Canada, 715-721.

Pastsakorn, K, Hashizume, Y and Matsumoto, T. Lateral load tests on model pile groups and piled raft foundations in sand, *Proc. Int. Conf. on Physical Modelling in Geotechnics* 2002, St. John's, Canada, 709-714.

Poulos, HG and Davis, EH. Pile Foundation Analysis and Design, John Wiley and Sons, New York, 1980.

Randolph, MF. Design methods for pile groups and piled rafts, *Proc. 13th ICSMFE* 1994, New Delhi; 2, 61-546.

CHAPTER 6

DEVELOPMENT OF A SIMPLIFIED ANALYSIS METHOD FOR PILED RAFT AND PILE GROUP FOUNDATIONS WITH BATTER PILES

(*N.B.* This chapter was published in Int. Jour. for Numerical Methods in Geomechanics, Vol.26, pp.1349-1369, entitled "A SIMPLIFIED ANALYSIS METHOD FOR PILED RAFT AND PILE GROUP FOUNDATIONS WITH BATTER PILES" by Pastsakorn Kitiyodom & Tatsunori Matsumoto)

SUMMARY

A simplified method of numerical analysis has been developed to estimate the deformation and load distribution of piled raft foundations subjected to vertical, lateral, and moment loads, using a hybrid model in which the flexible raft is modelled as thin plates and the piles as elastic beams and the soil is treated as springs. Both the vertical and lateral resistances of the piles as well as the raft base are incorporated into the model. Pile-soil-pile, pile-soil-raft and raft-soil-raft interactions are taken into account based on Mindlin s solutions for both vertical and lateral forces. The validity of the proposed method is verified through comparisons with several existing methods for single piles, pile groups and piled rafts. Workable design charts are given for the estimation of the lateral displacement and the load distribution of piled rafts from the stiffnesses of the raft alone and the pile group alone. Additionally, parametric studies were carried out concerning batter pile foundations. It was found that the use of batter piles can efficiently improve the deformation characteristics of pile foundations subjected to lateral loads.

KEY WORDS: piled raft; hybrid model; Mindlin s solution; batter piles; lateral load

6.1. INTRODUCTION

In recent years, there has been an increasing recognition that the inclusion of the resistance of the raft in pile foundation design can lead to a considerable economy without compromising the safety or the performance of the foundation. In highly seismic areas such as Japan, estimation of the behaviour of piled rafts during earthquakes becomes an important issue in the foundation design process, because better stability of pile rafts than pile groups would be expected during earthquakes. In one traditional method of seismic design in Japan, dynamic loads acting on the foundation are modelled by an equivalent static lateral load. And, as the behaviour of piled rafts under lateral loading has not been completely understood, piled raft foundations are generally treated as raft foundations or pile foundations. In addition, the use of batter piles in bridge foundation reinforcement works against earthquakes increase demands upon methods of estimation of the performance of piled raft foundations with batter piles.

Much research on the analysis of piled raft foundations has been done, for instance, the works of Hain & Lee[1], Poulos & Davis[2], Kuwabara[3] Clancy & Randolph[4], Poulos[5], Randolph[6], Yamashita *et al.*[7], Ta & Small[8], Horikoshi & Randolph[9] and Horikoshi & Randolph[10]. However, most of the previous research is related to piled rafts subjected to vertical loading. In the present study, a computer program PRAB (Piled Raft Analysis with Batter Piles) has been developed based on a hybrid model, which sufficiently minimizes the size of the stiffness matrix and the amount of computation. This model was first proposed by O Neill *et al.*[11]. The response of each pile is modelled using the load-transfer method, and the interaction between the piles through the soil, is calculated based on Mindlin s solution[12]. In Chow[13], this hybrid model was used for the analysis of general three-dimensional pile groups. Clancy & Randolph[4] extended the hybrid model by including thin plate bending finite elements to model the raft. The results of the analysis of piled rafts were presented in Clancy & Randolph[4], however, only vertical loading was considered in their work. In PRAB, the lateral resistance of the piles as well as the raft base is incorporated into the hybrid model so as to be able to analyze the deformation of piled rafts subjected to lateral and moment loads as well as vertical loads.

The validity of PRAB is examined in this paper by comparing the results calculated using PRAB with the results of the available previous research works. PRAB is then used for parametric studies of piled rafts. A simple design approach based on the reciprocal theorem for piled rafts in which the deformation of the foundation can be estimated directly from the separate deformation of the raft and the pile group was introduced in Randolph[14] and Clancy & Randolph[4]. In Clancy & Randolph[4], the parametric analyses were done for vertically loaded piled rafts. Similar parametric analyses are conducted in this paper for the case of piled rafts subjected to lateral loading. Additionally, PRAB is used for parametric studies of piled rafts and pile groups subjected to vertical,

lateral and moment loads to investigate the differences between the results of the two foundation types; piled raft and pile group, and the effects of factors such as pile rake angle and length.

6.2. METHOD OF ANALYSIS

6.2.1. Modelling of pile rafts

Figure 6.1 illustrates the analytical model for piled rafts employed in this study. This analytical model is similar to those used by O Neill *et al.*[11], Chow[13] and Clancy & Randolph[4], except that two additional soil springs in the horizontal plane are attached at each node of the piles and the raft to account for the bending of the piles, the lateral soil resistance to the piles, and the shear resistance between the raft base and the soil surface. The analytical model is incorporated in a computer program PRAB. Finite element modelling is used to model the structural elements of the foundation. The flexible raft is modelled as thin plate elements and the piles as elastic beam elements. These two element models are combined via the nodes at the pile heads. Unknown freedoms are linked at the pile head nodes. And it is assumed that there are no raft-soil springs at these nodes.

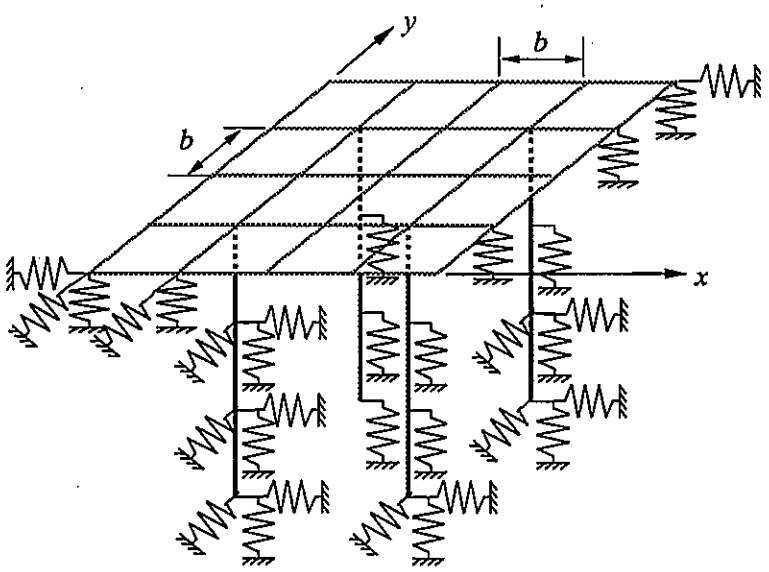

Figure 6.1. Plate-beam-spring modelling of a piled raft foundation.

The vertical soil spring values, K_z^R, and the horizontal soil spring values, K_x^R and K_y^R, at the raft nodes are estimated by means of Equations (6.1) and (6.2) following Muki(1961) (Poulos & Davis[15]), and the vertical shaft soil spring values, K_z^P, at the pile shaft nodes are estimated by means of Equation (6.3) following Randolph & Wroth[16].

$$K_z^R = \frac{4Ga}{1-\nu_s} \tag{6.1}$$

$$K_x^R = K_y^R = \frac{32(1-\nu_s)Ga}{7-8\nu_s} \tag{6.2}$$

where ν_s is the Poisson s ratio of the soil, G is the shear modulus of the soil, a is the equivalent radius of the raft element ($a = b/\sqrt{\pi}$, b = the width of the square raft element).

$$K_z^P = \frac{2\pi G\Delta L}{\ln(r_m/r_o)} \tag{6.3}$$

where r_o = the pile radius, ΔL = the pile segment length, $r_m = 2.5L(1-\nu_s)$. In estimation of r_m, for very slender piles, the pile length, L, is replaced by a limiting effective pile length $L_c = 1.5D\sqrt{2(1+\nu_s)E_p/E_s}$ (Clancy & Randolph[4]) in which D and E_p are the diameter and the Young s modulus of the pile respectively, and E_s is the Young s modulus of the soil.

The vertical and horizontal soil spring values at the pile base nodes are estimated also using Equations (6.1) and (6.2), replacing a by the pile radius, r_o.

There are many ways to estimate the horizontal shaft soil spring values, K_x^P and K_y^P. In this paper, the horizontal shaft soil spring values at each pile node are estimated based on Mindlin s solution which is similar to the solution of the integral equation method used by Poulos & Davis [2]. The equation becomes

$$K_x^P = K_y^P = \zeta E_s \Delta L \tag{6.4}$$

where $\zeta = pD/\rho E_s$ in which p is the lateral uniformly distributed force acting over the pile element and ρ is the corresponding lateral displacement at each pile node calculated using the integral equation method. The accuracy of the proposed method for estimation of K_x^P and K_y^P will be examined in Section 6.3.

6.2.2. The inclusion of batter piles

In order to model batter piles, it is necessary to relate the forces acting in all piles and the deformations of all piles to one set of global coordinates, x, y and z, as shown in **Figure 6.2.** The pile stiffness matrix $[K_p]$ is transformed from the local coordinates, x', y' and z', to the global coordinates using the transformation matrix $[T]$. The transformation matrix is given by Equation (6.5) following Saul[17].

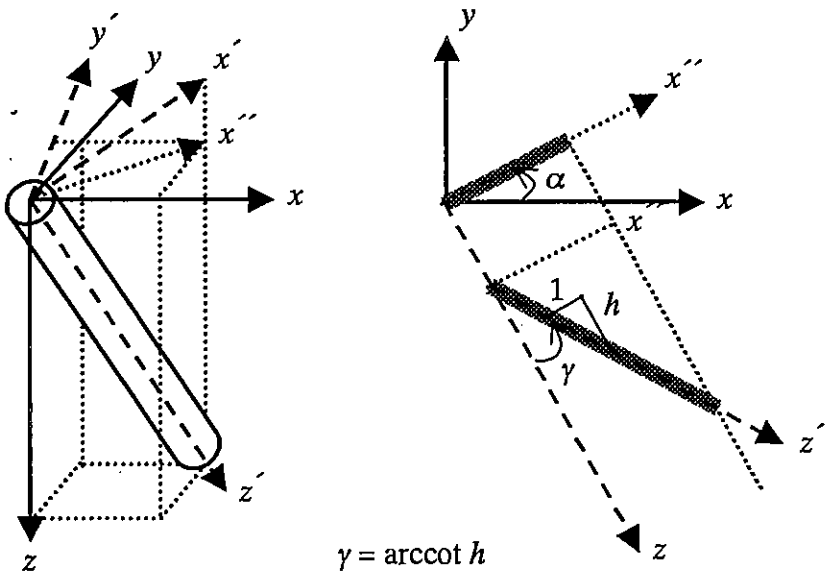

Figure 6.2. Global and local coordinates systems for pile element.

$$[T]=\begin{bmatrix}[R] & [0] & [0] & [0]\\ [0] & [R] & [0] & [0]\\ [0] & [0] & [R] & [0]\\ [0] & [0] & [0] & [R]\end{bmatrix},\quad [R]=\begin{bmatrix}\cos\gamma\cos\alpha & -\sin\alpha & \sin\gamma\cos\alpha\\ \cos\gamma\sin\alpha & \cos\alpha & \sin\gamma\sin\alpha\\ -\sin\gamma & 0 & \cos\gamma\end{bmatrix} \tag{6.5}$$

where $0^\circ \le \alpha \le 360^\circ, 0^\circ \le \gamma \le 90^\circ$. Then, we get

$$\{P\} = [T][K_p][T]^T\{w\} \tag{6.6}$$

$$\{P\} = [K_p^*]\{w\} \tag{6.7}$$

where $\{P\}$= the internal force vector, $[K_p]$ = the pile stiffness matrix, $[T]^T$ = the transpose of the transformation matrix, $\{w\}$= the displacement vector, and $[K_p^*] = [T][K_p][T]^T$.

In addition, for the normal range of pile rake angle (less than 30 degrees) employed in practice, it can be assumed that the stiffness of axial and lateral soil springs are independent of the pile rake angle (Poulos & Madhav[18]). Accordingly, Equations (6.1) to (6.4) are used to calculate the stiffness of the soil springs with respect to the local coordinates of the pile. Then it is again necessary to transform the soil spring stiffness matrix $[K_s]$ from the local to the global coordinates. The transformation submatrix $[R]$, which is a submatrix of $[T]$ in Equation (6.5), is used.

$$[K_s^*] = [R][K_s][R]^T \tag{6.8}$$

6.2.3. The interaction between structural members

The deformations of individual structural members occur due to loading. Since the soil is a continuous material, this deformation will induce additional deformations of other structural members in the piled raft system. The flexibility concept is employed in this paper to deal with the problem of the interaction between structural members as shown schematically in **Figure 6.3** for the example of a piled raft subjected to vertical loading. The overall deformation of any degree of freedom, w_i, at all nodes are written in the following discrete form.

$$w_i = \sum_{j=1}^{n} a_{ij} P_j \tag{6.9}$$

where a_{ij} is the soil flexibility coefficient denoting the deformation at degree of freedom i due to a unit load acting at degree of freedom j, and n is the total number of degrees of freedom in the piled raft system. Equation (6.9) is rewritten in the following matrix form.

$$\{w\} = [A]\{P\} \tag{6.10}$$

where $[A]$ is the soil flexibility matrix.

The diagonal coefficients of $[A]$ are determined by inverting the soil spring stiffness matrix $[K_s^*]$ in Equation (6.8). The off-diagonal nonzero coefficients in the matrix $[A]$ represent structural member-soil-structural member interactions and are calculated based on Mindlin s solutions for both vertical and lateral forces.

For further use, Equation (6.9) is rewritten as

$$[C]\{w\} = \{P\} \tag{6.11}$$

where $[C] = [A]^{-1}$.

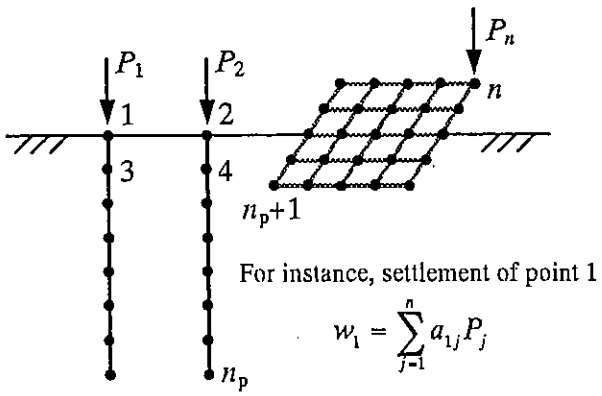

Figure 6.3. Structural member-soil-structural member interaction.

Note that interaction effects in the vertical direction between nodes within the same pile are ignored.

6.2.4. The stiffness matrix of the piled raft

The analysis of the raft is separately developed and can be written in the matrix form.

$$[K_r]\{w\} = \{F\} - \{P\} \tag{6.12}$$

where $[K_r]$ = the raft stiffness matrix, and $\{F\}$ = the external load vector acting on the raft.

Finally, from Equations (6.7), (6.11) and (6.12), we get

$$\left[C + K_r + K_p^*\right]\{w\} = [K]\{w\} = \{F\} \tag{6.13}$$

where $[K]$ is the global stiffness matrix of the piled raft system.

Note also that PRAB can also be used for the estimation of non-linear deformation of the foundations, due to the bi-linear (elastic-perfectly plastic) response of soil springs. In addition, for soil profiles that are arbitrarily layered and/or underlain by a rigid bed stratum, the soil spring values and the interaction may be modified approximately to include the influence of the soil profiles. These extensions are left for further work.

6.3. ACCURACY OF THE PROPOSED METHOD

In order to ensure the validity of the proposed method and to investigate the effects of mesh refinement of the pile and the raft, the results calculated using PRAB were compared with the results from related previous research.

6.3.1. The analysis of piled raft foundations subjected to vertical loading

In the work of Clancy & Randolph[4], analyses of foundations including single piles and piled rafts were conducted with the aim to verify the accuracy of their hybrid model and to investigate the effect of mesh refinement of the pile and the raft for vertical loading. It was stated that the use of 15 pile elements together with a raft mesh in which there are two thin plate finite elements between each pile leads to sufficient accuracy in the calculation of deformations and load distribution.

The same analyses were conducted using PRAB, and the same conclusions were obtained.

6.3.2. The analysis of single piles subjected to lateral loading

The use of the integral equation method for the analysis of the behaviour of piles subjected to lateral loads and moment loads was introduced by Poulos & Davis[2]. In the

integral equation method, a pile element subjected to a uniformly distributed force is modelled by a rectangular area, which has a width equal to the pile diameter and a length equal to the pile segment length. Based on Mindlin's solution for the lateral displacement due to a lateral force, integration is conducted twice on this rectangular area. Accordingly, the lateral displacement at any point on this rectangular plane can be calculated. This method was employed in PRAB in order to estimate the horizontal soil spring values at the pile shaft nodes. However, compared with the work of Poulos & Davis[2] in which single piles and pile groups subjected to lateral loads were analyzed, the main purpose of PRAB is to analyze the deformation of the piled raft. For this purpose, pile-soil-raft and raft-soil-raft interactions must be considered in the analysis in addition to pile-soil-pile interaction. Hence the analysis of piled rafts does require much more time than that of pile groups. In order to reduce the amount of time required for analysis, equivalent point forces acting at the nodal points were used instead of distributed forces in the estimation of the interaction coefficients. The accuracy of this assumption has been verified for vertical pile groups (Chow[19]). A comparison of the results for single piles subjected to lateral load, H, or moment load, M, at the pile head using the method of Poulos & Davis[2] and using PRAB is shown below.

In **Figure 6.4**, the deformations of piles subjected to lateral loading are shown in terms of the elastic influence factor of displacement, I_{hH}. The effect of the pile slenderness ratio, L/D, on the factor I_{hH} is shown in **Figure 6.4(a)**, while **Figure 6.4(b)** shows the effect of the pile-flexibility factor, K_R. The factors, I_{hH} and K_R, are defined in Equation (6.14).

$$I_{hH} = \frac{hE_sL}{H}, K_R = \frac{E_pI_p}{E_sL^4} \tag{6.14}$$

where h = the lateral displacement, H = the lateral load, E_p = theYoung's modulus of the pile, and I_p = the moment of inertia of a pile section.

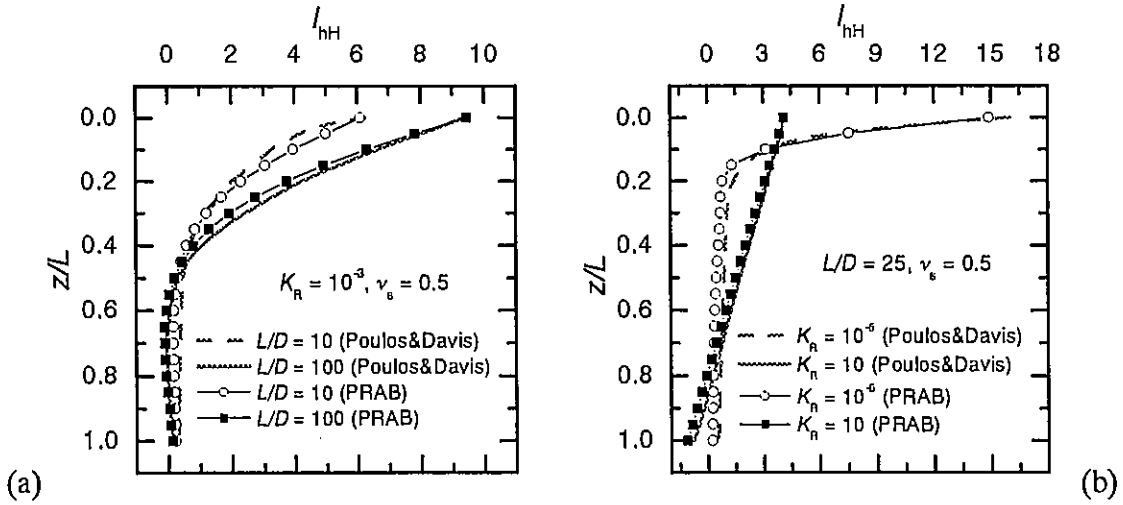

Figure 6.4. Comparisons of displacement profiles along pile.

Figure 6.5 shows the distributions of bending moments in a pile subjected to lateral load alone (**Figure 6.5(a)**) and moment load alone (**Figure 6.5(b)**). All the solutions above were obtained for piles which were divided into 20 elements. It can be seen from **Figures 6.4 and 6.5** that there was good agreement between the results from these two methods. Consequently, we believe the idea of using the equivalent point forces instead of the distributed forces to model the interactions in the horizontal direction to be valid.

In the work of Poulos[20], finite-difference analyses of laterally loaded single piles using the integral equation method were conducted for various numbers of pile elements: 6, 11, 21 and 31. It was stated that the accuracy of the solutions depended markedly on the number of pile elements. In order to investigate the effect of the number of pile elements used, laterally loaded single piles were analyzed using the same method as Poulos[20] except that the pile was modelled using beam finite elements, and the number of pile elements was varied up to 500. In the case of $K_R \geq 10^{-4}$, it was found that the solutions for the piles which had more than 100 elements were almost consistent. However, in the case of very flexible piles ($K_R \leq 10^{-5}$), consistency of the solution was found only when the number of pile elements exceeded 400. Accordingly, it was assumed that the solution obtained for 400 pile elements was a valid solution. For $K_R \geq 10^{-4}$, the solution obtained from PRAB using 20 pile elements underestimated the solution obtained for 400 pile elements by about 5%. For $K_R \leq 10^{-5}$, the solution of PRAB underestimated the solution obtained for 400 pile elements by about 20%. In most practical cases, the pile length in piled rafts is shorter than that of pile groups. So, it would be rare in piled rafts that $K_R \leq 10^{-5}$. Therefore, in analyses below, 20 pile elements were used together with a raft mesh in which there were two thin plate finite elements between each pile.

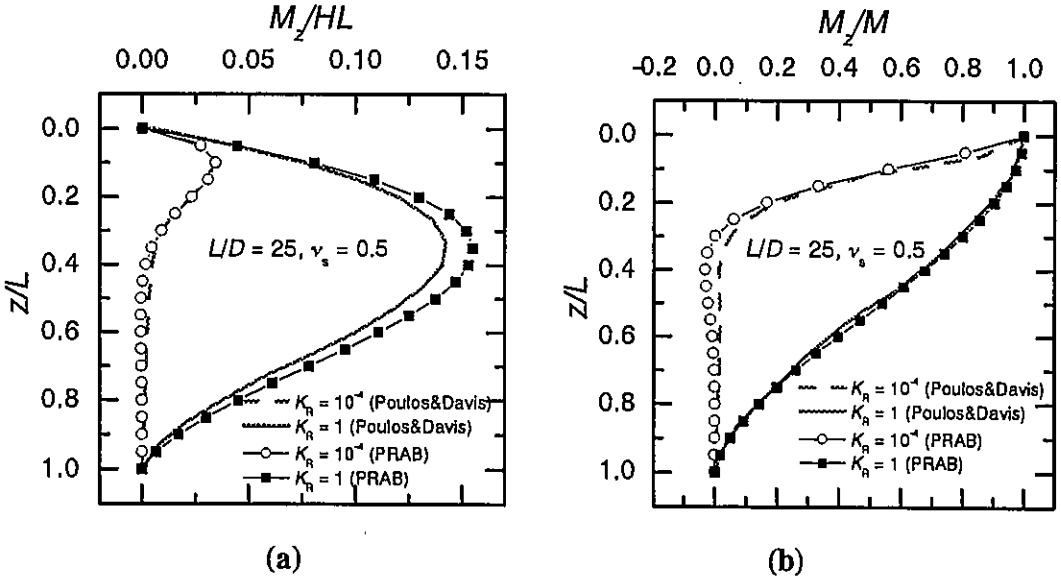

Figure 6.5. Comparisons of moment distributions along pile.

6.3.3. The analysis of pile group foundation with batter piles

In the work of Chow[13], the results of a computer hybrid model analysis for the performance of a typical 6 pile group (**Figure 6.6**) were compared with the results which were obtained from three widely used pile group analysis computer programs, PGROUP (Banerjee & Driscoll[21]), DEFPIG (Poulos[22]) and PIGLET (Randolph[23]). PGROUP is a computer program which was developed based on the boundary element method. The soil is modelled as a homogeneous linear elastic material. In the program DEFPIG, a simplified boundary element analyses for the response of single piles in an elastic soil mass and for the calculation of the interaction factors between two equally loaded piles were employed. The PIGLET program is based on analytical solutions that are either derived theoretically or fitted to finite element results to give the response of single piles. The interaction factors are also determined to fit the results of finite element analyses. In order to examine the validity of the use of PRAB to estimate the deformation and the load distribution of foundations with batter piles, the typical pile group was analyzed and the calculated results were compared with results from these four computer programs for pile group analysis.

The pile group examined is illustrated in **Figure 6.6**. The dimensionless parameters of the pile foundation are listed in **Table 6.1**. In order to model a rigid raft, the raft soil stiffness ratio, K_{rs}, was set equal to 10 following Brown[24]. Analyses were performed for cases where the corner piles were raked in the same plane at angles, γ, of 0, 7.5 and 15 degrees. When PRAB was used to analyze the pile group problem, the soil resistance (soil spring value) at the raft base was set to zero.

Comparisons were done in terms of deflection influence factors. The settlement, w, the lateral displacement, u, and the rotation, θ, of the foundation under vertical load, V, lateral load, H, and moment, M, are given by Equation (6.15).

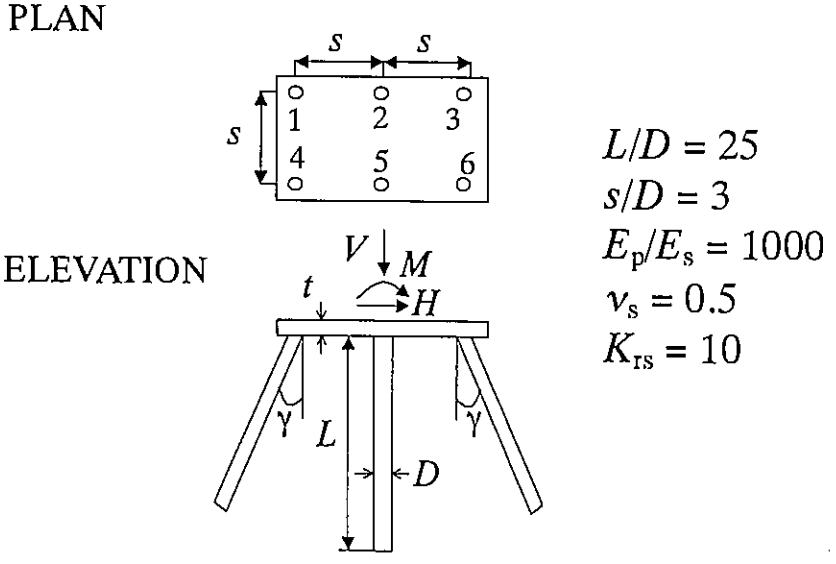

Figure 6.6. Configuration of typical 6-pile foundation.

Table. 6.1. Dimensionless parameters for piled raft foundation.

Dimensionless parameters	Definition
Pile spacing ratio	s/D
Pile slenderness ratio	L/D
Pile-soil stiffness ratio	$K_{ps} = E_p/E_s$
Raft-soil stiffness ratio	$K_{rs} = \dfrac{4E_r B_r t^3 (1-\nu_s^2)}{3\pi E_s L_r^4}$
Noted that s = pile spacing, E_r = Young s modulus of raft, B_r = raft breadth and L_r = raft length	

$$
\begin{aligned}
w &= \frac{V}{E_s D} I_{wV} + \frac{H}{E_s D} I_{wH} + \frac{M}{E_s D^2} I_{wM} \\
u &= \frac{V}{E_s D} I_{uV} + \frac{H}{E_s D} I_{uH} + \frac{M}{E_s D^2} I_{uM} \\
\theta &= \frac{V}{E_s D^2} I_{\theta V} + \frac{H}{E_s D^2} I_{\theta H} + \frac{M}{E_s D^3} I_{\theta M}
\end{aligned}
\tag{6.15}
$$

in which I_{wV}, I_{wH}, I_{wM}, I_{uV}, I_{uH}, I_{uM}, $I_{\theta V}$, $I_{\theta H}$ and $I_{\theta M}$ are the deflection influence factors. For symmetrical pile foundations I_{wH}, I_{wM}, I_{uV} and $I_{\theta V}$ are zero, and from the reciprocal theorem, $I_{\theta H} = I_{uM}$.

In addition, the calculated loads in the individual piles was compared in terms of the load influence factors, C_{aV}, C_{aH}, *etc.*, where the axial force, A, the shear force, S, and the bending moment, B, at the head of the individual piles in the foundation are given as

$$
\begin{aligned}
A &= VC_{aV} + HC_{aH} + \frac{MC_{aM}}{D} \\
S &= VC_{sV} + HC_{sH} + \frac{MC_{sM}}{D} \\
B &= VC_{bV}D + HC_{bH}D + MC_{bM}
\end{aligned}
\tag{6.16}
$$

Comparisons of the deflection influence factors and the load influence factors obtained from the results computed using PRAB and the other four programs are shown in **Figures 6.7 and 6.8**, respectively. It can be seen from **Figure 6.7** that the results obtained from PRAB match well with the results of Chow as well as PGROUP, which is thought to be the most rigorous method among the five methods. **Figure 6.8** shows the load influence factors for piles No. 3 and No. 6. Overall, good agreement between the three solutions can be seen again from **Figure 6.8**. From these comparisons, the validity of the proposed method to analyze pile foundations with batter piles is thought to be established.

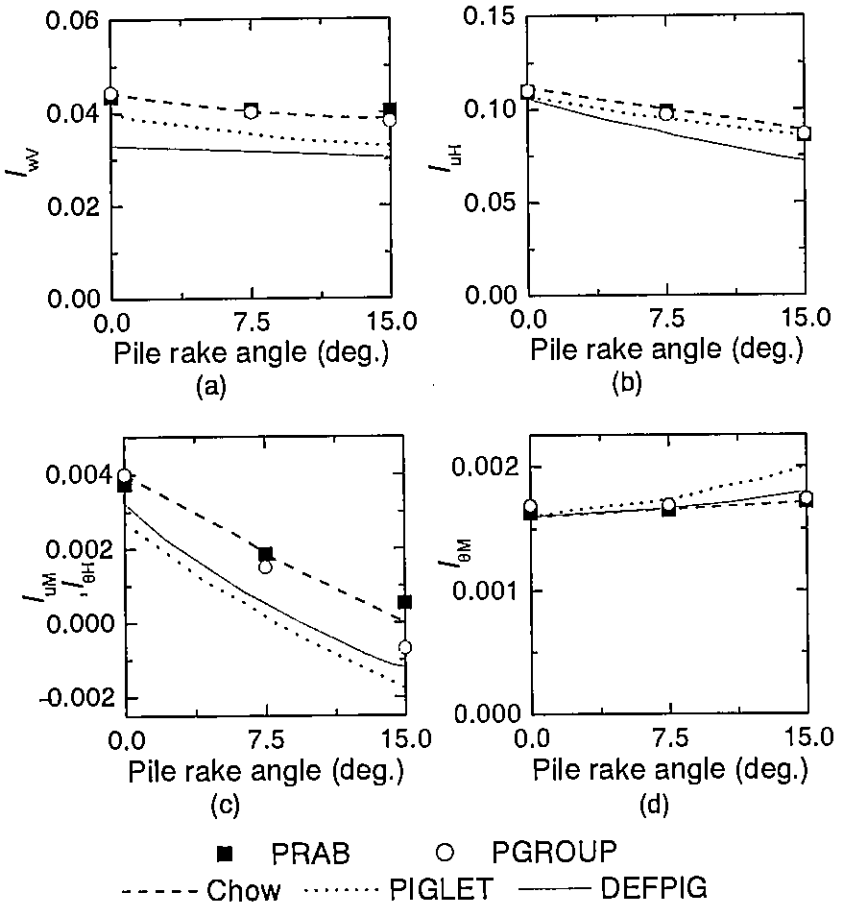

Figure 6.7. Comparisons of group deflection influence factors.

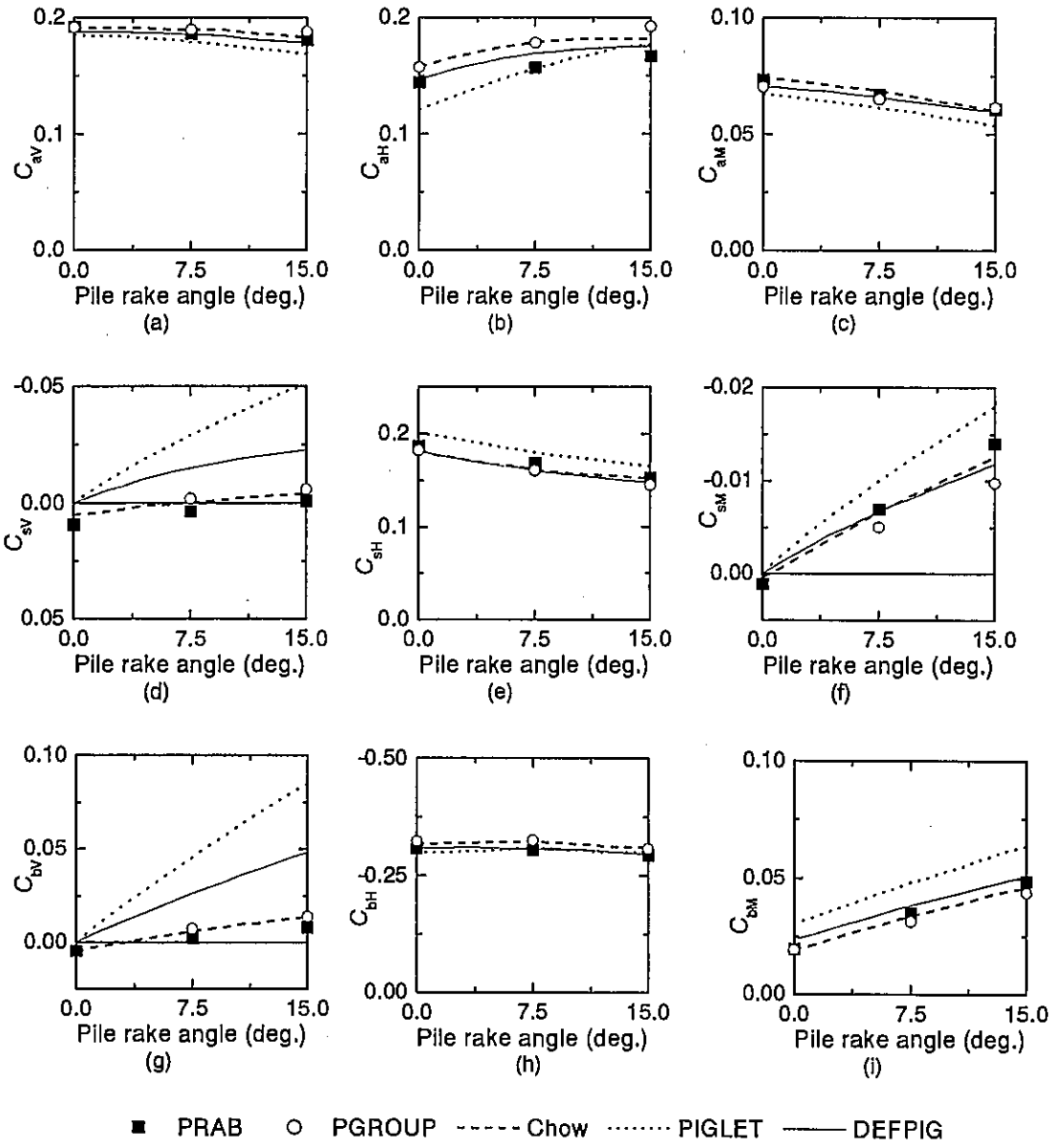

Figure 6.8. Comparisons of load influence factors.

6.4. PARAMETRIC ANALYSIS FOR PILED RAFTS

In the previous section, it was shown that the proposed method is a valid approach to analyze deformation and load distribution of pile foundations, such as piled rafts and pile groups, with vertical and/or batter piles, for elastic subsoil conditions.

Estimation of the load-deformation relationship of a pile foundation to failure is a vital issue in the framework of limit state design. In the current practice of the design of pile foundations, the serviceability limit load tends to be set in the region where subsoils still behave elastically. In order to keep the deformation of a piled raft foundation within an acceptable range, estimation of the deformation for loads within the serviceability limit

load is extremely important in the first design step of a piled raft foundation, in the determination of the raft size, the number of piles, the pile spacing, the pile length and the pile rake angle. Estimation of the deformation characteristics to failure of the piled raft foundation such determined will be conducted in the second design step. In common practice, the deformation stiffness of a single pile and the deformation stiffness of the raft alone are available from load tests or relatively simple calculations. Workable design charts may be useful to approximately estimate deformation and load distribution of a piled raft from the stiffnesses of the structural members. Such design charts for vertically loaded piled rafts have been given in Clancy & Randolph[4]. In this section, parametric calculations for laterally loaded piled rafts are conducted and the corresponding design charts are given for the purpose of aiding the preliminary design of laterally loaded piled rafts.

Additionally, parametric analyses of pile foundations are carried out to demonstrate the effectiveness of the piled raft with batter piles against lateral loads, since the use of batter piles in pile foundation reinforcement works against earthquakes has led to increased interest in the performance of foundations with batter piles.

6.4.1. Introduction of an approximate analysis method for square piled rafts

An approximate method, which employs a flexibility matrix method to combine the individual stiffnesses of a pile group and a raft, was introduced in Randolph[14]. This approximate method allows estimation of the piled raft response from the results of the analysis of the raft and the pile group in isolation. The method is written in the matrix form as

$$\begin{bmatrix} 1/k_p & \alpha_{pr}/k_r \\ \alpha_{rp}/k_p & 1/k_r \end{bmatrix} \begin{Bmatrix} P_p \\ P_r \end{Bmatrix} = \begin{Bmatrix} w_p \\ w_r \end{Bmatrix} \tag{6.17}$$

where w_p = the average displacement of the pile group in the piled raft
w_r = the average displacement of the raft in the piled raft
P_p = the total load carried by the pile group in the piled raft
P_r = the total load carried by the raft in the piled raft
k_p = the overall stiffness of the pile group in isolation
k_r = the overall stiffness of the raft in isolation
α_{rp} = the interaction factor of the pile group on the raft
α_{pr} = the interaction factor of the raft on the pile group

Randolph[14] assumed that the average displacement of the pile group, w_p, is equal to the average displacement of the raft, w_r (i.e. the average displacement of the piled raft w_{pr} =

$w_p = w_r$), and the off-diagonal terms of the flexibility matrix are equalled (i.e. $\alpha_{pr}/ k_r = \alpha_{rp}/ k_p$). He also suggested that the influence of the pile group on the raft is more likely than the influence of the raft on the pile group to result in an average displacement of the raft similar to the above work compatible value. Thus, α_{rp}/ k_p is a more reliable parameter for determining piled raft behaviour than α_{pr}/ k_r. The load carried by the pile group, P_p, and the raft, P_r, and the overall stiffness of the piled raft, k_{pr}, can be found in terms of α_{rp} as shown in Equations (6.18), (6.19) and (6.20).

$$P_p = \frac{\left[1 - k_r\left(\alpha_{rp}/k_p\right)\right] w_{pr}}{\left(1/k_p\right) - k_r\left(\alpha_{rp}/k_p\right)^2} \tag{6.18}$$

$$P_r = \frac{\left[\left(k_r/k_p\right) - k_r\left(\alpha_{rp}/k_p\right)\right] w_{pr}}{\left(1/k_p\right) - k_r\left(\alpha_{rp}/k_p\right)^2} \tag{6.19}$$

$$k_{pr} = \frac{\left(P_p + P_r\right)}{w_{pr}} = \frac{\left[k_p + k_r\left(1 - 2\alpha_{rp}\right)\right]}{\left[1 - \left(k_r/k_p\right)\alpha_{rp}^2\right]} \tag{6.20}$$

Randolph[14] also assumed that the value of α_{rp} for a single pile-raft unit is directly applicable to a piled raft foundation having more than one pile. This means that for a known value of α_{rp}, approximate values for the average displacement of the piled raft and the load distribution between the pile group and the raft can be calculated.

In Clancy & Randolph[4], a series of analyses of vertically loaded square piled rafts with a small number of piles up to 36, was carried out, and the influence of parameters (such as pile group size, pile spacing ratio, pile slenderness ratio, pile soil stiffness ratio, and raft soil stiffness ratio) on the values of α_{rp} and α_{pr} was investigated. The values of α_{rp} and α_{pr} were calculated from the values of P_p, P_r, k_p, k_r and w_{pr} by means of Equation (6.21).

$$\alpha_{rp} = \frac{k_p}{P_p}\left(w_{pr} - \frac{P_r}{k_r}\right), \alpha_{pr} = \frac{k_r}{P_r}\left(w_{pr} - \frac{P_p}{k_p}\right) \tag{6.21}$$

In order to obtain all the values of P_p, P_r, k_p, k_r and w_{pr}, it is necessary to perform three separate analyses. The values of k_p and k_r are obtained from analyses of the pile group and the raft in isolation. Then, a full analysis of the piled raft is performed to obtain P_p, P_r and w_{pr}.

Similar analyses of foundations subjected to lateral load were carried out in this paper to

obtain the values of α_{rp}^{L} and α_{pr}^{L} as will be described in section 6.4.2. Hereafter, superscript L will be used for the quantities related to the lateral direction. For an example, k_{p}^{L} is the pile group stiffness subjected to a lateral load.

6.4.2. Parametric study for laterally loaded square piled rafts

Analyses were conducted on square piled rafts varying the number of piles between 1 and 36. The ranges of the dimensionless parameters were set as 2–9 for the pile spacing ratio s/D, as 10–50 for the pile slenderness ratio L/D, as 10^2–10^5 for the pile soil stiffness ratio E_p/E_s, and as 0.01–10 for the raft soil stiffness ratio K_{rs}.

In Clancy & Randolph[4] the analyses were done without considering the interaction in the lateral direction due to a vertical point force, whereas this lateral interaction is considered in PRAB. In order to investigate the influence of this difference, analyses of vertically loaded single pile–raft units were conducted using PRAB. **Figure 6.9** shows the calculated values of α_{rp} and α_{pr} for the vertically loaded single pile–raft units. The results plotted in **Figure 6.9** are almost the same as those obtained in Clancy & Randolph[4]. This shows that consideration of the lateral interaction in the analyses of symmetrically vertically loaded foundations has only a small effect on the calculated values of α_{rp} and α_{pr}.

The calculated values of α_{rp}^{L} and α_{pr}^{L} for laterally loaded single pile–raft units are shown in **Figure 6.10**. It can be seen that α_{rp}^{L} decreases as the raft size of the single pile–raft units (pile spacing) increases, or as the pile stiffness decreases. On the other hand, there is no clear trend in the value of α_{pr}^{L}. For example, the value of α_{pr}^{L} even becomes negative when the pile is short and stiff. This may be caused by the use of the deformation profile of the laterally loaded single pile alone to calculate k_{p}^{L}, which is different from the deformation pattern of the pile as a component of the piled raft. As an example, in the case of L/D = 10, E_p/E_s = 10^5, and s/D = 9, the single pile alone deformed like a short pile in which all parts of the pile leaned due to the lateral load, and lateral displacement opposite to the loading direction occurred at the pile toe. On the other hand, in the case of the corresponding single pile in piled rafts, only the top part of the pile deformed laterally with little rotation of the pile head.

Figure 6.11 shows a similar set of plots obtained for various sized 3×3 piled rafts. Compared with the value of α_{rp}^{L} for the corresponding single pile–raft units, the value of α_{rp}^{L} for the 3×3 piled rafts are larger and the distribution of the values is narrower. The value of α_{pr}^{L} for the 3×3 piled rafts has a different trend from that for the corresponding single pile–raft units. The value of α_{pr}^{L} for the 3×3 piled rafts increases as the pile spacing increases, or as the pile stiffness decreases. This is due to the fact that the deformation pattern of piles in the piled rafts is similar to that of the piles in the corresponding pile groups.

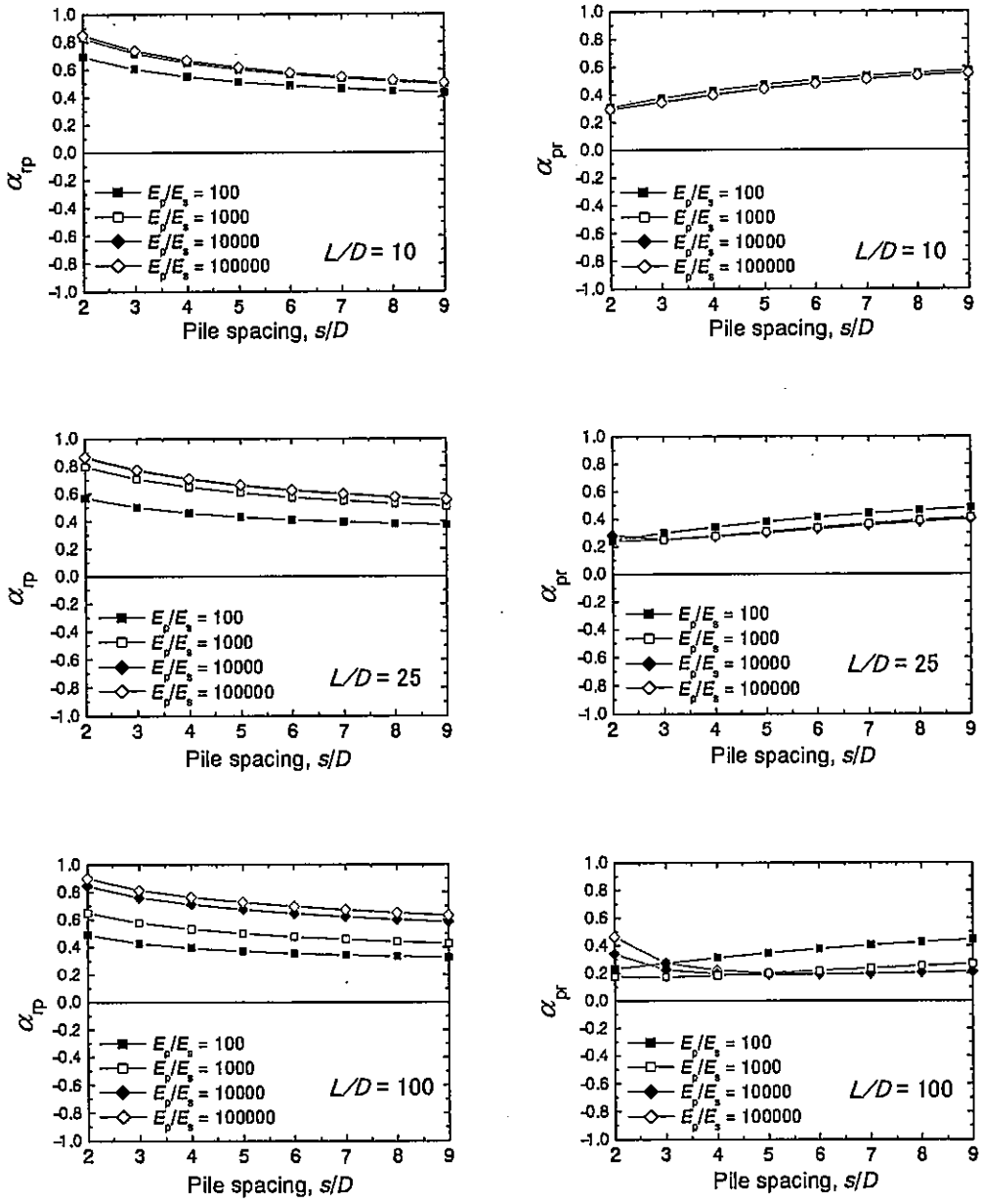

Figure 6.9. Calculated values for vertically loaded single pile-raft unit (K_{rs} = 10).

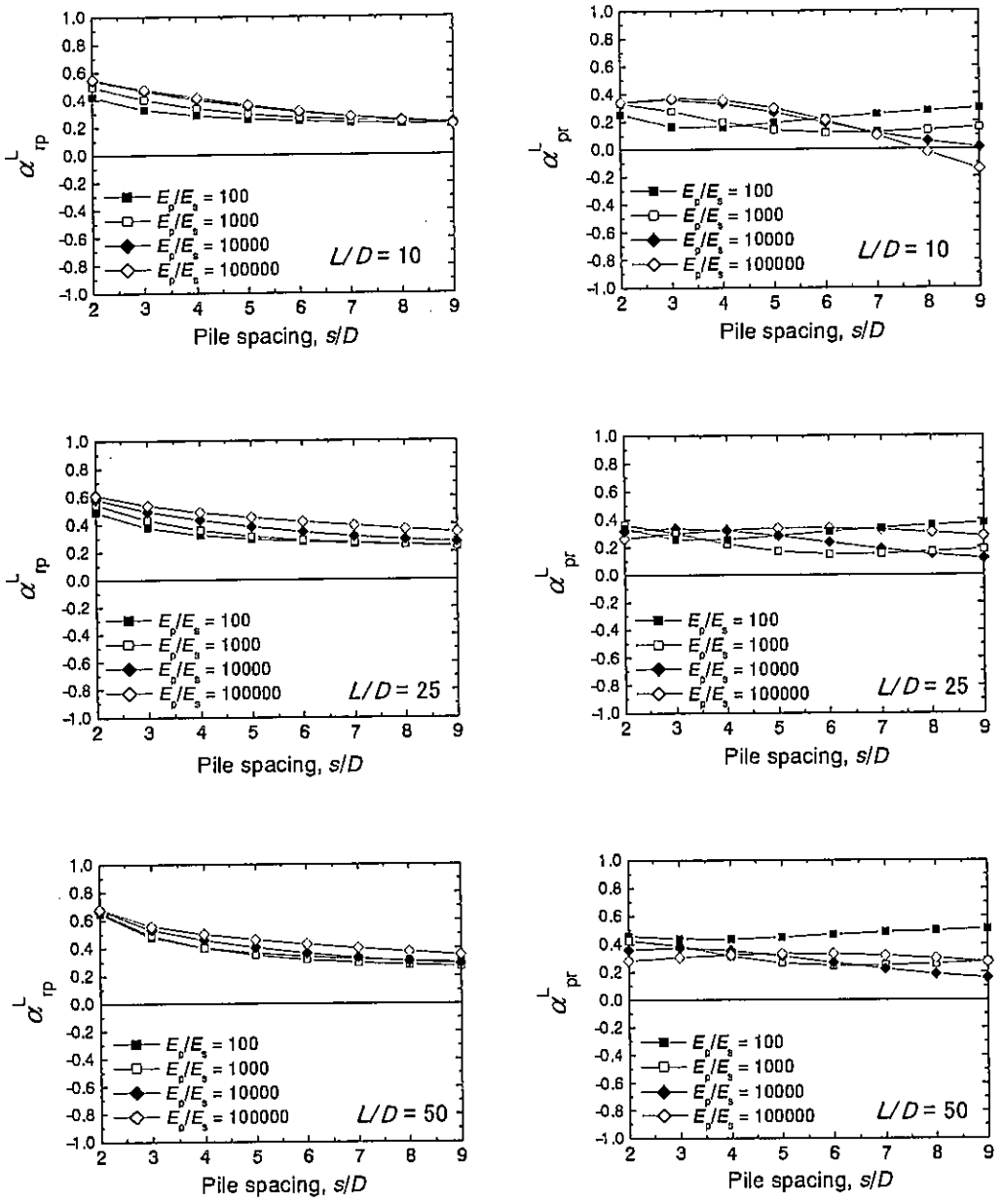

Figure 6.10. Calculated values for laterally loaded single pile-raft unit (K_{rs} = 10).

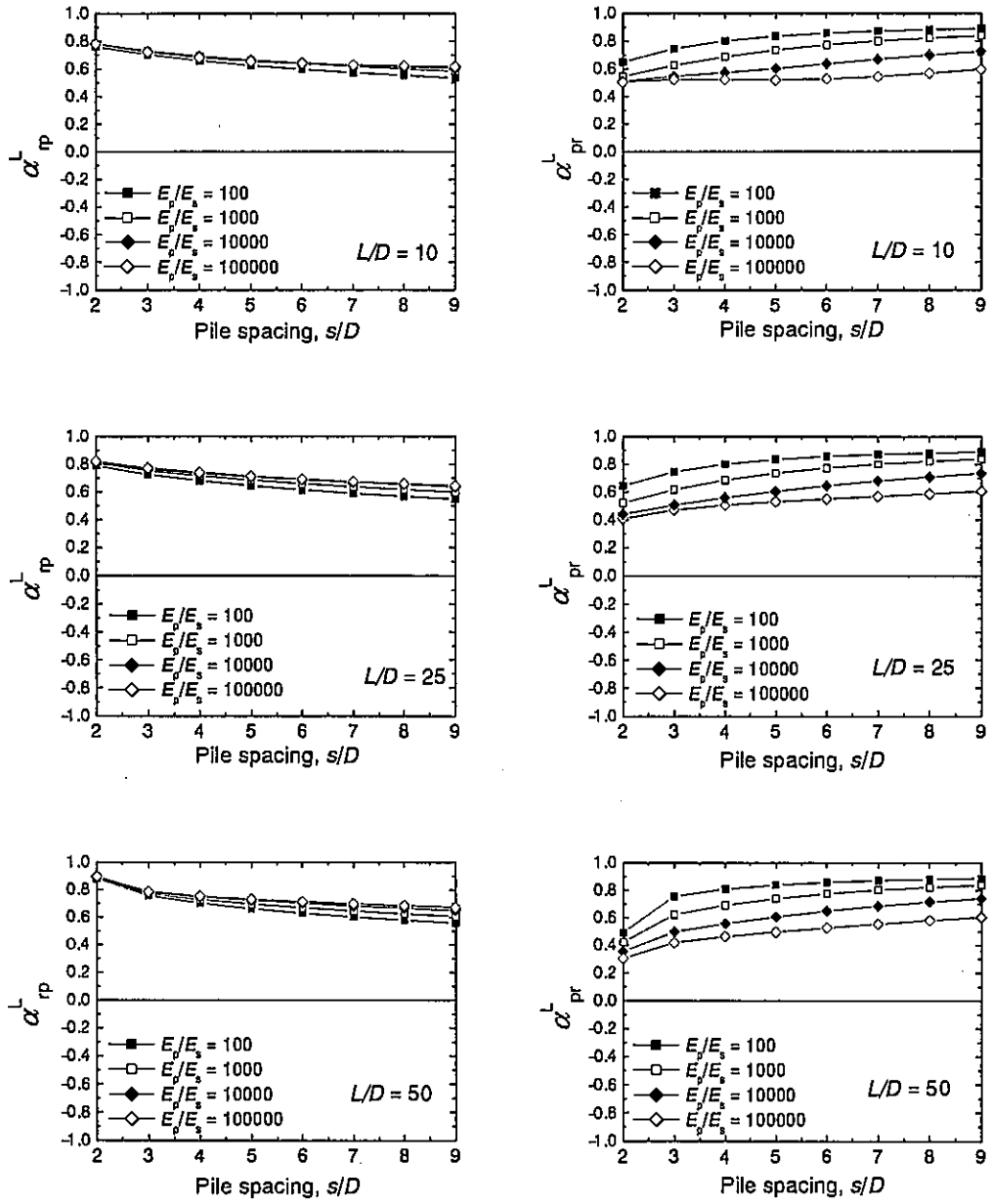

Figure 6.11. Calculated values for 3×3 piled raft (K_{rs} = 10).

Figure 6.12 shows the calculated values of α_{rp}^{L} and α_{pr}^{L} for square piled rafts in which the number of piles was varied between 1 and 36, and E_p/E_s was varied as 10^2 and 10^5, setting $L/D = 25$ and $K_{rs} = 10$ throughout. Both the values of α_{rp}^{L} and α_{pr}^{L} increase with the number of piles. It can be seen that the effect of E_p/E_s on α_{rp}^{L} is small except for the case of the single pile-raft unit (1×1 piled raft).

The effects of the pile slenderness ratio, L/D, and the raft soil stiffness ratio, K_{rs}, on the values of α_{rp}^{L} and α_{pr}^{L} for the 3×3 piled raft are shown in **Figures 13 and 14**, respectively. The figures show that the variations of the pile slenderness ratio and the raft soil stiffness ratio have little effect on the values of α_{rp}^{L} and α_{pr}^{L}.

Figures 6.10 to 6.14 may be used as design charts to estimate the stiffness of piled rafts subjected to lateral loading, k_{pr}^{L}, by substituting the value of α_{rp}^{L} from the figures into Equation (6.20), and to estimate the load distribution, P_p^L and P_r^L, using Equations (6.18) and (6.19).

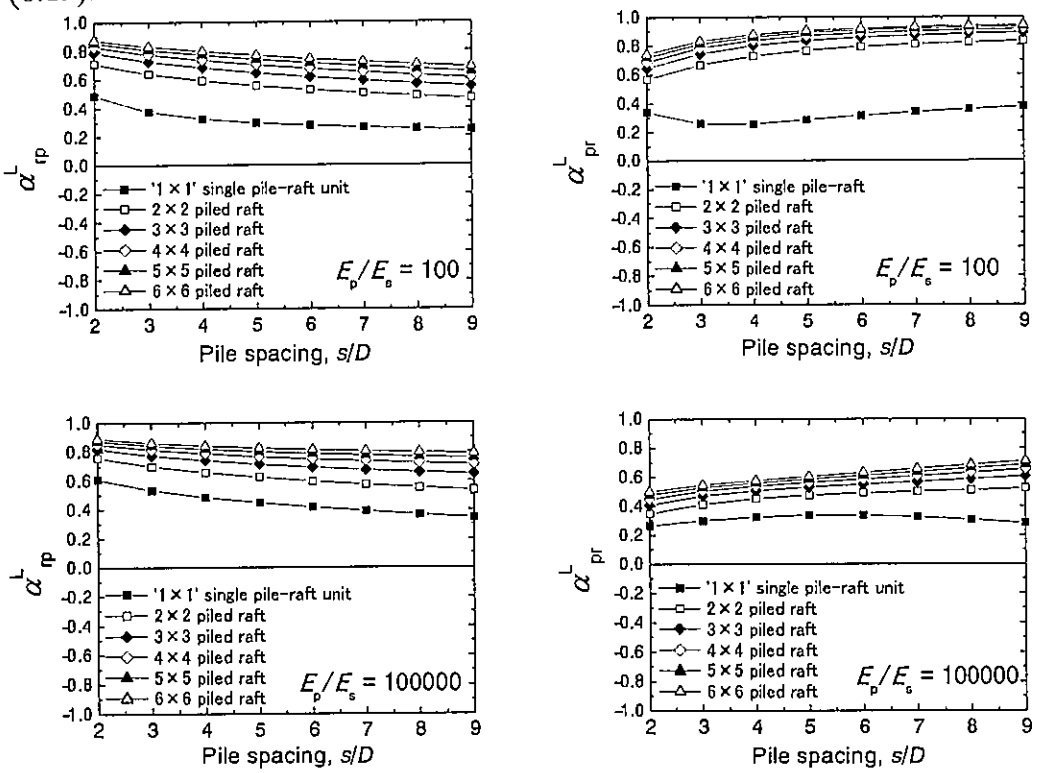

Figure 6.12. Calculated values: L/D = 25, K_{rs} = 10.

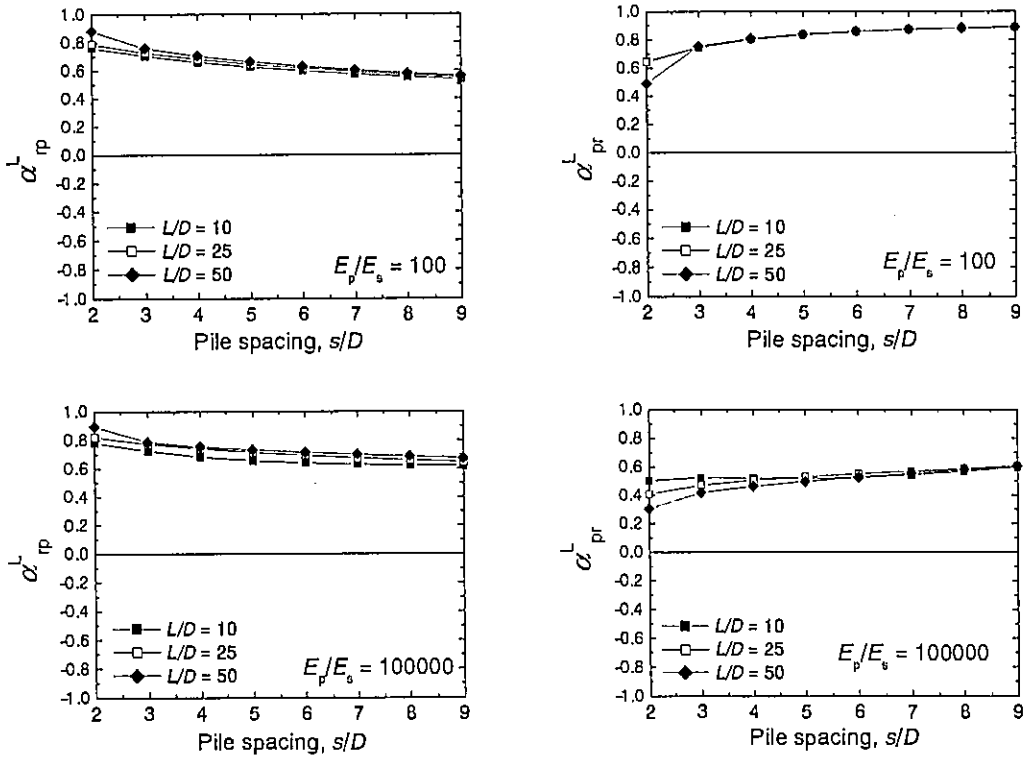

Figure 6.13. Calculated values for 3×3 piled raft (K_{rs} = 10).

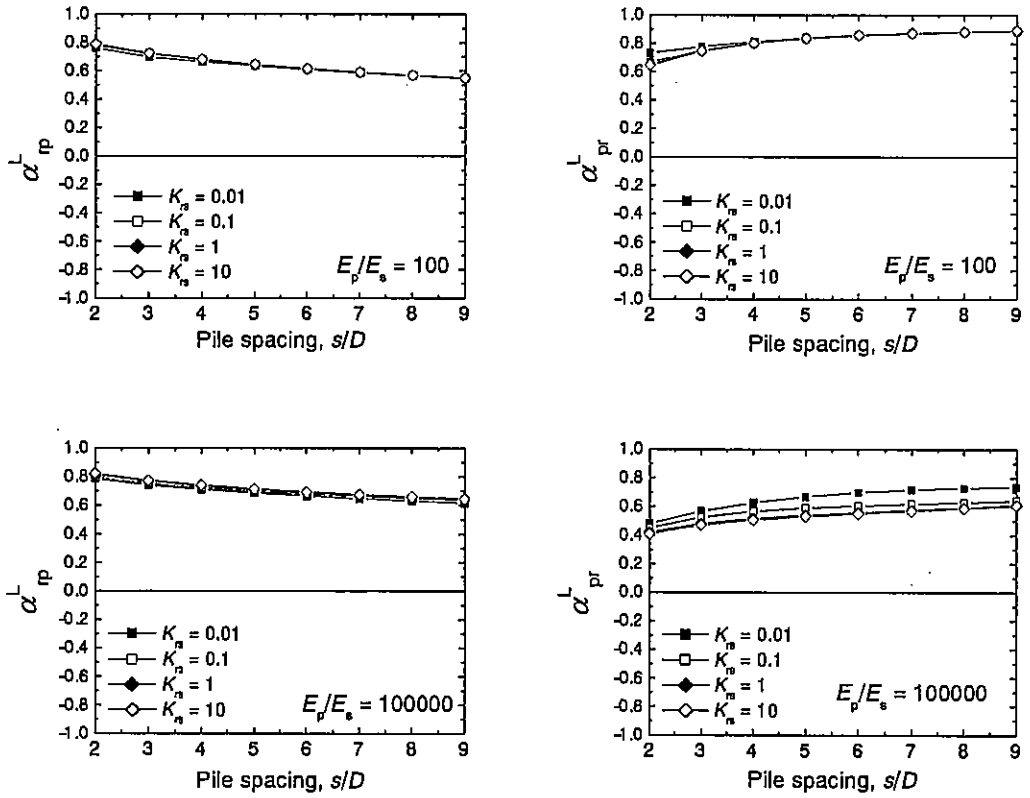

Figure 6.14. Calculated values for 3×3 piled raft (L/D = 25).

6.4.3. Parametric study for foundations with batter piles

In order to compare the performance of pile group and piled raft foundations with batter piles and to investigate the effects of the pile slenderness ratio and the pile rake angle on the deformation and load distribution of batter pile foundations, a typical 6-pile foundation (as shown in **Figure 6.6**) was analyzed. The pile length in the foundations was varied as L/D = 10, 25 and 50, while the corner piles were raked in the same plane at angles, γ, of 0, 7.5 and 15 degrees. Two types of foundations, pile groups and piled rafts, were analyzed. In the analysis of the pile groups, the soil spring value at the raft base was set to zero. Comparisons of the group deflection influence factors and the load influence factors (Equations (6.15) and (6.16)) of the calculated results for the two foundation types were made.

Figure 6.15 shows the comparisons of the group deflection influence factors. It can be clearly seen that the deflections of the piled rafts are smaller than those of the pile groups. The effect of the raft in reducing the deformations becomes smaller as the pile length increases. **Figure 6.15** also shows that the effects of pile rake angle on the deflections of the foundation are almost the same in both foundation types. **Figure 6.15(a)** shows that foundation with longer piles had smaller settlement, and that the pile rake angle has only a small effect on the settlement. On the other hand, **Figure 6.15(b)** shows that an increase in

the pile length does not efficiently improve the performance of a foundation subjected to lateral load, and that it would be better to slightly slant the piles than to increase the pile length. In addition, for foundations subjected to lateral load, an increase in the pile rake angle not only reduces the lateral displacement, but also reduces the inclination of the raft ($I_{\theta H}$ in **Figure 6.15(c)**). From the reciprocal theorem ($I_{uM} = I_{\theta H}$), it is noted that an increase in the pile rake angle can suppress the lateral displacement of foundations subjected to moment loads. **Figure 6.15(d)** shows the inclination of the foundations when subjected to moment load. It can be seen that for a short pile (L/D = 10), the inclination decreases with an increase in the pile rake angle whereas the inclination increased with increase in the pile rake angle for longer piles.

The axial and shear forces, and the bending moment at the head of piles No. 3 and No. 6 are shown in **Figure 6.16**. The load influence factors of C_{sM} for the shear force and C_{bM} for the bending moment at the pile head due to moment load for the pile raft are almost the same as those for the pile group. Except for these factors, the load influence factors for the piled rafts are small compared to those for the pile groups.

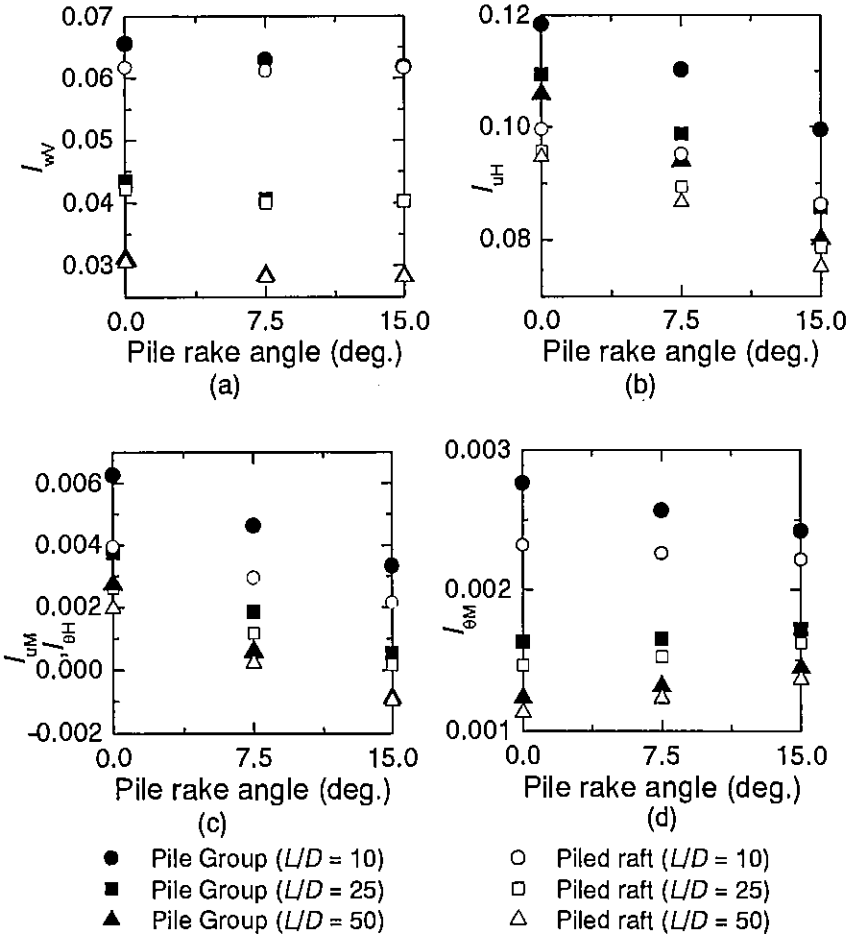

Figure 6.15. Comparisons of group deflection influence factors.

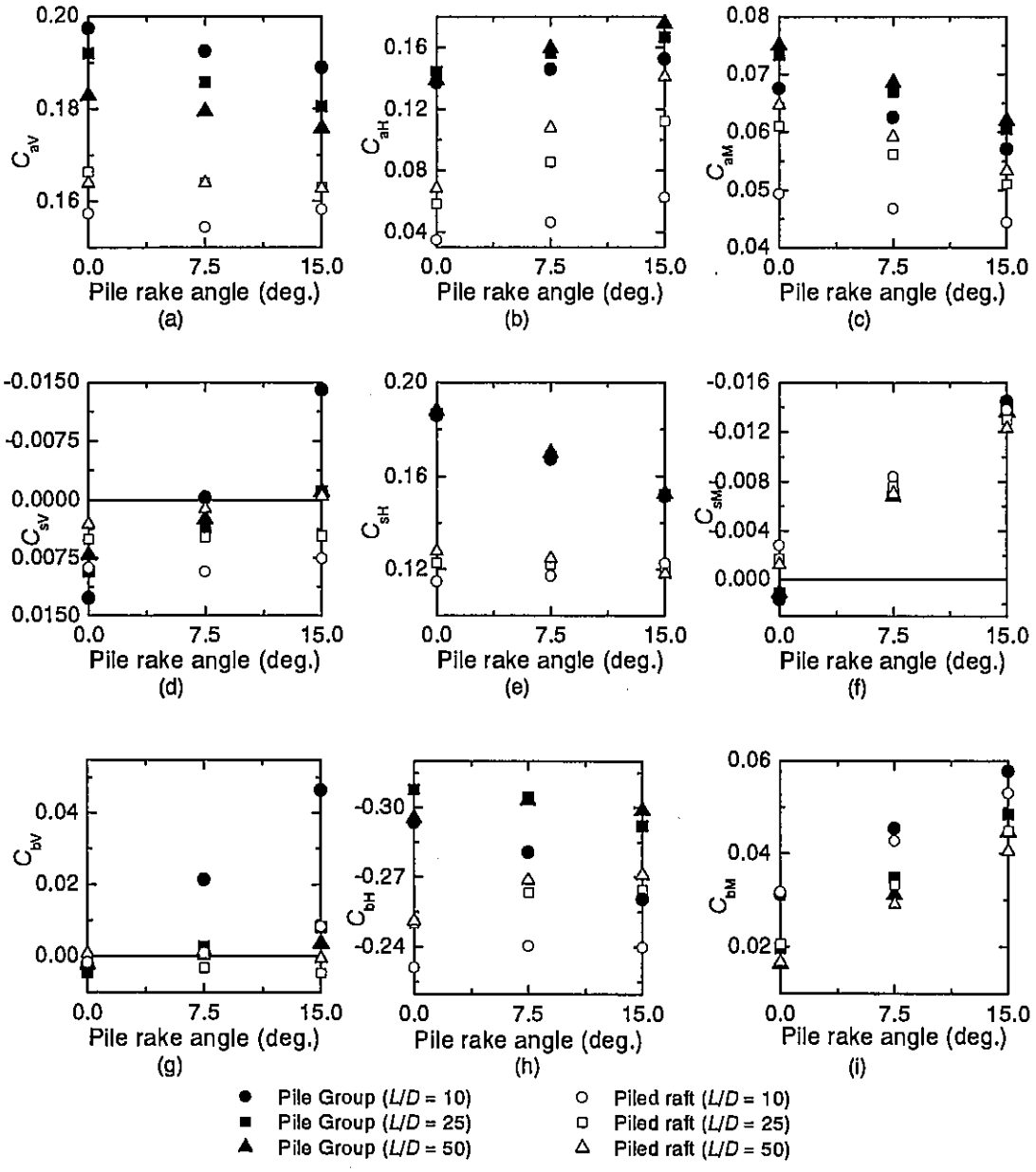

Figure 6.16. Comparisons of load influence factors.

6.5. CONCLUSIONS

A simplified analytical method for the analysis of the deformation of piled raft foundations subjected to vertical, lateral and moment loading has been developed, using a hybrid model. An important feature of the proposed method is that pile-soil-pile, pile-soil-raft, raft-soil-raft interactions due to lateral forces as well as vertical forces were incorporated in the analysis. The proposed method was verified through comparisons with the results from previous research. Workable design charts were given for the values of α_{rp}^{L}, which may be used for the estimation of the lateral displacement and the load distribution

of a piled raft from the stiffnesses of the raft alone and the pile group alone. Additionally, parametric studies were carried out concerning batter pile foundations. It was found that the use of batter piles can efficiently improve the performance of pile foundations subjected to lateral loads.

ACKNOLEDGEMENT

This study was supported by Grant-in-Aid for Scientific Research (Grant No. 12450188) of Japanese Ministry of Education, Culture, Sports, Science and Technology.

REFERENCES

1. Hain SJ, Lee IK. The analysis of flexible raft-pile systems. *Géotechnique* 1978; **28**(1):65-83.
2. Poulos HG, Davis EH. *Pile foundation analysis and design*. Wiley: New York, 1980.
3. Kuwabara F. An elastic analysis for piled raft foundations in a homogeneous soil. *Soils and Foundations* 1989; **29**(1):82-92.
4. Clancy P, Randolph MF. An approximate analysis procedure of piled raft foundations. *International Journal for Numerical and Analytical Methods in Geomechanics* 1993; 17:849-869.
5. Poulos HG. An approximate numerical analysis of pile-raft interaction. *International Journal for Numerical and Analytical Methods in Geomechanics* 1994; **18**:73-92.
6. Randolph MF. Design methods for pile groups and piled rafts. *Proc. 13th ICSMFE*, New Delhi 1994; **5**:61-82.
7. Yamashita K., Kakurai M., Yamada T. Investigation of a piled raft foundation on stiff clay. *Proc. 13th ICSMFE*, New Delhi 1994; **2**:543-546.
8. Ta LD, Small JC. Analysis of piled raft systems in layered soils. *International Journal for Numerical and Analytical Methods in Geomechanics* 1996; **20**:57-72.
9. Horikoshi K, Randolph MF. A contribution to optimum design of piled raft. *Géotechnique* 1998; **48**(3):301-317.
10. Horikoshi K, Randolph MF. Estimation of overall settlement of piled rafts. *Soils and Foundations* 1999; **39**(2):59-68.
11. O Neill MW, Ghazzaly OI, Ha HB. Analysis of three-dimensional pile groups with nonlinear soil response and pile-soil-pile interaction. *Proc. 9th Offshore Technology Conf.* 1977; **2**:245-256.
12. Mindlin RD. Force at a point interior of a semi-infinite solid. *Physics* 1936; **7**:195-202.
13. Chow YK. Three-dimensional analysis of pile groups. *Journal of Geotechnical Engineering ASCE* 1987; **113**(6):637-651.

14. Randolph MF. Design of piled raft foundations. *Proc. Int. Symp. Recent Developments in Laboratory and Field Tests and Analysis of Geotechnical Problems*, Bangkok 1983:525-537.
15. Poulos HG, Davis EH. *Elastic Solution for Soil and Rock Mechanics*. Wiley: New York, 1974.
16. Randolph MF, Wroth CP. Analysis of deformation of vertically loaded piles. *Journal of Geotechnical Engineering ASCE* 1978; **104**(12):1465-1488.
17. Saul WE. Static and dynamic analysis of pile foundations. *Journal of Structural Division ASCE* 1968; **94**(5):1077-1100.
18. Poulos HG, Madhav MR. Analysis of the movements of battered piles. *Proc. 1st Australia-New Zealand Conf. on Geomech.* 1971; **1**:268-275.
19. Chow YK. Analysis of vertically loaded pile groups. *International Journal for Numerical and Analytical Methods in Geomechanics* 1986; **10**(1):59-72.
20. Poulos HG. Behaviour of laterally loaded piles:I-Single Piles. *Journal of Soil Mechanics and Foundations Division ASCE* 1971; **97**(5):711-731.
21. Banerjee PK, Driscoll RMC. Three-dimensional analysis of raked pile groups. *Proc. Institution Civ. Engrs.* Part 2 1976; **61**:653-671.
22. Poulos HG. An approach for the analysis of offshore pile groups. *Proc. Int. Conf. Numer. Methods in Offshore Piling*, London, U.K. 1980:119-126.
23. Randolph MF. PIGLET:A computer program for the analysis and design of pile groups under general loading condition. *Soil Report TR91 CUED/D.* Cambridge Univ., England 1980.
24. Brown PT. Strip footing with concentrated loads on deep elastic foundations. *Geotech. Eng.* 1975;**6**:1-13.

CHAPTER 7

DEVELOPMENT OF A SIMPLIFIED ANALYSIS METHOD FOR PILED RAFT AND PILE GROUP FOUNDATIONS IN NONHOMOGENEOUS SOILS

(*N.B.* This chapter was published in Int. Jour. for Numerical Methods in Geomechanics, Vol.27, pp.85-109, entitled "A SIMPLIFIED ANALYSIS METHOD FOR PILED RAFT FOUNDATIONS IN NONHOMOGENEOUS SOILS" by Pastsakorn Kitiyodom & Tatsunori Matsumoto)

SUMMARY

A simplified method of numerical analysis based on elasticity theory has been developed for the analysis of axially and laterally loaded piled raft foundations embedded in nonhomogeneous soils and incorporated into a computer program PRAB . In this method, a hybrid model is employed in which the flexible raft is modelled as thin plates and the piles as elastic beams and the soil is treated as springs. The interactions between structural members, pile-soil-pile, pile-soil-raft and raft-soil-raft interactions, are approximated based on Mindlin s solutions for both vertical and lateral forces with consideration of nonhomogeneous soils. The validity of the proposed method is verified through comparisons with some published solutions for single piles, pile groups and capped pile groups in nonhomogeneous soils. Thereafter, the solutions from this approach for the analysis of axially and laterally loaded 4-pile pile groups and 4-pile piled rafts embedded in finite homogeneous and nonhomogeneous soil layers are compared with those from three-dimensional finite element analysis. Good agreement between the present approach and the more rigorous finite element approach is demonstrated.

KEY WORDS: piled raft; hybrid model; nonhomogenous soil; Mindlin s solution

7.1. INTRODUCTION

A simplified analysis method for an estimation of the deformation and load distribution of axially and laterally loaded piled raft foundations with batter piles has been presented previously by Kitiyodom & Matsumoto[1]. Finite element modelling was used to model the structural elements of the foundation, and the soil was modelled as springs attached at the structural nodes. The method made use of Mindlin s solutions[2] to account for the interactions between structural members. This analytical model has been incorporated into a computer program PRAB (Piled Raft Analysis with Batter piles). However, in this previous work, only semi-infinite homogeneous soils were considered. In practice, soil profiles may consist of different layers underlain by a stiff or rigid base soil stratum. The consideration of nonhomogeneous soils will be more realistic in many cases. Therefore, we decided to incorporate the effect of the soil profile into the analytical model.

Much work has been done on the analysis of pile foundations embedded in nonhomogeneous soils. Integral equation methods based on the theory of elasticity were used in the works of Banerjee & Davies[3,4], Poulos[5,6], and Poulos & Davis[7]. These methods make use of Mindlin s solutions to account for pile-soil-pile interaction, and the influence of soil nonhomogeneity is approximated using some averaging of the soil moduli. In the work of Chow[8], a hybrid approach is used and the pile-soil-pile interaction is determined from a finite element procedure. The hybrid approach is used with Mindlin s solutions for the settlement analysis of single piles and pile groups in the work of Lee[9]. Ta & Small[10,11] have analysed piled raft systems subjected to vertical loads in a layered soil. In their work, a finite layer method is introduced to analyse the layered soil, while a finite element method is used to analyse the piles and the raft. Zhang & Small[12] used the same method to analyse off-ground capped pile group systems subjected to both vertical and lateral loads. In their work, obviously, the vertical and lateral resistances of the raft base were not included in the analysis.

A complete three-dimensional analysis of a piled raft foundation system can be carried out by a finite element analysis (e.g. Smith & Wang[13]). The use of the finite element approach removes the need for the approximate assumptions inherent in the above-mentioned simplified approaches. However, a finite element analysis is more suited to obtaining benchmark solutions against which to compare simpler analysis methods, or to obtaining solutions of a detailed analysis for the final design of a foundation, rather than as a preliminary routine design tool.

Section 7.2 immediately below presents an extension of the computer program PRAB for the simplified analysis of piled raft foundations embedded in nonhomogeneous soils. In order to examine the validity of the improved PRAB, the results calculated using PRAB are compared with the solutions available from previous research in Section 7.3. In Section 7.4, comparative analyses between PRAB and a three-dimensional finite element analysis are

carried out for the interaction factor between two piles under lateral loading and for axially and laterally loaded piled raft and pile group foundations, and good agreement between these two solutions is demonstrated.

7.2. METHOD OF ANALYSIS

In this work, the simplified analysis method using a hybrid model developed by Kitiyodom & Matsumoto[1] (or Chapter 6 of this report) is employed, in which the flexible raft is modelled as thin plates and the piles as elastic beams, and the soil is treated as springs, as shown in **Figure 7.1.**

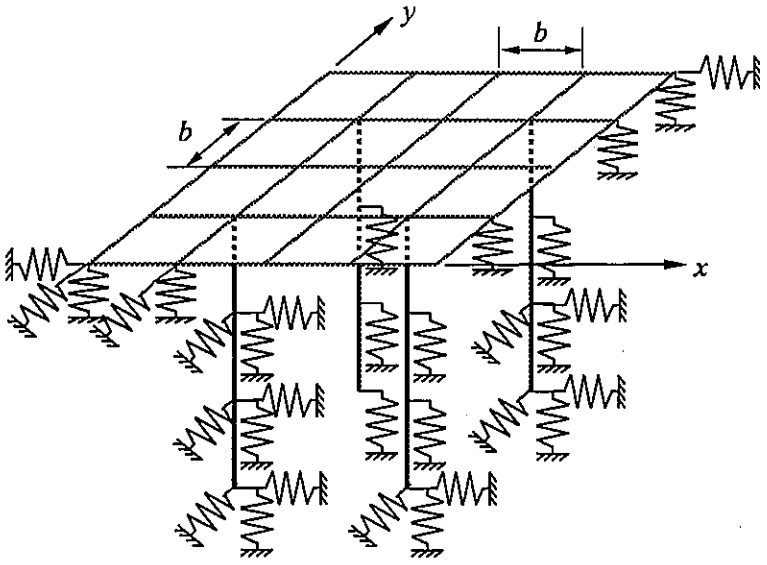

Figure 7.1. Plate-beam-spring modelling of a piled raft foundation.

For soil profiles that are arbitrarily layered and/or underlain by a rigid bed stratum, the vertical soil springs, K_z^{Pb}, at the pile base nodes and the vertical soil springs, K_z^{P}, at the pile shaft nodes are estimated using Equations (7.1) and (7.2), respectively, to include the influence of finite layered soils, following Lee[9]. Lee[9] also suggested the use of a general expression for the influential radius, r_m, given by Equation (7.3). In this work, the vertical soil springs, K_z^{R}, at the raft nodes are estimated by Equation (7.4).

$$K_z^{Pb} = \frac{4G_b r_o}{1-\nu_{sb}} \times \frac{1}{\left\{1-\exp\left(-h^*/2r_o\right)\right\}} \tag{7.1}$$

$$K_z^{P} = \frac{2\pi G \Delta L}{\ln\left(r_m/r_o\right)} \tag{7.2}$$

$$r_m = 2.5\left[\frac{\sum_{i=1}^{np} G_i L_i}{G_m L}\sqrt{\frac{G_m}{G_b}}\chi L\left(1-\bar{\nu}_s\right)\right], \quad \chi = 1-\exp\left(1-h/L\right) \tag{7.3}$$

$$K_z^{\mathrm{R}} = \frac{4\bar{G}a}{1-\bar{\nu}_s} \times \frac{1}{\left\{1-\exp\left(-h/2a\right)\right\}} \tag{7.4}$$

where h is the finite soil depth, h^* the distance between the pile base and the rigid bed stratum, a the equivalent radius of the raft element, r_o the pile radius, ΔL the pile segment length, and L the pile length. G_m is the maximum soil shear modulus, G_b and ν_{sb} are the shear modulus and the Poisson s ratio of the soil at the pile base. G_i and L_i are the shear modulus of the soil layer i and the length of pile embedded in soil layer i, and np is the total number of soil layers along the pile length. $\bar{G}$ and $\bar{\nu}_s$ are the equivalent shear modulus and the equivalent Poisson s ratio of the whole soil which can be determined as follows, following Fraser & Wardle[14]:

$$\bar{G} = \frac{\bar{E}_s^*}{2\left(1+\bar{\nu}_s\right)} \tag{7.5}$$

$$\bar{\nu}_s = \sum_{i=1}^{n} \nu_{s(i)} \Delta I_i / \Delta I_{\mathrm{total}} \tag{7.6}$$

where $\bar{E}_s^*$ is the equivalent Young s modulus for the whole soil given by Equation (7.7).

$$\frac{1}{\bar{E}_s^*} = \sum_{i=1}^{n} \frac{1}{E_{s(i)}^*} \Delta I_i / \Delta I_{\mathrm{total}} \tag{77.}$$

where $E_{s(i)}^*$ is the equivalent Young s modulus for the soil layer number i given by Equation (7.8).

$$E_{s(i)}^* = E_{s(i)} / \left(1-\nu_{s(i)}^2\right) \tag{7.8}$$

where $E_{s(i)}$ and $\nu_{s(i)}$ are the Young s modulus and the Poisson s ratio for soil layer number i in the n-layered system. ΔI_i and $\Delta I_{\mathrm{total}}$ in Equations (7.6) and (7.7) are the differences between the vertical settlement influence factors at different soil depths which can be determined by Equations (7.9) and (7.10).

$$\Delta I_i = I\left(z_{\mathrm{top}}^i\right) - I\left(z_{\mathrm{bottom}}^i\right) \tag{7.9}$$

$$\Delta I_{\mathrm{total}} = I\left(0\right) - I\left(h\right) \tag{7.10}$$

where z_{top}^i and z_{bottom}^i are the depths below the surface of the top and bottom of layer number i.

The vertical settlement influence factor I has been given by Harr[15] (see Appendix I).

Note that in Equations (7.1) to (7.3) only the nonhomogeneity of the soil along the pile shaft is considered. The influence of nonhomogeneous soil below the pile base may be calculated using an extension of the Steinbrenner approximation as described in Reference [7].

The horizontal soil springs, K_x^R and K_y^R, at the raft nodes, and the horizontal soil springs, K_x^{Pb} and K_y^{Pb}, at the pile base nodes are estimated by means of Equations (7.11) and (7.12), and the horizontal soil springs, K_x^P and K_y^P, at the pile shaft nodes are estimated by means of Equation (7.13). As for loading in the horizontal direction, the near surface soil layer seems to be the most influential. Hence, the soil shear modulus G_r and the Poisson's ratio ν_{sr} which are the shear modulus and the Poisson's ratio of the soil layer just beneath the raft is employed in the estimation of the horizontal springs at the raft nodes. The validity of this assumption will be demonstrated in Section 7.4.2.

$$K_x^R = K_y^R = \frac{32(1-\nu_{sr})G_r a}{7-8\nu_{sr}} \tag{7.11}$$

$$K_x^{Pb} = K_y^{Pb} = \frac{32(1-\nu_{sb})G_b r_o}{7-8\nu_{sb}} \tag{7.12}$$

$$K_x^P = K_y^P = \zeta E_s \Delta L \tag{7.13}$$

where $\zeta = pD/\rho E_s$ in which p is the lateral distributed force acting along a pile element, D the pile diameter and ρ the corresponding lateral displacement at each pile node calculated using the integral equation method by Poulos & Davis[7].

In order to obtain an approximate estimate of the influence of a finite depth on the interaction between structure member nodes, pile-soil-pile, pile-soil-raft and raft-soil-raft interactions may be determined using a modified form of Mindlin s solutions by employing the Steinbrenner approximation. The accuracy of this approximation has been discussed by Poulos[16] in relation to surface footings. From this approximation, the interaction factor for node i due to a unit force acting at node j in a finite soil of depth h is given by:

$$I_{ij(h)} = I_{ij(\infty)} - I_{im(\infty)} \tag{7.14}$$

where $I_{ij(\infty)}$ is the interaction factor for node i due to a unit force acting at node j in an infinite half space and $I_{im(\infty)}$ is the interaction factor for node i due to a unit force acting at the corresponding imaginary node m in the infinite half space directly beneath node j at the distance of h (see **Figure 7.2**).

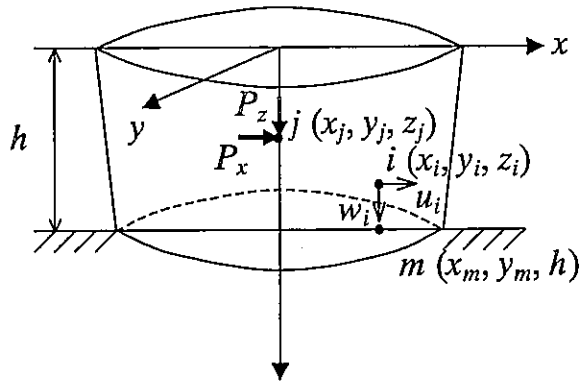

Figure 7.2. Estimation of the influence of a finite depth on the interactions.

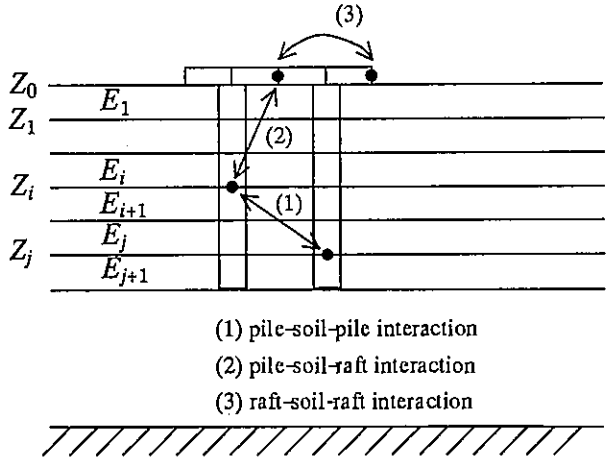

Figure 7.3. Averaged modulus used in the estimation of the interactions.

In addition, an averaging technique suggested by Poulos[5] is incorporated into the analysis to approximate the interaction between the structure members of a piled raft foundation embedded in nonhomogeneous soils. As shown in **Figure 7.3**, averaged Young's modulus, $E_{s(ij)}$, used in the approximation for pile-soil-pile, raft-soil-pile and raft-soil-raft interactions can be calculated using Equations (7.15), (7.16) and (7.17), respectively.

$$E_{s(ij)} = \frac{\left(E_{s(i)} + E_{s(i+1)}\right) + \left(E_{s(j)} + E_{s(j+1)}\right)}{4} \tag{15}$$

$$E_{s(1j)} = \frac{2E_{s(1)} + \left(E_{s(j)} + E_{s(j+1)}\right)}{4} \tag{16}$$

$$E_{s(11)} = E_{s(11)} \tag{17}$$

where $E_{s(ij)}$ is the averaged Young's modulus of the soil at the depths Z_i and Z_j, $E_{s(i)}$ and $E_{s(j)}$ are the Young s moduli for soil layer numbers i and j.

Employing the flexibility concept in the analysis of the piles and the raft, the stiffness matrix of the piled raft system can be written as:

$$\left[C + K_r + K_p\right]\{w\} = [K]\{w\} = \{F\} \tag{7.18}$$

where $[K_r]$ is the raft stiffness matrix, $[K_p]$ the pile stiffness matrix, $\{w\}$ the displacement vector, $\{F\}$ the external load vector acting on the raft, and $[C] = [A]^{-1}$. The diagonal coefficients in the soil flexibility matrix $[A]$ are determined by inverting the soil spring stiffness matrix. The off-diagonal non-zero coefficients in the matrix $[A]$ represent the structural member-soil-structural member interactions.

In the following sections, the feasibility of using the simplified analysis described in this section for foundations in finite homogeneous and nonhomogeneous soil layers will be examined by comparing solutions from the proposed method with those from previous research and those from three-dimensional finite element analysis.

7.3. VERIFICATION BY COMPARISON WITH PREVIOUS RESEARCH

7.3.1. Axially loaded pile foundations embedded in a finite homogeneous soil layer

Figures 7.4 and 7.5 show the results calculated using the proposed method compared with the results from the integral method by Poulos & Davis[7] for axially loaded single piles and pile groups embedded in a finite homogenous soil layer. Comparisons are shown in terms of a deflection influence factor, I_{wV}, and an interaction factor, α, which are defined as:

$$I_{wV} = \frac{E_s D w}{V} \tag{7.19}$$

$$\alpha = \frac{\text{additional settlement due to adjacent pile}}{\text{settlement of pile under its own load}} \tag{7.20}$$

where w is the settlement of the pile head and V the vertical load on the pile head.

Figure 7.4 shows the influence factor, I_{wV}, for single piles subjected to vertical load V. The pile-soil stiffness ratio, E_p/E_s, is made equal to 1000 and the Poisson s ratio of the soil is set as 0.5. The effect of pile spacing on the interaction factor, α, for five h/L ratios is plotted in **Figure 7.5** for rigid piles with a pile slenderness ratio, L/D, of 25. It can be seen from **Figures 7.4 and 7.5** that the results obtained from PRAB match very well with the results from the integral equation method.

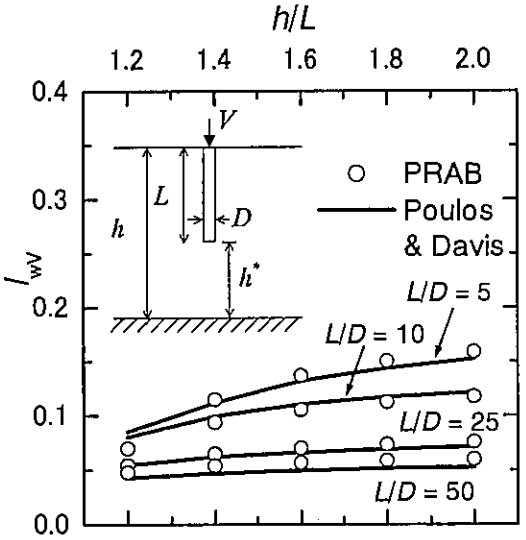

Figure 7.4. Comparison of the influence factor, I_{wv}.

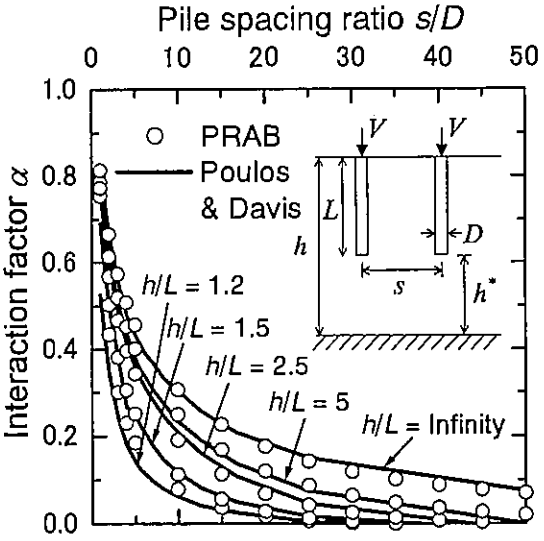

Figure 7.5. Comparison of the interaction factor, α.

7.3.2. Axially loaded pile foundations embedded in nonhomogeneous soils

In the case of a single pile embedded in layered soils, three idealized cases were considered as shown in **Figure 7.6**, and the solutions obtained for pile head settlement are given in **Table 7.1** in terms of the settlement influence factor, I_{wv}. The results calculated from PRAB are compared with those from the spring model by Lee[9], and the finite element and boundary element approaches by Poulos[5]. It can be seen that for Case 1 and Case 3, there are good agreements among the solutions. In Case 2, the finite element and boundary element approaches give the highest and the lowest values for the settlement influence factor, respectively. The solution of the proposed method and that of the spring model are around the middle value.

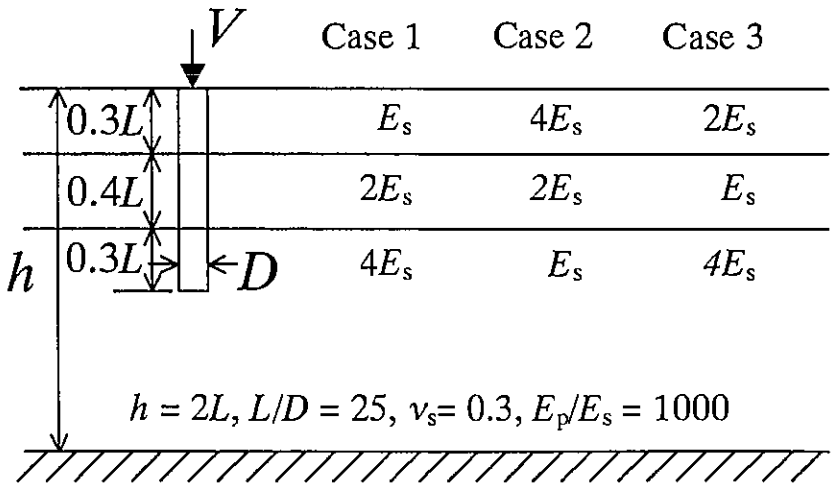

Figure 7.6. Layered soil problems analysed (a single pile).

Table 7.1. Comparison between solutions for settlement of a single pile in layered soils.

Case	Settlement Influence Factor, I_{wV}			
	PRAB	Lee	Poulos (FEM)	Poulos (BEM)
1	0.0377	0.0361	0.0377	0.0386
2	0.0356	0.0372	0.0430	0.0330
3	0.0360	0.0358	0.0382	0.0366

Note: $I_{wV} = wDE_s/V$; w is the settlement of the pile, D the pile diameter, E_s Young s modulus of the soil, and V the applied vertical load.

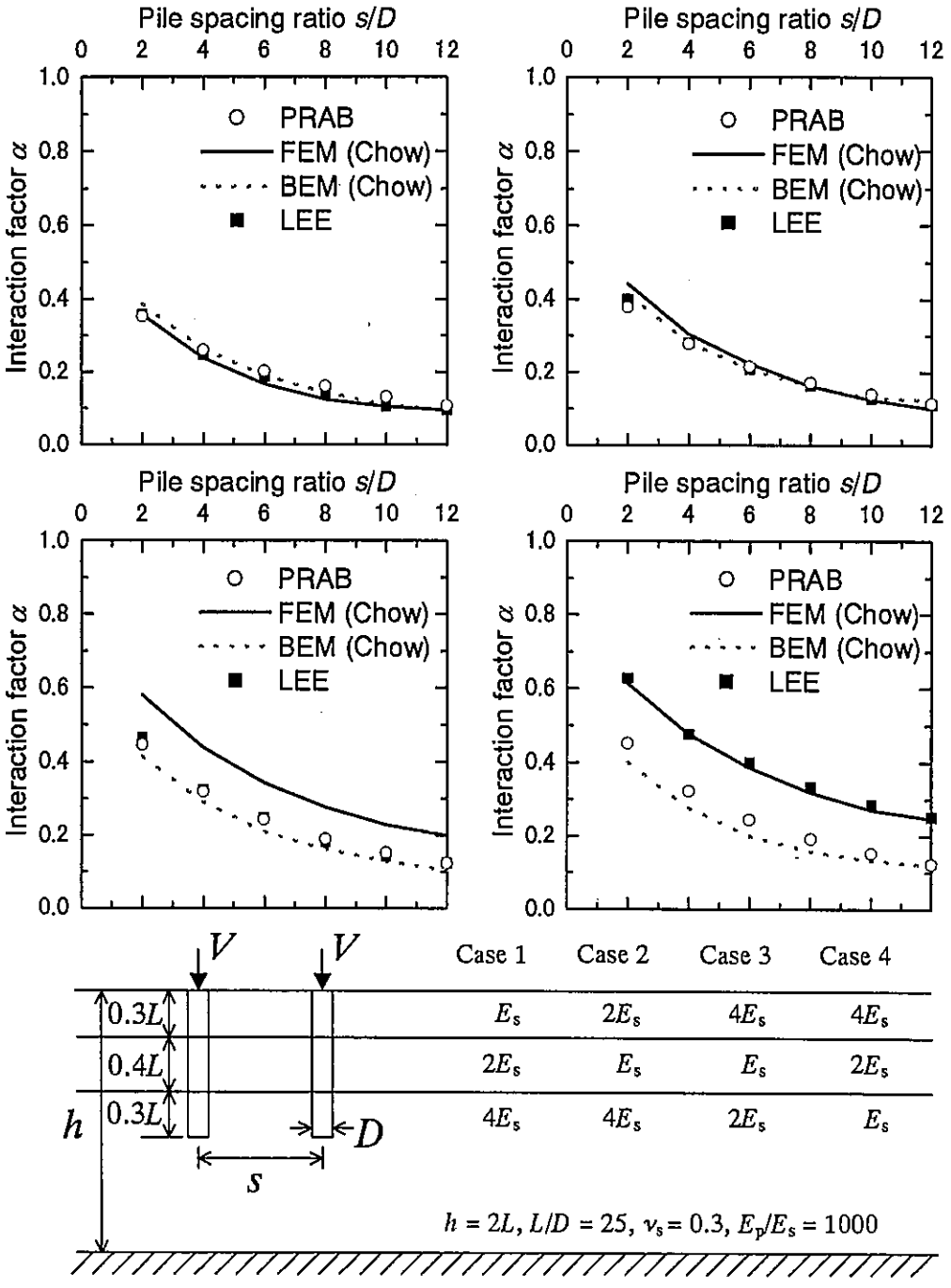

Figure 7.7. Layered soil problems analysed (interaction between two piles).

The influence of pile spacing between two piles on the interaction factor for four different layered soil profiles is shown in **Figure 7.7**. The results calculated using PRAB are compared with the results from the spring model by Lee[9], and the finite element and boundary element approaches by Chow[17]. It can be seen that there are good agreements among the solutions in Case 1 and Case 2. However, in Case 3 and Case 4 where the underlying stratum is softer than the soil in the top surface layer, the methods using the approximate average Mindlin approach tend to give lower values for the interaction factor.

In the case of single piles embedded in a Gibson s soil (see **Figure 7.8**), comparisons between various solutions for the pile head settlement and base load are shown in **Table 7.2**. The comparisons were made between the finite element (Poulos[5]), boundary element (Banerjee & Davies[3], Poulos[5]) and the present approaches. The pile geometry and soil modulus distribution are defined in **Figure 7.8**. **Table 7.2** reveals the good agreements between PRAB and FEM solutions for pile settlement and pile base load.

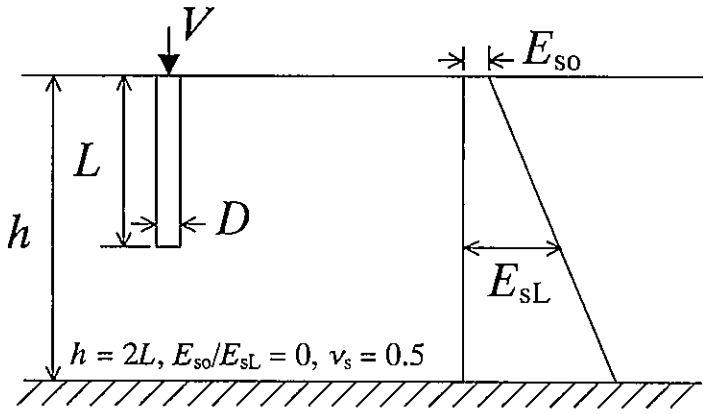

Figure 7.8. Gibson's soil problem analysed (a single pile).

Table 7.2. Comparison between solutions for settlement of single piles in Gibson s soils.

Method / E_p/E_{sL}	Settlement Influence Factor, I_{wV}				Relative Base Load, V_b/V			
	L/D = 10		L/D = 25		L/D = 10		L/D = 25	
	100	1000	100	1000	100	1000	100	1000
PRAB	0.235	0.170	0.257	0.115	0.193	0.212	0.977	0.142
Poulos (FEM)	0.231	0.184	0.250	0.118	0.18	0.22	0.12	0.20
Poulos (BEM)	0.249	0.176	0.274	0.122	0.242	0.270	0.088	0.126
Banerjee and Davies	0.241	0.233	0.204	0.116	0.113	0.140	0.047	0.078

Note: $I_{wV} = wDE_{sL}/V$; w is the settlement of the pile, D the pile diameter, E_{sL} Young s modulus of the soil at the pile length L, V the applied load, and V_b the load tranferred to the pile base.

Figure 7.9 shows the effect of the pile-soil stiffness ratio, E_p/E_{sL}, and the pile slenderness ratio, L/D, on the interaction factor between two piles in a Gibson s soil. For the four cases considered, the interaction factors computed by PRAB, the finite element (Chow[17]), the boundary element (Poulos[6]) and the boundary integral approaches (Banerjee[18]) are in reasonable agreement overall.

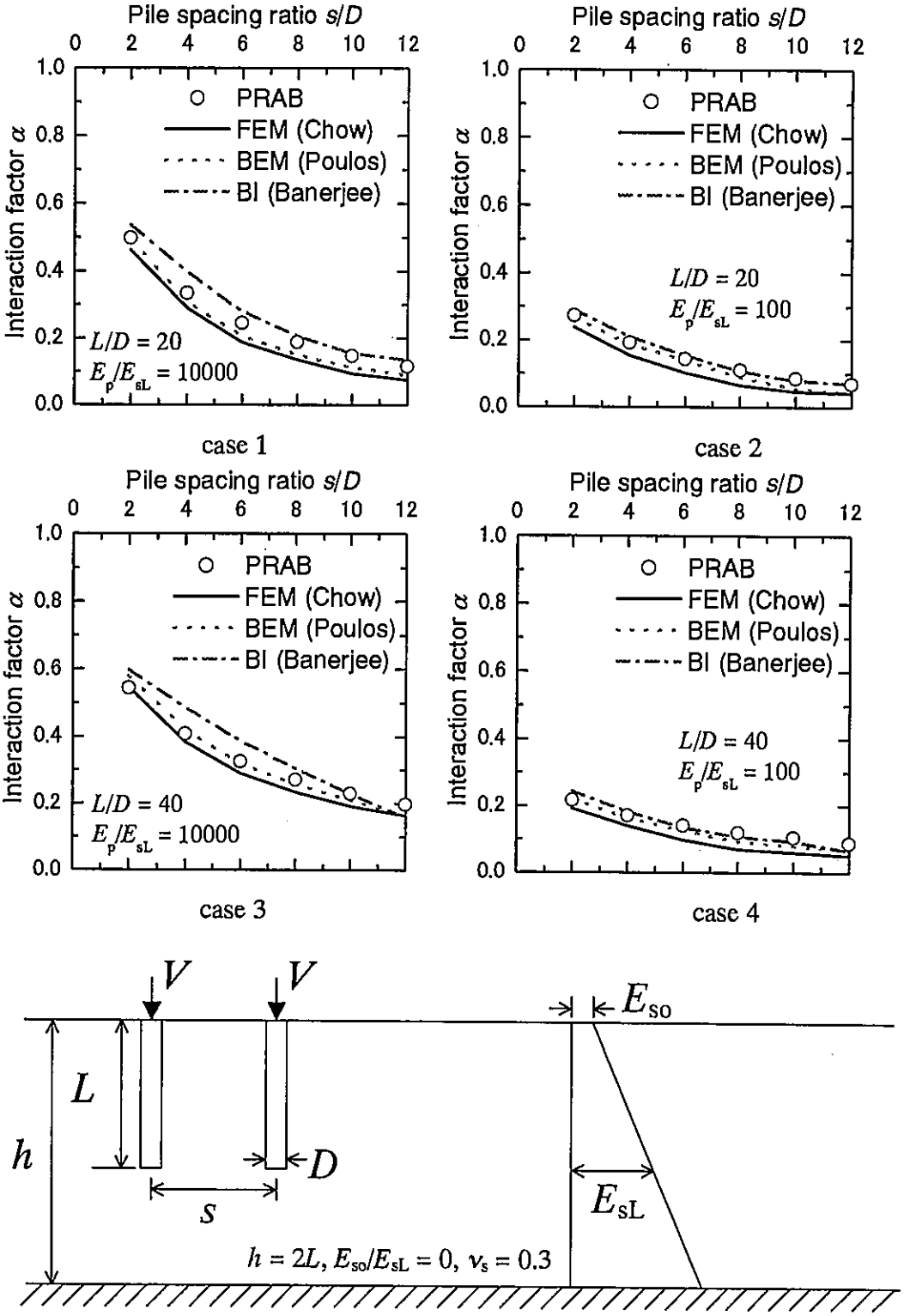

Figure 7.9. Gibson's soil problems analysed (interaction between two piles).

7.3.3. An axially and laterally loaded off-ground capped pile group

In Zhang & Small[12], off-ground capped pile group systems subjected to both vertical and lateral loads and embedded in homogeneous elastic soils or elastic soils where the modulus increases with depth, have been analysed by combining finite elements to model the cap and the piles with finite layer theory to model the soil. Here, the analyses of an off-ground cap supported by 12 piles (as shown in **Figure 7.10**) subjected to vertical load or lateral load are conducted using PRAB, and the results are compared with the results of Zhang & Small[12]. The soil profiles considered in the analyses are one case of a homogeneous soil and three cases of nonhomogeneous soil with soil modulus increasing with depth as shown in **Figure 7.10**. The soil modulus at the pile base, E_{sL}, was set at 7 MN/m^2 and the pile slenderness ratio, L_{em}/D, was set at 20. The pile-soil stiffness ratio, E_p/E_{sL}, and the raft-soil stiffness ratio, E_r/E_{sL}, were 4000 and 4285, respectively. The raft thickness, t_r, was chosen to be 1.0 m. The breadth, B_r, and length, L_r, of the raft were 15 and 20 m. Uniform vertical load, q_z, or lateral load, q_x, was applied separately on the raft in the analysis. Comparisons are shown in terms of vertical and horizontal displacement deflection influence factors, I_{wV} and I_{uH}, which are defined respectively as:

$$I_{wV} = \frac{wE_s D}{q_z B_r L_r} \tag{7.21}$$

$$I_{uH} = \frac{uE_s D}{q_x B_r L_r} \tag{7.22}$$

where w and u are the displacements at the pile head in the vertical and horizontal directions, respectively.

The vertical and horizontal displacement influence factors, I_{wV} and I_{uH}, for a pile No. 5 are shown in **Table 7.3**. It can be seen from **Table 7.3** that in the case of vertical loading, there are good agreements between the solutions from PRAB and those from the finite layer approach by Zhang & Small[12]. The lateral displacements at the pile head computed by PRAB tend to be lower than those computed by the finite layer approach in all the soil profiles.

Table 7.3. Comparison between solutions for displacements of an off-ground cap supported by piles.

	Vertical disp. influence factor, I_{wV}				Horizontal disp. influence factor, I_{uH}			
	Case 1	Case 2	Case 3	Case 4	Case 1	Case 2	Case 3	Case 4
PRAB	0.030	0.038	0.036	0.034	0.063	0.179	0.113	0.095
Zhang & Small	0.031	0.039	0.036	0.034	0.076	0.200	0.137	0.109

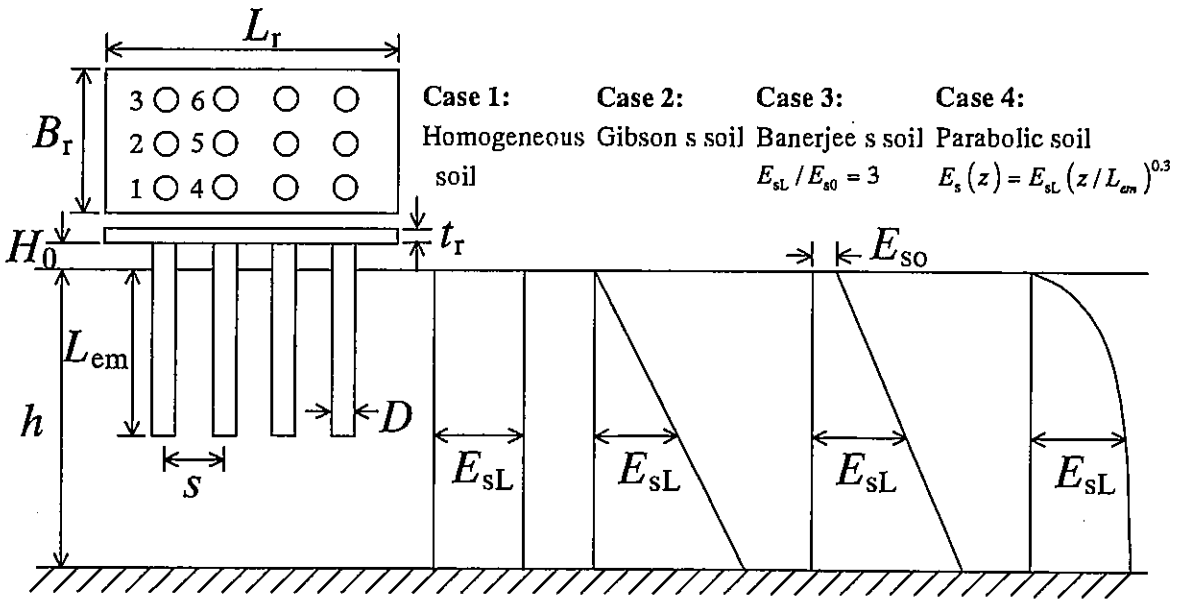

$h = 100L$, $H_0/D = 2.5$, $L_{em}/D = 20$, $s/D = 5$, $E_p/E_{sL} = 4000$, $E_r/E_{sL} = 4285$,
$\nu_s = 0.35$, $\nu_r = 0.15$, $E_{sL} = 7$ MN/m^2, $B_r = 15$ m, $L_r = 20$ m, $t_r = 1$ m

Figure 7.10. An off-ground capped pile group problem analysed.

7.4. VERIFICATION BY COMPARISON WITH FEM ANAYSIS

7.4.1. Laterally loaded pile foundations embedded in nonhomogeneous soils

Most of the previous research focused mainly on the problem of axially loaded pile foundations. The validity of the solutions for this problem has been widely verified. In this work, the problem of laterally loaded pile foundations is also considered. The same procedures as those used in the vertical loading are employed for the estimation of the influence of a finite depth on the interactions between structure member nodes under the lateral loading. The same averaging technique as used in the vertical loading analysis is also employed to approximate the interactions between the structure members of laterally loaded pile foundations embedded in nonhomogeneous soils. The performance of the present approach is examined by comparison with the more rigorous finite element solutions. Details of the finite element analysis will be described later in Section 7.4.2. The effect of pile spacing on the interaction factor under lateral loading α_L (i.e. the ratio of additional lateral displacement caused by an adjacent pile to the lateral displacement of pile under its own load) for five different layered soil profiles is plotted in **Figure 7.11**. The interaction factors computed by the finite element and the present approaches are similar over a wide range of pile spacing for all the soil profiles.

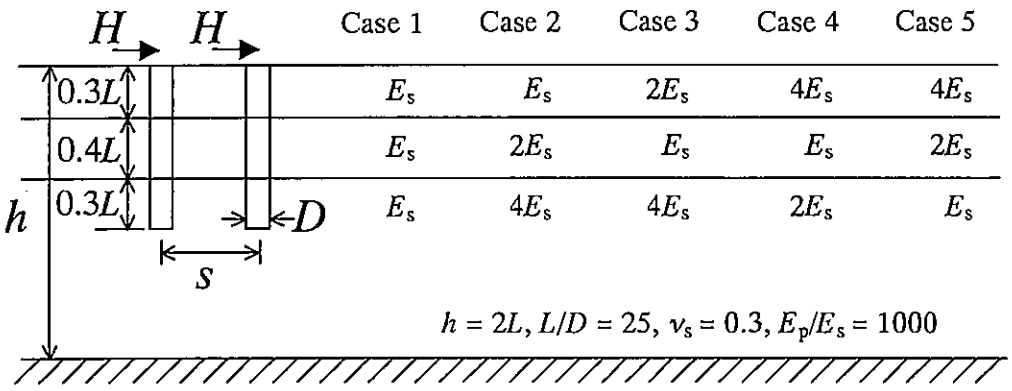

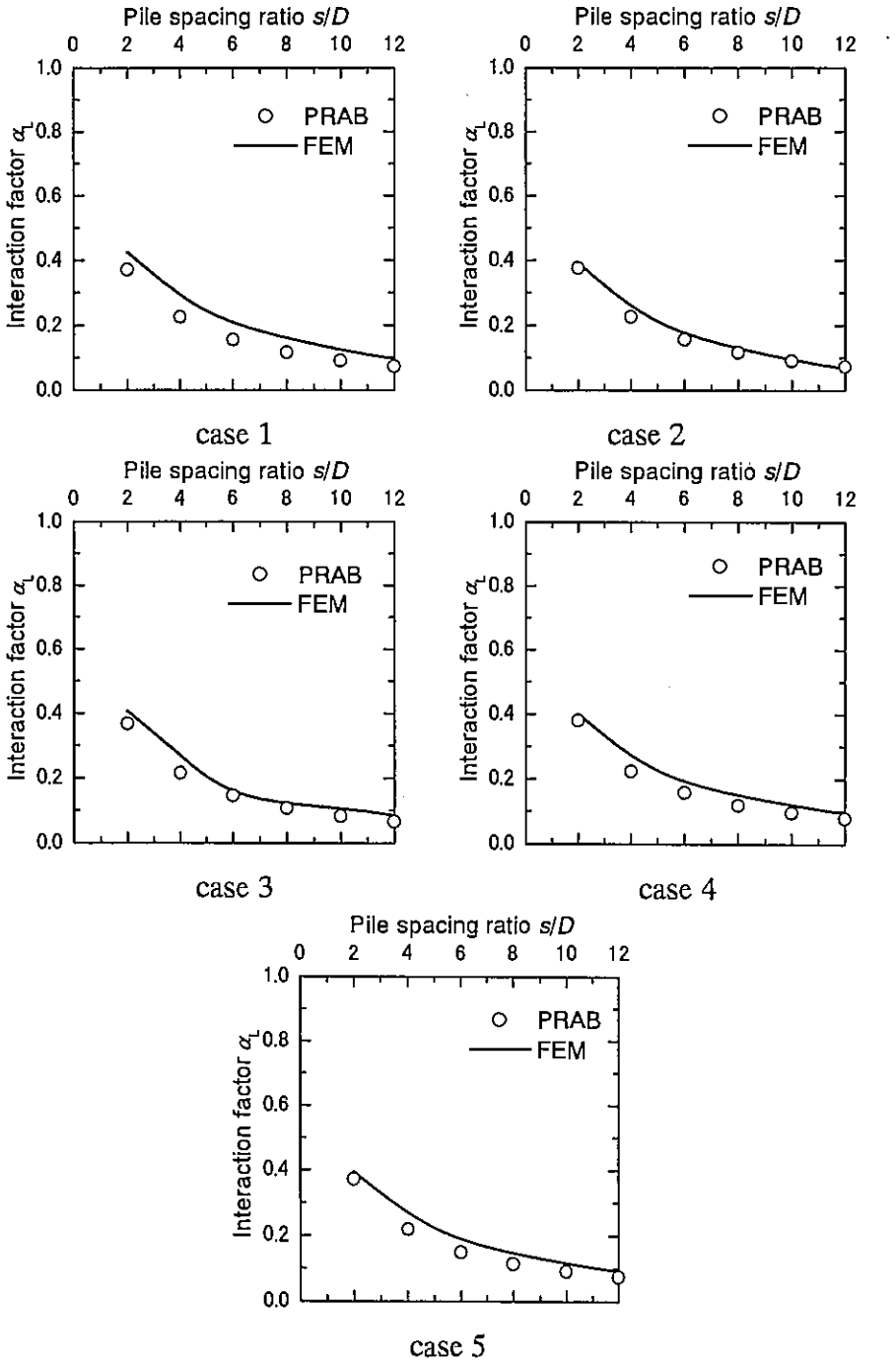

Figure 7.11. Layered soil problems analysed (interaction under lateral loading).

4.2. Piled raft and pile group foundations subjected to vertical and lateral loads

The analyses using PRAB and FEM were conducted for piled raft foundations and pile group foundations with a square raft supported by 4 piles as shown in **Figure 7.12.** The five soil profiles considered are also indicated in **Figure 7.12. Figure 7.13** illustrates the finite element discretization of the foundation and the soil, represented by eight-node hexahedron solid elements. Considering the condition of plane symmetry, one-half of the entire system was modelled. The circular pile cross-section was modelled by an octagon inscribed in the circle. The pile and the raft as well as the soil were modelled by linear elastic materials. In the analysis of pile groups, a gap of 10 mm was maintained between the raft base and the ground surface so that there was no raft base resistance. The geometrical and mechanical properties of the raft, the piles and the soil are shown in terms of dimensionless parameters in **Figure 7.12.** In order to model a rigid raft, the raft-soil stiffness ratio, K_{rs}, which can be calculated by Equation (7.23) was set equal to 10 following Brown[19].

$$K_{rs} = \frac{4E_r B_r t_r^3 \left(1-\nu_s^2\right)}{3\pi E_s L_r^4} \tag{7.23}$$

As for the displacement boundary conditions, displacements in the x, y and z-directions were fixed at zero on the side planes, the back plane and the bottom plane of the mesh. The displacement in the y-direction on the symmetric plane was also fixed at zero. The external load was applied on the top surface of the raft in the z-direction for the analysis of vertically loaded foundations and in the x-direction for the analysis of laterally loaded foundations.

Figures 7.14 to 7.23 show the calculated displacements and load distribution of the piled raft and the pile group embedded in the various soils. The calculated results are shown in terms of dimensionless parameters I_{wV} and I_{uH} (Equations (7.21) and (7.22)) for the settlement and the lateral displacement of a pile, and C_{aV}, C_{sH} and C_{bH} (Equations (7.24) to (7.26)) for the axial and shear forces, and the bending moment along the pile.

$$C_{aV} = \frac{A}{q_z B_r L_r} \tag{7.24}$$

$$C_{sH} = \frac{S}{q_x B_r L_r} \tag{7.25}$$

$$C_{bH} = \frac{B}{q_x D B_r L_r} \tag{7.26}$$

where A, S and B are the axial force, the shear force and the bending moment along the pile, respectively.

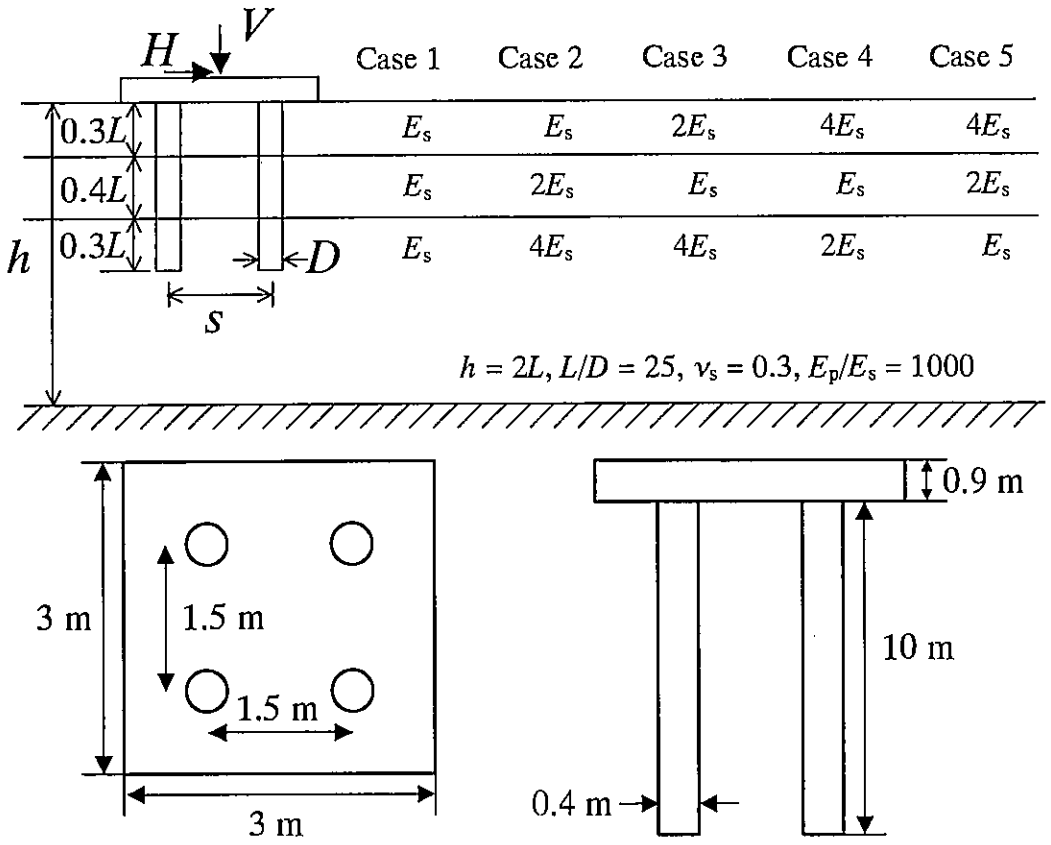

Figure 7.12. Configuration of foundation and soil profiles.

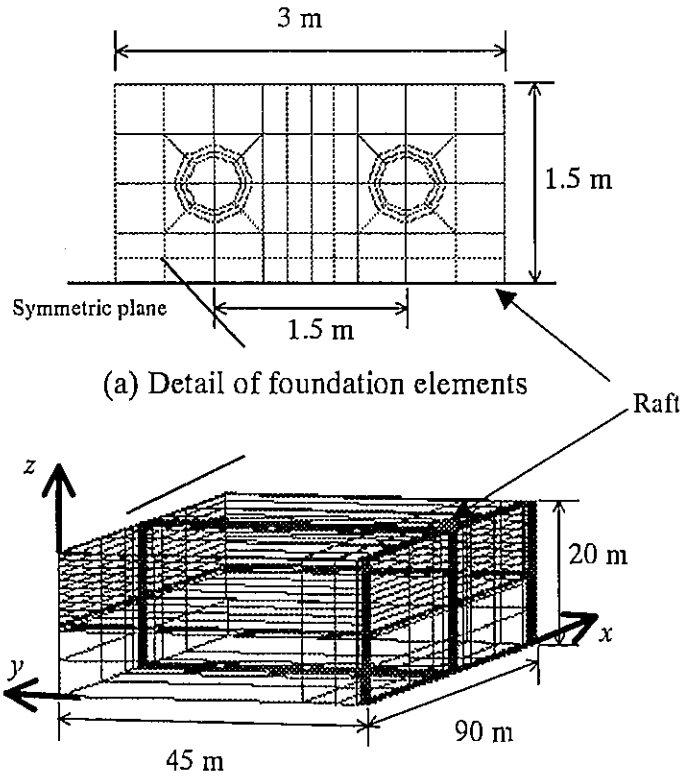

(a) Detail of foundation elements

(b) Whole mesh

Figure 7.13. Three-dimensional finite element mesh.

The settlement and the axial force along the pile were calculated in the vertical loading analysis, while the lateral displacement, the shear force and the bending moment along the pile were calculated in the lateral loading analysis.

The calculated results from the previous version of PRAB for the piled raft and pile group in Case 1 are also shown in **Figures 7.14 and 7.15**, respectively. It can be seen that the results from the extended PRAB, which includes the influence of finite layered soils, are closer to the results from the finite element approach, especially for the settlements, than the previous version of PRAB, in which the soil is treated as semi-infinite homogeneous soil. For all the soil profiles, it is obvious that in the case of a piled raft where the soil resistance of the raft is taken into account, the vertical and lateral displacements as well as the load distribution along the pile (i.e. axial force, shear force and bending moment) are smaller than those of the corresponding pile group.

In **Figures 7.16 to 7.23**, the results from the extended PRAB are compared with those from the finite element approach for foundations embedded in nonhomogeous soils. In Case 4 and Case 5, where softer layers lie under a much stiffer layer the interaction factors in the vertical loading computed using the present approach are lower than those computed using the finite element approach, as described in an earlier section. Consequently, the present method tends to underestimate the settlement of the foundations in the case of this type of soil profile. Except for the prediction of the settlement in this type of soil profile, there are reasonably good agreements between the calculated results from the proposed method and those from the more rigorous finite element approach. Thus, it is thought that this simplified method can be used with some confidence in the preliminary design of axially and laterally loaded piled raft and pile group foundations embedded in nonhomogeneous soils for the determination of the raft size, the number of piles, the pile spacing and the pile length.

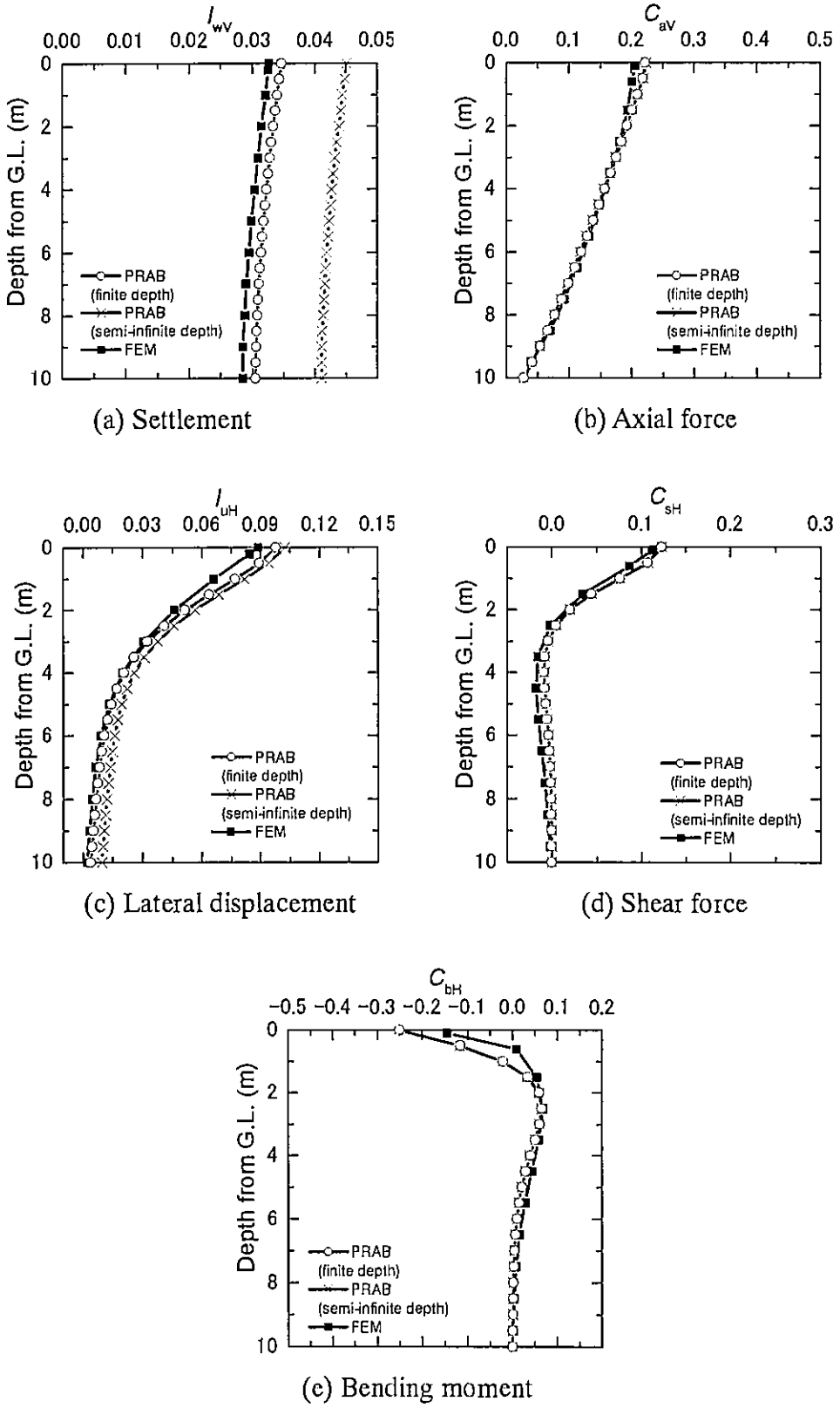

Figure 7.14. Comparison of calculated solutions for piled raft in Case 1.

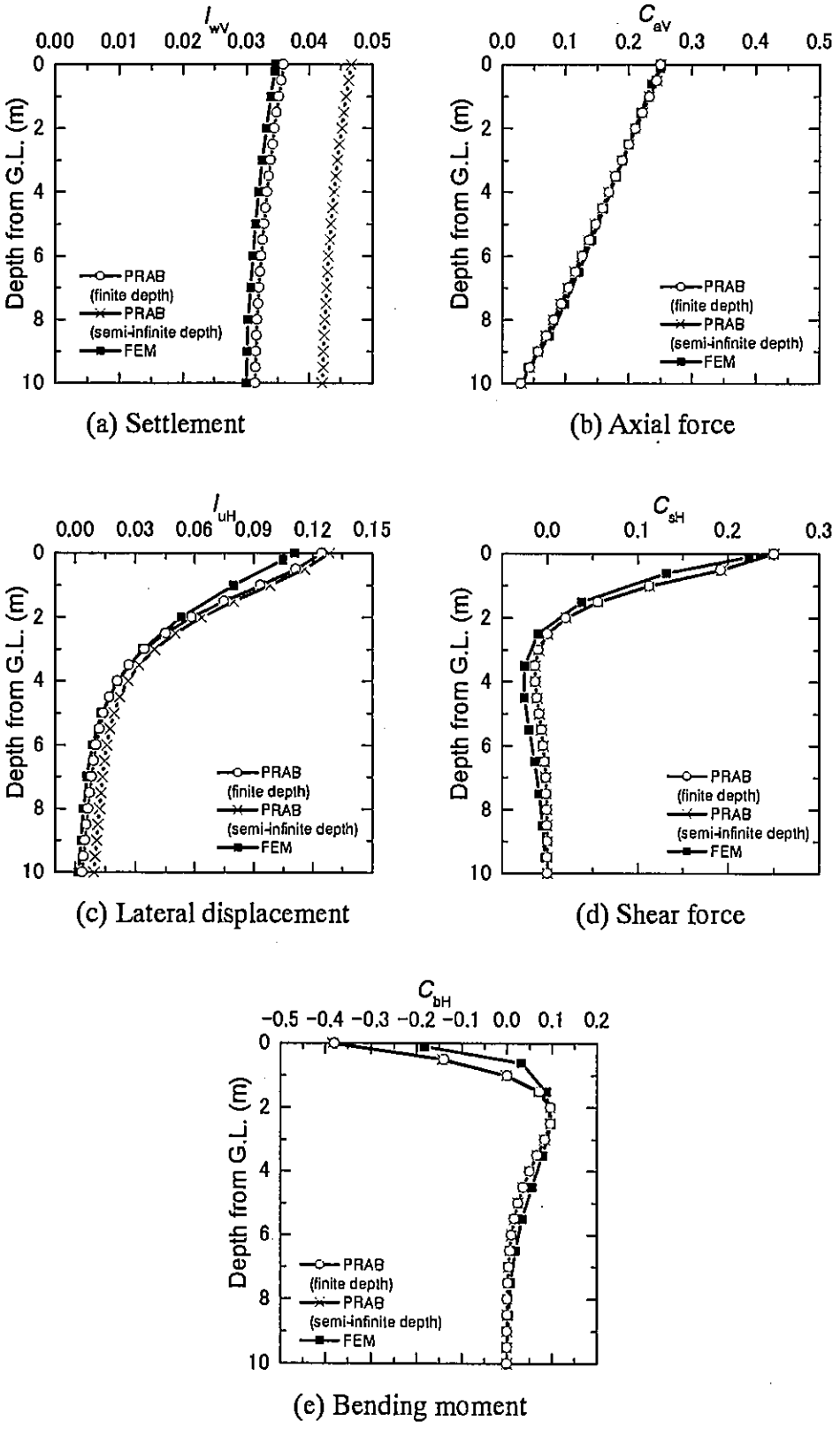

Figure 7.15. Comparison of calculated solutions for pile group in Case 1.

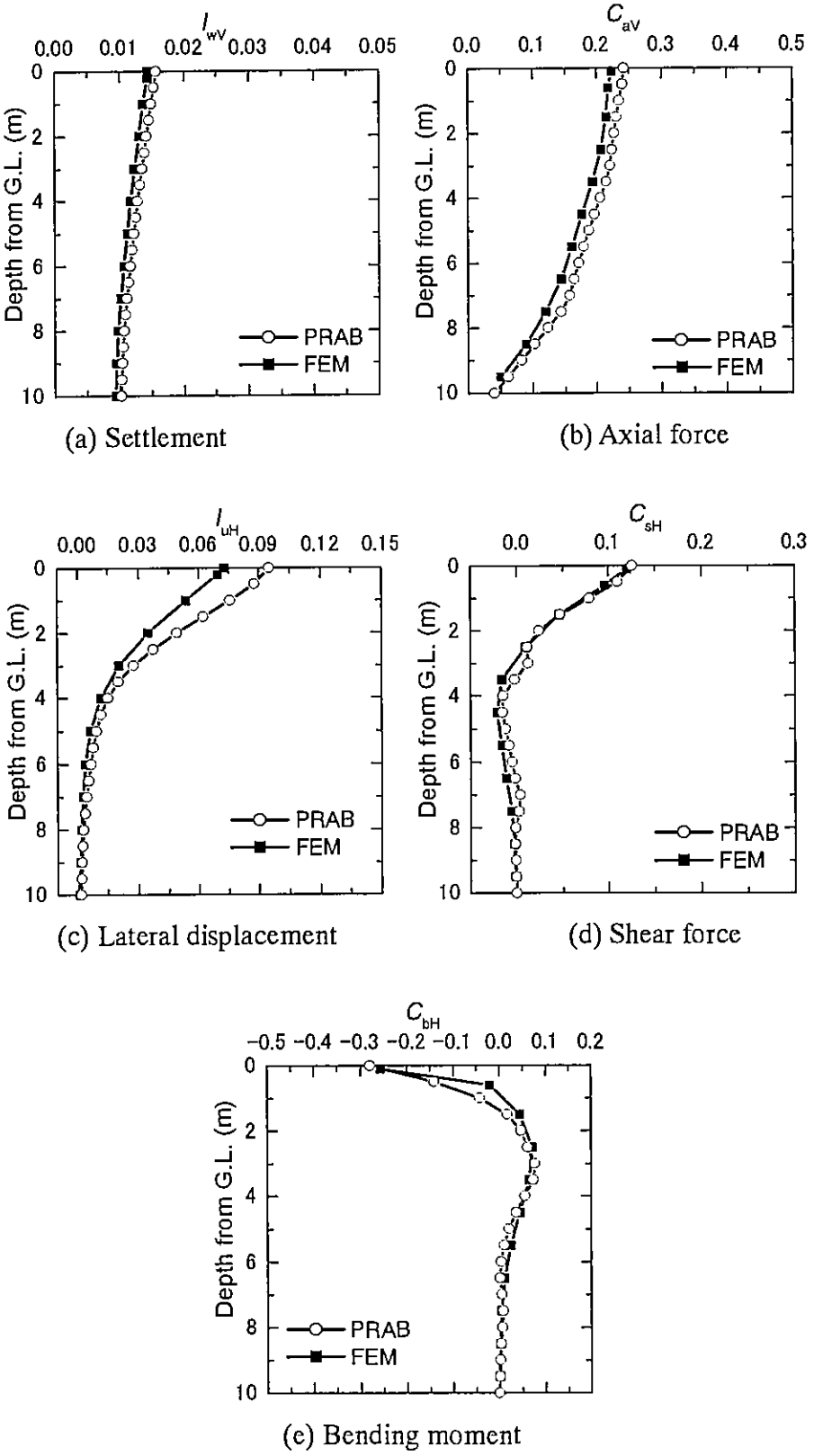

Figure 7.16. Comparison of calculated solutions for piled raft in Case 2.

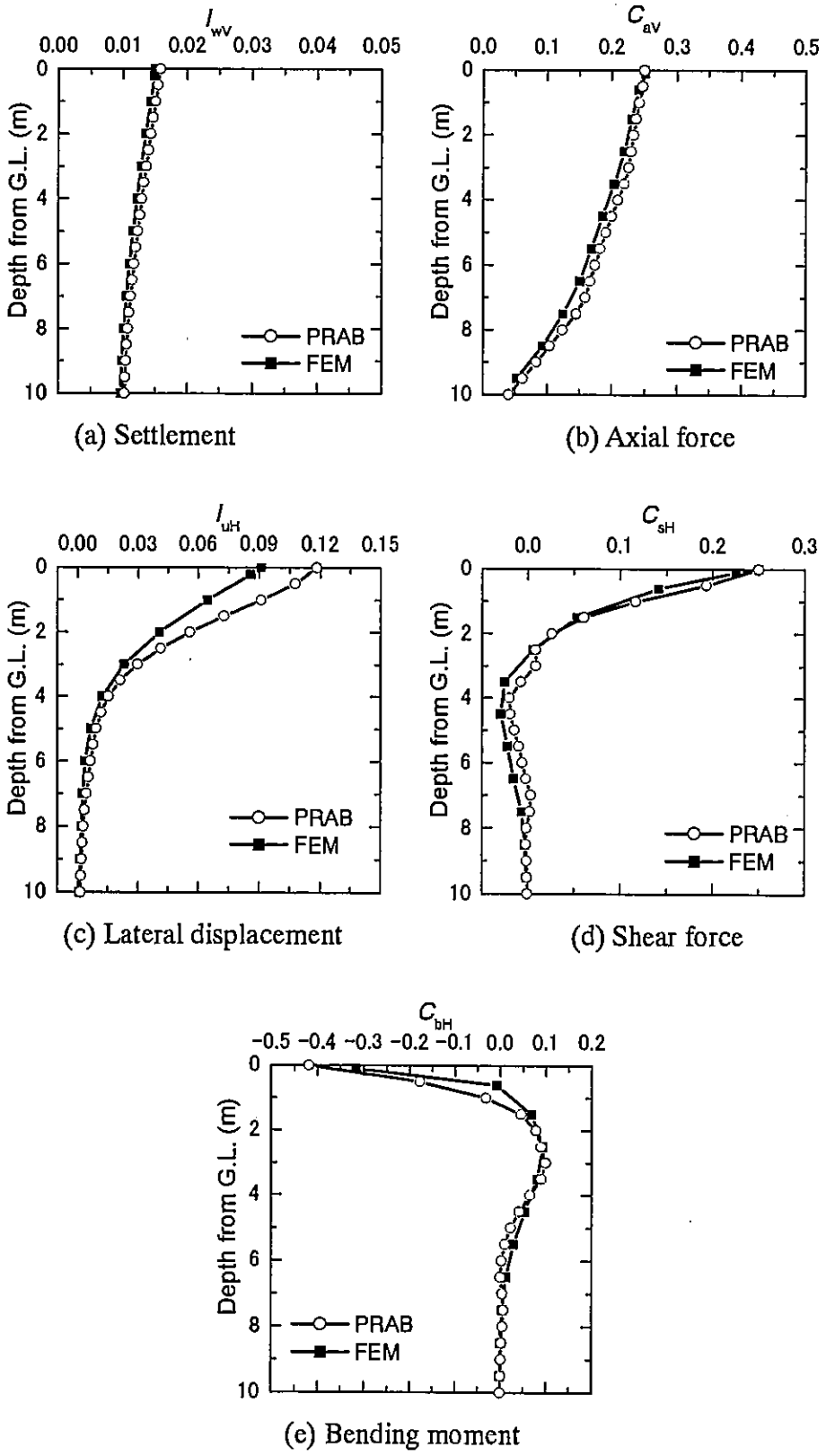

Figure 7.17. Comparison of calculated solutions for pile group in Case 2.

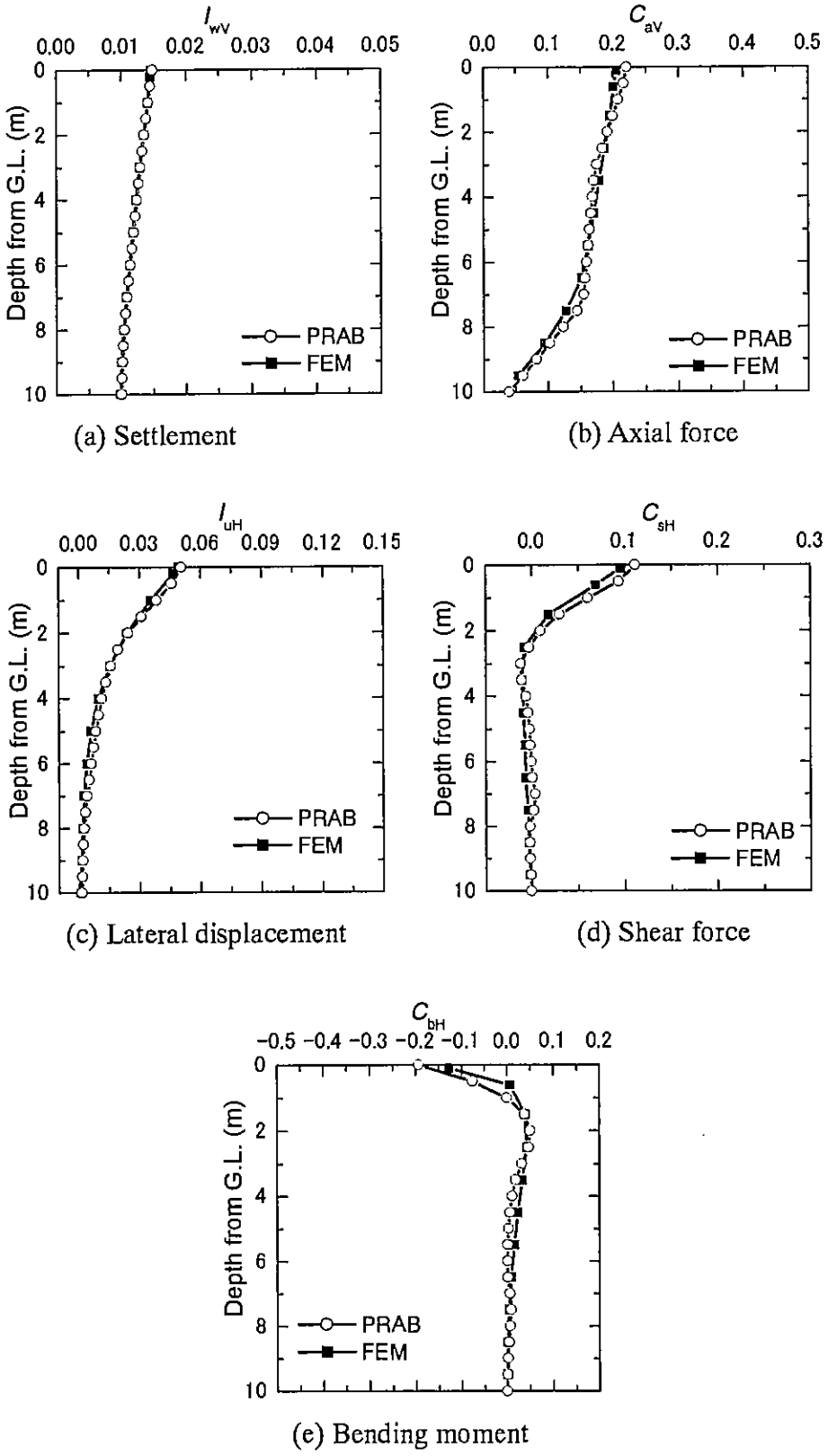

Figure 7.18. Comparison of calculated solutions for piled raft in Case 3.

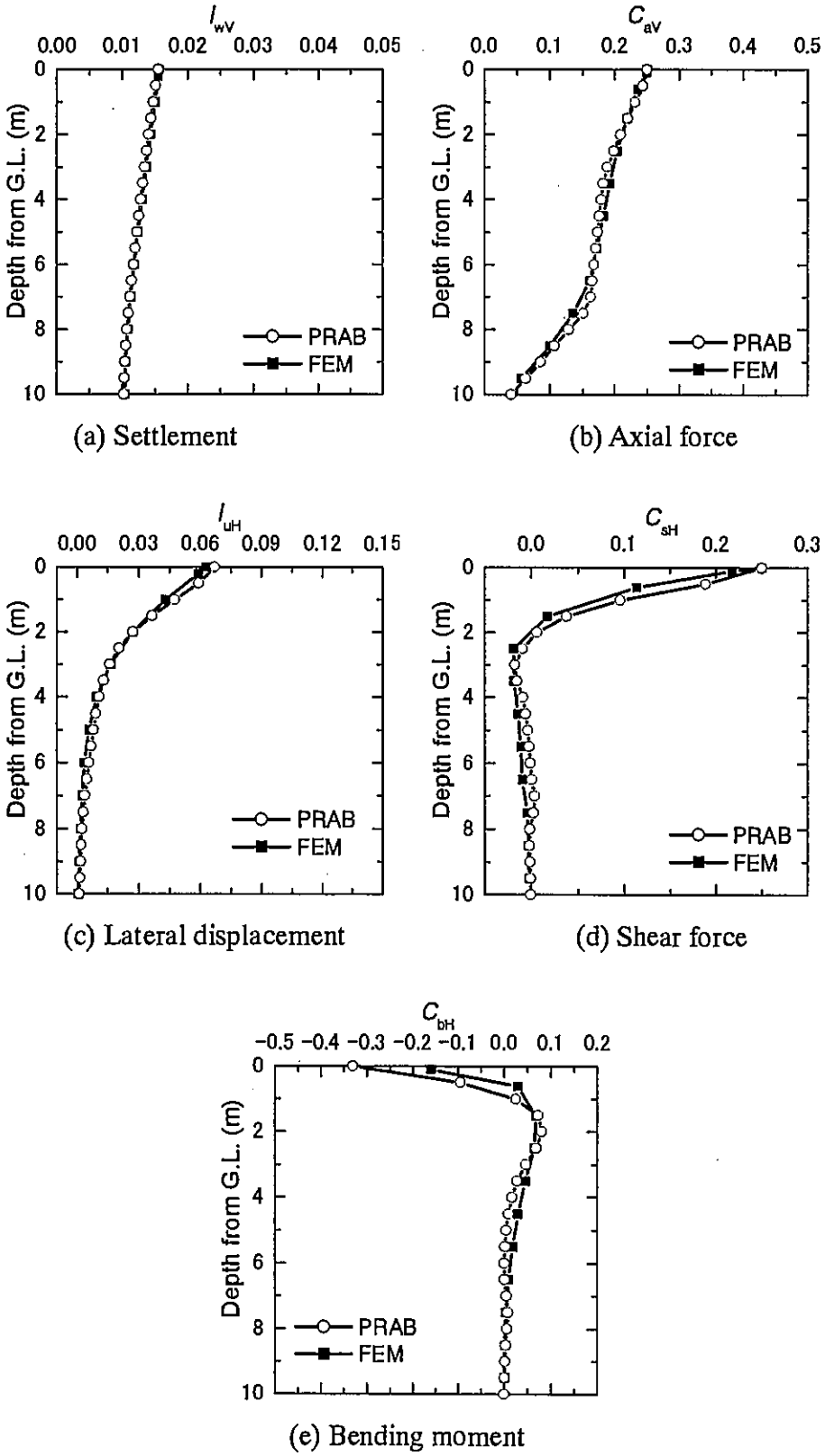

Figure 7.19. Comparison of calculated solutions for pile group in Case 3.

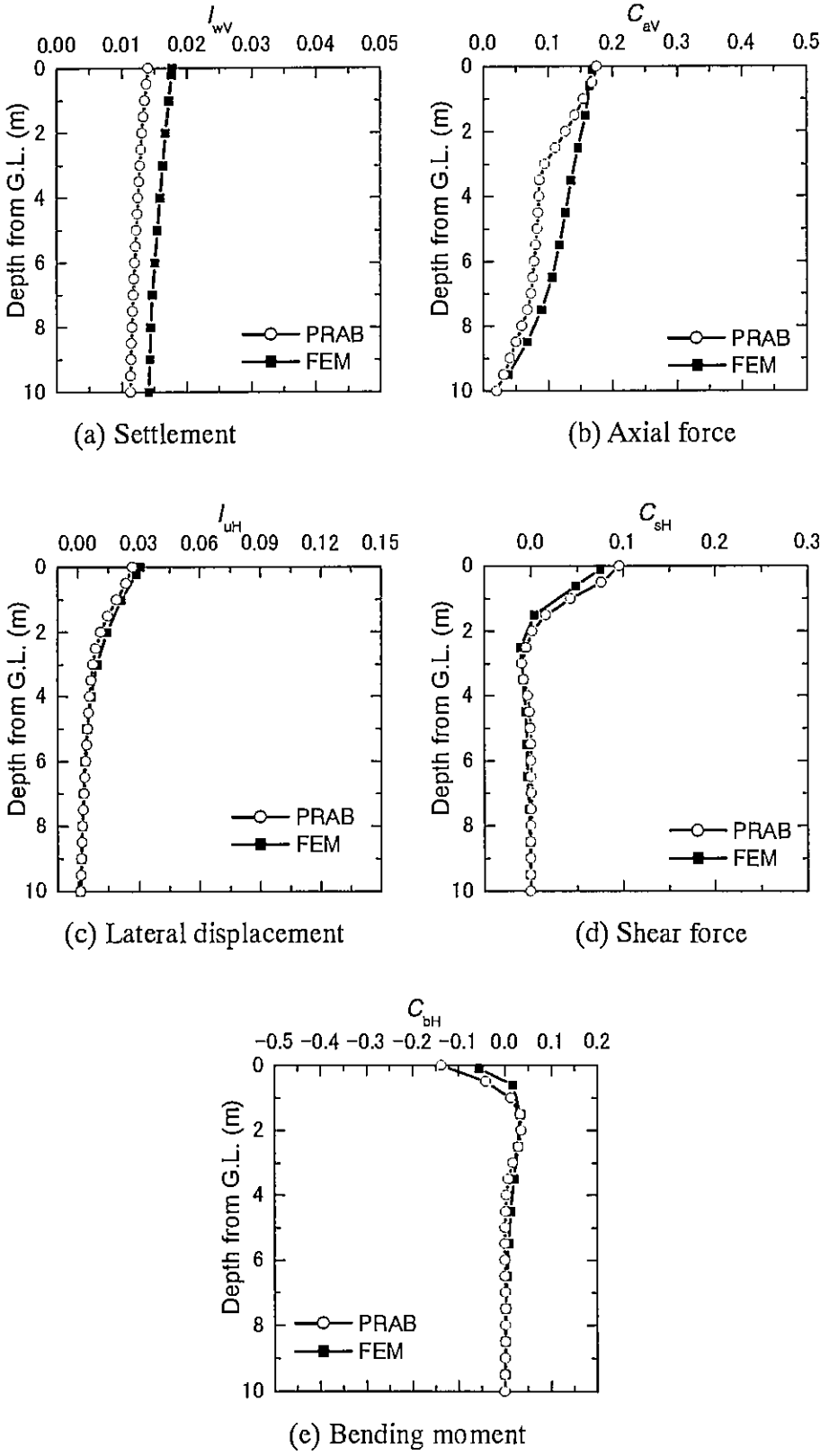

Figure 7.20. Comparison of calculated solutions for piled raft in Case 4.

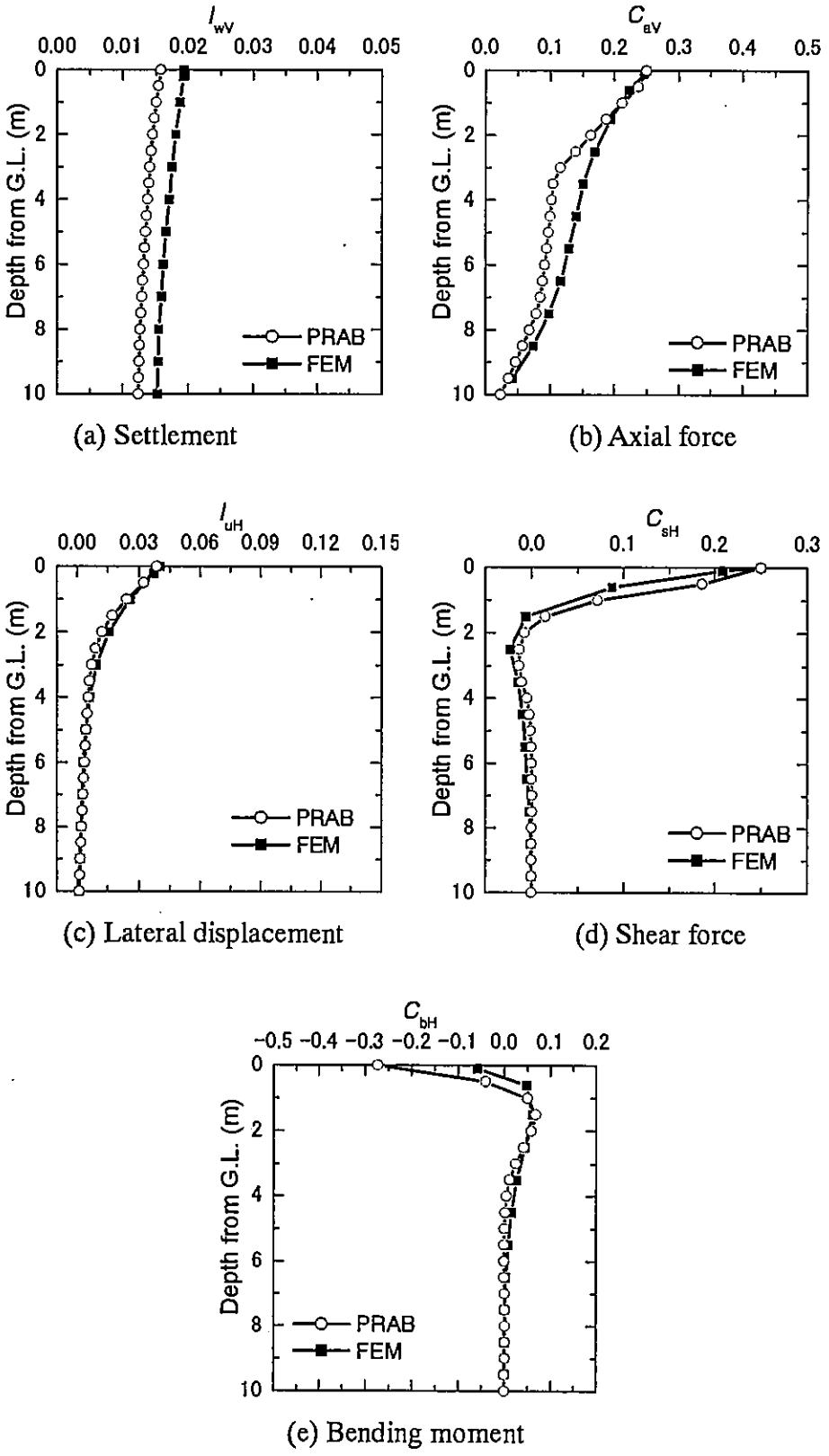

Figure 7.21. Comparison of calculated solutions for pile group in Case 4.

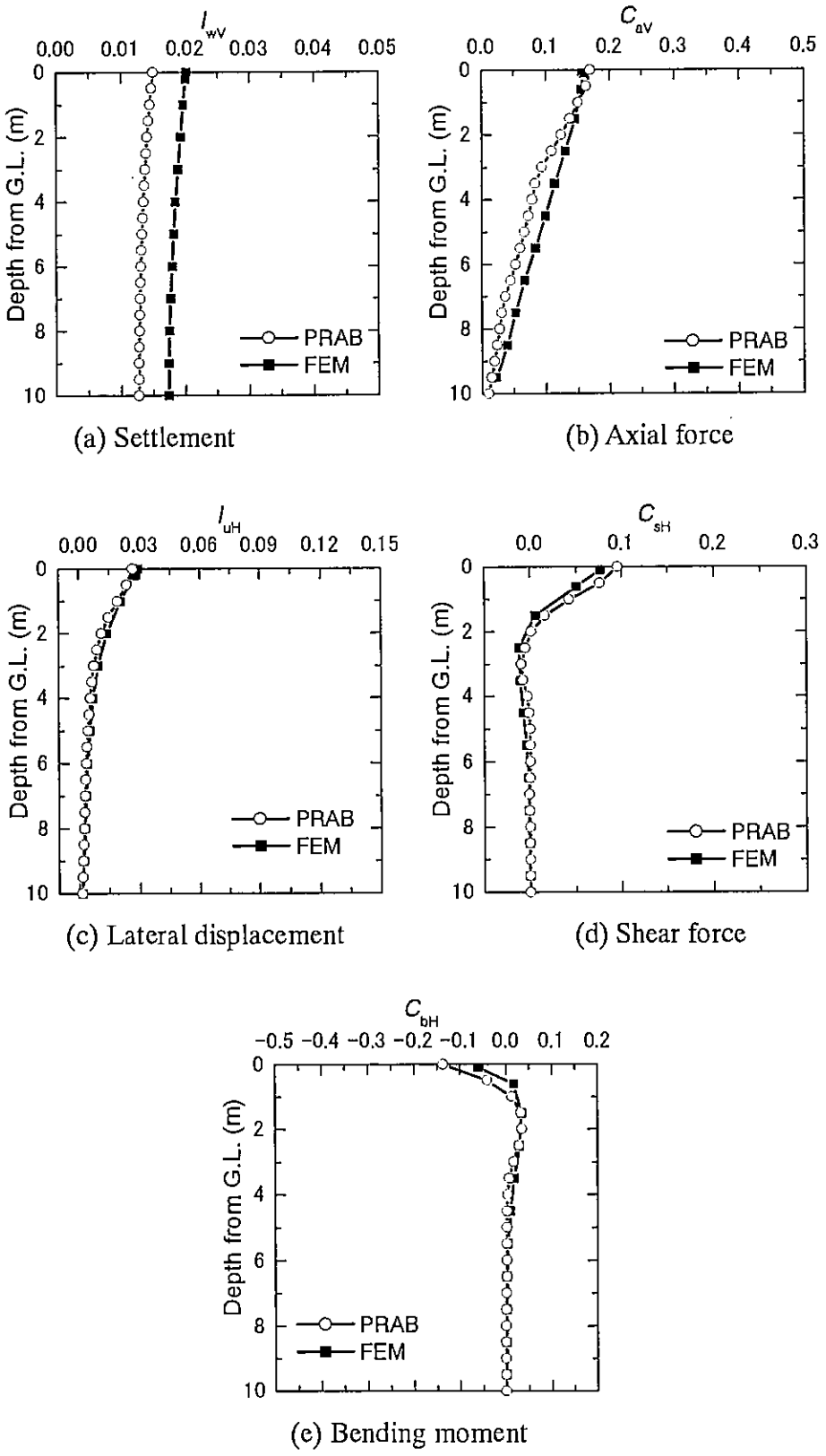

Figure 7.22. Comparison of calculated solutions for piled raft in Case 5.

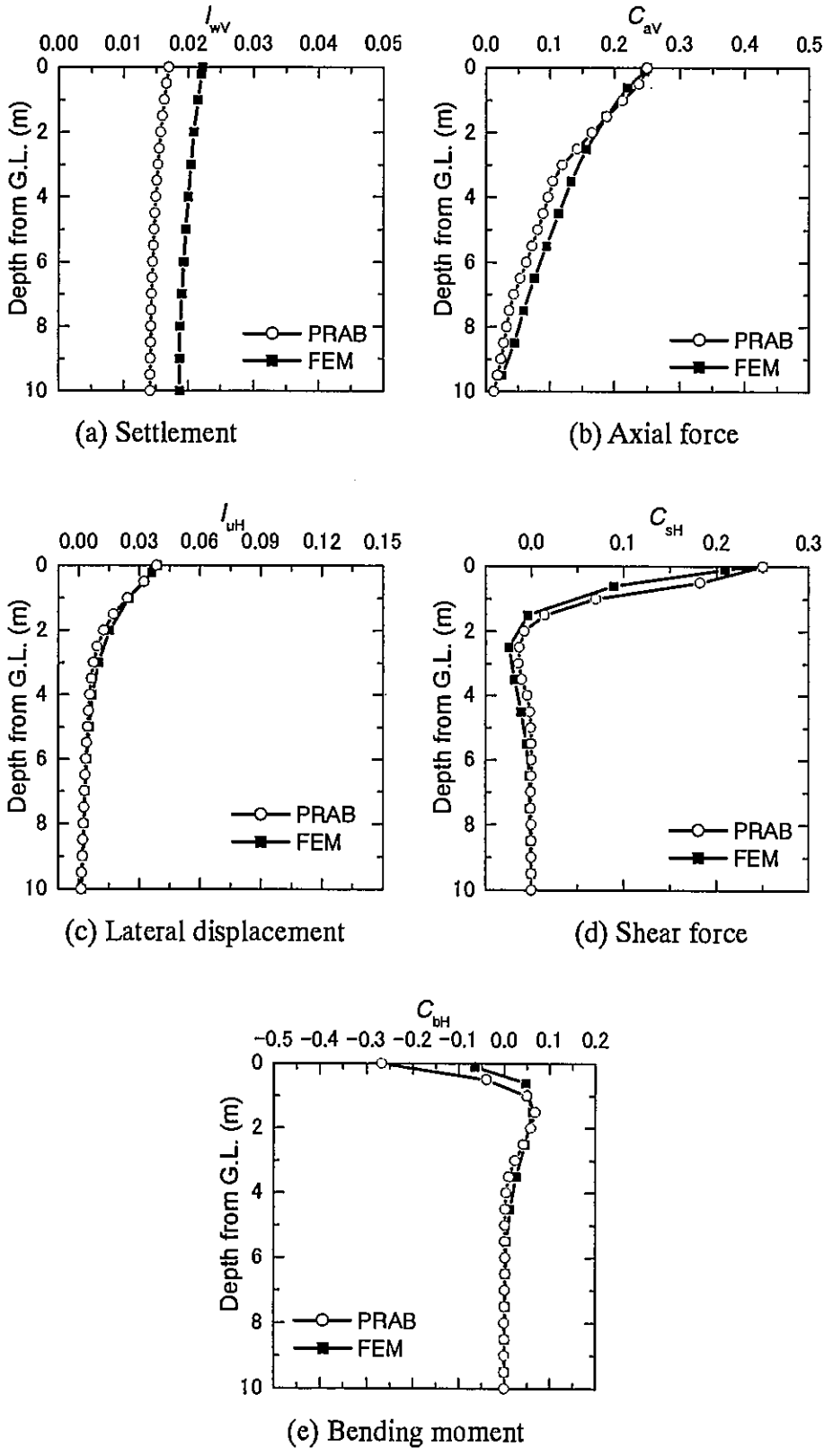

Figure 7.23. Comparison of calculated solutions for pile group in Case 5.

7.5. CONCLUSIONS

A simplified analytical method has been developed for the analysis of the deformation and the load distribution of axially and laterally loaded piled raft foundations embedded in nonhomogeneous soils. The proposed method was verified through comparisons with the results from previous research and the results from the more rigorous finite element approach. These comparisons suggest that the extended PRAB is capable of predicting reasonably well the deformation and the load distribution of single piles, pile groups and piled rafts in nonhomogeneous soils.

ACKNOWLEDGEMENT

This study was supported by a Grant-in-Aid for Scientific Research (Grant No. 12450188) of Japanese Ministry of Education, Culture, Sports, Science and Technology.

APPENDIX I: VERTICAL SETTLEMENT INFLUENCE FACTOR

The vertical settlement at depth z below the centre of a uniformly loaded square flexible raft is given by Harr[15].

$$\rho(z) = \frac{q_z a\left(1-\nu_s^2\right)}{2E_s} I(z) \tag{A-1}$$

where $\rho(z)$ is the settlement at depth z, q_z the uniform vertical load, a the equivalent radius of the raft element and $I(z)$ the vertical settlement influence factor which is defined as follows:

$$I(z) = A - \frac{1-2\nu_s}{1-\nu_s} B \tag{A-2}$$

$$A = \frac{1}{\pi}\left(\ln \frac{\sqrt{1+m^2+n^2}+m}{\sqrt{1+m^2+n^2}-m} + m \ln \frac{\sqrt{1+m^2+n^2}+1}{\sqrt{1+m^2+n^2}-1} \right) \tag{A-3}$$

$$B = \frac{n}{\pi} \tan^{-1} \frac{m}{n\sqrt{1+m^2+n^2}} \tag{A-4}$$

$$m = L_r / B_r,\ n = z/a \tag{A-5}$$

where L_r and B_r are the length and the breadth of the raft.

REFERENCES

1. Kitiyodom P, Matsumoto T. A simplified analysis method for piled raft and pile group foundations with batter piles. *International Journal for Numerical and Analytical Methods in Geomechanics* 2002; **26**: 1349-1369.
2. Mindlin RD. Force at a point in the interior of a semi-infinite solid. *Physics* 1936; **7**:195-202.
3. Banerjee PK, Davies TG. Analysis of pile groups embedded in Gibson soil. *Proc. 9th Int. Conf. Soil Mech. Found. Eng.*, Tokyo 1977.
4. Banerjee PK, Davies TG. The behaviour of axially and laterally loaded single piles embedded in nonhomogeneous soil. *Géotechnique* 1978; **28**(3):309-326.
5. Poulos HG.. Settlement of single piles in nonhomogeneous soil. *Journal of Geotechnical Engineering ASCE* 1979; **105**(5):627-641.
6. Poulos HG. Group factors for pile-deflection estimation. *Journal of Geotechnical Engineering ASCE* 1979; **105**(12):1489-1509.
7. Poulos HG, Davis EH. *Pile Foundation Analysis and Design*. Wiley: New York, 1980.
8. Chow YK. Axial and lateral response of pile groups embedded in nonhomogeneous soil. *Int. Journal for Numerical and Analytical Methods in Geomechanics* 1987; **11**:621-638.
9. Lee CY. Discrete layer analysis of axially loaded piles and pile groups. *Computers and Geotechnics* 1991; **11**:295-313.
10. Ta LD, Small JC. Analysis of piled raft systems in layered soils. *International Journal for Numerical and Analytical Methods in Geomechanics* 1996; **20**:57-72.
11. Ta LD, Small JC. An approximation for analysis of raft and piled raft foundations. *Computers and Geotechnics* 1997; **20**(2):105-123.
12. Zhang HH, Small JC. Analysis of capped pile groups subjected to horizontal and vertical loads. *Computers and Geotechnics* 2000; **26**:1-21.
13. Smith IM, Wang A. Analysis of piled rafts. *International Journal for Numerical and Analytical Methods in Geomechanics* 1998; **22**:777-790.
14. Fraser RA, Wardle LJ. Numerical analysis of rectangular rafts on layered foundations. *Géotechnique* 1976; **26**(4): 613-630.
15. Harr ME. *Foundations of Theoretical Soil Mechanics*. McGraw-Hill: New York, 1966.
16. Poulos HG. Stresses and displacements in an elastic layer underlain by a rough rigid base. *Géotechnique* 1967; **17**:378-410.
17. Chow YK. Behaviour of pile groups under axial loads. *3rd Int. Conf. on Numerical Methods in Offshore Piling*, Nantes 1986:237-251.
18. Banerjee R. Analysis of axially and laterally loaded pile groups. *In Developments in Soil Mechanics (Ed. C. R. Scott)*. Applied Science Publishers: UK, 1978.
19. Brown PT. Strip footing with concentrated loads on deep elastic foundations. *Geotech. Eng.* 1975;**6**:1-13.

CHAPTER 8

ANALYSES OF THE CENTRIFUGE TESTS USING THE SIMPLIFIED ANALYSIS METHOD

SUMMARY

A series of centrifuge static vertical and horizontal loading tests was conducted on model piled rafts in a dry sand. In the horizontal loading tests of the piled raft models, effects of two different connection types between the model pile head and the model raft, i.e., rigidly fixed and hinged, on the behaviour of the model piled rafts were investigated. In this work, in order to examine the applicability of the computer program PRAB, analyses of the above centrifuge tests are conducted. It is demonstrated that there are good agreements between the test results and the analysis results.

KEY WORDS: piled raft, simplified analysis, centrifuge test.

8.1. INTRODUCTION

Piled raft foundations have been widely recognized as one of the most economical methods of foundation systems since Burland et al (1977) presented the concept of 'settlement reducers'. The inclusion of the resistance of the raft in pile foundation design can lead to a considerable economy without compromising the safety or the performance of the foundation. Although a number of research works on the settlement of piled raft foundations have been reported, the work that deals with the behaviour of piled rafts under horizontal loading seems to be very limited. In highly seismic areas such as Japan, establishments of a seismic design concept and a design tool for piled raft foundations are necessary. Although piled raft foundations have been used for the foundations of actual buildings in Japan, most piled rafts were treated as rafts alone in the seismic design, since the behaviour of piled raft foundations during earthquakes has not been well explained.

The authors conducted a series of static and dynamic centrifuge model tests for piled raft foundation models on sand in a centrifugal field of 50g (Horikoshi *et al.*; 2003a, 2003b, or Chapters 3 and 4 in this report). An influence of the rigidity of the pile head connection on the horizontal behaviour of the foundation was investigated by designing two model piled rafts with two different pile head connections, i.e., rigidly fixed and hinged pile head connections. Much emphasis was placed on the stiffness and the proportion of the load carried by each component of the two different model piled rafts. It was also found that similar behaviours of the piled raft were obtained in the static and dynamic centrifuge model tests. These results support the idea of a traditional seismic design method of a foundation in which dynamic loads acting on the foundation are modelled by an equivalent static horizontal load.

Considering current trends toward the limit state design or performance based design in the area of foundation engineering, precise estimation of deformation of a pile foundation and of stresses of their structural members is a vital issue in the framework of this new design criteria. In the preliminary design stage, a number of alternative calculations are required, varying the number of piles, the pile length, the pile spacing, the locations of the piles, and so on. Hence, a feasible but reliable deformation analysis method of piled raft foundations is sought for. In Kitiyodom & Matsumoto (2002, 2003) or Chapters 6 and 7 in this report, a simplified method of numerical analysis was developed to estimate the deformation and load distribution of piled raft foundations subjected to static vertical, horizontal and moment loads. In this work, in order to examine the applicability of the method, analyses of the static centrifuge model tests were carried out. Good agreements between the test results and the analysis results are demonstrated.

8.2. METHOD OF ANALYSIS AND ANALYSIS CONDITIONS

The analysis was carried out using the program PRAB (Piled Raft Analysis with Batter

piles) which has been developed to estimate the deformation and load distribution of piled raft foundations subjected to vertical, horizontal, and moment loads (Kitiyodom & Matsumoto; 2002, 2003). In this program, a hybrid model is employed in which the flexible raft is modelled as thin plates and the piles as elastic beams and the soil is treated as springs (**Figure 8.1**). Both the vertical and horizontal resistances of the piles as well as the raft base are incorporated into the model. The interactions between structural members, pile-soil-pile, pile-soil-raft and raft-soil-raft interactions are taken into account based on Mindlin's solutions for both vertical and horizontal forces. The considered soil profile may be homogeneous semi-infinite, arbitrarily layered and/or underlain by a rigid base stratum. PRAB can also be used for the estimation of non-linear deformation of the foundations, due to the bi-linear (elastic-perfectly plastic) response of soil springs.

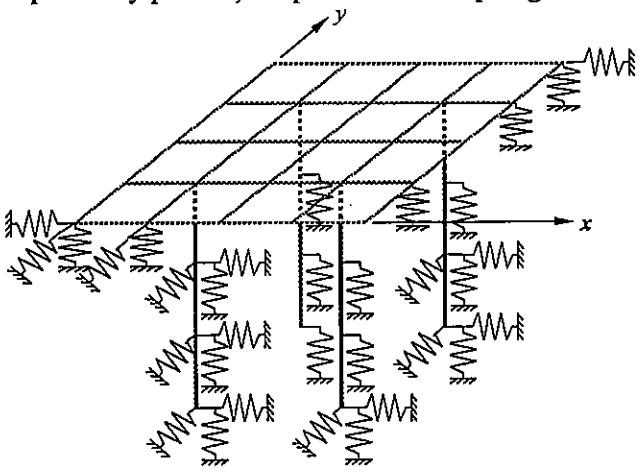

Figure 8.1. Plate-beam-spring modelling of a piled raft foundation.

Analyses of the centrifuge tests (Horikoshi *et al.*, 2003a) were carried out using the geometrical and mechanical properties given in **Table 8.1** and **Figure 8.2.** The soil was treated as a finite homogeneous layer. Hardin & Richart (1963) suggested the relationship between the shear modulus of sand at the low strain, G_0 (kgf/cm^2), and the void ratio, e, as shown in Equation (8.1). Using the effective confined pressure, p (kgf/cm^2), at the depth equal to 2/3 of the pile length, the shear modulus of the model ground at the low strain, G_0, was calculated as 58.2 GN/m^2, resulting in the young modulus at the low strain, E_0 = $2(1+\nu_s)\ G_0 = 2(1+0.3)\ G_0 = 151.4$ GN/m^2. Note that the coefficient of earth pressure at rest, K_0, was estimated using the empirical equation, $K_0 = 1 - \sin\phi'$, by Jaky (1944).

$$G_0 = 700\frac{(2.17-e)^2}{1+e}p^{0.5} \tag{8.1}$$

In the analyses, the Young's modulus of the soil were obtained by fitting the measured load-displacement curves at the initial loading stage. And it was found that the values of the Young's modulus are 15 GN/m^2 and 17.5 GN/m^2 for model piled raft subjected to vertical

and horizontal loading, respectively. These values are in the range of $0.1E_0$-$0.3E_0$ which is usually employed in the problem of pile foundation in practice (Yamashita *et al.*, 1994).

Table 8.1. Analysis condition

	Loading direction	
	Vertical loading	Horizontal loading
Pile	Pile length = 170 mm	Pile length = 180 mm
	Outer diameter = 10 mm, Inner diameter = 8 mm Young's modulus = 70.6 GN/m^2, Poisson ratio = 0.16	
Raft	Mass = 0.90 kg	Mass = 4.69 kg
	Width = 80 mm, Breadth = 80 mm Thickness = 25 mm (substantially rigid) Young's modulus = 70.6 GN/m^2, Poisson ratio = 0.16	
Soil	Layer depth = 470 mm	Layer depth = 460 mm
	Density = 1.52 t/m^3, Internal friction angle = 35° Void ratio = 0.76, Poisson ratio = 0.3 Finite homogeneous layer	

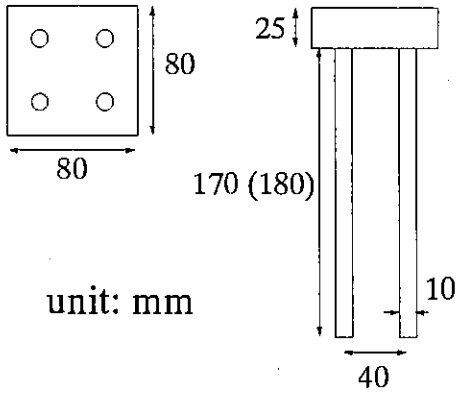

Figure 8.2. Configuration of piled raft.

8.3. ANALYSIS RESULTS

8.3.1. Model foundations subjected to vertical loading

For the analysis of the vertically loaded piled raft, in order to take into account the non-linear response, the value of the pile shaft resistance and the pile base bearing capacity were set as 100 kN/m^2 and 10000 kN/m^2, respectively. These values were obtained from the measured axial force distribution of piles in the piled raft at the settlement of 5-6 mm (**Figure 8.3**). Note that for the case of the centrifuge model test on sand, the modulus of the model sand ground significantly increases with the depth. Consequently, the pile in the piled raft didn t act purely like a friction pile (Watanabe *et al.*, 2001). In this analysis, an average value of the shaft resistance was employed. In addition, it was assumed that there is no failure occurred at the raft base.

Figure 8.4 shows the comparisons between the load-settlement behaviour of the model

piled raft calculated using PRAB and those obtained from the centrifuge tests. The load-settlement behaviour of the four piles in the piled raft are also shown in the figure. **Figure 8.5** shows the proportions of the vertical load carried by the raft and the four piles. It can be seen from the figures that there are good agreements between the calculated results using the simplified method and the measured results.

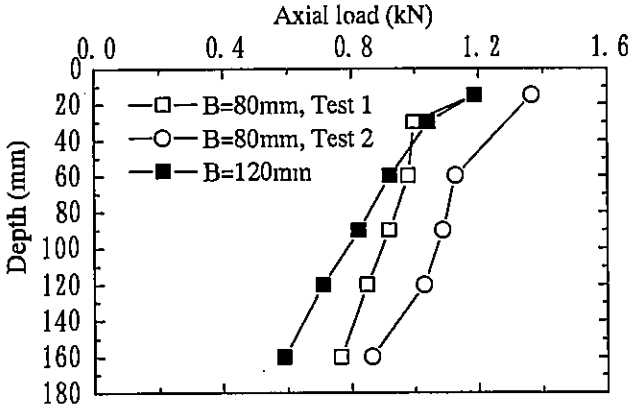

Figure 8.3. Axial force distribution of piles in piled raft model.

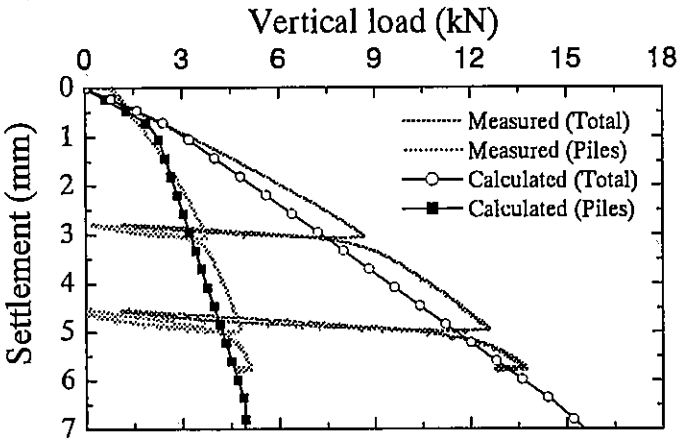

Figure 8.4. Load-settlement relationship.

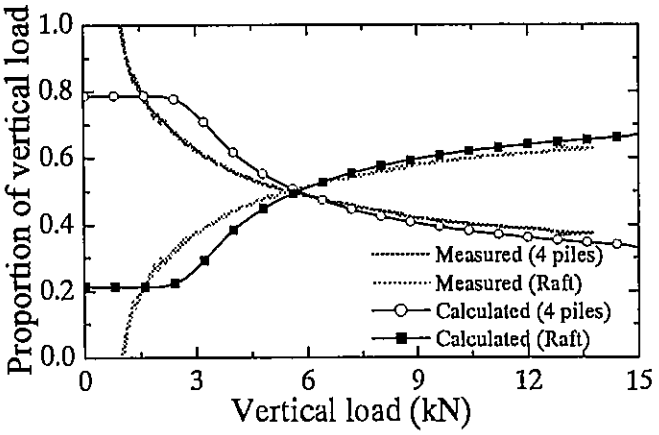

Figure 8.5. Proportion of vertical load carried by piles.

8.3.2. Model foundations subjected to horizontal loading

Although cyclic horizontal loads were applied to the model piled raft in the centrifuge tests, the horizontal load is applied in one direction in this analysis as shown in **Figure 8.6.** The analysis is conducted for only horizontal loading stage. The vertical load carried by the raft before the horizontal loading is taken into account as the initial condition. The vertical load carried by the raft base just before the horizontal load test (57% the raft weight of 2300 N) was assumed to distribute uniformly over the raft base. The friction coefficient at the raft base of 0.42 was obtained from the horizontal load test of the raft alone (**Figure 8.7**). In the estimation of the limit yield pressure of the piles located just beneath the raft in cohesionless soils, the effect of the increase in the vertical stress of the soil due to the vertical load transferred through the raft should be taken into account by using Equation (8.2).

$$p_u = K_p \sigma'_v = K_p \left(\sigma'_{v0} + \Delta\sigma'_v \right) \tag{8.2}$$

where K_p is the Rankine passive pressure coefficient, σ_v' is the total effective overburden pressure, σ_{v0}' is the initial effective overburden pressure and $\Delta\sigma_v'$ is the increase in the vertical stress of the soil beneath the raft and may be approximately estimated as follows:

$$\Delta\sigma'_v = \frac{q \times B \times L}{(B+z)(L+z)} \tag{8.3}$$

where q is the load per unit area, B and L are the breadth and the length of the raft, and z is the depth of the considered point below the raft. Note that Equation (8.3) is based on the assumption that the stress from the foundation spreads out along lines with a 2 vertical to 1 horizontal slope. The distribution of the limit soil pressures with depth is shown in **Figure 8.8.**

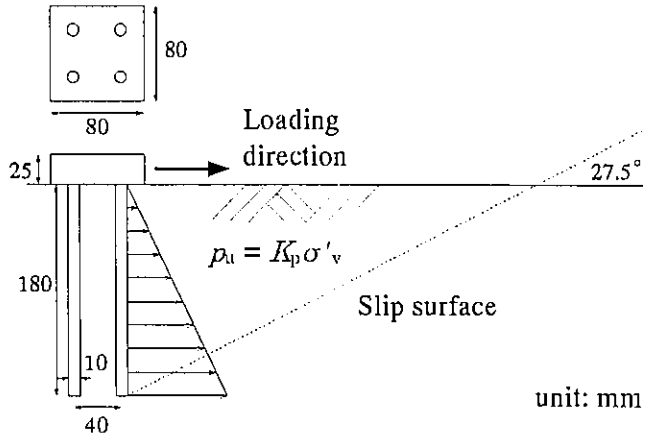

Figure 8.6. Problem analysed (horizontal loading).

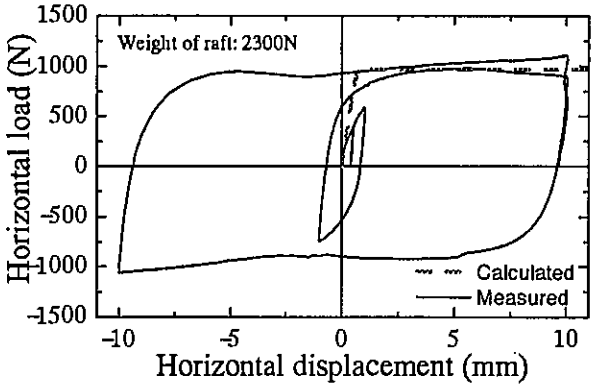

Figure 8.7. Horizontal load-displacement relationships (raft alone).

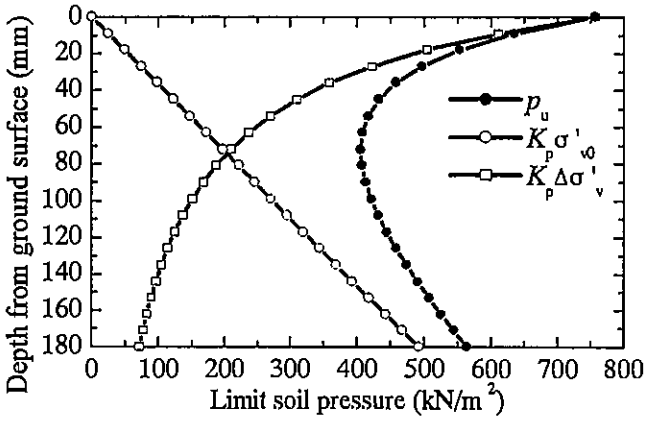

Figure 8.8. Recommend limit horizontal pressure of a pile in the piled raft.

Figure 8.9 shows the comparisons between the load-displacement behaviour of horizontally loaded model piled raft with the rigid pile head connection calculated using PRAB and those obtained from the centrifuge test. The horizontal load-displacement behaviour of the raft in the piled raft is also shown in the figure. **Figure 8.9(a)** shows the calculated results where the value of the limit horizontal pressure of the piles was estimated considering the effect of the increase in the soil stress beneath the raft, while the calculated results where the effect of the increase in the soil stress beneath the raft was neglected are shown in **Figure 8.9(b)**. The calculated results which considered the effect of the increase in the soil stress beneath the raft overestimate the measured total horizontal resistance, because of the overestimation of the horizontal pile resistance. This was thought to be due to the configuration of the model piled raft employed in this study. The raft breadth is relatively narrow compared to the pile length (**Figure 8.6**). The effect of the increase in the soil stress beneath the raft on the value of the limit horizontal pressure of the pile is small. Consequently, the calculated results which neglected the effect of the increase in the soil stress beneath the raft are closer to the measured values (**Figure 8.9(b)**). Note that the analysis results hereafter were calculated using the limit soil pressure value without the effect of the increase in the soil stress beneath the raft.

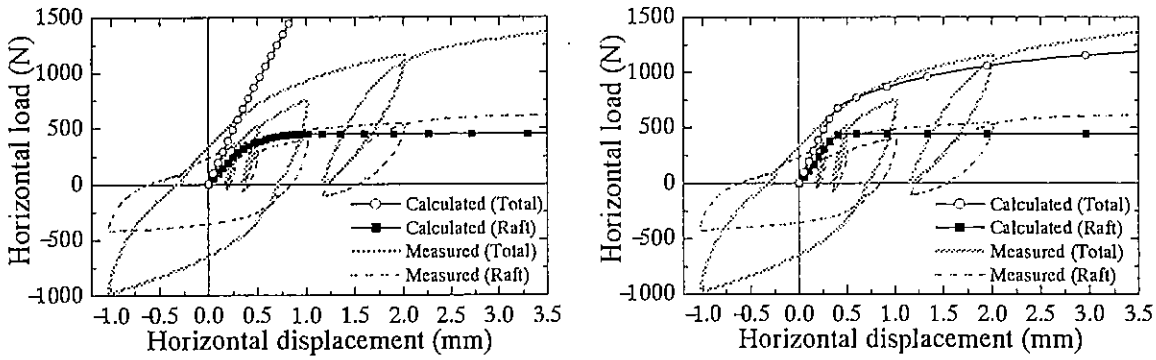

(a) consider increase in the soil stress beneath the raft (b) no increase in the soil stress beneath the raft.

Figure 8.9. Horizontal load-displacement relationships (rigid pile head connection).

An influence of the rigidity of the pile head connection on the horizontal behaviour of the piled raft foundation was also investigated in the centrifuge tests. The analysis of the horizontally load piled raft with the hinged pile head connection was carried out. Analysis parameters were set to be the same as the previous analysis of the piled raft with the rigid pile head connection. **Figure 8.10** shows the comparisons between the load-displacement behaviour of horizontally loaded model piled raft with the hinged pile head connection calculated using PRAB and those obtained from the centrifuge test. Good agreements were found between these two results. Comparing the results in **Figure 8.10** with those in **Figure 8.9(b)**, it can be seen from both the calculated results and the centrifuge results that the piles in the piled raft with the hinged pile head connection carry smaller amount of the horizontal load than those in the piled raft with the rigid pile head connection, while the amount of the horizontal load carried by the raft is almost the same.

Figure 8.11 shows the comparisons between the proportions of the horizontal load carried by four piles calculated using PRAB and those obtained from the centrifuge tests. The higher proportion of the horizontal load carried by the piles is shown in the case of the piled raft with the rigid piled head connection. The bending moment profiles at a horizontal displacement of 0.25 mm calculated using PRAB are compared with the centrifuge results in **Figure 8.12**. It was found from the figure that the values of the bending moments calculated using PRAB are a little bit higher than those of the measured values, and the points where maximum bending moment occurred are deeper in the calculation results. However, as a whole, the analysis results match well with the measured values obtained from the centrifuge tests.

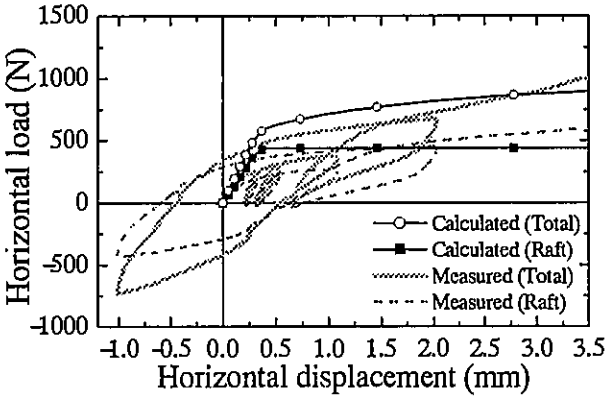

Figure 8.10. Horizontal load-displacement relationships (hinged pile head connection).

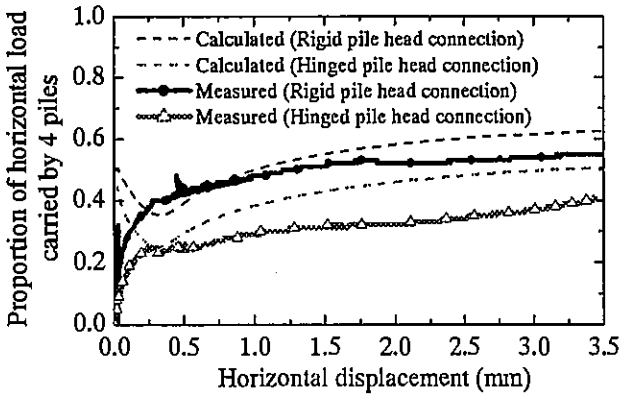

Figure 8.11. Proportion of horizontal load carried by piles.

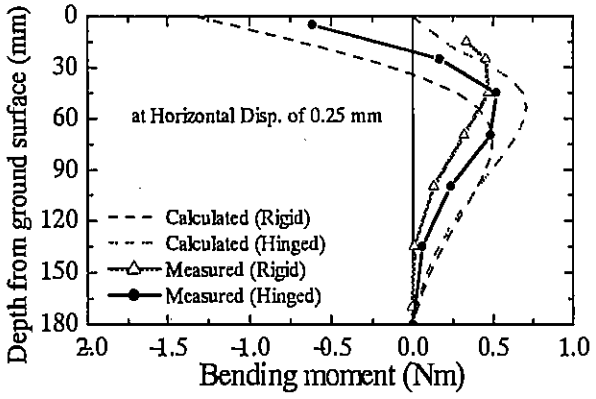

Figure 8.12. Distributions of bending moment.

8.4. CONCLUSIONS

The applicability of a computer program PRAB was examined by comparing the calculated values with the centrifuge test results. Good agreements between the calculated results and the measured values were demonstrated. It can be stated that even though the proposed method is simple, the method can be used with a confident as a design tool for a piled raft foundation subjected to vertical loads as well as horizontal loads.

ACKNOWLEDGEMENT

This study was supported by Grant-in-Aid for Scientific Research (Grant No. 12450188) of Japanese Ministry of Education, Culture, Sports, Science and Technology.

REFERENCES

1. Burland, J. B., Broms, B. B. and De Mello, V. F. B. (1977): Behaviour of foundations and structures , *Proc. 9th ICSMFE*, Tokyo, Vol. 2: 496-546.
2. Horikoshi, K., Matsumoto, T. , Hashizume, Y., Watanabe, T. and Fukuyama H.(2003a): Performance of piled raft foundations subjected to static horizontal loads , International Journal of Physical Modelling in Geomechanics.(submitted)
3. Horikoshi, K., Hashizume, Y., Matsumoto, T. and Watanabe, T. (2003b): Performance of piled raft foundations subjected to dynamic loading , International Journal of Physical Modelling in Geomechanics.(submitted)
4. Kitiyodom P, Matsumoto, T. (2002): A simplified analysis method for piled raft and pile group foundations with batter piles *International Journal for Numerical and Analytical Methods in Geomechanics*, **26**: 1649-1369.
5. Kitiyodom P, Matsumoto, T. (2003): A simplified analysis method for piled raft foundations in non-homogeneous soils *International Journal for Numerical and Analytical Methods in Geomechanics*, **27**: 85-109.
6. Yamashita, K., Kakurai, M. and Yamada, T. (1994): Investigation of a piled raft foundation on stiff clay. *Proc., 3rd Int. Geotech. Seminar Deep Found. on Bored and Auger Piles*, Belgium, Vol. 1: 457-464.
7. Watanabe, T., Fukuyama, H., Horikoshi, K. and Matsumoto, T. (2001): Centrifuge modeling of piled raft foundations subjected to horizontal loads, *Proc. 5th Int. Conf. Deep Foundation Practice incorporating Piletalk International 2001*, Singapore, 371-378.

CHAPTER 9

SUMMARY

9.1. INTRODUCTION

Experimental and analytical research on piled raft foundations subjected to static vertical and horizontal loading, and dynamic (seismic) loading was carried out in this research with the principle objectives as follows:

1. provide comprehensive experimental data of behaviors of piled rafts and freestanding pile groups, and their components such as single piles and rafts alone subjected to static vertical and horizontal loading,

2. provide comprehensive experimental data of behaviors of piled rafts and freestanding pile groups subjected to dynamic (seismic) loading,

3. provide comprehensive experimental data for calibration of piled rafts subjected to static horizontal loading and dynamic loading,

4. develop a simple method for deformation analysis of piled rafts and freestanding pile groups subjected to vertical, horizontal and moment loads,

5. examine the validity of the developed analysis method through comparisons with existing analytical methods and simulation of the experiments, and

6. give a design concept of piled rafts subjected to static horizontal loads and dynamic loads.

9.2 SUMMARY OF EACH CHAPTER

In Chapter 1, the background of the research, the review of previous research works, the objectives of the research, and the constitution of the report was described.

In Chapter 2, a series of static horizontal load tests of model piled rafts and free standing pile groups in model sand ground were conducted first to investigate the influence of the sharing of the vertical load by the raft and the piles on the raft base resistance and the resistance of the piles beneath the raft, varying the number of piles, the pile spacing and the raft size. It was shown that the horizontal resistance of a piled raft is greater than that of a freestanding pile group with the same number of piles as the piled raft, and that the

resistance of the pile beneath the raft also is larger than that of a single pile, and that the increase in the number of piles in a piled raft does not necessarily lead to the increase in the horizontal resistance of the piled raft.

In Chapter 3, a series of static vertical and horizontal load tests of model single piles, model rafts alone and model piled rafts in model sand ground was conducted in a centrifugal field of 50g, in order to explore the test results obtained in Chapter 1 in more detail and to provide comprehensive experimental data used for the design of pile raft foundations in sand. In the centrifuge experiments, the influences of the rigidity of the pile head connection on the horizontal behavior were investigated by designing rigidly fixed and hinged pile head connection models. Much emphasis was placed on the stiffness and the proportion of the load carried by each component of the two different pile head connections. The conclusions from Chapter 3 are summarized as follows:

1) The stiffness and the ultimate resistance of the single pile in the piled raft are highly different from those observed in the loading test of the isolated single pile. The increase in the confining stress around the pile due to the load transferred through the raft base should be considered in the evaluation of the pile response in the piled raft design, as well as the interaction effects between the components.
2) As for the rigid pile head connection model, the ultimate horizontal resistance was much higher than that of the raft alone. The piles play important roles in the ultimate resistance of piled raft foundations. Ignoring the pile existence in piled raft designs against horizontal loads may lead to conservative horizontal resistance.
3) As far as the present centrifuge models are concerned, the initial horizontal stiffness of the piled raft was not always higher than that of the raft alone. Since the smaller load is transferred from the raft base to the underlying soil in the piled raft, the stiffness of the sand beneath the raft may also be smaller due to the smaller confining stress. This behavior suggests that care is required in the selection of the soil modulus in the design of the piled raft foundations.
4) The ultimate frictional resistance of the raft component in the piled raft was smaller (rigid pile head connection) or almost the same (hinged pile head connection) compared with the estimates from the raft vertical loads and the coefficient of the friction between the raft base and the soil. It was thought that the soil beneath the raft was constrained by the piles which may reduce the shear deformation of the soil just beneath the raft base, and thus the mobilized shear stress at the interface was smaller. This constrained effect may be higher in the rigid pile head connection model.
5) As for the proportion of the horizontal load carried by each component, the raft initially carried more load than the piles, with larger displacements the piles more

than the raft in the piled raft with rigid pile head connection. In the piled raft with hinged pile head connection, the contribution of the piles was much smaller. Overall, however, the proportion is highly dependent on the piled raft displacement, and it is therefore important to consider such non-linear response in the designs of piled raft foundations.

6) The change in the proportion of the vertical load carried by the piles during the horizontal loading was smaller than that observed in the horizontal load. Hinged pile head connection gave the smaller change than the rigid pile head connection.
7) As far as the present centrifuge models are concerned, higher horizontal load was transferred to the piles with rigid pile head connection, which led to the higher initial horizontal stiffness compared with that of the hinged pile head connection. On the other hand, bending moments of the piles were much smaller in the piled raft with the hinged pile head connection for the same piled raft displacement.
8) In the piled raft with the hinged pile head connection, the horizontal resistance of the single pile in the piled raft was slightly smaller than that observed in the isolated single pile despite the higher confining stress around the piles beneath the raft. This was thought to be due to the possible interactions between the raft and the piles, i.e. the raft contribution was higher to the mobilization of the shear resistance.

In Chapter 4, dynamic (seismic) loading tests of 4-pile piled raft models with the rigid and the hinged pile head connections and a 4-pile freestanding pile group model with the hinged pile head connection were conducted in the centrifuge. Chapter 4 provided the behaviors of such foundation models and compared them with the results from the static horizontal loading tests. Main conclusions from Chapter 4 are summarized as follows:

9) In the piled raft designs, evaluation of the displacement (settlement, horizontal displacement, and inclination) and the proportion of the load carried by the components are the most important factors. The dynamic behaviors of the above factors were intensively examined in this paper.
10) As was also shown in the static modeling by the authors, the dynamic tests also indicate that the proportion of the horizontal load carried by each component is highly dependent on the horizontal displacement of the piled raft system. The evaluation of horizontal displacement is therefore important in the seismic design of piled rafts.
11) The change in the vertical load sharing between the piles and the raft base was relatively small compared with the horizontal load, even when the piled rafts were subjected to relatively strong input motion.
12) As far as the model conditions in the present study are concerned, the rigid pile head

connection gave higher horizontal stiffness than the hinged pile head connection. The acceleration response and the inclination of the model were also smaller in the rigid pile head connection model.

13) The proportion of the horizontal load carried by the piles was smaller in the hinged pile head connection model, indicating the role of piles in the horizontal resistance of the piled raft was smaller in the hinged pile head connection model.
14) According to the comparison of the behavior between the piled raft and the free-standing pile group, the contact of raft base with the soil surface played highly important roles in reducing the horizontal acceleration, the inclination, and the bending moments of the piles.

It is well known that centrifuge tests have many advantages in geotechnical modeling because the stress state in a prototype model can be realized in a corresponding model test and the similitude rules for the centrifuge testing has been established. However, the number of centrifuge tests is usually limited because of cost and time, and centrifuge apparatuses are available in limited numbers of institutions or organizations. Therefore, model tests at 1-g gravitational field still play important roles in pile foundation engineering area. Hence, in Chapter 5, shaking table tests of model piled rafts and model freestanding pile group models were conducted at 1-g gravitational field. In the dynamic loading tests conducted in Chapter 4, the frequency of the input motion was sufficiently lower than the natural frequencies of the foundation models. In contrast, frequencies of input motions ranged from very low to very high compared to the natural frequencies of the model foundations in the shaking table tests at 1-g gravitational field. The behaviors of the piled raft model and the freestanding pile group models near their natural frequencies were presented in Chapter 5. Main conclusions from Chapter 5 are summarized as follows:

15) The pile resistance in the piled raft in the horizontal load test was larger than that in the pile group, due to the increase in the stiffness and the strength of the soil beneath the raft caused by a vertical load transfer from the raft base to the soil. Under seismic loading, the pile resistance in the pile group was the same as that in the pile group.
16) The inclination of the piled raft in the horizontal load test was reduced compared to the pile group, indicating a contribution of the raft to suppress the inclination. Under seismic loading, the raft did not contribute effectively to reduce the inclination of the piled raft.
17) The distributions of the bending moments and the shear forces along the pile shaft were similar in each pile in the static horizontal load test. Under seismic loading, the bending moments and the shear forces of the piles fronted to the direction of

displacement at that moment were increased very much compared to the back piles.

18) The magnitude of he horizontal acceleration of the raft of the piled raft was about 2 times that of the pile group under seismic loading at near the natural frequencies of the piled raft and the pile group. Nevertheless, the bending moments and the shear forces of the piles in the piled raft were smaller than those in the pile group. This means that risk of structural failure of the piled raft is reduced compared to the pile group.

The design of pile foundations is changing from the conventional allowable stress design to a performance based design. A precise estimation of deformation of a pile foundation and of stresses of their structural members is a vital issue in the framework of the performance based design. In the preliminary design stage, a number of alternative calculations are required, varying the number of piles, the pile length, the pile spacing, the locations of the piles, and so on. Hence, a feasible but reliable deformation analysis method of piled raft foundations is sought for. In Chapter 6, a simplified method of numerical analysis was developed to estimate the deformation and load distribution of piled raft foundations subjected to vertical, lateral, and moment loads, using a hybrid model in which the flexible raft is modeled as thin plates and the piles as elastic beams and the soil is treated as springs. Both the vertical and lateral resistances of the piles as well as the raft base were incorporated into the model. Pile-soil-pile, pile-soil-raft and raft-soil-raft interactions were taken into account based on Mindlin s solutions for both vertical and lateral forces. The propose analysis method was incorporated into a computer program PRAB (Piled Raft Analysis with Batter Piles).

In Chapter 7, the computer program PRAB was extended for the analysis of axially and laterally loaded piled raft foundations embedded in nonhomogeneous soils that are encountered often in practice.

In Chapter 8, the program PRAB was employed to analyse the static horizontal load tests of the piled raft models conducted in Chapter 4. The applicability of a computer program PRAB was examined by comparing the calculated values with the centrifuge test results. Good agreements between the calculated results and the measured values were demonstrated. It can be stated that even though the proposed method is simple, the method can be used with a confident as a design tool for a piled raft foundation subjected to vertical loads as well as horizontal loads.

9.3. IMPLICATIONS FOR FUTURE STUDY

The experiments of model piled raft foundations in this research were carried out in a limited conditions such as:

1) experiments were conducted in uniform dry sand ground,
2) heights of superstructures (rafts) were low compared to the widths of the rafts, and
3) frequencies of the input motion in the centrifuge tests were lower than the natural frequencies of the foundations models.

Centrifuge experiments using saturated sands and clayey soils will be useful to investigate the behavior of piled rafts during seismic loading.

Centrifuge modeling with more realistic configurations of the superstructure and the foundation will be useful to investigate the interaction between the superstructure and the foundation structure during seismic loading.

Calibration between static the behavior of a piled raft and that under seismic loading with the input motion near the natural frequency of the piled raft will be required, in order to employ a simplified design method where the dynamic load is replaced by a equivalent static horizontal force.

As for analytical methods, comparison of the PRAB and FEM in which the stress dependency of the soil stiffness is adequately modeled will be required especially for sands of which stiffness is largely dependent of the effective stresses.

In practice, pile foundations may be subjected to ground movements induced by nearby excavation operations, settling embankments, pile driving operations, tunneling operations, moving slopes, landslides and so on. The investigation of the behavior of piled rafts subjected to the soil movement is also one of research objectives for piled rafts.